POLSKIE TOWARZYSTWO MIKROBIOLOGÓW
POLISH SOCIETY OF MICROBIOLOGISTS

# Polish Journal of Microbiology

2022

Polish Journal of Microbiology
formerly Acta Microbiologica Polonica
2022, Vol. 71, No 4

# CONTENTS



INSTRUCTIONS FOR AUTHORS
Instructions for authors: https://www.sciendo.com/journal/PJM

MINIREVIEW
Polish Journal of Microbiology
2022, Vol. 71, No 4, 481–489
https://doi.org/10.33073/pjm-2022-050

# Rapid and Simple Approaches for Diagnosis of *Staphylococcus aureus* in Bloodstream Infections

RUI DUAN and PEI WANG*

Department of Laboratory Medicine and Blood Transfusion, The First People's Hospital of Jingmen, Jingmen, Hubei Province, China

Submitted 29 August 2022, accepted 1 November 2022, published online 9 December 2022

Abstract

*Staphylococcus aureus* is an important causative pathogen of bloodstream infections. An amplification assay such as real-time PCR is a sensitive, specific technique to detect *S. aureus*. However, it needs well-trained personnel, and costs are high. A literature review focusing on rapid and simple methods for diagnosing *S. aureus* was performed. The following methods were included: (a) Hybrisep *in situ* hybridization test, (b) T2Dx system, (c) BinaxNow *Staphylococcus aureus* and PBP2a, (d) Gram staining, (e) PNA FISH and QuickFISH, (f) Accelerate Pheno™ system, (g) MALDI-TOF MS, (h) BioFire FilmArray, (i) Xpert MRSA/SA. These rapid and simple methods can rapidly identify *S. aureus* in positive blood cultures or direct blood samples. Furthermore, BioFire FilmArray and Xpert MRSA/SA identify methicillin-resistant *S. aureus* (MRSA), and the Accelerate Pheno™ system can also provide antimicrobial susceptibility testing (AST) results. The rapidity and simplicity of

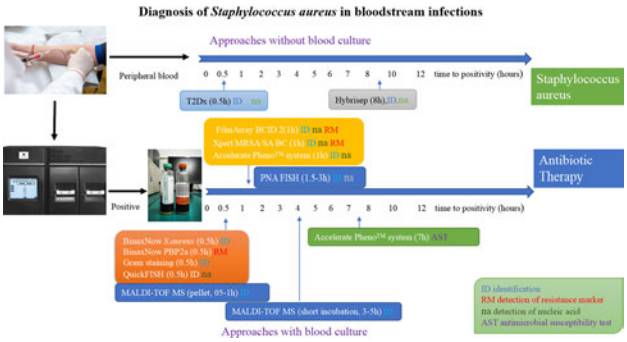


results generated by these methods have the potential to improve patient outcomes and aid in the prevention of the emergence and transmission of MRSA.

K e y w o r d s: bloodstream infections, *Staphylococcus aureus*, rapid diagnostics, antimicrobial stewardship, bacteremia

## Introduction

*Staphylococcus aureus* (SA) is a leading cause of bacteremia. High mortality rates from 20% to 50%, frequent recurrences from 5% to 10%, and lasting impairment in more than one-third of the survivors characterize *S. aureus* bloodstream infections (BSI) (Asgeirsson et al. 2018; Kern and Rieg 2020). *S. aureus* infections are particularly problematic due to the frequent antibiotic resistance, among which methicillin resistance is the most clinically relevant (Turner et al. 2019). Patients with methicillin-resistant *S. aureus* (MRSA) bacteremia stay longer in hospitals and generate higher costs than those with bacteremia caused by methicillin-susceptible *S. aureus* (MSSA) (Tsuzuki et al. 2021).

MRSA often requires vancomycin therapy. Vancomycin use is associated with increased antimicrobial and monitoring costs and may bring about drug-induced acute kidney injury in up to 15% of patients (Pritchard et al. 2010). Furthermore, empirical anti-MRSA treatment for MSSA bacteremia can lead to poor outcomes compared with standard therapy (Jones et al. 2020). Therefore, rapid and accurate discrimination of MRSA from MSSA is essential for clinical diagnosis to facilitate a specific antimicrobial therapy (Srisrattakarn et al. 2022).

When the positive blood culture starts, conventional *S. aureus* identification takes about 48 to 72 h to complete. Recent advances in molecular and nonmolecular testing methods significantly reduced the turnaround

* Corresponding author: P. Wang, Department of Laboratory Medicine and Blood Transfusion, The First People's Hospital of Jingmen, Jingmen, Hubei Province, China; **e-mail: peiwwien@outlook.com**

time for MRSA reporting (Gonzalez et al. 2020; Sze et al. 2021; Parkes-Smith et al. 2022).

Rapid and simple techniques are required to address the challenges raised by *S. aureus* BSI, employing rapid pathogen identification and susceptibility testing to enable specific targeted antibiotic therapy on time.

This review updates recent advances in rapid and simple assays to identify *S. aureus* in bloodstream infections and discusses the advantages and limitations of these methods.

## Methods

The authors searched PubMed and Google Scholar with the following terms: bloodstream infections, *S. aureus*, rapid diagnostics, bacteremia, and blood cultures. English and Japanese literature for randomized clinical trials (RCTs), meta-analyses, systematic reviews, and observational studies were evaluated (1999–2022). The author agreed with the quality of included studies.

## Direct detection of *S. aureus* from blood samples

**Hybrisep – an *in situ* hybridization method.** Hybrisep is an *in situ* hybridization-based assay which detects specific bacterial DNA in smears enriched in polymorphonuclear neutrophils (PMN) from the blood of suspected BSI individuals. At an early stage of sepsis, neutrophils ingest bacteria, and bacterial DNA can be detected in the blood smears by an *in situ* hybridization (ISH) method. In 1999, an ISH assay targeted phagocyted bacteria from blood was developed by collecting the blood and preparing neutrophil-enriched smears. The neutrophils were then permeabilized and incubated with specific probes (Shimada et al. 1999). Digoxygenin-labelled probes and anti-digoxygenin-alkaline phosphatase conjugates were utilized. BCIP (5-bromo-4-chloro-3-indolyl-phosphate) with NBT (nitro blue tetrazolium) was used as a substrate for ALP and allowed the signal visualization. These signals were observed in the cell cytoplasm under a microscope. Blue-colored dots represented the phagocytized bacteria in neutrophils, and it was assumed a positive result. The first available kit Hybrisep (Fuso Pharmaceuticals, Japan), provided five probes, including those specific to *S. aureus*. In 2014, Enomoto et al. (2014) introduced a new ISH assay that contained a universal probe targeting 59 species of 35 genera. The hybridization and washing procedures were performed automatically by Hybristat. The whole process takes about eight hours.

The ISH assay was used to investigate blood smears from 60 patients with suspected sepsis (Kudo et al. 2009). Nine *S. aureus* strains were detected with ISH assay, while only one blood was found to be positive for *S. aureus* by conventional culture. Discrepancies were found to be due to the effect of antibiotic treatment. Three of the nine patients with positive *S. aureus* blood cultures underwent antibiotic therapy before blood sampling. Therefore, the ISH method appeared less affected by antibiotic treatment than blood culture.

Over 40% of patients can take antibiotics before blood collection (Roh et al. 2012). Although new blood culture bottles contain neutralization of antimicrobial substances, the elimination effect for antibiotics is limited by the concentration of antibiotics in the blood (Mitteregger et al. 2013). ISH depends on the hybridization performed in neutrophils; thus, a reduced number of neutrophils resulting from immunosuppressive therapy may decrease the sensitivity of the ISH assay. As an independent-culture method, ISH is beneficial for managing patients with BSI, despite the absence of *S. aureus* in blood culture. So far, the Hybrisep kit and Hybristat are available only in Japan. Only limited studies on ISH for *S. aureus* detection in blood have been reported (Kudo et al. 2009). Further studies of ISH for *S. aureus* detection in blood should be conducted through multicenter cooperation.

**T2Dx magnetic resonance assay.** The T2Dx system (T2 Biosystems, USA), an automated instrument, uses a method based on magnetic resonance changes in the water proton T2 relaxation signal in the presence of a magnetic field (Neely et al. 2013). The protocol includes a pathogen-specific amplification step, and the amplicons are hybridized into specific probe-enriched nanoparticles (Paolucci et al. 2010). The T2Bacteria Panel enables multiplex detection of the ESKAPE pathogens (*Enterococcus faecium*, *Staphylococcus aureus*, *Klebsiella pneumoniae*, *Acinetobacter baumannii*, *Pseudomonas aeruginosa*, and *Enterobacter* species). De Angelis et al. (2018), upon evaluation of 140 suspected BSI samples, detected two of two *S. aureus* strains with the T2Bacteria Panel and confirmed this finding by blood culture. The remaining 138 samples were negative when using the T2Bacteria Panel and a paired blood culture. The sensitivity and specificity of T2Dx for *S. aureus* identification was 100% compared to the blood culture. Another study by Drevinek et al. (2021) found a good sensitivity of the T2Dx system. In 55 samples, two of two *S. aureus* strains were detected by the T2Bacteria Panel, but the corresponding blood culture detected only one strain. Nguyen et al. (2019) conducted a prospective multicenter study involving 1,427 samples. The T2Dx system and blood culture identified 41 and 16 *S. aureus* strains, respectively. The turnaround time of the T2Dx system was shorter than that of the blood culture (3.6–7.7 h vs. 38.5–71.7 h, respectively). It demonstrates that the T2Dx system has value over blood culture in patients receiving antimicrobial therapy.

## Rapid detection of *S. aureus* from positive blood cultures

**BinaxNOW *Staphylococcus aureus* test with BinaxNow PBP2a assay.** The principle of BinaxNow *Staphylococcus aureus* (Alere, USA) and BinaxNowPBP2a (Alere SAS, France) assays is an immunochromatographic test for the identification of *S. aureus* and the determination of methicillin resistance, respectively. BinaxNow *Staphylococcus aureus* test was FDA approved for direct identification of *S. aureus*. It uses polyclonal antibodies to qualitatively detect an *S. aureus*-specific protein in a positive blood culture (Dhiman et al. 2013). Qian et al. (2014) collected 104 blood cultures from 2012 to 2013 that were tested with this method. The blood cultures included 41 *S. aureus* (14 MRSA, 27 MSSA), 60 CoNS (coagulase-negative *Staphylococci*), three other Gram-positive cocci in pairs and clusters (one of *Micrococcus* species, one anerobic Gram-positive coccus, and one of *Gemella* species). The BinaxNow *Staphylococcus aureus* test showed 97.6% sensitivity, 100% specificity, and positive and negative predictive values of 100% and 98.4%, respectively, upon *S. aureus* identification in positive blood culture. The performance was equally efficient in both aerobic and anaerobic bottles. Only one false-negative result was found due to antibiotic treatment of the patient and the resulting reduction in the antigen's level. Dhiman et al. (2013) evaluated 319 positive blood cultures containing clusters of Gram-positive cocci using the BinaxNow *Staphylococcus aureus* test. The study achieved 95.8% of sensitivity and 99.6% of specificity. One false-positive result occurred in the blood culture containing a presumptive *Staphylococcus lugdunensis* isolate not later confirmed. One false-negative result was confirmed by repeated testing. It might have resulted from a decrease in the bacterial concentration below the detection limit ($5.42 \times 10^8$ cells/ml). One study combined BinaxNow *Staphylococcus aureus* for species identification and BinaxNow PBP2a assay to detect methicillin resistance (Heraud et al. 2015). Seventy-nine positive blood cultures with Gram-positive cocci in clusters were tested. A sensitivity of 94% and specificity of 98% in identifying *S. aureus* and 100% sensitivity and specificity of methicillin resistance detection were reported. These tests are valuable alternatives for the diagnosis of MRSA bacteremia.

**Gram staining.** Gram staining is an essential technique in microbiology. It was invented by Danish bacteriologist Hans Christian Gram in 1882 (Wu and Yang 2020). Gram staining distinguishes Gram-positive from Gram-negative organisms based on differences in their cell walls. The thick cell walls of Gram-positive bacteria retain the purple crystal violet-iodine complex after treatment with ethanol (O'Toole 2016). Once a blood culture is detected as positive by an automated, continuously monitoring blood culture system, a smear is Gram stained, providing a quick presumptive identification of pathogens. It might be helpful in directing the bread antibiotic therapy (Boyanova 2018). Gram staining is a crucial but easy, rapid, and inexpensive method for pathogen detection in a positive blood culture. A series of evaluating criteria were developed based on the type of blood culture bottle, bacterial species, and cluster characteristics (Murdoch and Greenlees 2004). These criteria may help an experienced microbiological technician to distinguish *S. aureus* from CoNS in positive blood cultures. It allowed for achieving the overall sensitivity and specificity of 89% and 98%, respectively. A prospective observational study with 118 blood samples showed that a pink-colored "oozing sign" could also be used to distinguish *S. aureus* from CoNS (Hadano et al. 2018). The study demonstrated a sensitivity and specificity of 78.7% and 95.0%, respectively. Compared to the previous study by Murdoch and Greenlees (2004), this method focused on the "oozing sign" regardless of blood culture bottle type, organism species, and cluster characteristics. Therefore, it is simpler and more suitable than the previous method for application in routine work. A significant advantage of Gram staining is to be a good alternative for a community hospital without a diagnostic microbiology laboratory. The quality of Gram staining depends on the skills and can vary over time and between technicians. With the development of automated Gram staining systems, the comparability and consistency of results can be improved in laboratories (Baron et al. 2010). It also holds for new automated image acquisition systems as a convolutional neural network-based classification of Gram staining results (Smith et al. 2018). Integrating these techniques with previous evaluation criteria in *S. aureus* identification may make the Gram staining method more uncomplicated and accurate. Early identification of *S. aureus* in blood cultures is vital because the clinical signs of *S. aureus* bacteremia may be unspecific and therefore, the patients may be no symptomatic early in the course of the infection (Mitchell and Howden 2005).

**PNA FISH and QuickFISH assays.** Fluorescent *in situ* hybridization (FISH) is a diagnostic technique using a probe (e.g., peptide nucleic (PNA) probe) to target the 16S rRNA gene of *S. aureus* directly in the blood culture smears. Fluorescence *in situ* hybridization using the PNA probes is a useful diagnostic tool for pathogen-directed therapy (Weaver et al. 2019). PNA probes have unique performance characteristics that render PNA FISH to be applied widely to positive blood cultures. The first commercially available kit was PNA FISH (OpGen®, USA, previously AdvanDx). González et al. (2004) evaluated 285 blood cultures containing Gram-positive cocci similar to staphylococci using PNA FISH. The results showed 100% sensitivity,

and 99.4% specificity, and their positive and negative predictive values were 99.2% and 100%, respectively. The PNA probe recognizes both MRSA and MSSA. In ten positive blood cultures mixed with other bacteria, *S. aureus* was correctly identified. Only one weak positive hybridization was obtained with a positive blood culture of *Staphylococcus schleiferi*. Oliveira et al. (2003) performed a blinded comparison of *S. aureus* PNA FISH in eight centres with three types of blood culture bottles produced by different manufacturers (ESP, BACTEC, and BacT/Alert). The sensitivity ranged from 98.5% to 100%, the specificity was between 98.5% and 99.1%.

Even a potentially interfering substance as charcoal did not affect the performance of *S. aureus* PNA FISH. The total analysis time is up to 2.5 h, and hands-on time is below 30 min. QuickFISH was launched in 2013 (Carretto et al. 2013), a modified PNA FISH version with several timesaving innovations. It takes less than 30 min. because procedure does not include washing or mounting of slides, and the hands-on time is about 5 min. Deck et al. (2012) tested 722 positive blood cultures containing Gram-positive cocci in cluster using the *Staphylococcus* QuickFISH method. The sensitivity was 99.5%, and the combined specificity was 89.5%. Two false positive and seven false negative results were found. The discrepancies between the *Staphylococcus* QuickFISH method and the standard method were due to human errors or to the limited sequence alignment of the probes designed. The *Staphylococcus* QuickFISH method can speed up the *S. aureus* identification in blood cultures. It would help in the patient's management when catheter-related BSI is suspected. Early catheter removal is recommended when *S. aureus* is detected to decrease the risks of persistent bacteremia and hematogenous complications.

**Accelerate Pheno™ system.** The fully automated Accelerate Pheno™ system provides rapid identification and susceptibility of microorganisms in positive blood samples (Cenci et al. 2020). The system combines FISH for bacterial identification and an automated microscope for assessing bacterial growth rates and calculating the MIC value (Marschal et al. 2017). Molecular methods and MALDI-TOF MS can also identify microorganisms in positive blood cultures and their susceptibility phenotype in a few hours. However, these methods must provide the susceptibility phenotype that clinicians request to make a therapeutic decision. This need drove Accelerate Diagnostic™ (USA) to develop an Accelerate Pheno™ system (APS). The multiplex fluorescence *in situ* hybridization using target-specific probes is a diagnostic strategy APS uses to identify on-panel microbes. The minimum inhibitory concentration (MIC) is evaluated after analyzing the bacterial morphokinetic growth pattern in the presence of a given antimicrobial agent (Marschal et al. 2017). Charnot-Katsikas et al. (2017) investigated 232 blood cultures using APS and compared the results with the standard method. After considering the discrepant results, the sensitivity and specificity for *S. aureus* were 94.7% and 99.0%, respectively.

The categorical agreement between APS and standard antimicrobial susceptibility tests (AST) was 98.5%. Only two minor errors were found upon conventional testing of 68 *S. aureus* strains. When using APS for blood culture, the turnaround time was shortened to about 23.47 h, 41.86 h, and 25.5 min. for identification, susceptibility, and hands-on time, respectively. Lutgring et al. (2018) demonstrated that the sensitivity and specificity of *S. aureus* detection using APS in positive blood cultures were 96.9%, and 95.2%, respectively. The categorical agreement between APS and culture-based AST was 100% upon *S. aureus* testing. Since the identification and AST were performed in 1.5 h and 7 h, respectively, as opposed to a few days with conventional testing, it would decrease morbidity and mortality of patients with BSI. It is due to the switch from broad-spectrum empiric therapy to targeted specific antibiotic therapy since it decreases adverse effects and the emergence of multi-drug resistance organisms. However, APS has low performance for correct identification, and AST results in polymicrobial blood cultures. It is also of a high cost compared to standard methods. All these APS characteristics should be considered for a diagnostic and treatment decision.

**MALDI-TOF MS.** One of the soft ionization techniques, a matrix-assisted laser desorption ionization-time of flight mass spectrometry (MALDI-TOF MS), generates a protein-based spectral profile or "fingerprint" unique to a given species of pathogen. The microorganism identification relies on the characteristic spectrum of each species.

MALDI-TOF MS has revolutionized microorganism identification and is now widely used in routine laboratory testing. Two main commercial systems are used worldwide, the Vitek MS (bioMerieux, France) and Microflex LT Biotyper (Bruker Daltonics, USA). The detection limit is $10^8$ CFU/ml of positive blood culture broth (Christner et al. 2010).

*S. aureus* identification from positive blood culture with MALDI-TOF MS can be conducted according to two protocols: (a) after short-term incubation on a solid medium or (b) directly from the positive blood culture pellet. Curtoni et al. (2017) reported reliable species identification in less than 5 h. The identification of *S. aureus* was successful at 85.7% and 100% after 3 h and 5 h of incubation, respectively. It means that MALDI-TOF MS can be a reliable, easy, and rapid method for the *S. aureus* identification from positive blood culture when performed after a short-term culture of bacteria on a solid medium. Direct identification from blood

culture involves the protein extraction after bacterial lysis and filtration (Foster 2013; Lin et al. 2018), use of a Sepsityper® kit (Bruker) or serum separator tube (Zengin and Bayraktar 2021), and in-house saponin-based bacterial extraction (Hu et al. 2020; Ponderand et al. 2020). Tsuchida et al. (2018) compared an in-house lysis filtration protocol with a Sepsityper® kit for *S. aureus* identification. Out of a total of 19 *S. aureus* strains, 17 were identified to species level by a lysis filtration protocol, two to genus level, whereas 11 of these strains were identified to species level and four to genus level. Four strains could not be identified by the Sepsityper® kit. The results showed that Sepsityper® kit failed to identify completely Gram-positive cocci in positive blood cultures.

Another study employed a serum separator tube followed by MALDI-TOF MS for *S. aureus* identification (Zengin and Bayraktar 2021). A total of 36 *S. aureus* strains were confirmed by a short-term incubation routine identification (SIRID) method and 32 strains from 36 monomicrobial cultures were correctly identified by direct rapid identification (RID) method using a serum separator tube followed by MALDI-TOF MS. The mean turnaround time of RID method was significantly lower compared to SIRID method (2.86 h vs. 19.49 h, $p < 0.001$). This study indicated that the serum separator tube method was suitable for the rapid identification of *S. aureus* in a blood culture.

MALDI-TOF MS has been proposed to detect strains susceptible or resistant to several antibiotics. Some studies reported accurate discrimination of *S. aureus* isolates susceptible to vancomycin (Mather et al. 2016). Recently, Liu et al. (2021) presented the machine learning algorithms for rapid MALDI-TOF MS-based MRSA screening. By selecting 38 *m*/*z* features for the classifying model and coupling it with machine-learning algorithms, a rapid and simple method to distinguish MRSA from MSSA was established. This method makes resistance detection more convenient and effective in routine microbiology laboratories.

**FilmArray system.** The FilmArray is a multiplex-PCR-based system that combines samples the preparation, PCR amplification, detection, and analysis (Peker et al. 2018). The BioFire FilmArray BCID2 panel can simultaneously identify 43 pathogens and ten antimicrobial resistance genes (Cortazzo et al. 2021). It takes about 2 min. of hands-on time and 1 h turnaround time. Sze et al. (2021) compared BioFire FilmArray BCID2 with MALDI-TOF MS for the *S. aureus* identification in blood cultures and reported both sensitivity and specificity of 100%. Furthermore, two out of two MRSA were detected by the BCID2 panel. Holma et al. (2022) presented similar results. These findings showed that the BioFire FilmArray BCID2 proves to be a good tool for the early detection of MRSA and the administration of effective antimicrobial therapy.

**Xpert MRSA/SA BC assay.** The Xpert MRSA/SA BC assay is based on a multiplex PCR. It targets the junction between *S. aureus* conserved open reading frame (*orfx*) and the SCC containing the *mec*A gene (SCC *mec*A). It enables Xpert MRSA/SA BC to detect and identify MRSA and MSSA in 1 h (Belmekki et al. 2013). A prospective study at two clinical centers investigated the impact of rapid detection of *S. aureus* in positive blood cultures on patient management (McHugh et al. 2020). In 264 blood cultures, 39 were positive for *S. aureus,* and one strain was identified as MRSA. Compared with the culture method, Xpert MRSA/SA BC has 100% sensitivity and 100% specificity for identifying *S. aureus* and 100% specificity for MRSA detection. For the Xpert MRSA/SA BC assay, the median turnaround time from blood culture processing to the final result was 1.7 h, compared to the 25.7 h turnaround time of the culture method. Xpert MRSA/SA BC results allowed early specific therapy for *S. aureus* and de-escalation of antimicrobial therapy for MSSA. Reddy and Whitelaw (2021) explored whether Xpert MRSA/SA BC assay can be utilized as an antimicrobial stewardship tool. Of 231 samples tested, concordance was 100% between the Xpert MRSA/SA BC assay and culture method. It can discriminate MRSA from MSSA and significantly reduce the laboratory turnaround time. This study showed the potential benefit of time reduction for the appropriate therapy introduction in most patients with *S. aureus* BSI.

## Conclusions

Timely and targeted specific antibiotic therapy of *S. aureus* BSI improves survival and decreases the length of hospital stay and adverse effects of antibiotics. Although new approaches are utilized for rapid identification and AST, conventional methods are still indispensable.

Several rapid and simple methods, such as PNA FISH, MALDI-TOF MS, and the Accelerate Pheno™ system, are being used to diagnose positive blood cultures. PNA FISH and QuickFISH are well-validated methods. Utilization of MALDI-TOF MS directly from blood culture pellets is still in progress. The pre-treatment of the sample is being recognized as a standard approach. The Accelerate Pheno™ system provides not only rapid identification but also susceptibility reports (as the MIC values), while the low throughput of one sample per machine hinder this method from wide utilization. Gram staining integrated with machine-learning-based image analysis may lead to the rapid identification of *S. aureus* from blood culture. The BinaxNow *Staphylococcus aureus* and BinaxNow PBP2a appear to be a golden pair for the rapid identification and determination of methicillin resistance of *S. aureus.* The Hybrisep *in situ* hybridization and T2Dx assays

have a high detection positive rate compared to blood cultures. Limited studies have been here reported and validated. Further validation and studies should be performed to determine its performance for the rapid identification of *S. aureus* from blood cultures. FilmArray BCID2 and Xpert MRSA/SA BC are very useful tools in routine microbiology laboratories for rapid discrimination of MRSA from MSSA.

Every approach has its characteristics (summarized in Table I and II). Each laboratory should con-

Table I
Characteristics and performance of different methods for the identification of *S. aureus* in the blood or blood cultures.

| Assays | Resistance markers | Sensitivity | Turnaround time (h) | Specificity | References |
|---|---|---|---|---|---|
| Hybrisep | none | NA | NA | 8 | Shimada et al. 1999 |
| T2Dx | none | 100% | 100% | 3–5 | De Angelis et al. 2018 |
| BinaX Now *S.aureus* | none | 97.6% | 100% | 0.5 | Qian et al. 2014 |
| BinaX Now PBP2a | yes | 100% | 100% | 0.5 | Heraud et al. 2015 |
| Gram staining | none | 78.7% | 95% | 0.5 | Hadano et al. 2018 |
| PNA FISH | none | 100% | 99.4% | 1.5–3 | González et al. 2004 |
| QuickFISH | none | 99.5% | 89.5% | 0.5 | Deck et al. 2012 |
| Accelerate Pheno™ system | susceptibility | 94.7% | 99% | ID1/AST 7 | Charnot-Katsikas et al. 2017 |
| MALDI-TOF MS | in development | 85.7–100% | NA | 0.5–1 (pellet)/3–5 (short incubation) | Foster 2013; Curtoni et al. 2017 |
| FilmArray BCID2 | yes | 100% | 100% | 1 | Holma et al. 2022 |
| Xpert MRSA/SA BC | yes | 100% | 100% | 1 | McHugh et al. 2020 |

FISH – fluorescent *in situ* hybridization, PNA – peptide nucleic acid, MALDI-TOF MS – matrix-assisted laser desorption/ionisation-time of flight mass spectrometry, NA – not available

Table II
Comments on rapid and simple methods for the identification of *S. aureus* from the blood or blood cultures.

| Assays | Automated | Personnel experience | Equipment requirement | Throughput | Cost | Comments |
|---|---|---|---|---|---|---|
| Hybrisep | yes | yes | proprietary equipment | low | moderate | +: rapid, sensitive and specific<br>–: limited number of publications |
| T2Dx | yes | no | proprietary equipment | low | high | +: rapid, sensitive, and specific<br>–: no resistance markers |
| BinaX Now *S. aureus* | no | no | no | low | low | +: rapid, sensitive and specific<br>–: cross-reaction with *S. lugdunensis* |
| BinaX Now PBP2a | no | no | no | low | low | +: rapid, sensitive, and specific<br>–: no identification |
| Gram staining | yes | yes | generic equipment | low | low | +: rapid, simple<br>–: variable sensitivity and specificity |
| PNA FISH | no | yes | generic equipment | low | high | +: rapid, sensitive, and specific<br>–: no resistance markers |
| QuickFISH | no | yes | generic equipment | low | high | +: rapid, sensitive, and specific<br>–: no resistance markers |
| Accelerate Pheno™ system | yes | no | proprietary equipment | low | high | +: rapid, sensitive, and specific, with AST results<br>–: low throughout |
| MALDI-TOF MS | no | yes | proprietary equipment | high | low | +: rapid, sensitive, and specific, cost-effective<br>–: enrichment, not standardization |
| FilmArray BCID2 | yes | no | proprietary equipment | low | high | +: rapid, sensitive, and specific, with resistance results<br>–: low throughout |
| Xpert MRSA/SA BC | yes | no | proprietary equipment | low | high | +: rapid, sensitive, and specific, with resistance results<br>–: expensive |

FISH – fluorescent *in situ* hybridization, PNA – peptide nucleic acid, MALDI-TOF MS – matrix-assisted laser desorption/ionisation-time of flight mass spectrometry

sider some important factors such as turnaround time, panels of antibiotics offered, and hands-on time when searching for an appropriate method (Sze et al. 2021). Polymicrobial infections in BSI are not infrequent. It is essential to select an accurate method for such samples (Abat et al. 2015). Direct identification of *S. aureus* from blood rather than blood culture should be a direction of future development to maximize the benefits of rapid identification of *S. aureus* from blood cultures. Rapid identification methods combined with rapid AST determination are also necessary (Pliakos et al. 2018). Simple and rapid identification of *S. aureus* from blood culture plus phenotype AST will significantly impact the optimizing BSI management.

**ORCID**

Rui Duan https://orcid.org/0000-0002-0187-9331
Pei Wang https://orcid.org/0000-0002-0550-1029

**Author contributions**

RD and PW performed the literature search and data analysis. RD and PW drafted the work. All authors critically revised the work.

**Conflict of interest**

The authors do not report any financial or personal connections with other persons or organizations, which might negatively affect the contents of this publication and/or claim authorship rights to this publication.

## Literature

**Abat C, Chaudet H, Colson P, Rolain JM, Raoult D.** Real-time microbiology laboratory surveillance system to detect abnormal events and emerging infections, Marseille, France. Emerg Infect Dis. 2015 Aug;21(8):1302–1310. https://doi.org/10.3201/eid2108.141419

**Asgeirsson H, Thalme A, Weiland O.** *Staphylococcus aureus* bacteraemia and endocarditis – epidemiology and outcome: a review. Infect Dis (Lond). 2018 Mar;50(3):175–192. https://doi.org/10.1080/23744235.2017.1392039

**Baron EJ, Mix S, Moradi W.** Clinical utility of an automated instrument for gram staining single slides. J Clin Microbiol. 2010 Jun; 48(6):2014–2015. https://doi.org/10.1128/jcm.02503-09

**Belmekki M, Mammeri H, Hamdad F, Rousseau F, Canarelli B, Biendo M.** Comparison of Xpert MRSA/SA nasal and MRSA/SA ELITe MGB assays for detection of the *mec*A gene with susceptibility testing methods for determination of methicillin resistance in *Staphylococcus aureus* isolates. J Clin Microbiol. 2013 Oct;51(10):3183–3191. https://doi.org/10.1128/jcm.00860-13

**Boyanova L.** Direct Gram staining and its various benefits in the diagnosis of bacterial infections. Postgrad Med. 2018 Jan;130(1):105–110. https://doi.org/10.1080/00325481.2018.1398049

**Carretto E, Bardaro M, Russello G, Mirra M, Zuelli C, Barbarini D.** Comparison of the *Staphylococcus* QuickFISH BC test with the tube coagulase test performed on positive blood cultures for evaluation and application in a clinical routine setting. J Clin Microbiol. 2013 Jan;51(1):131–135. https://doi.org/10.1128/jcm.02103-12

**Cenci E, Paggi R, Socio GV, Bozza S, Camilloni B, Pietrella D, Mencacci A.** Accelerate Pheno™ blood culture detection system: a literature review. Future Microbiol. 2020 Oct;15:1595–1605. https://doi.org/10.2217/fmb-2020-0177

**Charnot-Katsikas A, Tesic V, Love N, Hill B, Bethel C, Boonlayangoor S, Beavis KG.** Use of the Accelerate Pheno system for identification and antimicrobial susceptibility testing of pathogens in positive blood cultures and impact on time to results and workflow. J Clin Microbiol. 2017 Dec 26;56(1):e01166-17. https://doi.org/10.1128/jcm.01166-17

**Christner M, Rohde H, Wolters M, Sobottka I, Wegscheider K, Aepfelbacher M.** Rapid identification of bacteria from positive blood culture bottles by use of matrix-assisted laser desorption-ionization time of flight mass spectrometry fingerprinting. J Clin Microbiol. 2010 May;48(5):1584–1591. https://doi.org/10.1128/jcm.01831-09

**Cortazzo V, D'Inzeo T, Giordano L, Menchinelli G, Liotti FM, Fiori B, De Maio F, Luzzaro F, Sanguinetti M, Posteraro B, et al.** Comparing BioFire FilmArray BCID2 and BCID panels for direct detection of bacterial pathogens and antimicrobial resistance genes from positive blood cultures. J Clin Microbiol. 2021 Mar 19;59(4): e03163-20. https://doi.org/10.1128/jcm.03163-20

**Curtoni A, Cipriani R, Marra ES, Barbui AM, Cavallo R, Costa C.** Rapid identification of microorganisms from positive blood culture by MALDI-TOF MS after short-term incubation on solid medium. Curr Microbiol. 2017 Jan;74(1):97–102. https://doi.org/10.1007/s00284-016-1161-2

**De Angelis G, Posteraro B, De Carolis E, Menchinelli G, Franceschi F, Tumbarello M, De Pascale G, Spanu T, Sanguinetti M.** T2Bacteria magnetic resonance assay for the rapid detection of ESKAPEc pathogens directly in whole blood. J Antimicrob Chemother. 2018 Mar 1;73(suppl 4):iv20–iv26. https://doi.org/10.1093/jac/dky049

**Deck MK, Anderson ES, Buckner RJ, Colasante G, Coull JM, Crystal B, Della Latta P, Fuchs M, Fuller D, Harris W, et al.** Multicenter evaluation of the *Staphylococcus* QuickFISH method for simultaneous identification of *Staphylococcus aureus* and coagulase-negative staphylococci directly from blood culture bottles in less than 30 minutes. J Clin Microbiol. 2012 Jun;50(6):1994–1998. https://doi.org/10.1128/jcm.00225-12

**Dhiman N, Trienski TL, DiPersio LP, DiPersio JR.** Evaluation of the BinaxNOW *Staphylococcus aureus* test for rapid identification of Gram-positive cocci from VersaTREK blood culture bottles. J Clin Microbiol. 2013 Sep;51(9):2939–2942. https://doi.org/10.1128/jcm.01087-13

**Drevinek P, Hurych J, Antuskova M, Tkadlec J, Berousek J, Prikrylova Z, Bures J, Vajter J, Soucek M, Masopust J, et al.** Direct detection of ESKAPEc pathogens from whole blood using the T2Bacteria Panel allows early antimicrobial stewardship intervention in patients with sepsis. Microbiologyopen. 2021 Jun;10(3):e1210. https://doi.org/10.1002/mbo3.1210

**Enomoto H, Inoue S, Matsuhisa A, Nishiguchi S.** Diagnosis of spontaneous bacterial peritonitis and an *in situ* hybridization approach to detect an "unidentified" pathogen. Int J Hepatol. 2014; 2014:634617. https://doi.org/10.1155/2014/634617

**Foster AG.** Rapid Identification of microbes in positive blood cultures by use of the Vitek MS matrix-assisted laser desorption ionization-time of flight mass spectrometry system. J Clin Microbiol. 2013 Nov;51(11):3717–3719. https://doi.org/10.1128/jcm.01679-13

**Gonzalez MD, Chao T, Pettengill MA.** Modern blood culture: management decisions and method options. Clin Lab Med. 2020 Dec; 40(4):379–392. https://doi.org/10.1016/j.cll.2020.07.001

**González V, Padilla E, Giménez M, Vilaplana C, Pérez A, Fernández G, Quesada MD, Pallarés MA, Ausina V.** Rapid diagnosis of *Staphylococcus aureus* bacteremia using *S. aureus* PNA FISH. Eur J Clin Microbiol Infect Dis. 2004 May;23(5):396–398. https://doi.org/10.1007/s10096-004-1112-x

**Hadano Y, Isoda M, Ishibashi K, Kakuma T.** Validation of blood culture gram staining for the detection of *Staphylococcus aureus* by

the 'oozing sign' surrounding clustered gram-positive cocci: a prospective observational study. BMC Infect Dis. 2018 Sep 29;18(1):490. https://doi.org/10.1186/s12879-018-3412-2

**Heraud S, Freydiere AM, Doleans-Jordheim A, Bes M, Tristan A, Vandenesch F, Laurent F, Dauwalder O.** Direct identification of *Staphylococcus aureus* and determination of methicillin susceptibility from positive blood-culture bottles in a Bact/ALERT system using Binax Now *S. aureus* and PBP2a tests. Ann Lab Med. 2015 Jul; 35(4):454–457. https://doi.org/10.3343/alm.2015.35.4.454

**Holma T, Torvikoski J, Friberg N, Nevalainen A, Tarkka E, Antikainen J, Martelin JJ.** Rapid molecular detection of pathogenic microorganisms and antimicrobial resistance markers in blood cultures: evaluation and utility of the next-generation FilmArray Blood Culture Identification 2 panel. Eur J Clin Microbiol Infect Dis. 2022 Mar;41(3):363–371. https://doi.org/10.1007/s10096-021-04314-2

**Hu YL, Hsueh SC, Ding GS, Chuang PC, Chen JM, Lu CY, Chang LY, Huang LM, Lee PI, Hsueh PR.** Applicability of an in-house saponin-based extraction method in Bruker Biotyper matrix-assisted laser desorption/ionization time-of-flight mass spectrometry system for identifying bacterial and fungal species in positively flagged pediatric VersaTREK blood cultures. J Microbiol Immunol Infect. 2020 Dec;53(6):916–924. https://doi.org/10.1016/j.jmii.2020.01.004

**Jones BE, Ying J, Stevens V, Haroldsen C, He T, Nevers M, Christensen MA, Nelson RE, Stoddard GJ, Sauer BC, et al.** Empirical anti-MRSA vs standard antibiotic therapy and risk of 30-day mortality in patients hospitalized for pneumonia. JAMA Intern Med. 2020 Apr 1;180(4):552–560. https://doi.org/10.1001/jamainternmed.2019.7495

**Kern WV, Rieg S.** Burden of bacterial bloodstream infection – a brief update on epidemiology and significance of multidrug-resistant pathogens. Clin Microbiol Infect. 2020 Feb; 26 (2):151–157. https://doi.org/10.1016/j.cmi.2019.10.031

**Kudo M, Matsuo Y, Nakasendo A, Inoue S, Goto H, Tsukiji J, Watanuki Y, Ueda A, Kaneko T, Ishigatsubo Y.** Potential clinical benefit of the *in situ* hybridization method for the diagnosis of sepsis. J Infect Chemother. 2009 Feb;15(1):23–26. https://doi.org/10.1007/s10156-008-0655-7

**Lin JF, Ge MC, Liu TP, Chang SC, Lu JJ.** A simple method for rapid microbial identification from positive monomicrobial blood culture bottles through matrix-assisted laser desorption ionization time-of-flight mass spectrometry. J Microbiol Immunol Infect. 2018 Oct;51(5):659–665. https://doi.org/10.1016/j.jmii.2017.03.005

**Liu X, Su T, Hsu YS, Yu H, Yang HS, Jiang L, Zhao Z.** Rapid identification and discrimination of methicillin-resistant *Staphylococcus aureus* strains via matrix-assisted laser desorption/ionization time-of-flight mass spectrometry. Rapid Commun Mass Spectrom. 2021 Jan 30;35(2):e8972. https://doi.org/10.1002/rcm.8972

**Lutgring JD, Bittencourt C, McElvania TeKippe E, Cavuoti D, Hollaway R, Burd EM.** Evaluation of the Accelerate Pheno system: results from two academic medical centers. J Clin Microbiol. 2018 Mar 26;56(4):e01672-17. https://doi.org/10.1128/jcm.01672-17

**Marschal M, Bachmaier J, Autenrieth I, Oberhettinger P, Willmann M, Peter S.** Evaluation of the Accelerate Pheno system for fast identification and antimicrobial susceptibility testing from positive blood cultures in bloodstream infections caused by Gram-negative pathogens. J Clin Microbiol. 2017 Jul;55(7):2116–2126. https://doi.org/10.1128/jcm.00181-17

**Mather CA, Werth BJ, Sivagnanam S, SenGupta DJ, Butler-Wu SM.** Rapid detection of vancomycin-intermediate *Staphylococcus aureus* by matrix-assisted laser desorption ionization-time of flight mass spectrometry. J Clin Microbiol. 2016 Apr;54(4):883–890. https://doi.org/10.1128/jcm.02428-15

**McHugh MP, Parcell BJ, MacKenzie FM, Templeton KE; Scottish Microbiology and Virology Network Smvn Molecular Diagnostics Evaluation Group.** Rapid molecular testing for *Staphylococcus aureus* bacteraemia improves clinical management. J Med Microbiol. 2020 Apr;69(4):552–557. https://doi.org/10.1099/jmm.0.001171

**Mitchell DH, Howden BP.** Diagnosis and management of *Staphylococcus aureus* bacteraemia. Intern Med J. 2005 Dec;35 Suppl 2:S17–S24. https://doi.org/10.1111/j.1444-0903.2005.00977.x

**Mitteregger D, Barousch W, Nehr M, Kundi M, Zeitlinger M, Makristathis A, Hirschl AM.** Neutralization of antimicrobial substances in new BacT/Alert FA and FN Plus blood culture bottles. J Clin Microbiol. 2013 May;51(5):1534–1540. https://doi.org/10.1128/jcm.00103-13

**Murdoch DR, Greenlees RL.** Rapid identification of *Staphylococcus aureus* from BacT/ALERT blood culture bottles by direct Gram stain characteristics. J Clin Pathol. 2004 Feb;57(2):199–201. https://doi.org/10.1136/jcp.2003.10538

**Neely LA, Audeh M, Phung NA, Min M, Suchocki A, Plourde D, Blanco M, Demas V, Skewis LR, Anagnostou T, et al.** T2 magnetic resonance enables nanoparticle-mediated rapid detection of candidemia in whole blood. Sci Transl Med. 2013 Apr 24;5(182):182ra54. https://doi.org/10.1126/scitranslmed.3005377

**Nguyen MH, Clancy CJ, Pasculle AW, Pappas PG, Alangaden G, Pankey GA, Schmitt BH, Rasool A, Weinstein MP, Widen R, et al.** Performance of the T2Bacteria panel for diagnosing bloodstream infections: a diagnostic accuracy study. Ann Intern Med. 2019 Jun 18;170(12):845–852. https://doi.org/10.7326/m18-2772

**Oliveira K, Brecher SM, Durbin A, Shapiro DS, Schwartz DR, De Girolami PC, Dakos J, Procop GW, Wilson D, Hanna CS, et al.** Direct identification of *Staphylococcus aureus* from positive blood culture bottles. J Clin Microbiol. 2003 Feb;41(2):889–891. https://doi.org/10.1128/jcm.41.2.889-891.2003

**O'Toole GA.** Classic spotlight: how the Gram stain works. J Bacteriol. 2016 Nov 4;198(23):3128. https://doi.org/10.1128/jb.00726-16

**Paolucci M, Landini MP, Sambri V.** Conventional and molecular techniques for the early diagnosis of bacteraemia. Int J Antimicrob Agents. 2010 Dec;36(Suppl2):S6–S16. https://doi.org/10.1016/j.ijantimicag.2010.11.010

**Parkes-Smith J, Bergh H, Harris PNA.** Assessing the performance of the Cepheid Xpert in identifying and differentiating methicillin-susceptible *Staphylococcus aureus* and methicillin-resistant *Staphylococcus aureus* from blood culture bottles. Pathology. 2022 Sep 5:S0031-3025(22)00232-X. https://doi.org/10.1016/j.pathol.2022.07.006

**Peker N, Couto N, Sinha B, Rossen JW.** Diagnosis of bloodstream infections from positive blood cultures and directly from blood samples: recent developments in molecular approaches. Clin Microbiol Infect. 2018 Sep;24(9):944–955. https://doi.org/10.1016/j.cmi.2018.05.007

**Pliakos EE, Andreatos N, Shehadeh F, Ziakas PD, Mylonakis E.** The cost-effectiveness of rapid diagnostic testing for the diagnosis of bloodstream infections with or without antimicrobial stewardship. Clin Microbiol Rev. 2018 May 30;31(3):e00095-17. https://doi.org/10.1128/cmr.00095-17

**Ponderand L, Pavese P, Maubon D, Giraudon E, Girard T, Landelle C, Maurin M, Caspar Y.** Evaluation of Rapid Sepsityper® protocol and specific MBT-Sepsityper module (Bruker Daltonics) for the rapid diagnosis of bacteremia and fungemia by MALDI-TOF-MS. Ann Clin Microbiol Antimicrob. 2020 Dec 9;19(1):60. https://doi.org/10.1186/s12941-020-00403-w

**Pritchard L, Baker C, Leggett J, Sehdev P, Brown A, Bayley KB.** Increasing vancomycin serum trough concentrations and incidence of nephrotoxicity. Am J Med. 2010 Dec;123(12):1143–1149. https://doi.org/10.1016/j.amjmed.2010.07.025

**Qian Q, Eichelberger K, Kirby JE.** Rapid identification of *Staphylococcus aureus* directly from Bactec blood culture broth by the BinaxNOW *S. aureus* test. J Clin Microbiol. 2014 Jan; 52(1):319–320. https://doi.org/10.1128/jcm.02291-13

**Reddy K, Whitelaw A.** Can the Xpert MRSA/SA BC assay be used as an antimicrobial stewardship tool? A prospective assay validation and descriptive impact assessment study in a South African setting. BMC Infect Dis. 2021 Feb 15;21(1):177. https://doi.org/10.1186/s12879-021-05857-7

**Roh KH, Kim JY, Kim HN, Lee HJ, Sohn JW, Kim MJ, Cho Y, Kim YK, Lee CK.** Evaluation of BACTEC Plus aerobic and anaerobic blood culture bottles and BacT/Alert FAN aerobic and anaerobic blood culture bottles for the detection of bacteremia in ICU patients. Diagn Microbiol Infect Dis. 2012 Jul;73(3):239–242. https://doi.org/10.1016/j.diagmicrobio.2012.03.022

**Shimada J, Hayashi I, Inamatsu T, Ishida M, Iwai S, Kamidono S, Kurosawa H, Masaoka T, Matsumoto F, Monden M, et al**. Clinical trial of in-situ hybridization method for the rapid diagnosis of sepsis. J Infect Chemother. 1999 Mar;5(1):21–31. https://doi.org/10.1007/s101560050004

**Smith KP, Kang AD, Kirby JE.** Automated interpretation of blood culture Gram stains by use of a deep convolutional neural network. J Clin Microbiol. 2018 Feb 22;56(3):e01521-17. https://doi.org/10.1128/jcm.01521-17

**Srisrattakarn A, Panpru P, Tippayawat P, Chanawong A, Tavichakorntrakool R, Daduang J, Wonglakorn L, Lulitanond A.** Rapid detection of methicillin-resistant *Staphylococcus aureus* in positive blood-cultures by recombinase polymerase amplification combined with lateral flow strip. PLoS One. 2022 Jun 30;17(6):e0270686. https://doi.org/10.1371/journal.pone.0270686

**Sze DTT, Lau CCY, Chan TM, Ma ESK, Tang BSF.** Comparison of novel rapid diagnostic of blood culture identification and antimicrobial susceptibility testing by Accelerate Pheno system and BioFire FilmArray Blood Culture Identification and BioFire FilmArray Blood Culture Identification 2 panels. BMC Microbiol. 2021 Dec 18; 21(1):350. https://doi.org/10.1186/s12866-021-02403-y

**Tsuchida S, Murata S, Miyabe A, Satoh M, Takiwaki M, Matsushita K, Nomura F.** An improved in-house lysis-filtration protocol for bacterial identification from positive blood culture bottles with high identification rates by MALDI-TOF MS. J Microbiol Methods. 2018 May;148:40–45. https://doi.org/10.1016/j.mimet.2018.03.014

**Tsuzuki S, Yu J, Matsunaga N, Ohmagari N**. Length of stay, hospitalisation costs and in-hospital mortality of methicillin-susceptible and methicillin-resistant *Staphylococcus aureus* bacteremia in Japan. Public Health. 2021 Sep;198:292–296. https://doi.org/10.1016/j.puhe.2021.07.046

**Turner NA, Sharma-Kuinkel BK, Maskarinec SA, Eichenberger EM, Shah PP, Carugati M, Holland TL, Fowler VG Jr.** Methicillin-resistant *Staphylococcus aureus*: an overview of basic and clinical research. Nat Rev Microbiol. 2019 Apr;17(4):203–218. https://doi.org/10.1038/s41579-018-0147-4

**Weaver AJ, Brandenburg KS, Sanjar F, Wells AR, Peacock TJ, Leung KP.** Clinical utility of PNA-FISH for burn wound diagnostics: a noninvasive, culture-independent technique for rapid identification of pathogenic organisms in burn wounds. J Burn Care Res. 2019 Jun 21;40 (4):464–470. https://doi.org/10.1093/jbcr/irz047

**Wu KY, Yang TX.** A novel improved Gram staining method based on the capillary tube. Pol J Microbiol. 2020 Dec;69(4):503–508. https://doi.org/10.33073/pjm-2020-043

**Zengin Canalp H, Bayraktar B.** Direct rapid identification from positive blood cultures by MALDI-TOF MS: specific focus on turnaround times. Microbiol Spectr. 2021 Dec 22;9(3):e0110321. https://doi.org/10.1128/spectrum.01103-21

ORIGINAL PAPER
Polish Journal of Microbiology
2022, Vol. 71, No 4, 491–497
https://doi.org/10.33073/pjm-2022-042

# Screening of Toxin Genes in Methicillin-Resistant *Staphylococcus aureus* Clinical Isolates from a Hospital Setting in a Tertiary Hospital in Northern Cyprus

TCHAMOU M.F. POTINDJI[1], OSAID A.A. MOMANI[1], BAKARE B. OMOWUMI[1] and BUKET BADDAL[1, 2*]

[1] Department of Medical Microbiology and Clinical Microbiology, Faculty of Medicine, Near East University, Nicosia, Cyprus
[2] Microbial Pathogenesis Research Group, DESAM Institute, Near East University, Nicosia, Cyprus

Submitted 23 June 2022, accepted 29 August 2022, published online 12 November 2022

Abstract

Methicillin-resistant *Staphylococcus aureus* (MRSA) is a significant opportunistic pathogen with a wide repertoire of virulence characteristics. Data regarding the molecular profile of MRSA in Northern Cyprus is limited. The current study aimed to examine the virulence profiles of MRSA with a focus on toxin-associated factors. Ninety-one *S. aureus* isolates collected at a university hospital were included in the study. Identification and antibiotic susceptibility testing were performed with BD Phoenix™ automated system. Methicillin resistance was evaluated by the disc diffusion assay and *mecA* detection. The presence of *nuc* was confirmed by conventional PCR. Confirmed MRSA isolates were assessed for the presence of virulence genes *hla*, *eta*, *etb*, *etd* and *tst* using molecular methods. Among 91 *S. aureus* isolates identified as MRSA using the BD Phoenix™ platform, 80.85% (n = 76/91) were confirmed as MRSA using phenotypic and genotypic methods. All confirmed MRSA isolates (n = 76, 100%) were positive for the *nuc*. MRSA rates were statistically higher in elderly inpatients. The prevalence of toxin-encoding genes was 97.3% (n = 74/76) for *hla,* 2.63% (n = 2/76) for *eta,* 1.3% (n = 1/76) for *etb*, and 2.63% (n = 2/76) for *tst*. None of the screened isolates harbored the *etd* gene. These results represent the first report to investigate multiple virulence factors in MRSA isolates in Northern Cyprus.

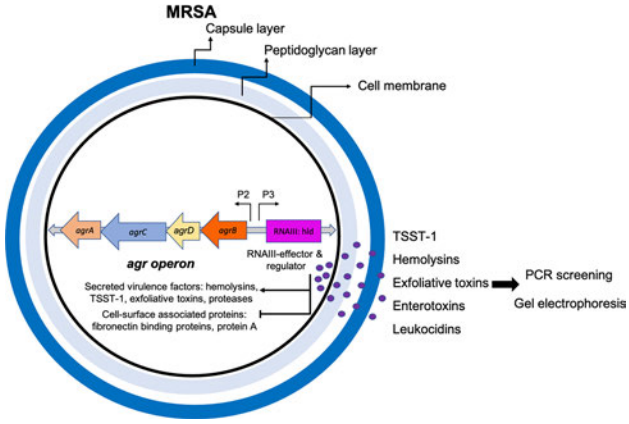


K e y w o r d s: methicillin-resistant *Staphylococcus aureus*, toxins, virulence, Northern Cyprus

## Introduction

Methicillin-resistant *Staphylococcus aureus* (MRSA) represents one of the most concerning pathogens worldwide, responsible for community-acquired and hospital-acquired infections (Kourtis et al. 2019; Turner et al. 2019). According to the Centers for Disease Prevention and Control (CDC), antibiotic-resistant *S. aureus* causes over 2 million cases of disease and 23,000 deaths each year in the United States alone (Okwu et al. 2019). In addition to their intrinsic resistance to β-lactam antibiotics, hospital-associated MRSA strains often exhibit a variable yet alarming level of multi-drug resistance which narrows treatment alternatives to the limited remaining efficient drugs (Bispo et al. 2020; Jernigan et al. 2020).

The molecular characteristics of *S. aureus* can change over time, and the population structure varies regionally, according to epidemiological studies of *S. aureus* (Barcudi et al. 2020; Junnila et al. 2020; Lu et al. 2021). Over 94% of *S. aureus* strains are reported to be resistant to penicillin and its derivatives due to the release of the penicillinase enzyme, beta-lactamase, which inhibits penicillin by hydrolyzing the beta-lactam ring (Algammal et al. 2020). MRSA is characterized predominantly by the presence of either the *mecA* gene or

* Corresponding author: B. Baddal, Department of Medical Microbiology and Clinical Microbiology, Faculty of Medicine, Near East University, Nicosia, Cyprus; Microbial Pathogenesis Research Group, DESAM Institute, Near East University, Nicosia, Cyprus; **email: buket.baddal@neu.edu.tr**

its homologs *mecB*, *mecC* and *mecD*, that are located on the staphylococcal chromosomal cassette *mec* (*SCCmec* type I–XIV) and code for the penicillin-binding protein 2a (PBP2-a) that has a reduced affinity for beta-lactam antibiotics (Urushibara et al. 2020; Uehara 2022).

From a clinical perspective, the increasing use of molecular and other bioinformatics tools has facilitated the mapping of the *S. aureus* virulome and clarified its epidemiological and clinical significance. *S. aureus* generates an array of virulence factors that allow the bacteria to survive extreme conditions within the human host and damages biological membranes, resulting in cell death (Shettigar and Murali 2020; Nisar et al. 2021). *S. aureus* maintains fine control of the expression of virulence factors which include hemolysins, leukocidins, proteases, exfoliative toxins, enterotoxins, and immunemodulatory factors.

The development of clinical management and infection control policies presents a significant challenge as there is still insufficient data on the infection transmission rate and clone characteristics. It is, therefore, of paramount importance to investigate the epidemiology and the molecular profile of *S. aureus*. The current study aims to characterize toxin-associated virulence determinants in a wide range of clinical isolates in a previously understudied region of Northern Cyprus.

## Experimental

### Materials and Methods

**Clinical isolates.** In total, 91 clinical non-repetitive *S. aureus* strains isolated between January 2012 and November 2020, identified initially to be MRSA by BD Phoenix™ 100 automated identification and antibiotic susceptibility system, were collected and investigated in this study. Isolates were cultured from wound/abscess, blood, bronchoalveolar lavage, nasal swab, tracheal aspiration, and sputum samples from different departments at the Near East University Hospital in Northern Cyprus.

**Identification and phenotypic detection of methicillin resistance.** All isolates were cultured on sheep blood agar. Agar plates were incubated at 35°C for 24–48 h in 5% $CO_2$. The isolates were subsequently confirmed as *S. aureus* based on colony morphology and ability to coagulate human plasma. Methicillin resistance was assessed using the disc diffusion method with cefoxitin (30 µg) (Bioanalyse, Turkey) on Mueller-Hinton agar (Difco, Becton Dickinson, USA) plates. Antibiotic susceptibility was assessed with the European Committee on Antimicrobial Susceptibility Testing guidelines (EUCAST 2020).

**DNA extraction.** Rapid extraction of genomic DNA was performed with the boiling method described by Barbosa et al. (2016). Briefly, a few colonies cultured on blood agar were suspended in nuclease-free water in a microcentrifuge tube. The cell suspension was then incubated at 100°C for 15 min and centrifuged at 13,000 rpm for 5 min to sediment the debris. After centrifugation, the supernatant was collected and utilized as a DNA template in polymerase chain reaction (PCR) reactions.

**Molecular identification of the isolates.** The preliminary identification procedures were followed by the PCR analysis using *S. aureus* species-specific thermonuclease (*nuc*) primers, as previously shown (Amin et al. 2020). The *nuc* gene was amplified in a 25-µl reaction which contained: PCR Master Mix 2× (Thermo Fisher Scientific, USA), Taq DNA polymerase (0.05 U/µl), 0.4 mM of each dNTP, 4 mM $MgCl_2$, 4 µl of template DNA, and 10 pmol of forward and reverse primer nuc-F 5'-GCGATTGATGGTGATACGGTT-3', nuc-R 5'-AGCCAAGCCTTGACGAACTAAAGC-3'. DNA amplification was performed involving denaturation at 94°C for 10 min, 30 cycles at 94°C for 30 s, 55°C for 30 s, and 72°C for 1 min, and a final elongation step at 72°C for 5 min. The PCR detection of *mecA* confirmed the methicillin resistance. Amplification was achieved as described before (Rahman et al. 2018) except for a denaturation step at 94°C for 10 min. The strain of *S. aureus* SCC*mec* type IV (*mecA*+, *pvl*–, *nuc*+) was used as a positive control. Distilled water was used as a negative control. Verification of PCR products was obtained using 1.5% agarose gel. Ethidium bromide was used for staining the gels, and amplicons were observed with MiniBIS Pro Gel Documentation Platform (DNR, Israel).

**Screening for virulence genes in MRSA.** The occurrence of virulence-associated genes was investigated by PCR detection of *hla*, *eta*, *etb*, *etd* and *tst* in all confirmed MRSA isolates. Single PCR reactions were performed as described above. PCR amplification for each primer set was performed using Bio-Rad MyCycler™ Thermal Cycler (Bio-Rad Laboratories, Israel) according to the cycling parameters summarized in Table I. PCR products were analyzed with gel electrophoresis through 2% agarose gel and visualized using a transilluminator. The positive controls included the genomic DNA from isolates in which the presence of the genes mentioned above was formerly found in the genome.

**Statistical analysis.** Statistical data analysis was performed using SPSS Version 25.0 (SPSS, Inc., USA). Comparison of variables was achieved using independent t-tests and Chi-square test of association. A $p$-Value of $\leq 0.05$ was considered statistically significant.

**Ethics approval.** The Institutional Review Board approved this study at Near East University with a waiver of patient consent (YDU/2020/80-1115, YDU/2021/90-1331).

Table I
Oligonucleotides used in this study.

| Target | Sequence (from 5' to 3') | Product size (bp) | Annealing temp. (°C) | Reference |
|---|---|---|---|---|
| *mecA* | | | | |
| Forward | AAAATCGATGGTAAAGGTTGGC | 533 | 55 | Kot et al. 2020 |
| Reverse | AGTTCTGCAGTACCGGATTTGC | | | |
| *nuc* | | | | |
| Forward | GCGATTGATGGTGATACGGTT | 279 | 55 | Amin et al. 2020 |
| Reverse | AGCCAAGCCTTGACGAACTAAAGC | | | |
| *hla* | | | | |
| Forward | CTGATTACTATCCAAGAAATTCGATTG | 209 | 57 | Rasheed and Hussein 2020 |
| Reverse | CTTTCCAGCCTACTTTTTTATCAGT | | | |
| *eta* | | | | |
| Forward | GCAGGTGTTGATTTAGCATT | 93 | 58 | Rasheed and Hussein 2020 |
| Reverse | AGATGTCCCTATTTTTGCTG | | | |
| *etb* | | | | |
| Forward | ACAAGCAAAAGAATACAGCG | 226 | 50 | Rasheed and Hussein 2020 |
| Reverse | GTTTTTGGCTGCTTCTCTTG | | | |
| *etd* | | | | |
| Forward | AACTATCATGTATCAAGG | 376 | 47 | Liu et al. 2018 |
| Reverse | CAGAATTTCCCGACTCAG | | | |
| *tst* | | | | |
| Forward | ACCCCTGTTCCCTTATCATC | 326 | 57 | Rasheed and Hussein 2020 |
| Reverse | TTTTCAGTATTTGTAACGCC | | | |

## Results

**Patients features.** A total of 91 non-duplicate samples were initially screened. Of these, 80.85% (76/91) strains were identified as MRSA using phenotypic and genotypic methods, among which 57.9% (44/76) were recovered from male patients. The distribution of isolates according to patient admission status indicated that 75% (57/76) of the isolates were obtained from inpatients. Despite the predominance of the male gender, no statistically significant difference was observed in gender distribution across inpatient and outpatient groups ($p = 0.107$) (Table II). Patient age at admission ranged from 1 to 99 years (mean: 60.16, median: 63.00, standard deviation: 22.21), and the majority of patients with MRSA infection were over the age of 45 ($p < 0.005$) (Table II) with the inpatients group being significantly older ($p < 0.001$). No significant association was observed between patient age and gender ($p = 0.901$).

Table II
Distribution of MRSA isolates according to age, gender, and admission status.

| Demographic data | n (%) | *p*-value |
|---|---|---|
| Age groups | | |
| Under 15 | 2 (2.6) | < 0.005 |
| 15–44 | 16 (21.1) | |
| 45–64 | 22 (28.9) | |
| 65 and above | 36 (47.4) | |
| Gender | | |
| Male | 44 (57.9) | 0.107 |
| Female | 32 (42.1) | |
| Admissions | | |
| Inpatients | 57 (75) | < 0.001 |
| Outpatients | 19 (25) | |

Majority of the isolates obtained in this study originated from patients admitted to cardiology (n = 14; 18.4%), pulmonary infections (n = 10; 13.2%), infectious diseases (n = 10; 13.2%), anesthesiology (n = 7; 9.2%), orthopedics and traumatology (n = 6; 7.9%), cardiovascular surgery (n = 5; 6.6%), general surgery (n = 5; 6.6%), neurosurgery (n = 4; 5.3%), dermatology (n = 4; 5.3%), brain surgery (n = 2; 2.6%), gastroenterology (n = 2; 2.6%), intensive care unit (n = 2; 2.6%), and the remaining departments; dialysis, neurology, plastic surgery, urology, and pediatrics (n = 5; 6.6%). The distribution of isolates by the hospital department is shown in Table III.

Majority of the samples from which MRSA were cultured were isolated from abscess-wound (n = 19; 25.0%), blood (n = 17; 22.4%), nasal swabs (n = 13; 17.1%), and tracheal aspirates (n = 13; 17.1%). The distribution of the isolates according to the sample type is given in Table IV.

Table III
Distribution of MRSA isolates according to the hospital department.

| Department | n (%) |
|---|---|
| Cardiology | 14 (18.4) |
| Pulmonary infections | 10 (13.2) |
| Infectious diseases | 10 (13.2) |
| Anesthesiology | 7 (9.2) |
| Orthopedics and traumatology | 6 (7.9) |
| Cardiovascular surgery | 5 (6.6) |
| General surgery | 5 (6.6) |
| Dermatology | 4 (5.3) |
| Neurosurgery | 4 (5.3) |
| Brain surgery | 2 (2.6) |
| Gastroenterology | 2 (2.6) |
| Intensive care unit | 2 (2.6) |
| Dialysis | 1 (1.3) |
| Neurology | 1 (1.3) |
| Pediatrics | 1 (1.3) |
| Plastic surgery | 1 (1.3) |
| Urology | 1 (1.3) |
| Total | 76 (100) |

Table IV
Distribution of MRSA isolates according to the sample source.

| Sample source | n (%) |
|---|---|
| Abscess-wound | 19 (25.0) |
| Blood | 17 (22.4) |
| Nasal swab | 13 (17.1) |
| Tracheal aspirate | 13 (17.1) |
| Sputum | 5 (6.6) |
| Urine | 4 (5.3) |
| Catheter tip | 3 (3.9) |
| Bronchioalveolar lavage | 1 (1.3) |
| Urethral swab | 1 (1.3) |
| Total | 76 (100) |

**Confirmation of MRSA isolates.** Seventy-six isolates that were found to be non-susceptible to cefoxitin in the disc diffusion assay were verified to be MRSA with the amplification of the *mecA* gene via single-target PCR. The presence of the *mecA* gene is demonstrated in Fig. 1.

**Detection of virulence determinants.** Among the investigated virulence genes, the α-toxin encoding gene (*hla*) was found in 97.3% (n = 74/76) of the isolates and it was the most frequently virulence gene detected. Among the MRSA isolates, the frequencies of exfoliative toxin A, B, D and TSST-1 encoding genes (*eta*, *etb*, *etd*, *tst*) were 2.63% (n = 2/76), 1.3%, (n = 1/76), 0%, and 2.63% (n = 2/76), respectively.

## Discussion

MRSA represents a significant public health threat, particularly in developing countries owing to its ability to lead to life-threatening infections (Li et al. 2021; Pannewick et al. 2021). Regarding MRSA-induced infections and their burden in healthcare, studies focusing on regional epidemiology have demonstrated significant differences among regions (Gagliotti et al. 2021; Tsuzuki et al. 2021). For the first time, our present study pro-

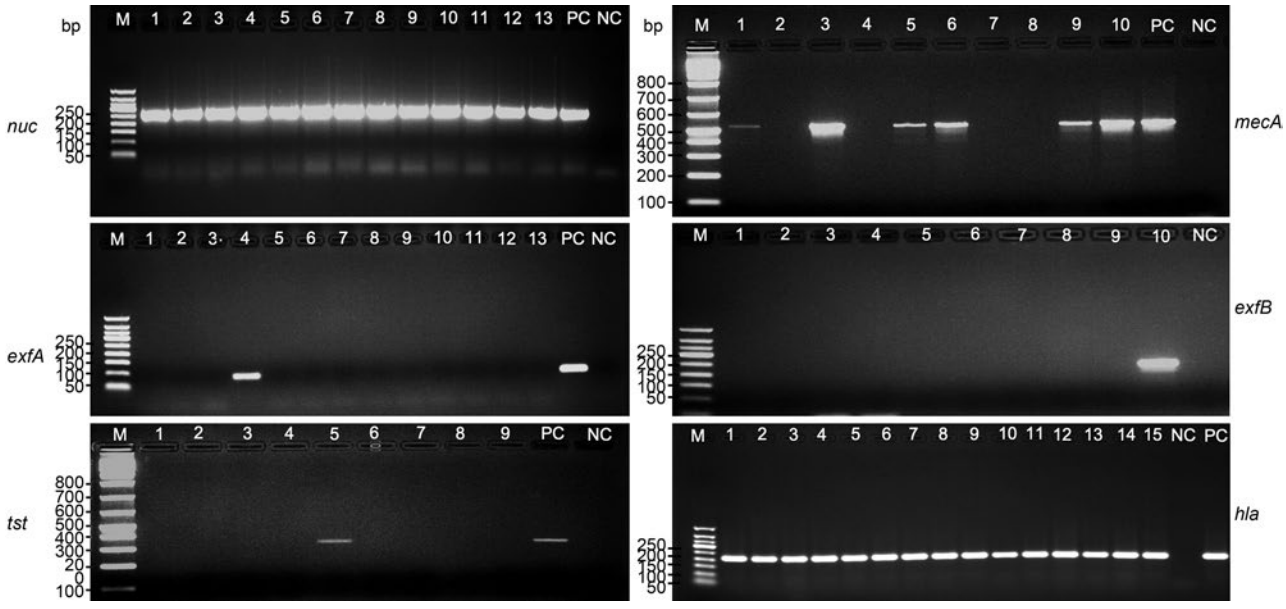


Fig. 1. Molecular detection of the *nuc*, *mecA*, *exfA*, *exfB*, *tst* and *hla* genes by single target PCR.
PC – positive control, NC – negative control, M – 100 bp DNA ladder (Hibrigen) for *mecA* (533 bp) and *tst* (326 bp), 50 bp DNA ladder (Hibrigen) for *nuc* (270 bp), *exfA* (93 bp), *exfB* 226 bp) and *hla* (209 bp), bp – base pairs

vides insights into multiple virulence characteristics of *S. aureus* from clinical specimens in Northern Cyprus.

In the current study, at a trend analysis level, although the gender of the patients had no statistical association with the detection of MRSA, the isolation rate was markedly higher in males. MRSA infections occur less frequently in patients below 45 years of age. Both age and gender-related trends observed in this study were similar to those previously investigated by others (Pomorska-Wesołowska et al. 2017; Thorlacius-Ussing et al. 2019). The isolation frequency of MRSA was highest in wounds and abscesses (25%; n = 19/76) and blood samples (22%; n = 17/76). These findings reinforce the association of skin and soft tissue infections (SSTIs) as a predisposing factor to *S. aureus* bacteremia (Jorgensen et al. 2019; Horino and Hori 2020).

The effects of *S. aureus* virulome on the progression of infections have been broadly investigated (Lebughe et al. 2017; Park et al. 2019). While virulence genes can play an important role in the pathogenicity of *S. aureus*, the circulation of these genes may vary among strains. Therefore, defining the distribution of virulence-associated genes is invaluable for the epidemiological control of *S. aureus.* The *hla* gene was detected in 97% of MRSA strains and had the highest frequency of all genes among the virulence factors investigated. This finding is comparable to another study in China in which authors reported that 98.7% (n = 224/227) of the *S. aureus* isolates were *hla*-positive (Li et al. 2019). In a separate investigation conducted in Iraq in 2020, *S. aureus* strains isolated from Syrian and Iraqi refugees were screened, and the *hla* gene was found in 93.4% (n = 117/125) of the Iraqi community. In contrast, the frequency of *hla* positivity was 71.4% (n = 89/125) in the Syrian refugee group (Rasheed and Hussein 2020). Alpha-hemolysin is by far the most well studied among the *S. aureus* cytotoxins, as it is produced by many strains and is toxic to a broad spectrum of mammalian cells.

Exfoliative toxins secreted by *S. aureus* are essential virulence factors of the bacterium. In our study *eta* was detected in 3% (n = 2) and *etb* in 1.5% (n = 1) of the isolates, whereas *etd* was not detected among the isolates tested. Our study results differed from those obtained by Mohseni et al. in 2018, in which a high frequency of *eta* (76.7%), *etb* (16.7%), and *etd* (54%) in *S. aureus* clinical isolates was observed. These findings contrast with a previous study in Korea on staphylococcal scalded skin syndrome patient-derived strains, which reported 53.8% of MRSA isolates to be *etb*-positive (Choi et al. 2021). According to the literature, *eta* is more common in Europe, Africa, and North America, contributing to over 80% of exfoliative toxin-producing strains, whereas *etb* is more common in Japan (Mariutti et al. 2017).

Toxic shock syndrome (TSS) manifests as either non-menstrual or menstrual-associated infection. However, cases of menstrual TSS are rarely seen (0.03–0.5/ 100.000), although the strains producing the toxin are often reported (Tong et al. 2015; Berger et al. 2019). It is suggests that the production of the toxin is under tight control (Tuffs et al. 2019). Only 3% (n = 2) of the isolates investigated in this study harbored the *tst* gene. In other studies, the prevalence of the toxin among the strains was found to be between 14% and 36.8% (Papadimitriou-Olivgeris et al. 2017; Shahini Shams-Abadi et al. 2018; Zhao et al. 2019; Abbasi Montazeri et al. 2021).

In this study, we gained insights into the prevalence of toxin genes among *S. aureus* clinical isolates. We also identified that the elderly and inpatient population were at high risk of developing an MRSA infection. These findings are invaluable for the genetic characterization of bacterial isolates circulating in Northern Cyprus and call our attention to the need for regular surveillance of MRSA epidemiology. In-depth studies covering the clonal diversity of MRSA strains and the correlation of antimicrobial resistance and toxin gene profiles with specific clones have highlighted these features as variables driving the complex epidemiology of this pathogen (Peterson et al. 2019; Maalej et al. 2019). The recent development of rapid diagnostic technologies contributes to the fast and reliable identification of infectious pathogens. For example, integrated sensing platforms using microfluidics technology and mass spectrometry techniques such as MALDI-TOF have significantly increased the rate of detection of MRSA in clinical samples (Schulz et al. 2020; Zhou et al. 2021). Concurrently, novel therapeutic approaches such as antivirulence drugs and phage therapy are being developed and hold promise for tackling antimicrobial resistance (He et al. 2021; Chang et al. 2022; Naorem et al. 2022).

## Conclusion

The data presented indicate that while most strains carry the alpha-toxin gene, the frequency of *tst*, *eta*, *etb,* and *etd* genes were considerably low in the strains circulating at the main hospital in this region. Our results provide new epidemiological data of *S. aureus* strains in this region.

## Limitations

This work represents a preliminary study with a limited sample size from a single center; therefore the data is not representative of isolates in all hospitals across Cyprus. Additional analyses with a higher number of isolates are required to identify the overall frequency of virulence determinants. Another limitation of the study was the absence of measurements of expression levels of the virulence factors at gene and protein levels.

**ORCID**
Buket Baddal https://orcid.org/0000-0003-3319-2179

**Acknowledgments**
The authors are thankful to the Near East University Hospital Microbiology Laboratory members for their assistance with the collection of specimens.

**Conflict of interest**
The authors do not report any financial or personal connections with other persons or organizations, which might negatively affect the contents of this publication and/or claim authorship rights to this publication.

## Literature

**Abbasi Montazeri E, Khosravi AD, Khazaei S, Sabbagh A.** Prevalence of methicillin resistance and superantigenic toxins in *Staphylococcus aureus* strains isolated from patients with cancer. BMC Microbiol. 2021 Dec;21(1):262. https://doi.org/10.1186/s12866-021-02319-7

**Algammal AM, Hetta HF, Elkelish A, Alkhalifah DHH, Hozzein WN, Batiha GES, El Nahhas N, Mabrok MA.** Methicillin-resistant *Staphylococcus aureus* (MRSA): One health perspective approach to the bacterium epidemiology, virulence factors, antibiotic-resistance, and zoonotic impact. Infect Drug Resist. 2020 Sep; 13:3255–3265. https://doi.org/10.2147/IDR.S272733

**Amin DHM, Guler E, Baddal B.** Prevalence of Panton-Valentine leukocidin in methicillin-resistant *Staphylococcus aureus* clinical isolates at a university hospital in Northern Cyprus: A pilot study. BMC Res Notes. 2020 Oct 20;13(1):490. https://doi.org/10.1186/s13104-020-05339-0

**Barbosa C, Nogueira S, Gadanho M, Chaves S.** Chapter 7 – DNA extraction: finding the most suitable method. In: Cook N, D'Agostino M, Thompson KC, editors. Molecular microbial diagnostic methods. San Diego (USA): Academic Press; 2016. p. 135–154. https://doi.org/10.1016/B978-0-12-416999-9.00007-1

**Barcudi D, Sosa EJ, Lamberghini R, Garnero A, Tosoroni D, Decca L, Gonzalez L, Kuyuk MA, Lopez T, Herrero I, et al.; Study Group of S. aureus in Córdoba, Argentina.** MRSA dynamic circulation between the community and the hospital setting: new insights from a cohort study. J Infect. 2020 Jan;80(1):24–37. https://doi.org/10.1016/j.jinf.2019.10.001

**Berger S, Kunerl A, Wasmuth S, Tierno P, Wagner K, Brügger J.** Menstrual toxic shock syndrome: Case report and systematic review of the literature. Lancet Infect Dis. 2019 Sep;19(9):e313–e321. https://doi.org/10.1016/S1473-3099(19)30041-6

**Bispo PJM, Ung L, Chodosh J, Gilmore MS.** Hospital-associated multidrug-resistant MRSA lineages are trophic to the ocular surface and cause severe microbial keratitis. Front Public Health. 2020 Jun 3;8:204. https://doi.org/10.3389/fpubh.2020.00204

**Chang RYK, Nang SC, Chan HK, Li J.** Novel antimicrobial agents for combating antibiotic-resistant bacteria. Adv Drug Deliv Rev. 2022 Aug;187:114378. https://doi.org/10.1016/j.addr.2022.114378

**Choi JH, Lee H, Choi EH.** Antimicrobial resistance and molecular analysis of *Staphylococcus aureus* in staphylococcal scalded skin syndrome among children in Korea. J Korean Med Sci. 2021;36(3):e22. https://doi.org/10.3346/jkms.2021.36.e22

**EUCAST.** Antimicrobial susceptibility testing EUCAST disk diffusion method. Version 8.0 January 2020. Basel (Switzerland): The European Committee on Antimicrobial Susceptibility Testing; 2020 [cited 2022 Apr 8]. Available from https://www.eucast.org/fileadmin/src/media/PDFs/EUCAST_files/Disk_test_documents/2020_manuals/Manual_v_8.0_EUCAST_Disk_Test_2020.pdf

**Gagliotti C, Högberg LD, Billström H, Eckmanns T, Giske CG, Heuer OE, Jarlier V, Kahlmeter G, Lo Fo Wong D, Monen J, et al.; EARS-Net study group participants.** *Staphylococcus aureus* bloodstream infections: diverging trends of meticillin-resistant and meticillin-susceptible isolates, EU/EEA, 2005 to 2018. Euro Surveill. 2021 Nov 18;26(46):2002094. https://doi.org/10.2807/1560-7917.ES.2021.26.46.2002094

**He S, Deng Q, Liang B, Yu F, Yu X, Guo D, Liu X, Dong H.** Suppressing alpha-hemolysin as potential target to screen of flavonoids to combat bacterial coinfection. Molecules. 2021 Dec 14;26(24):7577. https://doi.org/10.3390/molecules26247577

**Horino T, Hori S.** Metastatic infection during *Staphylococcus aureus* bacteremia. J Infect Chemother. 2020 Feb;26(2):162–169. https://doi.org/10.1016/j.jiac.2019.10.003

**Jernigan JA, Hatfield KM, Wolford H, Nelson RE, Olubajo B, Reddy SC, McCarthy N, Paul P, McDonald LC, Kallen A, et al.** Multidrug-resistant bacterial infections in U.S. hospitalized patients, 2012–2017. N Engl J Med. 2020 Apr 02;382(14):1309–1319. https://doi.org/10.1056/NEJMoa1914433

**Jorgensen SCJ, Lagnf AM, Bhatia S, Singh NB, Shammout LK, Davis SL, Rybak MJ.** Diagnostic stewardship: A clinical decision rule for blood cultures in community-onset methicillin-resistant *Staphylococcus aureus* (MRSA) skin and soft tissue infections. Infect Dis Ther. 2019 Jun;8(2):229–242. https://doi.org/10.1007/s40121-019-0238-1

**Junnila J, Hirvioja T, Rintala E, Auranen K, Rantakokko-Jalava K, Silvola J, Lindholm L, Gröndahl-Yli-Hannuksela K, Marttila H, Vuopio J.** Changing epidemiology of methicillin-resistant *Staphylococcus aureus* in a low endemicity area – new challenges for MRSA control. Eur J Clin Microbiol Infect Dis. 2020 Dec;39(12):2299–2307. https://doi.org/10.1007/s10096-020-03824-9

**Kot B, Wierzchowska K, Piechota M, Gruzewska A.** Antimicrobial resistance patterns in methicillin-resistant *Staphylococcus aureus* from patients hospitalized during 2015-2017 in hospitals in Poland. Med Princ Pract. 2020;29(1):61–68. https://doi.org/10.1159/000501788

**Kourtis AP, Hatfield K, Baggs J, Mu Y, See I, Epson E, Nadle J, Kainer MA, Dumyati G, Petit S, et al.; Emerging Infections Program MRSA author group.** *Vital Signs:* Epidemiology and recent trends in methicillin-resistant and in methicillin-susceptible *Staphylococcus aureus* bloodstream infections – United States. MMWR Morb Mortal Wkly Rep. 2019 Mar 08;68(9):214–219. https://doi.org/10.15585/mmwr.mm6809e1

**Lebughe M, Phaku P, Niemann S, Mumba D, Peters G, Muyembe-Tamfum JJ, Mellmann A, Strauß L, Schaumburg F.** The impact of the *Staphylococcus aureus* virulome on infection in a developing country: A cohort study. Front Microbiol. 2017 Aug 29;8(AUG):1662. https://doi.org/10.3389/fmicb.2017.01662

**Li X, Huang T, Xu K, Li C, Li Y.** Molecular characteristics and virulence gene profiles of *Staphylococcus aureus* isolates in Hainan, China. BMC Infect Dis. 2019 Dec;19(1):873. https://doi.org/10.1186/s12879-019-4547-5

**Li Z, Zhuang H, Wang G, Wang H, Dong Y.** Prevalence, predictors, and mortality of bloodstream infections due to methicillin-resistant *Staphylococcus aureus* in patients with malignancy: Systemic review and meta-analysis. BMC Infect Dis. 2021 Dec;21(1):74. https://doi.org/10.1186/s12879-021-05763-y

**Liu B, Sun H, Pan Y, Zhai Y, Cai T, Yuan X, Gao Y, He D, Liu J, Yuan L, et al.** Prevalence, resistance pattern, and molecular characterization of *Staphylococcus aureus* isolates from healthy animals and sick populations in Henan Province, China. Gut Pathog. 2018 Jul 17;10(1):31. https://doi.org/10.1186/s13099-018-0254-9

**Lu H, Zhao L, Si Y, Jian Y, Wang Y, Li T, Dai Y, Huang Q, Ma X, He L, et al.** The surge of hypervirulent ST398 MRSA lineage with

higher biofilm-forming ability is a critical threat to clinics. Front Microbiol. 2021 Mar 4;12(March):636788.
https://doi.org/10.3389/fmicb.2021.636788

**Maalej SM, Trabelsi JJ, Claude-alexandre G, Boutiba I, Mastouri M, Besbes S, Barguellil F, Laurent F, Hammami A.** Antimicrobial susceptibility and molecular epidemiology of methicillin-resistant *Staphylococcus aureus* in Tunisia: Results of a multicenter study. J Infect Dis Epidemiol. 2019 Mar 11;5(2):071.
https://doi.org/10.23937/2474-3658/1510071

**Mariutti RB, Tartaglia NR, Seyffert N, de Paula Castro T, Arni RK, Azevedo VA, Le Loir Y, Nishifuji K.** Exfoliative toxins of *Staphylococcus aureus*. In: Enany S, Alexander LEC, editors. The rise of virulence and antibiotic resistance in *Staphylococcus aureus*. London (UK): IntechOpen; 2017.
https://doi.org/10.5772/66528

**Mohseni M, Rafiei F, Ghaemi EA.** High frequency of exfoliative toxin genes among *Staphylococcus aureus* isolated from clinical specimens in the north of Iran: Alarm for the health of individuals under risk. Iran J Microbiol. 2018 Jun;10(3):158–165.

**Naorem RS, Pangabam BD, Bora SS, Goswami G, Barooah M, Hazarika DJ, Fekete C.** Identification of putative vaccine and drug targets against the methicillin-resistant *Staphylococcus aureus* by reverse vaccinology and subtractive genomics approaches. Molecules. 2022 Mar 24;27(7):2083.
https://doi.org/10.3390/molecules27072083

**Nisar S, Kirkpatrick LD, Shupp JW.** Bacterial virulence factors and their contribution to pathophysiology after thermal injury. Surg Infect (Larchmt). 2021 Feb;22(1):69–76.
https://doi.org/10.1089/sur.2020.188

**Okwu MU, Olley M, Akpoka AO, Izevbuwa OE.** Methicillin-resistant *Staphylococcus aureus* (MRSA) and anti-MRSA activities of extracts of some medicinal plants: A brief review. AIMS Microbiol. 2019 Apr 15;5(2):117–137.
https://doi.org/10.3934/microbiol.2019.2.117

**Pannewick B, Baier C, Schwab F, Vonberg RP.** Infection control measures in nosocomial MRSA outbreaks – Results of a systematic analysis. PLoS One. 2021 Apr 7;16(4):e0249837.
https://doi.org/10.1371/journal.pone.0249837

**Papadimitriou-Olivgeris M, Drougka E, Fligou F, Dodou V, Kolonitsiou F, Filos KS, Anastassiou ED, Petinaki E, Marangos M, Spiliopoulou I.** Spread of *Tst*-positive *Staphylococcus aureus* strains belonging to ST30 clone among patients and healthcare workers in two intensive care units. Toxins (Basel). 2017 Sep 4;9(9):270.
https://doi.org/10.3390/TOXINS9090270

**Park KH, Greenwood-Quaintance KE, Cunningham SA, Rajagopalan G, Chia N, Jeraldo PR, Mandrekar J, Patel R.** Lack of correlation of virulence gene profiles of *Staphylococcus aureus* bacteremia isolates with mortality. Microb Pathog. 2019 Aug;133:103543.
https://doi.org/10.1016/j.micpath.2019.103543

**Peterson JC, Durkee H, Miller D, Maestre-Mesa J, Arboleda A, Aguilar MC, Relhan N, Flynn HW Jr, Amescua G, Parel JM, et al.** Molecular epidemiology and resistance profiles among healthcare- and community-associated *Staphylococcus aureus* keratitis isolates. Infect Drug Resist. 2019 Apr;12:831–843.
https://doi.org/10.2147/IDR.S190245

**Pomorska-Wesołowska M, Różańska A, Natkaniec J, Gryglewska B, Szczypta A, Dzikowska M, Chmielarczyk A, Wójkowska-Mach J.** Longevity and gender as the risk factors of methicillin-resistant *Staphylococcus aureus* infections in southern Poland. BMC Geriatr. 2017 Dec;17(1):51.
https://doi.org/10.1186/s12877-017-0442-3

**Rahman MM, Amin KB, Rahman SMM, Khair A, Rahman M, Hossain A, Rahman AKMA, Parvez MS, Miura N, Alam MM.** Investigation of methicillin-resistant *Staphylococcus aureus* among clinical isolates from humans and animals by culture methods and multiplex PCR. BMC Vet Res. 2018 Oct 3;14(1):300.
https://doi.org/10.1186/s12917-018-1611-0

**Rasheed NA, Hussein NR.** Characterization of different virulent factors in methicillin-resistant *Staphylococcus aureus* isolates recovered from Iraqis and Syrian refugees in Duhok city, Iraq. PLoS One. 2020 Aug 17;15(8):e0237714.
https://doi.org/10.1371/journal.pone.0237714

**Schulz M, Calabrese S, Hausladen F, Wurm H, Drossart D, Stock K, Sobieraj AM, Eichenseher F, Loessner MJ, Schmelcher M, et al.** Point-of-care testing system for digital single cell detection of MRSA directly from nasal swabs. Lab Chip. 2020 Jul 14;20(14):2549–2561.
https://doi.org/10.1039/D0LC00294A

**Shahini Shams-Abadi M, Halaji M, Hoseini-Alfatemi SM, Gholipour A, Mojtahedi A, Sedigh Ebrahim-Saraie H.** Epidemiology of toxic shock syndrome toxin-1 harboring *Staphylococcus aureus* obtained from clinical samples in Iran: A systematic review and meta-analysis. Ann Ig. 2018 Sep–Oct;30(5):391–400.
https://doi.org/10.7416/ai.2018.2239

**Shettigar K, Murali TS.** Virulence factors and clonal diversity of *Staphylococcus aureus* in colonization and wound infection with emphasis on diabetic foot infection. Eur J Clin Microbiol Infect Dis. 2020 Dec;39(12):2235–2246.
https://doi.org/10.1007/s10096-020-03984-8

**Thorlacius-Ussing L, Sandholdt H, Larsen AR, Petersen A, Benfield T.** Age-dependent increase in incidence of *Staphylococcus aureus* bacteremia, Denmark, 2008–2015. Emerg Infect Dis. 2019 May;25(5):875–882. https://doi.org/10.3201/eid2505.181733

**Tong SYC, Davis JS, Eichenberger E, Holland TL, Fowler VG Jr.** *Staphylococcus aureus* infections: epidemiology, pathophysiology, clinical manifestations, and management. Clin Microbiol Rev. 2015 Jul;28(3):603–661. https://doi.org/10.1128/CMR.00134-14

**Tsuzuki S, Matsunaga N, Yahara K, Shibayama K, Sugai M, Ohmagari N.** Disease burden of bloodstream infections caused by antimicrobial-resistant bacteria: A population-level study, Japan, 2015–2018. Int J Infect Dis. 2021 Jul;108:119–124.
https://doi.org/10.1016/j.ijid.2021.05.018

**Tuffs SW, Herfst CA, Baroja ML, Podskalniy VA, DeJong EN, Coleman CEM, McCormick JK.** Regulation of toxic shock syndrome toxin-1 by the accessory gene regulator in *Staphylococcus aureus* is mediated by the repressor of toxins. Mol Microbiol. 2019 Oct;112(4):1163–1177. https://doi.org/10.1111/mmi.14353

**Turner NA, Sharma-Kuinkel BK, Maskarinec SA, Eichenberger EM, Shah PP, Carugati M, Holland TL, Fowler VG Jr.** Methicillin-resistant *Staphylococcus aureus*: An overview of basic and clinical research. Nat Rev Microbiol. 2019 Apr;17(4):203–218.
https://doi.org/10.1038/s41579-018-0147-4

**Uehara Y.** Current status of staphylococcal cassette chromosome *mec* (SCC*mec*). Antibiotics (Basel). 2022 Jan 11;11(1):86.
https://doi.org/10.3390/antibiotics11010086

**Urushibara N, Aung MS, Kawaguchiya M, Kobayashi N.** Novel staphylococcal cassette chromosome *mec* (SCC*mec*) type XIV (5A) and a truncated SCC*mec* element in SCC composite islands carrying *speG* in ST5 MRSA in Japan. J Antimicrob Chemother. 2020 Jan 1;75(1):46–50. https://doi.org/10.1093/jac/dkz406

**Zhao H, Xu S, Yang H, He C, Xu X, Hu F, Shu W, Gong F, Zhang C, Liu Q.** Molecular typing and variations in amount of *tst* gene expression of TSST-1-producing clinical *Staphylococcus aureus* isolates. Front Microbiol. 2019 Jun 19;10(JUN):1388.
https://doi.org/10.3389/fmicb.2019.01388

**Zhou W, Wu R, Duraiswamy S, Wang W, Zhu L, Wang Z.** Development of microfluidic cartridge for culture-free detection of *Staphylococcus aureus* in blood. J Micromech Microeng. 2021 May 01;31(5):055012. https://doi.org/10.1088/1361-6439/abf32f

ORIGINAL PAPER
Polish Journal of Microbiology
2022, Vol. 71, No 4, 499–507
https://doi.org/10.33073/pjm-2022-043

# Evaluation of Cell-Free DNA-Based Next-Generation Sequencing for Identifying Pathogens in Bacteremia Patients

CHAOQIN ZHANG[1, 2#], HANG CHENG[1, 2#], YUXI ZHAO[1, 2#], JINLIAN CHEN[1, 2#], MENG LI[3], ZHIJIAN YU[1, 2], XIANG SUN[1], PEIYU LI[1, 2], YONGPENG SHANG [1, 2], JINMIN MA[3*] and JINXIN ZHENG[1, 2*]

[1] Department of Infectious Diseases and the Key Lab of Endogenous Infection, Huazhong University of Science and Technology Union Shenzhen Hospital, Shenzhen, China
[2] Department of Infectious Diseases and the Key Lab of Endogenous Infection, Shenzhen Nanshan People's Hospital and the 6th Affiliated Hospital of Shenzhen University Health Science Center, Shenzhen, China
[3] BGI-Shenzhen, Shenzhen, China

Submitted 14 May 2022, accepted 30 August 2022, published online 12 November 2022

Abstract

Rapid detection of bloodstream pathogens would greatly facilitate clinicians to make precise antimicrobial treatment in patients with bacteremia. In this study, 114 plasma samples were collected from patients with identified or suspected bacteremia, and pathogens were detected by the conventional blood culture (BC) and cell-free DNA metagenomics next-generation sequencing (cfDNA mNGS). The present study indicated that 76% (38/50) of positive conventional blood culture ($BC^+$ group) patients were positively detected by cfDNA mNGS, and only 4% were mismatched between cfDNA mNGS and conventional bacteria culture. Pathogens in 32.8% of suspected bacteremia patients with negative conventional blood culture ($BC^-$ group) were determined accurately by cfDNA mNGS combined with analyzing the patients' clinical manifestations. *Escherichia coli* and *Klebsiella pneumoniae* were the most detected pathogens in identified bacteremia patients by cfDNA mNGS. 76.2% (16/21) of *E. coli* and 92.3% (12/13) of *K. pneumoniae* in bacteremia patients were identified by conventional blood cultures that were also detected by cfDNA mNGS. This study demonstrated that genomic coverage of *E. coli* and *K. pneumoniae* were more often detected in $BC^+$ group patients and genomic coverage of *Acinetobacter johnsonii* and *Paucibacter* sp. KCTC 42545 was more often detected in $BC^-$ group patients. In conclusion, cfDNA mNGS could rapidly and precisely provide an alternative detection method for the diagnosis of bacteremia.

K e y w o r d s: cell-free DNA, next-generation sequencing, bacteremia, blood culture, pathogens

## Introduction

Bacteremia can result in many serious diseases, such as sepsis, septic shock, and multi-organ failure (Laupland et al. 2004). Rapid detection of causative pathogens will be clinically helpful in optimizing accurate antimicrobial therapy in patients with suspected bacteremia. Conventional culture-based diagnostic procedures (e.g., blood cultures) currently remain the most reliable and clinically commonly used method for pathogens detection in patients with suspected bacteremia. However, the limitations of the conventional culture-based strategies for microbial tests in clinical practice have been widely discussed (e.g., it takes over 24 h to get results). Thus, several culture-independent molecular diagnostic procedures (such as polymerase chain reaction (PCR)-based techniques) have been introduced in clinics to identify the causative pathogens in patients with infectious diseases (Rutanga and Nyirahabimana 2016). Mounting evidence has demonstrated the diagnostic values of PCR-based techniques as additional tools to the conventional culture-based methods for identifying some known pathogens of patients with bacteremia and other infectious diseases (Blauwkamp et al. 2019).

# Chaoqin Zhang, Hang Cheng, Yuxi Zhao and Jinlian Chen contributed equally to this study.
* Corresponding authors: J. Ma, BGI-Shenzhen, Shenzhen, China; **email: majinmin@genomics.cn**
J. Zheng, Department of Infectious Diseases and the Key Lab of Endogenous Infection, Huazhong University of Science and Technology Union Shenzhen Hospital, Shenzhen, China; Department of Infectious Diseases and the Key Lab of Endogenous Infection, Shenzhen Nanshan People's Hospital and the 6th Affiliated Hospital of Shenzhen University Health Science Center, Shenzhen, China; **email: jinxinzheng@fudan.edu.cn**

Several recent studies have demonstrated the diagnostic values of cell-free DNA metagenomics next-generation sequencing (cfDNA mNGS) as a rapid and accurate method for identifying pathogens in patients with infectious diseases (Simner et al. 2018; Chiu and Miller 2019). The performance of the cfDNA mNGS for the identifying infectious microorganisms is based on the unbiased sequence analyses of the microbiome from the patient's plasma (human DNA is removed) (Grumaz et al. 2016; Long et al. 2016). The conventional bacterial culture methods are commonly used as a gold standard for identifying bloodstream pathogens in patients with suspected bacteremia. Comparing diagnostic values of cfDNA mNGS and the conventional culture-based methods is seldomly reported in suspected bacteremia patients. In this study, the clinical values of the cfDNA mNGS were compared with the conventional culture-based methods. Moreover, the utility of cfDNA mNGS in suspected bacteremia patients was further evaluated as an alternative detection method.

## Experimental

### Materials and Methods

**Patients and diagnostic standards.** One hundred fourteen patients hospitalized at the Huazhong University of Science and Technology Union Shenzhen Hospital (Shenzhen, China) between August 2017 and May 2020 were enrolled in this study. The pathogen detection was performed synchronically in the sera of all 114 patients by both the conventional blood culture and cfDNA mNGS. The clinical diagnosis of these patients was shown in Table SI, and they were divided into two groups with identified or suspected bacteremia. Identified bacteremia patients were defined as those with the clinical symptoms of bloodstream infection and positive conventional bacteria culture from the blood samples ($BC^+$ group). Suspected bacteremia patients were defined as those with the clinical symptoms of bloodstream infection and negative microbial detection in the conventional bacteria culture from the blood samples and other clinical specimens. The clinical symptoms of bloodstream infection mainly included as the following: 1) fevers with body temperatures > 38.0°C and recurrent chills; 2) clinical evidence of bacterial infection in some organs or systems; 3) no evidences of fever caused by non-infectious diseases. Suspected bacteremia patients were described as the $BC^-$ group in this study.

**The conventional blood culture method.** The conventional blood culture method was performed according to standard operations and incubated in the BD Bactec™ FX400 system (Becton Dickinson, USA). The bacterial species and antimicrobial susceptibility of blood culture positive samples were identified by the BD Phoenix™ M50 automated microbiology system (Becton Dickinson, USA).

**Plasma preparation and cfDNA mNGS performance.** Plasma samples were separated from the whole blood samples (before antibiotics were used) in EDTA anticoagulation blood collection tubes. The serum samples were collected from the whole blood samples in the tube without an anticoagulant. Plasma samples from five healthy volunteers were used as negative controls to calibrate and set detection thresholds. The cfDNA was extracted from 300 µl of plasma or serum using the TIANamp Micro DNA Kit (DP316, TIANGEN Biotech(Beijing)Co.,Ltd., China) according to the manufacturer's protocol. The nucleic acid concentration was measured using the Qubit dsDNA HS Assay Kit (Life Technologies, Invitrogen, China). Library construction and mNGS were performed according to the sequencing protocol (BGI, China). DNA library quality was assessed using an Agilent 2100 Bioanalyzer (Agilent Technologies, USA) combined with quantitative PCR to measure the adapters before sequencing. Qualified DNA libraries were prepared in a OneTouch system by emulsion PCR and then sequenced on the BGISEQ-100 or BGISEQ-50 sequencing platform (BGI, China).

**NGS data processing.** Raw data were preprocessed by removing short reads, low-quality reads, and sequencing adapters to generate clean reads. Raw data generated from the BGISEQ-50 sequencing platform were filtered using SOAPnuke software (version:1.5.6, BGI, China, https://github.com/BGI-flexlab/SOAPnuke), which included removing reads in which at least 30% of the total reads had quality scores < 20, a proportion of unknown nucleotides > 2%, and less than 50 bp, and trimming adapters sequences. For raw data generated from the BGISEQ-100 sequencing platform, reads with less than 50 bp were discarded, and those with average quality scores of < 10 per 15 window lengths and sequencing adapters were trimmed. The alignment and analysis of the cfDNA reads by mNGS were performed according to the previous reports (Altschul et al. 1990; Wood and Salzberg 2014). Reads were normalized per 20 million mapped reads according to the clean reads as the relative abundance. Species with detection rates > 0.8 and sample standard deviations > 0.6 were retained. The ratio of the relative bacterial abundance in each sample was calculated and placed in descending order. Criteria for a positive cfDNA mNGS result were as per Miao and coworkers (Miao et al. 2018). Consistency between the microbial species identified by cfDNA mNGS and the BC results combined with clinical manifestations was evaluated. For $mNGS^+/BC^-$ samples, whether the pathogen results were reliable after the combined analysis with clinical symptoms was assessed by three clinicians.

**Statistical analysis.** Data were analyzed using R software, version 3.5.0. A chi-square test was used to compare the prevalence of each species and their resistance and virulence genes between positive and negative BC samples. $p < 0.05$ was considered statistically significant. The Wilcoxon rank-sum test was used to calculate differences in the relative abundances of the resistance and virulence genes between positive and negative BC samples, with $p < 0.05$.

## Results

**Clinical information and cfDNA quantification from bacteremia patients' plasma or serum samples.** The microbes-derivative read numbers of the cfDNA extracted from bacteremia patients' plasma and serum samples were compared. It suggested that more microbes-derivative read numbers could be detected in plasma compared to serum ones. It demonstrated that the plasma was more suitable for detecting cfDNA mNGS (Fig. 1a). Subsequently, 114 patients were divided into two groups according to the blood culture results and the criteria described above. Fifty patients were diagnosed with bacteremia ($BC^+$ group) and 64 with suspected bacteremia ($BC^-$ group), and the diagnostic value of cfDNA mNGS in these groups was evaluated. The total cfDNA read numbers/concentrations (copies/ml) by cfDNA mNGS were significantly higher in the plasma samples of the $BC^+$ group compared with the $BC^-$ group (Fig. 1b). The microbes-derivative cfDNA reads/total cfDNA reads showed no significant differences between these two groups (Fig. 1c).

Table I
Comparison of the consistency of the pathogen identification between cfDNA mNGS and BC.

| | cfDNA mNGS$^+$ | cfDNA mNGS$^-$ | Consistency |
|---|---|---|---|
| $BC^+$ | 38 | 12 | 36[a] |
| $BC^-$ | 26 | 38 | 21[b] |
| Total | 64 | 50 | |

BC – blood culture, cfDNA mNGS – cell-free DNA metagenomics next-generation sequencing, [a] – consistency between the microbial species identified by cfDNA mNGS and the BC results, [b] – for $NGS^+/BC^-$ samples, whether the pathogen results were reliable after the combined analysis with clinical symptoms were assessed by three clinicians

**Comparison of the diagnostic value between the conventional blood culture and cfDNA mNGS.** The diagnostic values of pathogen detection by cfDNA mNGS and conventional blood culture were compared and are presented in Table I. In this study, 76% of the $BC^+$ group (38/50) were positively recognized by cfDNA mNGS, indicating that 72% (36/50) were consistent with the BC results, and only two cases were mismatched between these two methods. Moreover, among the 64 cfDNA $mNGS^+$ samples, 26 were $BC^-$, and 80.7% (21/26) of cfDNA $mNGS^+/BC^-$ samples were consistent with the clinical manifestation. This observation indicated that the pathogens in $BC^-$ samples were reliable determined by cfDNA mNGS. Thus, to promise

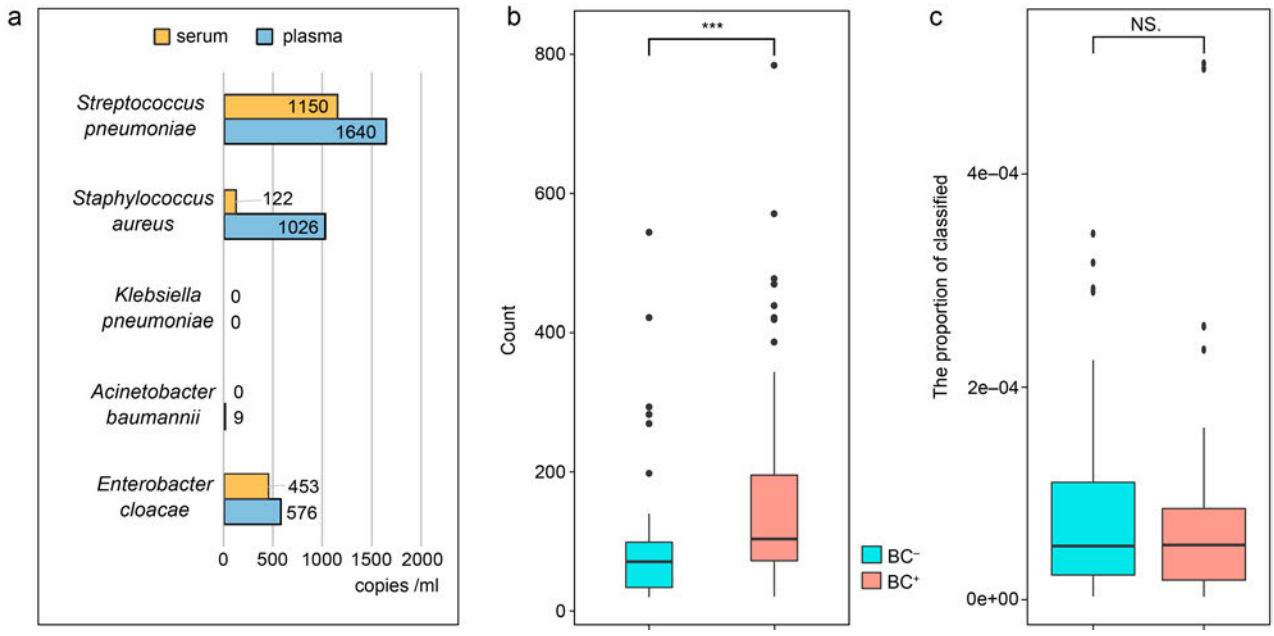


Fig. 1. a) Comparison of cfDNA reads number/concentrations (copies/ml) of pathogens by cfDNA mNGS between plasma and serum; b) comparison of cfDNA read numbers/concentrations (copies/ml) between $BC^+$ and $BC^-$; c) comparison of the microbes-derivative cfDNA reads/total cfDNA reads between $BC^+$ and $BC^-$ patients.

*** – $p < 0.001$, NS – not significant, BC – blood culture, cfDNA mNGS – cell-free DNA metagenomics next-generation sequencing, $^+$ – positive, $^-$ – negative

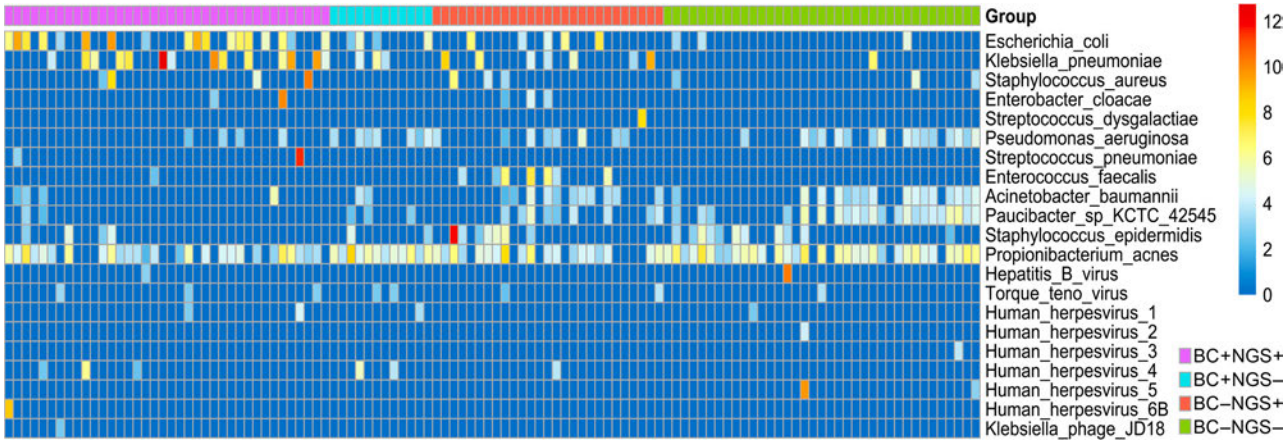


Fig. 2. The relative abundance of cfDNA mNGS-detected bacteria and viruses in the 114 samples were shown by Heatmap. The relative abundance data used in the heatmap were $\log_2$-transformed to compare among species. *Staphylococcus epidermidis* and *Propionibacterium acnes* were discarded as contaminants in the downstream analysis.

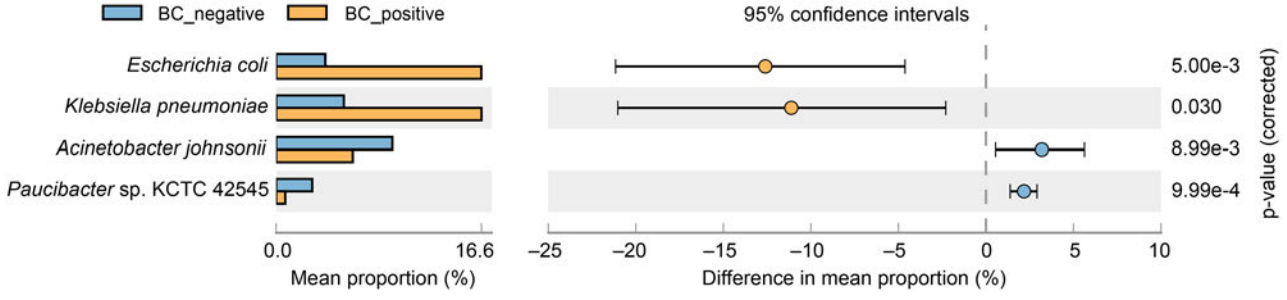


Fig. 3. Relative abundances of read numbers of microbial species between the BC$^+$ and BC$^-$ samples. Confidence intervals and *p*-values are indicated for each species, and the differences in proportions were calculated as the mean proportion of BC$^-$ minus BC$^+$ samples with 95% confidence intervals.

the accuracy of cfDNA mNGS results in BC$^-$ groups, performing analysis combined with the clinical manifestation is necessary.

In this study, *Escherichia coli* and *Klebsiella pneumoniae* were the most detected pathogens in identified bacteremia patients by cfDNA mNGS (Fig. 2). cfDNA mNGS detected 76.2% (16/21) of *E. coli* and 92.3% (12/13) of *K. pneumoniae* in the patients in whom the bacteriemia was detected by conventional blood culture (Table SII).

In addition to bacterial pathogens, cfDNA mNGS indicated that 54.39% of the blood samples (62/114) came from patients with coexisting viral infections (Table SIII). The Torque Teno virus (TTV) and human herpesvirus 4 (EBV) were the top two species detected in this study. EBV had a significantly higher detection rate in the BC$^+$ samples than in the BC$^-$ group. Notably, most viral read numbers were $<20$, and the relative abundance of the hepatitis B virus (HBV) in the BC$^-$ group was over 1,000, which nearly equaled the viral copy number determined by quantitative fluorescent PCR (Fig. 2).

**The genomic mapping of the microbes detected by cfDNA mNGS in BC$^+$ and BC$^-$ groups.** Furthermore, the whole genome of individual microbial species, such as *E. coli* and *K. pneumoniae* were mapped from the cfDNA reads detected by mNGS, and compared between the BC$^+$ and BC$^-$ groups. This study demonstrated that genomic coverage of *E. coli* and *K. pneumoniae* was most often detected in BC$^+$ group patients, and genomic coverage of *Acinetobacter johnsonii* and *Paucibacter* sp. KCTC 42545 was more often detected in BC$^-$ patients (Fig. 3).

Proteobacteria was the most common phylum in both BC$^+$ and BC$^-$ patients (Fig. 4a). Gammaproteobacteria had the highest relative abundance ratio at the class level, and was more abundant in the BC$^+$ patients ($p=0.03$), whereas Alphaproteobacteria ($p<0.001$) and Betaproteobacteria ($p<0.001$) were more abundant in the BC$^-$ samples (Fig. 4b). At the order level, Enterobacterales ($p<0.001$) was significantly abundant in the BC$^+$ samples, whereas Rhizobiales ($p=0.001$) and Pseudomonadales ($p=0.01$) were more abundant in the BC$^-$ samples. At the family level, *Enterobacteriaceae* ($p<0.001$) was significantly abundant in the BC$^+$ samples, whereas *Moraxellaceae* ($p=0.01$) and *Caulobacteraceae* ($p<0.001$) were more abundant in the BC$^-$ group. At the genus level, *Escherichia* ($p<0.001$) was relatively higher

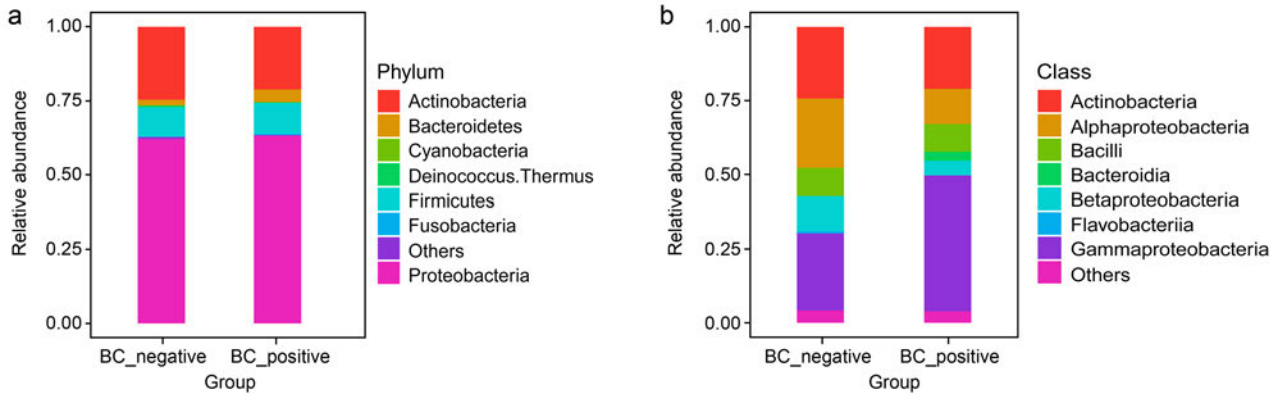


Fig. 4. Microbial compositions of the BC⁺ and BC⁻ samples.
a) At phylum level; b) at class level.

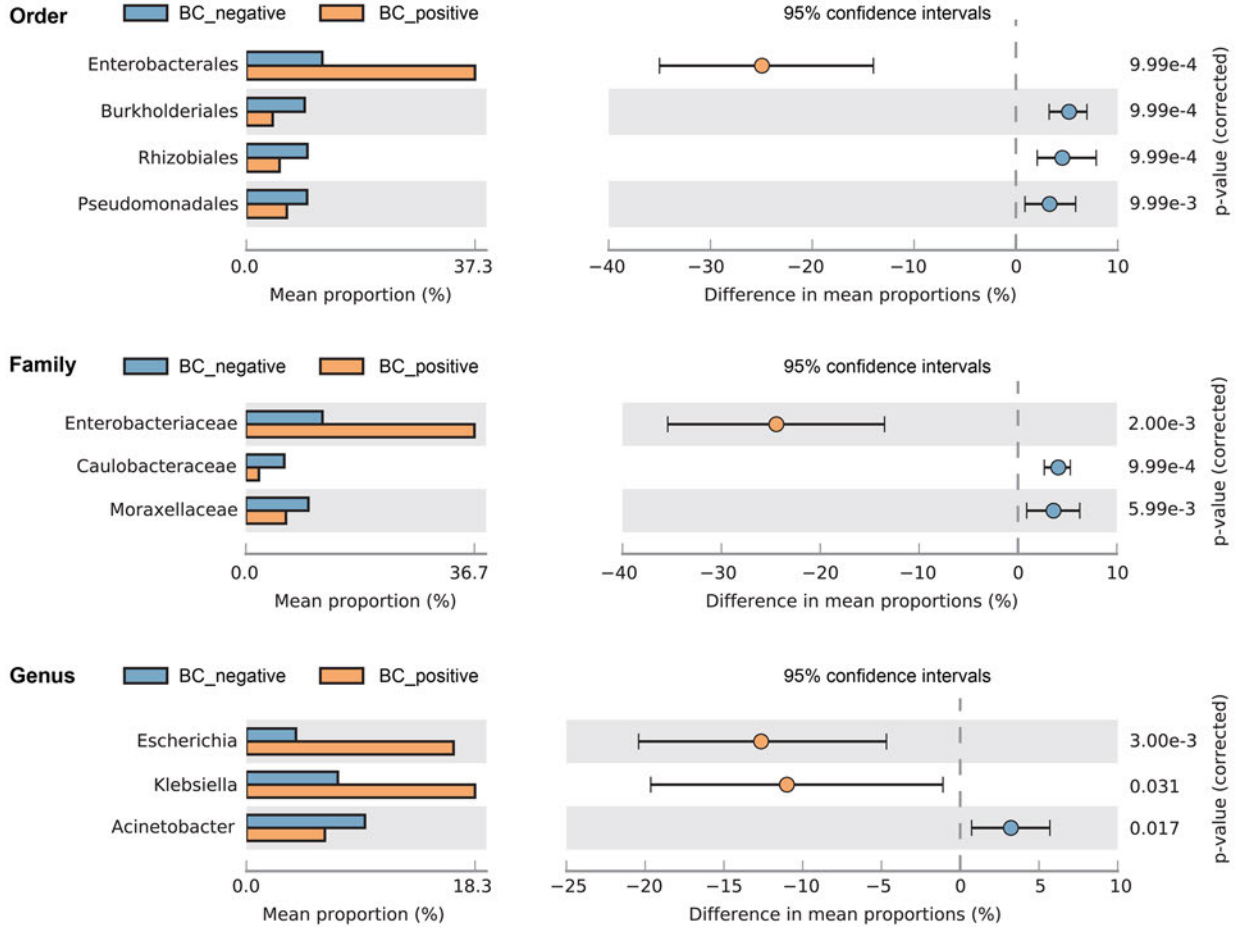


Fig. 5. Comparison of community compositions at the order, family and genus levels. Confidence intervals and *p*-values are indicated in each case, and the difference in proportions was calculated by the mean proportion of BC⁻ minus BC⁺ samples with 95% confidence intervals.
BC – blood culture, ⁺ – positive, ⁻ – negative

in the BC⁺ samples, whereas *Acinetobacter* ($p = 0.01$) was relatively higher in the BC⁻ samples (Fig. 5).

**Dynamics of microbial derivative cfDNA read numbers determined by mNGS during antibiotic treatment.** The read numbers of cfDNA from the plasma samples collected from three patients at different time points were analyzed to investigate the dynamic changes of the microbial derivative cfDNA read numbers during antimicrobial treatment (Fig. 6). In patients of A47 and A45, the cfDNA read numbers of *K. pneumoniae* and *E. coli* significantly decreased after of the effective antimicrobial treatment. It showed that

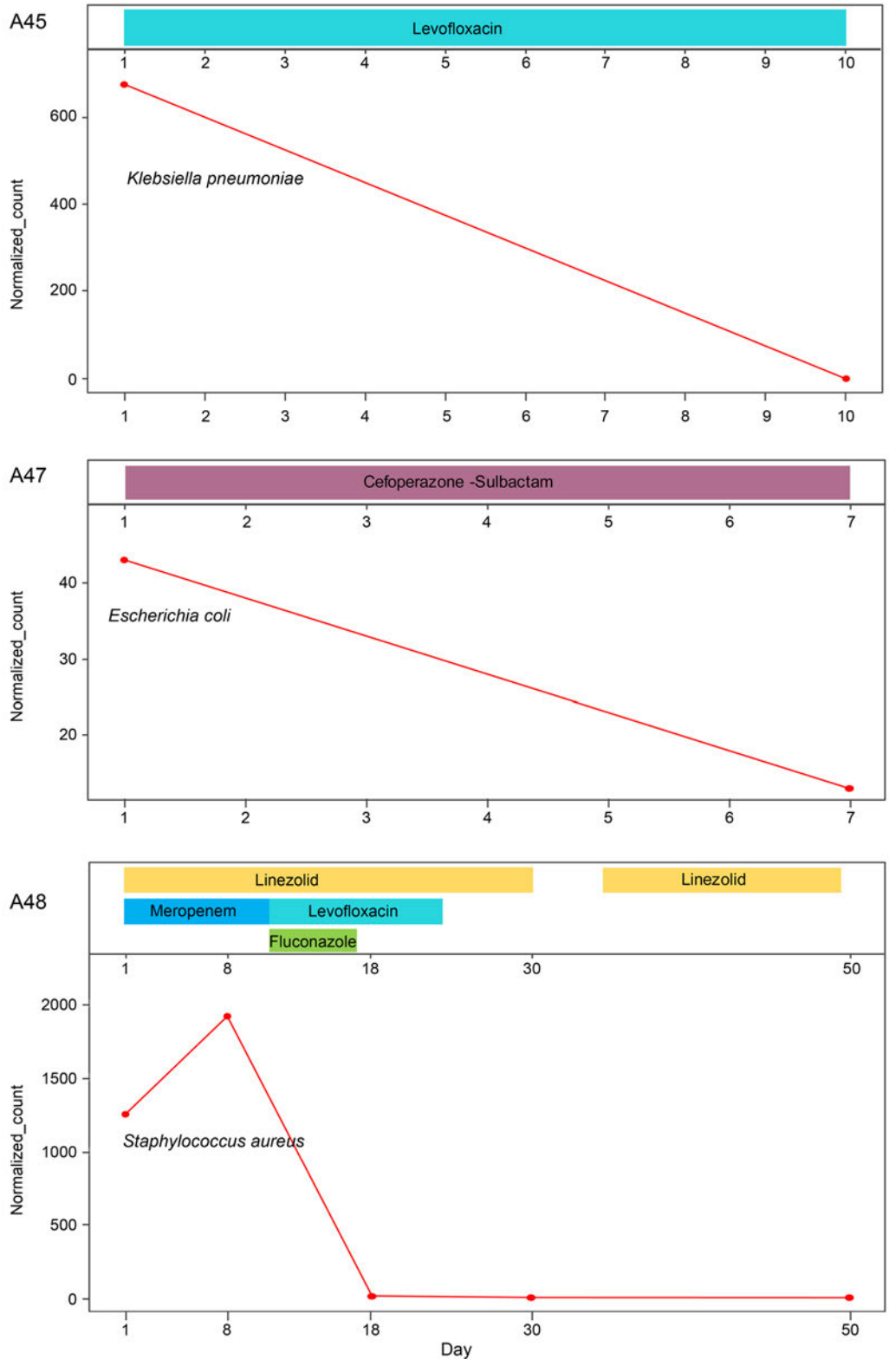


Fig. 6. Antibiotic treatments and relative pathogen abundances at different times after disease onset.

the dynamics of the bacterial read numbers in these two cases reflected the efficacy of the antibiotic treatment. However, the cfDNA read numbers of *Staphylococcus aureus* in patient A48 remained positive with a transient increase of cfDNA read number after eight days of antibiotic treatment with remission of clinical symptoms. Subsequently, with persistent antibiotic treatment, the *S. aureus* cfDNA read numbers decreased and became negative (Fig. 6). With the decrease of cfDNA read numbers, the fever symptoms gradually improved, and while blood cells, C-reactive protein, and procalcitonin were gradually reduced (Fig. 7).

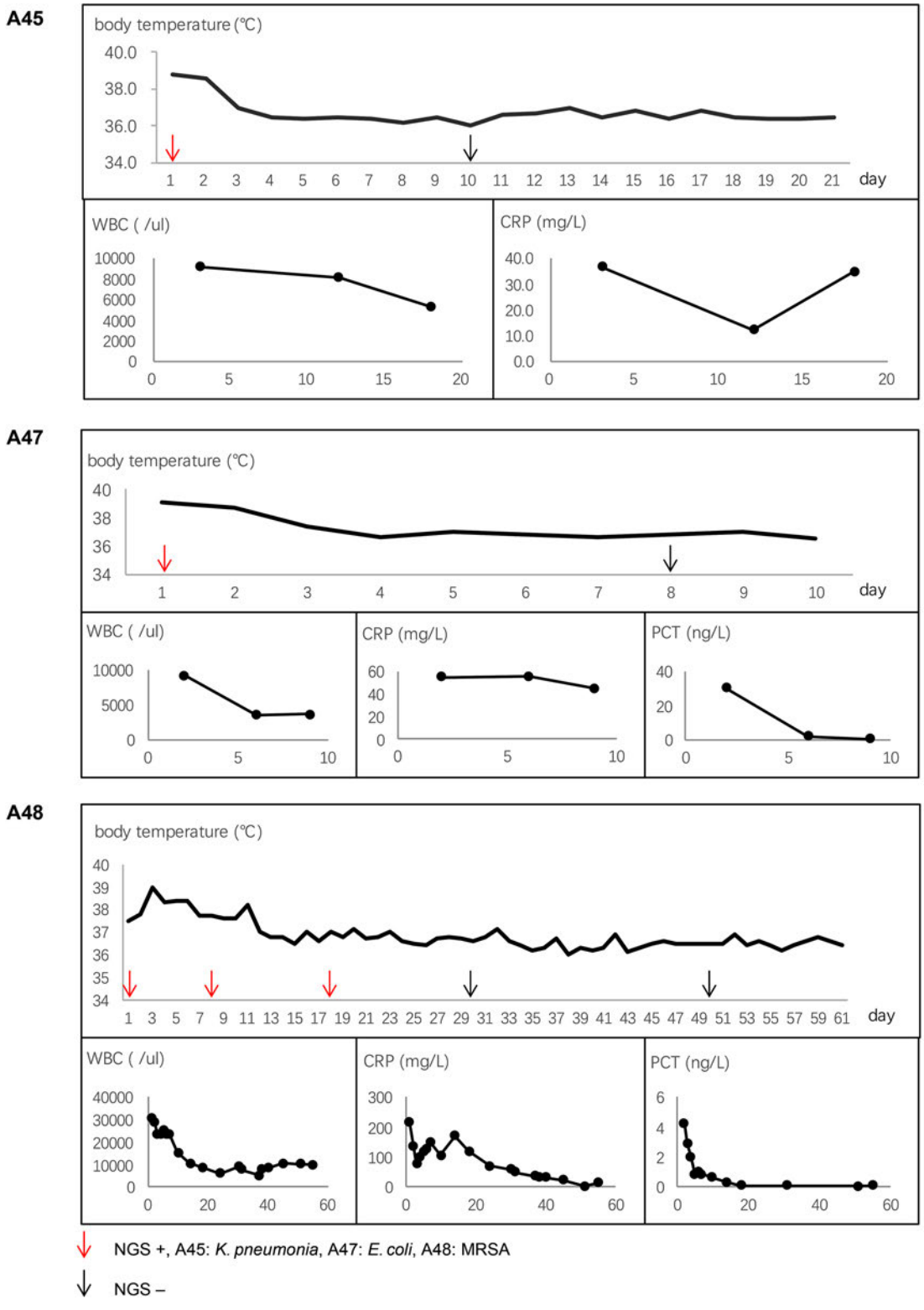


Fig. 7. Patient symptoms with antibiotic treatment.
WBC – white blood cells, CRP – C-reactive protein, PCT – procalcitonin, MRSA – methicillin-resistant *S. aureus*, NGS – cell-free DNA metagenomics next-generation sequencing

## Discussion

An ideal diagnostic test would enable the simultaneous detection and identification of pathogens from various clinical specimens, including rare or unculturable ones. cfDNA-based mNGS has been widely reported as a promising diagnostic tool for detecting microorganism from various clinical samples, such as bronchoalveolar lavage fluid and cerebrospinal fluid (Horiba et al. 2018; Miao et al. 2018; Miller et al. 2019). However, the

evaluation of the diagnostic values of cfDNA mNGS for microbial testing of bacteremia patients' blood samples has rarely been reported. Here, our data showed that cfDNA mNGS could detect pathogens in plasma samples independently of BC tests, demonstrating that 72% of the mNGS-positive samples were consistent with the gold standard approach of BC.

One of the most urgent needs in clinics is to evaluate the clinical significance of cfDNA mNGS for determining microbial species in the $BC^-$ group. i.e., patients with suspected bacteremia (Horiba et al. 2018). Our data indicated that cfDNA mNGS yielded accurate microbial results in 32.8% of the $BC^-$ group of patients with suspected bacteremia, supporting the future application of this approach in clinics. Although the cost of cfDNA NGS is five to six times that of conventional blood culture method, it takes only 24 hours from blood sample collection to NGS detection, bioinformatics analysis, and final results. Especially for those patients with severe bloodstream infections, it might be helpful to obtain a clinical prognosis in the shortest time and start timely anti-infection treatment.

Previous studies have indicated that herpes viruses (cytomegalovirus, Epstein-Barr virus, herpes simplex virus types 1, and human herpesviruse types 6), polyomaviruses (JC and BK), and an anellovirus (Torque Teno virus) are significant and commonly found in plasma samples of septic patients (Béland et al. 2014; Walton et al. 2014). Whether the increased propensity for infections with relatively weakly pathogenic organisms results from viral-mediated effects to impair immunity and whether viral reactivation occurs more readily in more profoundly immunosuppressed septic patients remains unknown. Applying cfDNA-based NGS may facilitate monitoring serum viral titers and identifying viral reactivation or flare in serum samples of patients with identified or suspected bacteremia. Therefore, discovering occult DNA viruses in host plasma samples may be an advantage in the future.

The antimicrobial susceptibility of traditional microbial culture depends on the microbial isolation and identification. Some molecular diagnostic methods, such as PCR, can both analyze the microbial species and determine the antimicrobial-resistance genes to provide the additional guidance for the antibiotic treatments (Gu et al. 2019). Previous researches have indicated that mNGS detection of clinical samples can reveal information about both the microbial species and the antimicrobial gene distribution, which can facilitate undertaking treatment choices for bacteremia patients (Grumaz et al. 2016; Horiba et al. 2018; Charalampous et al. 2019). In this study, blood culture results showed that these bacteria were not resistant to commonly used antibiotics, so we did not conduct in-depth analysis of resistance genes in cfDNA mNGS sequencing results. This study was probably limited by its single-center nature, and small number of patients. Thus, to some extent, it may affect the accuracy and reliability of the results.

## Conclusion

In conclusion, cfDNA mNGS may be an alternative detection method for pathogen identification in the patients with bacteremia. Applying cfDNA mNGS, especially combined with BC and clinical manifestation, can significantly enhance the detection rate and accuracy of cfDNA microbial detection in patients with bacteremia. High read numbers of microbial cfDNA will facilitate using cfDNA mNGS to determine the antimicrobial susceptibility and dynamical detection of the cfDNA-derivative microbial read numbers. The achieve the accurate diagnosis by cfDNA mNGS one should avoid the operational contamination and exclude the interference from the extra or occult microbial species. Additional clinical trials are needed to determine the sensitivity and specificity of this NGS method.

**ORCID**
Jinxin Zheng https://orcid.org/0000-0003-4064-2430

**Availability of data and material**

The raw whole-genome sequencing data was posted in the Sequence Read Archive (SRA) database under accession number PRJNA837746 (https://dataview.ncbi.nlm.nih.gov/object/ PRJNA837746).

**Ethical statement**

All procedures involving human participants were performed following the ethical standards of Huazhong University of Science and Technology Union Shenzhen Hospital and with the 1964 Helsinki Declaration and its later amendments or comparable ethical standards. As this study only involves the detection of patients' blood samples and does not carry out drug treatment, patients do not need to sign informed consent according to the requirements of the Ethics Committee of Huazhong University of Science and Technology Union Shenzhen Hospital.

**Acknowledgments**

The authors would like to thank these organizations for financial supports and the anonymous reviewers are acknowledged for their critical comments and suggestions which have considerably improved the manuscript.

**Author contributions**

CZ participated in the design of this study, collected strains, extracted cfDNA from plasma or serum, and drafted the manuscript. HC analyze the cfDNA mNGS data. YZ participated in the collection of strains and cfDNA mNGS test. JC participated in the collection of strains and extraction of cfDNA from plasma or serum. ML, ZY and XS participated in the design of this study, collected strains and analyze the cfDNA mNGS data. PL and YS collected clinical informa-

tion of patients and participated in the cfDNA mNGS test. JM and JZ designed the study, conducted the data analysis, and provided critical revisions of the manuscript for valuable intellectual content.

**Funding**

This work was supported by the Technology and Innovation Commission of Shenzhen Municipality of Key Funds (JCYJ20180302144721183; JCYJ20170412143551332) and Basic Research Funds (JCYJ20180302144345028; JCYJ20180302144403714) and National Key R&D Program of China O.2016YFE0205800, Science, Technology and Shenzhen Key Medical Discipline Construction Fund (No. SZXK06162).

**Conflict of interest**

The authors do not report any financial or personal connections with other persons or organizations, which might negatively affect the contents of this publication and/or claim authorship rights to this publication.

## Literature

**Altschul SF, Gish W, Miller W, Myers EW, Lipman DJ.** Basic local alignment search tool. J Mol Biol. 1990 Oct 5;215(3):403–410. https://www.doi.org/10.1016/S0022-2836(05)80360-2

**Béland K, Dore-Nguyen M, Gagné MJ, Patey N, Brassard J, Alvarez F, Halac U.** Torque Teno virus in children who underwent orthotopic liver transplantation: New insights about a common pathogen. J Infect Dis. 2014 Jan 15;209(2):247–254. https://www.doi.org/10.1093/infdis/jit423

**Blauwkamp TA, Thair S, Rosen MJ, Blair L, Lindner MS, Vilfan ID, Kawli T, Christians FC, Venkatasubrahmanyam S, Wall GD, et al.** Analytical and clinical validation of a microbial cell-free DNA sequencing test for infectious disease. Nat Microbiol. 2019 Apr;4(4):663–674. https://www.doi.org/10.1038/s41564-018-0349-6

**Charalampous T, Kay GL, Richardson H, Aydin A, Baldan R, Jeanes C, Rae D, Grundy S, Turner DJ, Wain J, et al.** Nanopore metagenomics enables rapid clinical diagnosis of bacterial lower respiratory infection. Nat Biotechnol. 2019 Jul;37(7):783–792. https://www.doi.org/10.1038/s41587-019-0156-5

**Chiu CY, Miller SA.** Clinical metagenomics. Nat Rev Genet. 2019 Jun;20(6):341–355. https://www.doi.org/10.1038/s41576-019-0113-7

**Grumaz S, Stevens P, Grumaz C, Decker SO, Weigand MA, Hofer S, Brenner T, von Haeseler A, Sohn K.** Next-generation sequencing diagnostics of bacteremia in septic patients. Genome Med. 2016 Jul 1;8(1):73. https://www.doi.org/10.1186/s13073-016-0326-8

**Gu W, Miller S, Chiu CY.** Clinical metagenomic next-generation sequencing for pathogen detection. Annu Rev Pathol. 2019 Jan 24;14:319–338. https://www.doi.org/10.1146/annurev-pathmechdis-012418-012751

**Horiba K, Kawada JI, Okuno Y, Tetsuka N, Suzuki T, Ando S, Kamiya Y, Torii Y, Yagi T, Takahashi Y, et al.** Comprehensive detection of pathogens in immunocompromised children with bloodstream infections by next-generation sequencing. Sci Rep. 2018 Feb 28;8(1):3784. https://www.doi.org/10.1038/s41598-018-22133-y

**Laupland KB, Gregson DB, Zygun DA, Doig CJ, Mortis G, Church DL.** Severe bloodstream infections: A population-based assessment. Crit Care Med. 2004 Apr;32(4):992–997. https://www.doi.org/10.1097/01.ccm.0000119424.31648.1e

**Long Y, Zhang Y, Gong Y, Sun R, Su L, Lin X, Shen A, Zhou J, Caiji Z, Wang X, et al.** Diagnosis of sepsis with cell-free DNA by next-generation sequencing technology in ICU patients. Arch Med Res. 2016 Jul;47(5):365–371. https://www.doi.org/10.1016/j.arcmed.2016.08.004

**Miao Q, Ma Y, Wang Q, Pan J, Zhang Y, Jin W, Yao Y, Su Y, Huang Y, Wang M, et al.** Microbiological diagnostic performance of metagenomic next-generation sequencing when applied to clinical practice. Clin Infect Dis. 2018 Nov 13;67(suppl_2):S231–S240. https://www.doi.org/10.1093/cid/ciy693

**Miller S, Naccache SN, Samayoa E, Messacar K, Arevalo S, Federman S, Stryke D, Pham E, Fung B, Bolosky WJ, et al.** Laboratory validation of a clinical metagenomic sequencing assay for pathogen detection in cerebrospinal fluid. Genome Res. 2019 May;29(5):831–842. https://www.doi.org/10.1101/gr.238170.118

**Rutanga JP, Nyirahabimana T.** Clinical significance of molecular diagnostic tools for bacterial bloodstream infections: A systematic review. Interdiscip Perspect Infect Dis. 2016;2016:6412085. https://www.doi.org/10.1155/2016/6412085

**Simner PJ, Miller S, Carroll KC.** Understanding the promises and hurdles of metagenomic next-generation sequencing as a diagnostic tool for infectious diseases. Clin Infect Dis. 2018 Feb 10;66(5):778–788. https://www.doi.org/10.1093/cid/cix881

**Walton AH, Muenzer JT, Rasche D, Boomer JS, Sato B, Brownstein BH, Pachot A, Brooks TL, Deych E, Shannon WD, et al.** Reactivation of multiple viruses in patients with sepsis. PLoS One. 2014 Jun 11;9(2):e98819. https://www.doi.org/10.1371/journal.pone.0098819

**Wood DE, Salzberg SL.** Kraken: ultrafast metagenomic sequence classification using exact alignments. Genome Biol. 2014 Mar 3;15(3):R46. https://www.doi.org/10.1186/gb-2014-15-3-r46

Supplementary materials are available on the journal's website.

ORIGINAL PAPER
Polish Journal of Microbiology
2022, Vol. 71, No 4, 509–518
https://doi.org/10.33073/pjm-2022-044

# Retrospective Analysis of the *Ureaplasma* spp. Prevalence with Reference to Other Genital Tract Infections in Women of Reproductive Age

KATARZYNA RAK[1], ANETA KIECKA[1], JOANNA BIAŁECKA[1], ANNA KAWALEC[2], PAWEŁ KRZYŚCIAK[3] and ANNA BIAŁECKA[1]

[1] Centre of Microbiological Research and Autovaccines, Cracow, Poland
[2] Department of Microbiology and Biomonitoring, University of Agriculture, Cracow, Poland
[3] Department of Infections Control and Mycology, Jagiellonian University Medical College, Cracow, Poland

Submitted 1 June 2022, accepted 11 September 2022, published online 20 November 2022

Abstract

*Ureaplasma* spp. are frequently isolated from the genital tract of women of reproductive age. To date, it remains unclear whether they are commensal or pathogenic. In our study, we assessed the prevalence of *Ureaplasma* spp. in a group of 1,155 women of childbearing age. In addition, we assessed how often women with positive *Ureaplasma* spp. develop genital tract co-infections and how the vaginal pH changes. This study showed a relationship between colonization by *Ureaplasma* spp. and presenting symptoms. In fact, we showed that colonization of the genital tract by *Ureaplasma* spp.


can affect the occurrence of co-infections such as *Gardnerella vaginalis*. We also observed a relationship between increased pH values and the presence of *Ureaplasma* spp.

K e y w o r d s: female genital tract microbiota, *Ureaplasma* spp., bacterial vaginosis, vaginal infections

## Introduction

The vaginal microbiota demonstrates its important role in the reproductive age women's health or disease. Many studies show that *Lactobacillus* spp. dominates the vaginal microbiota of healthy women (Ravel et al. 2011; Gajer et al. 2012; Kiecka et al. 2021). Due to *Lactobacillus* spp. colonization, a pH value up to 4 is maintained, and the binding of pathogenic microorganisms to vaginal epithelial cells is blocked. Bacteriocins, $H_2O_2$, and lactic acid produced by lactobacilli can inhibit the growth of different microorganisms (Aroutcheva et al. 2001; Vallor et al. 2001; Karaoğlu et al. 2003; Amabebe and Anumba 2018).

*Ureaplasma* spp. are frequently isolated from the genital tract of women at childbearing age (Leli et al. 2018). Based on nucleic acid amplification techniques (NAAT) *Ureaplasma urealyticum* species was split into *Ureaplasma parvum* and *U. urealyticum*. Despite the many studies conducted, it has not been resolved whether *Ureaplasma* spp. are pathogenic or commensal. Some authors describe *Ureaplasma* spp. as pathogenic in nongonococcal urethritis in men (NGU), pyelonephritis, endometritis (Kundsin et al. 1996; Dewan et al. 1997), and pregnancy complications (Horowitz et al. 1995; Abele-Horn et al. 1997; Harada et al. 2008) while others consider them commensal (Donders et al. 2017). These problems in determining their impact on women's health may be related to the design of a study and the diagnostic technique used: culture, serology, or polymerase chain reaction (PCR), among others.

The aim of this study was to assess the prevalence of *Ureaplasma* spp. colonization in a large group of women of childbearing age reporting to a microbiology laboratory for follow-up examinations or by presenting symptoms (itching, burning, discharge, pain, or discomfort). In addition, the objective was to determine the prevalence and co-occurrence of other microorganisms, both common components of the genital tract microbiota and pathogens.

* Corresponding author: K. Rak, Centre of Microbiological Research and Autovaccines, Cracow, Poland; **email: katarzyna.rak@cbm.com.pl**

## Experimental

### Materials and Methods

**Study population.** This study was a retrospective analysis of the populations of women aged 18 to 49 who had microbiological tests of the genital tract in the Microbiology and Autovaccine Research Center in Cracow, Poland, from April to August 2019, as recommended by a gynecologist. All included patients had to undergo a set of tests such as pH determination, microscopic examination of vaginal smear, microbial culture, and molecular testing for *Chlamydia trachomatis*, *Mycoplasma hominis*, *U. urealyticum*, *U. parvum*, *Mycoplasma genitalium*. Moreover, a thorough history of reported symptoms and previous antibiotic treatment were recorded. Women with a history of antibiotic treatment within the past two months were excluded from the study. Information on antibiotic treatment was obtained from the worksheets and referrals for examinations from attending physicians. The following patient data were used for analysis: age, symptoms--reported complaints, pH of vaginal contents, *Lactobacillus* presence or absence, presence of other bacteria, yeast-like fungi, and *Trichomonas vaginalis*.

The clinical signs divide the patients into symptomatic and asymptomatic groups. The group of symptomatic women included those who reported at least one symptom in the genital tract: itching, burning, discharge, pain, or discomfort. The asymptomatic group reported no such complaints.

**Microbiological methods.** The material for microbiological examination consisted of two vaginal swabs (one for Gram-staining microscopy and one for culture) and one cervical swab for molecular testing (NAAT). The vaginal fluid pH was measurand during sample collecting. All tests were performed at the Microbiology and Autovaccination Research Center in Cracow, Poland.

Swabs were taken from the posterior vaginal vault and endocervical canal using a sterile speculum. The vaginal content remaining on the speculum was used to measure the pH value using pH indicator strips with a pH range of 2.0–9.0 (MERCK, Germany). One vaginal swab was used for Gram staining with PREVI® Color Gram stainer (bioMerieux, France). The vaginal Gram stain smears were assessed using the scale according to Kuczyńska modified by Kasprowicz (Kasprowicz and Białecka 2012). The presence of leukocytes, lactobacilli, other bacteria, fungi, and clue cells was assessed based on an abundance scale ranging from 0 to 3 in oil-immersion microscope fields (× 1000). The degrees III, III/IV, and IV with clue cells detected indicated BV, which is comparable to a score from 7 to 10 according to Nugent criteria (Nugent et al. 1991; Kuczyńska 2003; Kasprowicz and Białecka, 2008). The specimen from the first vaginal swab was also inoculated in Trichomedium (GRASO, Poland). After 48 hours of culture, a direct preparation was made and viewed under a microscope (200 × magnification) to identify *T. vaginalis*.

The second vaginal swab was used to perform cultures on TSA with 5% sheep blood (GRASO, Poland) for the detection of aerobic bacteria, Gardnerella Agar (bioMerieux, France) for anaerobic bacteria, CANDIselect (BioRad, USA) for yeasts, and Chocolate Agar + P.V.S. + VCAT (BioRad, USA) for *Neisseria gonorrhoeae*. The media were incubated for 24 h or 48 h at 35°C under appropriate conditions. The cultured microorganisms were isolated and identified using VITEK2 (bioMerieux, France) or MALDI-TOF MS (Brucker, USA).

Material collected from the cervical swabs was preserved on UTM medium (Copan Italia, Italy) and tested for *C. trachomatis*, *M. hominis*, *U. urealyticum*, *U. parvum,* and *M. genitalium*. The DNA was isolated with croBEE 201A Nucleic Acid Extraction Kit (GeneProof, Czech Republic) with croBEE NA16 Nucleic Acid Extraction System (GeneProof, Czech Republic) according to the manufacturer's instructions. The NAAT was performed with a commercially available PCR – AmpliSens test, according to the manufacturer's instructions in a Cobas Z480 real-time thermocycler (ROCHE, Switzerland).

**Statistical analysis.** A language and environment for statistical computing R were used for statistical analysis (R Core Team 2022). The significance level was assumed at $p = 0.05$. The Chi-square test of independence, Fisher exact test (for qualitative features) and Mann-Whitney $U$ test (for quantitative features) were used to compare distributions of variables across two independent groups. The odds ratios [ORs] with 95% confidence intervals [CIs] were calculated with Firth's bias reduction method of logistic regression with the Wald test (Wang 2014, Heinze et al. 2022). The multivariable logistic regression model was built and evaluated to associate various independent factors, such as the presence of different microorganisms or the age of women, with clinical symptoms or elevated pH. The Akaike information criterion was extracted and based on this statistic best-suited (with minimal AIC), the most parsimonious models were selected from a collection of fitted models. Bearing in mind the possible coexistence of some microorganisms, we tested second-order interactions between them. Due to non-significant results, none of the interaction terms was incorporated into the final model.

## Results

**Study patients' population.** A total of 1,155 women aged from 18 to 49 years were included in the study. Seven hundred fifty-six women in the study group did not report symptoms, while 399 women presented symptoms.

Among 1,155 women, *Lactobacillus* spp. was found in vaginal swabs of 1,107 (95.8%) (single/few/numerous lactobacilli). The differences in the abundance of *Lactobacillus* spp. in the patients' group (n = 1,107) were analyzed; 964 women presented the vaginal smear with few or numerous lactobacilli, and 143 presented only single lactobacilli.

*Ureaplasma* spp. was detected in 274 women (23.7%). Aerobic bacteria were identified in 153 vaginal swabs (13.2%), and yeast-like fungi in 192 (16.6%). *Gardnerella vaginalis* was found in 56 specimens (4.8%) from patients with vaginosis. *M. hominis* (1.8%) and sexually transmitted pathogens *C. trachomatis* (0.7%) and *M. genitalium* (0.2%) were found rarely in the study group. *T. vaginalis* and *N. gonorrhoeae*, two other etiological agents of STI, were not identified in any specimen in this study. Complete data on genital tract microorganisms' prevalence are summarized in Table I.

The occurrence of urogenital mycoplasmas (*U. parvum, U. urealyticum,* and *M. hominis*) was analyzed regarding multiple colonization with these species and co-infection with *C. trachomatis* and *M. genitalium*. The overall incidence of urogenital mycoplasmas in this study group was 24.22%. Most patients (23.02%) presented single mycoplasma species in the genital tract. Both double (1.03%) and triple mycoplasma colonization (0.17%) and co-infections of urogenital mycoplasmas with *C. trachomatis* and *M. genitalium* (0.35%) were very rarely observed (Fig. 1).

**Urogenital microorganisms and symptoms.** Our data show that the presence of different microorganisms in the genital tract is associated with symptoms including itching, burning, discharge, pain, and discomfort. The results of univariable and multivariable logistic regression models are depicted in Table I and II, respectively.

Univariable analysis showed that women in whom *G. vaginalis* was isolated were more likely to report symptoms (OR = 8.32, 95% CI: 4.30–16.08). Women with identified *Ureaplasma* spp. were about four times more likely to be symptomatic (OR = 4.26, 95% CI: 3.21–5.66), and a similar trend was found for *C. trachomatis*, but the group of *C. trachomatis* positives

Table I
The prevalence of specific microorganisms across groups of women manifesting or not clinical symptoms.

| Microorganisms | Microbiological method | Total | Without symptoms (n = 756) | With symptoms (n = 399) | $p^*$ | OR*** (95% CI) | $p^{**}$ |
|---|---|---|---|---|---|---|---|
| | | n (%) | n (%) | n (%) | | | |
| *Lactobacillus* spp. | microscopic | 1,107 (95.8) | 737 (97.5) | 370 (92.7) | < 0.001 | 0.33 (0.18–0.60) | < 0.001 |
| *Gardnerella vaginalis* | microscopic, culture | 56 (4.8) | 11 (1.5) | 45 (11.3) | < 0.001 | 8.32 (4.30–16.08) | < 0.001 |
| *Ureaplasma* spp. | PCR | 276 (23.9) | 108 (14.3) | 166 (41.6) | < 0.001 | 4.26 (3.21–5.66) | < 0.001 |
| *Ureaplasma parvum* | PCR | 187 (16.2) | 81 (10.7) | 106 (26.6) | < 0.001 | 3.01 (2.19–4.14) | < 0.001 |
| *Ureaplasma urealyticum* | PCR | 89 (7.7) | 27 (3.6) | 62 (15.5) | < 0.001 | 4.91 (3.08–7.83) | < 0.001 |
| *Mycoplasma hominis* | PCR | 21 (1.8) | 0 (0.0) | 21 (5.3) | < 0.001# | 85.94 (5.19–1,422.62) | 0.002 |
| *Mycoplasma genitalium* | PCR | 2 (0.2) | 0 (0.0) | 2 (0.5) | 0.119# | 9.52 (0.46–198.69) | 0.146 |
| *Chlamydia trachomatis* | PCR | 8 (0.7) | 1 (0.1) | 7 (1.8) | 0.003# | 9.62 (1.66–55.79) | 0.012 |
| Aerobic bacteria (with GBS) | culture | 153 (13.2) | 95 (12.6) | 58 (14.5) | 0.396 | 1.19 (0.84–1.68) | 0.339 |
| *Streptococcus* group B (GBS) | culture | 88 (7.6) | 57 (7.5) | 31 (7.8) | 0.981 | 1.04 (0.66–1.63) | 0.865 |
| Yeast | microscopic, culture | 192 (16.6) | 100 (13.2) | 92 (23.1) | < 0.001 | 1.97 (1.44–2.69) | < 0.001 |
| *Neisseria gonorrhoeae* | culture | | – | – | – | – | – |
| *Trichomonas vaginalis* | culture | | – | – | – | – | – |

* – all *p*-values denoted by # are from Fisher's exact test; the remaining comparisons are made with the chi-square test of independence
** – *p*-values calculated by Wald method using Firth's logistic regression
*** – OR of prevalence symptoms in women with specific microorganisms detected when compared with those without symptoms

Table II
Association between the prevalence of microorganisms and clinical symptoms – multivariable analyses. The fully adjusted model and the most parsimonious model.

| Microorganisms | Model 1* | | Model 2** | |
|---|---|---|---|---|
| | OR*** (95% CI) | $p$** | OR*** (95% CI) | $p$** |
| *Ureaplasma parvum* | 3.06 (2.17–4.31) | < 0.001 | 3.07 (2.18–4.31) | < 0.001 |
| *Ureaplasma urealyticum* | 5.25 (3.20–8.62) | < 0.001 | 5.20 (3.17–8.51) | < 0.001 |
| *Mycoplasma hominis* | 49.30 (3.09–787.71) | 0.006 | 48.97 (2.94–815.88) | 0.007 |
| *Chlamydia trachomatis* | 10.03 (1.66–60.42) | 0.012 | 10.04 (1.66–60.66) | 0.012 |
| *Lactobacillus* spp. | 0.47 (0.23–0.98) | 0.045 | 0.48 (0.24–0.94) | 0.033 |
| *Gardnerella vaginalis* | 3.92 (1.89–8.14) | < 0.001 | 3.87 (1.90–7.91) | < 0.001 |
| Yeast | 1.73 (1.23–2.43) | 0.002 | 1.73 (1.23–2.43) | 0.002 |
| DF | 12 | | 7 | |
| AICc | 207.5 | | 197.8 | |
| ΔAICc | 9.7 | | 0.0 | |

* – Model 1 – a fully adjusted model to variables presented in Table II and additionally to *Mycoplasma genitalium*, *Streptococcus* group B, aerobic bacteria (with GBS), age, pH > 4.5
** – Model 1 – the most parsimonious model adjusted to variables presented in Table II
*** – OR of prevalence symptoms in women with detected specific microorganisms compared with those without symptoms

was small, so estimates were imprecise (OR = 9.62, 95% CI: 1.66–55.79). All 21 women diagnosed with *M. hominis* were symptomatic in the study group. The data on the diagnosis of *M. genitalium* was not significant, as it was identified in only two patients. The results also showed a positive correlation between candidiasis and symptoms in the analyzed group of women. In the present study, neither the prevalence of aerobic bacteria, nor Gram-negative and Gram-positive, like *Escherichia coli*, *Klebsiella pneumoniae*, *Streptococcus* spp., *Staphylococcus* spp., *Enterococcus* spp., nor the prevalence of GBS was statistically different in women manifesting symptoms compared to the non-symptomatic women. Complete data on the presence of specific microorganisms in the genital tract and their relationship to symptoms are presented in Table I.

Multivariable analysis found the vaginal colonization by *G. vaginalis*, urogenital *Mycoplasma* spp., *Chlamydia*, and yeast-like fungi as independent predictors of vaginitis symptoms, while *Lactobacillus* spp. was shown as protective against it (Table II).

***Ureaplasma parvum* and co-infections.** Among 1,155 examined women, 274 women had a positive PCR result for *Ureaplasma* spp., 187 for *U. parvum* (68%), and 89 cases for *U. urealyticum* (32%). Both *U. urealyticum* and *U. parvum* were diagnosed in two women. Genital tract colonization by *U. parvum* more than for times increased the chance of bacterial vaginosis with *G. vaginalis* (OR = 4.30, 95% CI: 2.44–7.49), almost tripled the prevalence of *M. hominis* infection (1.4% vs. 3.7%), and contributed to the more frequently recorded infection by yeast-like fungi (OR = 1.58, 95% CI: 1.07–2.32). However, it also significantly reduced the chance of *U. urealyticum* detection (OR = 0.11, 95% CI: 0.03–0.45) (Table III).

Among the 187 women with positive *U. parvum*, 81 showed no symptoms, and 106 reported symptoms. The presence of *Lactobacillus* spp. was analyzed in both groups and was at a similar level (Table I). The prevalence of *U. parvum* increased the chance of clinical symptoms about three times (OR = 3.07, 95% CI: 2.18–4.31) (Table II).

***Ureaplasma urealyticum* and co-infections.** The colonization of the genital tract by *U. urealyticum* increased four times the chance of bacterial vaginosis (OR = 4.07, 95% CI: 2.10–7.89). The possibility of *M. hominis* detection was also significantly increased (OR = 8.00, 95% CI: 3.22–19.86*)* (Table IV).

Among 89 women with positive *U. urealyticum*, 27 were asymptomatic, while 62 women were symptomatic. In all asymptomatic women with *U. urealyticum*, the presence of *Lactobacillus* spp. in the vagina was

Table III
Relationship between the presence of *U. parvum* and other microorganisms.

| Microorganisms | Without *Ureaplasma parvum* (n = 968) | With *Ureaplasma parvum* (n = 187) | $p^*$ | OR*** (95% CI) | $p^{**}$ |
|---|---|---|---|---|---|
| | n (%) | n (%) | | | |
| *Lactobacillus* spp. | 930 (96.1) | 177 (94.7) | 0.489 | 0.72 (0.35–1.48) | 0.372 |
| *Garderella vaginalis* | 32 (3.3) | 24 (12.8) | < 0.001 | 4.30 (2.44–7.49) | < 0.001 |
| *Chlamydia trachomatis* | 5 (0.5) | 3 (1.6) | 0.125# | 2.60 (0.86–12.81) | 0.101 |
| *Mycoplasma hominis* | 14 (1.4) | 7 (3.7) | 0.064# | 2.65 (1.05–6.66) | 0.0313 |
| *Mycoplasma genitalium* | 2 (0.2) | 0 (0.0) | 1.000# | 0.00 (0.05–21.56) | 0.534 |
| *Ureaplasma urealyticum* | 87 (9.0) | 2 (1.1) | < 0.001 | 0.11 (0.03–0.45) | < 0.001 |
| Aerobic bacteria | 134 (13.8) | 19 (10.2) | 0.214 | 0.70 (0.42–1.17) | 0.174 |
| Yeast | 150 (15.5) | 42 (22.5) | 0.025 | 1.58 (1.07–2.32) | 0.019 |
| *Streptococcus* group B | 82 (8.5) | 6 (3.2) | 0.020 | 0.36 (0.14–0.77) | 0.017 |

* – all *p*-values denoted by # are from Fisher's exact test; the remaining comparisons are made with the chi-square test of independence
** – *p*-values calculated by Wald method using Firth's logistic regression
*** – OR of prevalence of specific microorganisms in women with *Ureaplasma parvum* compared with those without *Ureaplasma parvum*

Table IV
Relationship between the presence of *U. urealyticum* and other microorganisms.

| Microorganisms | Without *Ureaplasma urealyticum* (n = 1,066) | With *Ureaplasma urealyticum* (n = 89) | $p^*$ | OR*** (95% CI) | $p^{**}$ |
|---|---|---|---|---|---|
| | n (%) | n (%) | | | |
| *Lactobacillus* spp. | 1,024 (96.1) | 83 (93.3) | 0.319 | 0.57 (0.23–1.37) | 0.203 |
| *Garderella vaginalis* | 43 (4.0) | 13 (14.6) | < 0.001 | 4.07 (2.10–7.89) | < 0.001 |
| *Chlamydia trachomatis* | 8 (0.8) | 0 (0.0) | 1.000# | 0.00 (0.04–12.15) | 0.412 |
| *Mycoplasma hominis* | 13 (1.2) | 8 (9.0) | < 0.001# | 8 (3.22–19.86) | < 0.001 |
| *Mycoplasma genitalium* | 1 (0.1) | 1 (1.1) | 0.148# | 5.98 (1.24–116.95) | 0.025 |
| *Ureaplasma parvum* | 185 (17.4) | 2 (2.2) | < 0.001 | 0.11 (0.03–0.45) | < 0.001 |
| Aerobic bacteria | 137 (12.9) | 16 (18.0) | 0.227 | 1.48 (0.84–2.63) | 0.171 |
| Yeast | 173 (16.2) | 19 (21.3) | 0.272 | 1.40 (0.82–2.39) | 0.213 |
| *Streptococcus* group B | 77 (7.2) | 11 (12.4) | 0.122 | 1.81 (0.88–3.42) | 0.083 |

* – all *p*-values denoted by # are from Fisher's exact test; the remaining comparisons are made with the chi-square test of independence
** – *p*-values calculated by Wald method using Firth's logistic regression
*** – OR of prevalence specific microorganisms in women with *Ureaplasma urealyticum* compared with those without *Ureaplasma urealyticum*

Table V
Relationship between the detection of *Ureaplasma* spp. and pH > 4.5 regarding *Gardnerella vaginalis* coinfections.

| | pH ≤ 4.5 n (%) | pH > 4.5 n (%) | OR*** (95% CI) | *p*** |
|---|---|---|---|---|
| *Ureaplasma* spp. | 180 (15.6%) | 94 (8.1%) | 2.1 (1.56–2.84) | < 0.005 |
| *Ureaplasma* spp. without *Garnerella vaginalis* coinfection | 173 (15.7%) | 65 (5.9%) | 1.60 (1.15–2.24) | 0.004 |

** – *p*-values calculated by Wald method using Firth's logistic regression
*** – OR of prevalence pH > 4.5 in women with *Ureaplasma* spp. (without *Garderella vaginalis* coinfection) compared with those without *Ureaplasma* spp. infection

Table VI
Distribution of vaginal pH values in women with and without the presence of specific microorganisms.

| Microorganisms | Not prevalent | | Prevalent | | *p** | pH > 4.5 OR (95% CI)** | *p*** |
|---|---|---|---|---|---|---|---|
| | n | Q2 (Q1-Q3) | n | Q2 (Q1-Q3) | | | |
| *Lactobacillus* spp. | 48 | 5.5 (5.0–5.5) | 1,107 | 4.5 (4.0–4.5) | < 0.001 | 0.01 (0.00–0.05) | < 0.001 |
| *Gardnerella vaginalis* | 1,099 | 4.5 (4.0–4.5) | 56 | 5.0 (4.9–5.5) | < 0.001 | 11.18 (6.05–20.65) | < 0.001 |
| *Ureaplasma* spp. | 881 | 4.5 (4.0–4.5) | 274 | 4.5 (4.5–5.0) | < 0.001 | 2.09 (1.55–2.82) | < 0.001 |
| *Ureaplasma parvum* | 968 | 4.5 (4.0–4.5) | 187 | 4.5 (4.5–5.0) | 0.001 | 1.71 (1.21–2.41) | 0.002 |
| *Ureaplasma urealyticum* | 1,066 | 4.5 (4.0–4.5) | 89 | 4.5 (4.5–5.0) | 0.004 | 2.42 (1.55–3.78) | < 0.001 |
| *Mycoplasma hominis* | 1,134 | 4.5 (4.0–4.5) | 21 | 4.5 (4.5–5.0) | 0.008 | 3.07 (1.31–7.16) | 0.010 |
| Aerobic bacteria (with GBS) | 1,002 | 4.5 (4.0–4.5) | 153 | 5.0 (4.5–5.0) | < 0.001 | 7.44 (5.17–10.69) | < 0.001 |
| *Streptococcus group B* | 1,067 | 4.5 (4.0–4.5) | 88 | 5.0 (4.5–5.1) | < 0.001 | 5.89 (3.76–9.24) | < 0.001 |
| Yeast | 963 | 4.5 (4.0–4.5) | 192 | 4.5 (4.5–5.0) | 0.003 | 1.49 (1.06–2.10) | 0.023 |

* – based on Mann-Whitney *U* test
** – based on logistic regression, crude models, Firth method, OR of prevalence pH > 4.5 in women with specific microorganisms compared with those without their presence Q2 (Q1-Q3) – median (interquartile range)

Table VII
Association between the prevalence of microorganisms and pH > 4.5 – multivariable analyses. The fully adjusted model and the most parsimonious model.

| Microorganisms | Model 1* | | Model 2** | |
|---|---|---|---|---|
| | OR (95% CI) | *p**** | OR (95% CI) | *p**** |
| *Ureaplasma parvum* | 1.81 (1.21–2.73) | 0.004 | 1.86 (1.24–2.79) | 0.003 |
| *Ureaplasma urealyticum* | 2.23 (1.31–3.78) | 0.003 | 2.32 (1.37–3.92) | 0.002 |
| *Lactobacillus* spp. | 0.03 (0.01–0.11) | < 0.001 | 0.03 (0.01–0.11) | < 0.001 |
| *Gardnerella vaginalis* | 5.91 (2.91–12.00) | < 0.001 | 6.54 (3.25–13.18) | < 0.001 |
| Aerobic bacteria (with GBS) | 7.31 (4.14–12.91) | < 0.001 | 6.85 (4.61–10.18) | < 0.001 |
| DF | 11 | | 5 | |
| AICc | 287.7 | | 275.0 | |
| ΔAICc | 12.7 | | 0.0 | |

* – Model 1 – fully adjusted model variables presented in the Table and additionally to yeast, Streptococcus group B, *Mycoplasma hominis*, *Mycoplasma genitalium, Chlamydia trachomatis*, and age
** – Model 2 – the most parsimonious model, adjusted to variables presented in the Table; OR of prevalence pH > 4.5
*** – *p*-values calculated by the Wald method using Firth's logistic regression

demonstrated (Table I). The prevalence of *U. urealyticum* increased about five times the chance of clinical symptoms (OR = 5.20, 95% CI: 3.17–8.51) (Table II).

***Ureaplasma* spp. and the pH value.** Among 1,155 vaginal smears, 76.6% of samples showed the correct vaginal pH range from 3.5 to 4.5. In 23.3% of samples,

pH was increased > 4.5. The statistical analysis indicated a strong association between *Ureaplasma* spp. presence in the genital tract with higher pH (Fig. 2, Table VI). According to our data, a higher pH value (pH > 4.5) increases the chance of *Ureaplasma* spp. detection regardless *G. vaginalis* infection (Table V).

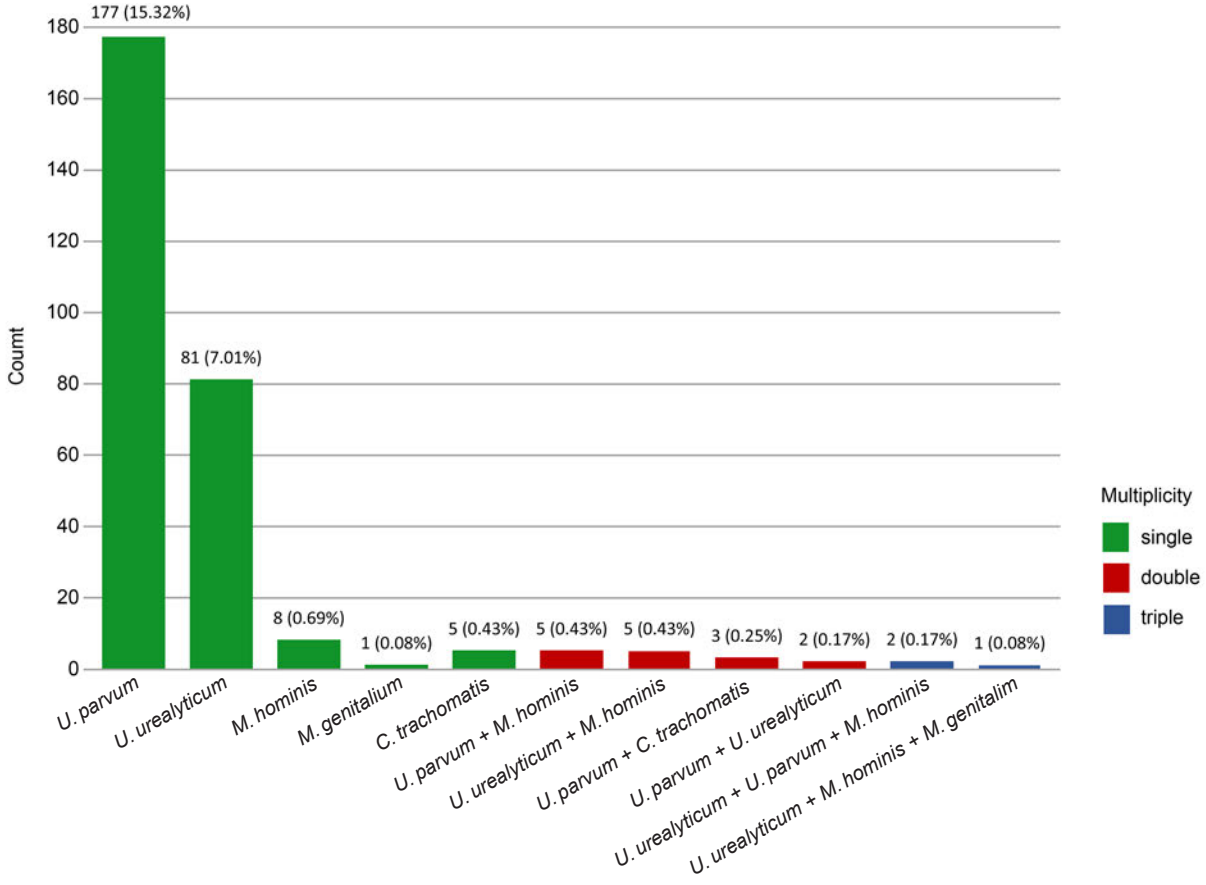


Fig. 1. The prevalence of mycoplasmas and *C. trachomatis* according to the multiplicity of colonization in the population studied (n = 1,155).

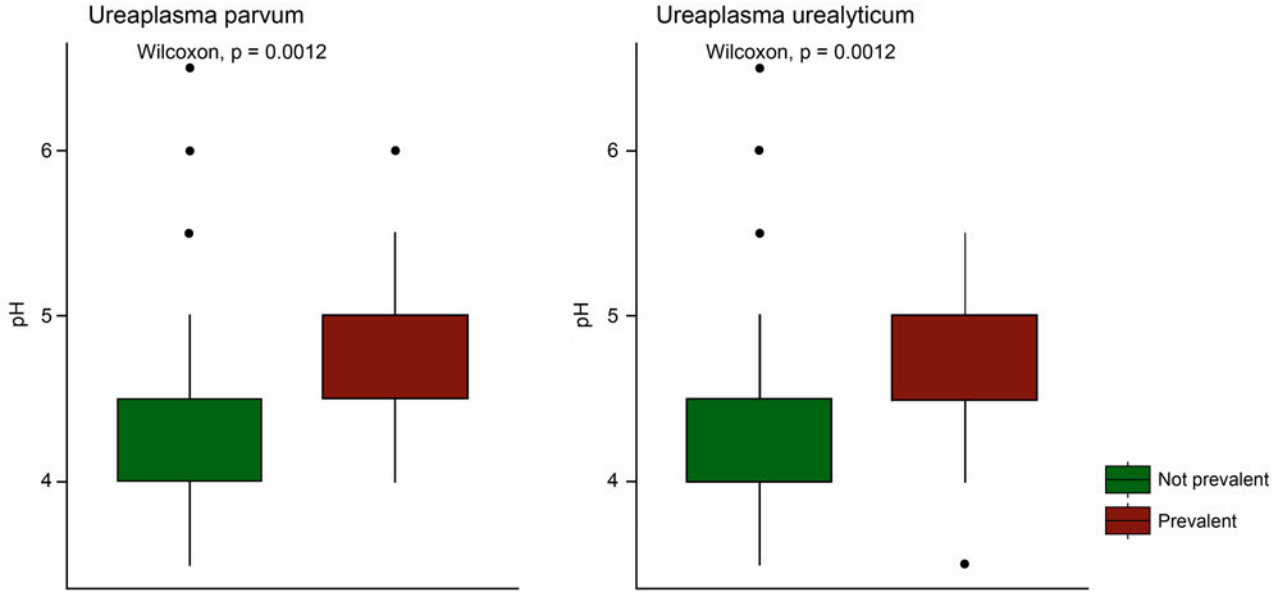


Fig. 2. Distribution of vaginal pH values in women with and without the presence of specific microorganisms. Dots denote extreme values; vertical segments are placed at median values, and boxes are located at quartile values. All differences in pH levels between groups were statistically significant.

## Discussion

This presented retrospective study showed a set of results from women in reproductive age diagnosed at the Microbiology and Autovaccine Research Center in Cracow, Poland. Gynecologists referred patients participating in the study to the laboratory for preventive or diagnostic examinations in case of suspected infection in the genital tract. The relationship between the presence of specific microorganisms and the manifestation of various symptoms was investigated. The significant positive associations between vaginal infection of *G. vaginalis* or *Candida* spp. with symptoms such as itching, burning, discomfort, discharge, and pain were detected. The results connecting BV or candidiasis with typical vaginitis or cervicitis symptoms have also been described by Leli et al. (2018). This study also found that in women with symptoms, *C. trachomatis* genital tract infections were over nine times more often identified than in the group without symptoms. It may be related to the previously studied occurrence of the pelvic inflammatory disease reported after *C. trachomatis* infection (O'Connell and Ferone 2016). Statistically significant differences in our study were observed in colonization by *U. urealyticum* of symptomatic or asymptomatic women as others reported (Hunjak et al. 2014; Marovt et al. 2015). Similarly, our results conformed the observations by De Francesco et al. (2013) on a relationship between symptom onset and infection by *Ureaplasma* spp.

Among 1,155 women in our study, 24,2% were colonized by single or multiple species of genital mycoplasmas. Most patients (23.02%) presented single mycoplasma species versus infrequent double and triple colonization, which was detected only in 1.2% of women. The other observational study conducted on a group of 1,761 women showed a much higher general prevalence of mycoplasmas (56.4%). In 39.4% of patients, single species colonization was detected (Leli el al. 2018). Contrary to our results, no association between *Ureaplasma* spp. and symptoms of vaginitis or cervicitis was reported in the study mentioned above.

The study shows that women with *Lactobacillus* spp. in the vagina reported symptoms less frequently, confirming the long-known protective role of *Lactobacillus* spp. (Boskey et al. 2001; Ravel et al. 2011; Witkin and Linhares 2017). No relationship was shown between *Lactobacillus* spp. and infection by *Ureaplasma* spp. *Lactobacillus* spp. was presented in women without *Ureaplasma* spp. and in women with *Ureaplasma* spp. symptomatic and asymptomatic. There was also no relationship between *Ureaplasma* spp. and *C. trachomatis* infection, as identified by Yamazaki et al. (2012) with only a statistically insignificant trend. A similar trend was shown by Leli et al. (2013). Moreover, *U. urealyticum* colonization in symptomatic women increases the prevalence of *M. hominis* (Leli et al. 2013).

Several observational studies have shown that BV and undetectable vaginal lactobacilli are important risk factors for STIs, such as HIV (Martin et al. 1999) and HPV infections (Watts et al. 2005; Biernat-Sudolska et al. 2011). BV microbiota assessed by Gram staining is associated with a significantly increased risk for acquisition of *T. vaginalis, N. gonorrhoeae,* and *C. trachomatis* infection (Schwebke and Desmond 2007; Brotman et al. 2010). Our results show that the colonization of the genital tract with *U. urealyticum* and *U. parvum* increased four times the chance of bacterial vaginosis. These results are consistent with reports on the epidemiology of *U. urealyticum* and *M. hominis* infections associated with the presence of BV and BV markers in pregnant women (Donders et al. 2017).

Excessive growth of *G. vaginalis* with a reduced number of *Lactobacillus* spp. leads to an increase of vaginal pH (Mączyńska 2008; Kasprowicz and Białecka 2012). The correlation between increased vaginal pH and BV is well established, making pH testing one of the predictors of BV according to Amsel's criteria (Amsel et al. 1983). In our study, the interesting association between colonization by *Ureaplasma* spp. and higher pH was detected regardless of co-infection with *G. vaginalis* indicating bacterial vaginosis. During *Ureaplasma* spp. colonization, the increase of vaginal pH may be partially mediated by urea hydrolysis into ammonia. Also, *M. hominis* produces ammonia from arginine, thus alkalizing the environment. Alkalization of the vaginal environment by mycoplasmas is opposite to the acidifying effect of *Lactobacillus*. Since our retrospective study lacks data on urogenital mycoplasmas and *Lactobacillus* load, quantitatively comparing their presence with a pH value is impossible. In addition to the microbiota, the vaginal pH can also be affected by hormonal status, sexual, and hygiene behavior. Our results show an interesting relationship between genital mycoplasmas, bacterial vaginosis, and symptoms of genital tract infections that needs further confirmation.

Our many years of experience in microbial diagnostics were starting points for retrospective analysis of microorganisms' prevalence, including urogenital mycoplasmas, in the south Poland population of women. The paper is retrospective, based on patients' charts who underwent routine microbiological diagnosis of the genital tract and answered questions regarding symptoms and antibiotic treatment and medical referrals. The paper attempts to use a large pool of data on the microbiota of the genital tract in a population of women in the south of Poland. Information on the prevalence of specific etiological factors of reproductive tract infections could be valuable for clinics. As a part of routine work, our diagnostic laboratory of the CBMiA

carries out diagnostics of the reproductive tract, including microscopic technique, microbial culture technique, and molecular methods (NAAT).

Infections of *C. trachomatis, N. gonorrhoeae*, and *M. genitalium* developing in the cervix cause many complications. Colonization of lower genital tract with mycoplasmas can lead to asymptomatic infections of the woman's upper reproductive system (Kasprzykowska et al. 2014). Often asymptomatic or sparsely symptomatic cervical infections cause complications such as pelvic inflammatory disease (PID), fallopian tube inflammation, fallopian tube obstruction, and ectopic pregnancies. Also, the incidences of sexually transmitted diseases differ regionally; therefore, the knowledge of the occurrence of STI pathogens is valuable. In Poland, women of childbearing age who are sexually active are often referred by gynecologists for prophylactic testing to diagnose infections with *C. trachomatis*, *N. gonorrhoeae*, *T. vaginalis*, but also *Ureaplasma* spp., and *Mycoplasma* spp. However, women reporting complaints in the genitourinary tract such as increased vaginal discharge, soreness on urination, soreness during intercourse, and lower abdominal pain are often treated empirically based on the reported symptoms.

The strength of our study is the numerous patient group and the broad picture of microorganisms that have been investigated. On the other hand, the impact of microbiota on women's health and often co-infections certainly cannot be solved by methods used in routine microbiological diagnostics. The diversity of the vaginal microbiota requires further studies with high-throughput sequencing. However, classic diagnostic microbiology can still broaden the knowledge of the microorganism prevalence in the genital tract and support women's reproductive health.

In addition, the group of women with symptoms was smaller than the asymptomatic group. It is mainly because of the retrospective character of the analysis and the chosen exclusions parameters. Some women who reported symptoms were not tested with all three microbiological methods; microscopy, culture, and NAAT, and, therefore, were excluded from the analysis. In some cases of STI risk, only NAAT was proceed according to the physician's prescription. Also, when candidiasis or BV were suspected, only microscopic evaluation of vaginal smear and culture were conducted along with the gynecologist's recommendation. In our opinion, the picture of coinfections needs more attention from physicians, diagnosticians, and scientists. Future studies should include more numerous groups of women with particular attention to symptoms. The symptoms assessment is an important factor in the analysis. It may result in bias since not every woman experiences the symptoms to the same degree, and many factors can influence this assessment.

In conclusion, a relationship between colonization of the female genital tract by *Ureaplasma* spp. and coinfection by *G. vaginalis* were observed in our study group. It was shown that the presence of *Lactobacillus* spp. significantly reduces the risk of symptoms in women. It was also assessed that BV with *G. vaginalis* isolation was more often detected in the group of symptomatic women. However, with a view to studies from other groups, further analyses of coinfections and potential associations with symptoms occurring in genital tract infections are needed.

**Conflict of interest**

The authors do not report any financial or personal connections with other persons or organizations, which might negatively affect the contents of this publication and/or claim authorship rights to this publication.

## Literature

**Abele-Horn M, Peters J, Genzel-Boroviczény O, Wolff C, Zimmermann A, Gottschling W.** Vaginal *Ureaplasma urealyticum* colonization: Influence on pregnancy outcome and neonatal morbidity. Infection. 1997 Sep–Oct;25(5):286–291. https://doi.org/10.1007/BF01720398

**Amabebe E, Anumba DOC.** The vaginal microenvironment: The physiologic role of *Lactobacilli*. Front Med (Lausanne). 2018 Jun 13;5:181. https://doi.org/10.3389/fmed.2018.00181

**Amsel R, Totten PA, Spiegel CA, Chen KC, Eschenbach D, Holmes KK.** Nonspecific vaginitis. Diagnostic criteria and microbial and epidemiologic associations. Am J Med. 1983 Jan;74(1):14–22. https://doi.org/10.1016/0002-9343(83)91112-9

**Aroutcheva A, Gariti D, Simon M, Shott S, Faro J, Simoes JA, Gurguis A, Faro S.** Defense factors of vaginal lactobacilli. Am J Obstet Gynecol. 2001 Aug;185(2):375–379. https://doi.org/10.1067/mob.2001.115867

**Biernat-Sudolska M, Szostek S, Rojek-Zakrzewska D, Klimek M, Kosz-Vnenchak M.** Concomitant infections with human papillomavirus and various mycoplasma and ureaplasma species in women with abnormal cervical cytology. Adv Med Sci. 2011;56(2):299–303. https://doi.org/10.2478/v10039-011-0028-9

**Boskey ER, Cone RA, Whaley KJ, Moench TR.** Origins of vaginal acidity: high D/L lactate ratio is consistent with bacteria being the primary source. Hum Reprod. 2001 Sep;16(9):1809–1813. https://doi.org/10.1093/humrep/16.9.1809

**Brotman RM, Klebanoff MA, Nansel TR, Yu KF, Andrews WW, Zhang J, Schwebke JR.** Bacterial vaginosis assessed by gram stain and diminished colonization resistance to incident gonococcal, chlamydial, and trichomonal genital infection. J Infect Dis. 2010 Dec 15;202(12):1907–1915. https://doi.org/10.1086/657320

**De Francesco MA, Caracciolo S, Bonfanti C, Manca N.** Incidence and antibiotic susceptibility of *Mycoplasma hominis* and *Ureaplasma urealyticum* isolated in Brescia, Italy, over 7 years. J Infect Chemother. 2013 Aug;19(4):621–627. https://doi.org/10.1007/s10156-012-0527-z

**Dewan B, Sharma M, Nayak N, Sharma SK.** Upper urinary tract stones and *Ureaplasma urealyticum*. Indian J Med Res. 1997 Jan; 105:15–21.

**Donders GGG, Ruban K, Bellen G, Petricevic L.** Mycoplasma/Ureaplasma infection in pregnancy: To screen or not to screen. J Perinat Med. 2017 Jul 26;45(5):505–515. https://doi.org/10.1515/jpm-2016-0111

**Gajer P, Brotman RM, Bai G, Sakamoto J, Schütte UM, Zhong X, Koenig SS, Fu L, Ma ZS, Zhou X, et al.** Temporal dynamics of the human vaginal microbiota. Sci Transl Med. 2012 May 2; 4(132): 132ra52. https://doi.org/10.1126/scitranslmed.3003605

**Harada K, Tanaka H, Komori S, Tsuji Y, Nagata K, Tsutsui H, Koyama K.** Vaginal infection with *Ureaplasma urealyticum* accounts for preterm delivery via induction of inflammatory responses. Microbiol Immunol. 2008 Jun;52(6):297–304. https://doi.org/10.1111/j.1348-0421.2008.00039.x

**Heinze G, Ploner M, Dunkler D, Southworth H, Jiricka L.** Firth's bias-reduced logistic regression [Internet]. Vienna (Austria): Center for Medical Statistics, Informatics and Intelligent Systems, Medical University of Vienna; 2022 [cited 2022 Mar 1]. Available from https://cran.r-project.org/web/packages/logistf/logistf.pdf

**Horowitz S, Horowitz J, Mazor M, Porath A, Glezerman M.** *Ureaplasma urealyticum* cervical colonization as a marker for pregnancy complications. Int J Gynaecol Obstet. 1995 Jan;48(1):15–19. https://doi.org/10.1016/0020-7292(94)02236-4

**Hunjak B, Sabol I, Vojnović G, Fistonić I, Erceg AB, Peršić Z, Grce M.** *Ureaplasma urealyticum* and *Ureaplasma parvum* in women of reproductive age. Arch Gynecol Obstet. 2014 Feb;289(2):407–412. https://doi.org/10.1007/s00404-013-2980-z

**Karaoğlu ŞA, Aydin F, Kiliç SS, Kiliç AO.** Antimicrobial activity and characteristics of bacteriocins produced by vaginal lactobacilli. Turk J Med Sci. 2003;33(1):7–13.

**Kasprowicz A, Białecka A.** [Assessment of vaginal biocenosis, degrees of vaginal cleanliness] (in Polish). Diagnosta laboratoryjny. 2008;6(2):21–24.

**Kasprowicz A, Białecka A.** [Atlas of vaginal purity degrees. Research procedures, interpretation of results] (in Polish). Wrocław (Poland): MesPharm; 2012. p. 5–45.

**Kasprzykowska U, Elias J, Elias M, Mączyńska B, Sobieszczańska BM.** Colonization of the lower urogenital tract with *Ureaplasma parvum* can cause asymptomatic infection of the upper reproductive system in women: A preliminary study. Arch Gynecol Obstet. 2014 May;289(5):1129–34. https://doi.org/10.1007/s00404-013-3102-7

**Kiecka A, Macura B, Szczepanik M.** Can *Lactobacillus* spp. be a factor reducing the risk of miscarriage? Pol J Microbiol. 2021 Dec; 70(4):431–446. https://doi.org/10.33073/pjm-2021-043

**Kuczyńska K.** [Female vaginal biocenosis] (in Polish). Studia Medyczne Akademii Świętokrzyskiej. 2003;11:17–21.

**Kundsin RB, Leviton A, Allred EN, Poulin SA.** *Ureaplasma urealyticum* infection of the placenta in pregnancies that ended prematurely. Obstet Gynecol. 1996 Jan;87(1):122–127. https://doi.org/10.1016/0029-7844(95)00376-2

**Leli C, Mencacci A, Latino MA, Clerici P, Rassu M, Perito S, Castronari R, Pistoni E, Luciano E, De Maria D, et al.** Prevalence of cervical colonization by *Ureaplasma parvum*, *Ureaplasma urealyticum*, *Mycoplasma hominis* and *Mycoplasma genitalium* in childbearing age women by a commercially available multiplex real-time PCR: An Italian observational multicentre study. J Microbiol Immunol Infect. 2018 Apr;51(2):220–225. https://doi.org/10.1016/j.jmii.2017.05.004

**Leli C, Meucci M, Vento S, D'Alò F, Farinelli S, Perito S, Bistoni F, Mencacci A.** Microbial and vaginal determinants influencing *Mycoplasma hominis* and *Ureaplasma urealyticum* genital colonization in a population of female patients. Infez Med. 2013 Sep;21(3):201–206.

**Mączyńska B.** [Diagnostics of bacterial vaginosis and atypical sexually transmitted infections] (in Polish). Diagnosta laboratoryjny. 2008;6(2):13–17.

**Marovt M, Keše D, Kotar T, Kmet N, Miljković J, Šoba B, Matičič M.** *Ureaplasma parvum* and *Ureaplasma urealyticum* detected with the same frequency among women with and without symptoms of urogenital tract infection. Eur J Clin Microbiol Infect Dis. 2015 Jun;34(6):1237–45. https://doi.org/10.1007/s10096-015-2351-8

**Martin HL, Richardson BA, Nyange PM, Lavreys L, Hillier SL, Chohan B, Mandaliya K, Ndinya-Achola JO, Bwayo J, Kreiss J.** Vaginal lactobacilli, microbial flora, and risk of human immunodeficiency virus type 1 and sexually transmitted disease acquisition. J Infect Dis. 1999 Dec;180(6):1863–1868. https://doi.org/10.1086/315127

**Nugent RP, Krohn MA, Hillier SL.** Reliability of diagnosing bacterial vaginosis is improved by a standardized method of gram stain interpretation. J Clin Microbiol. 1991 Feb;29(2):297–301. https://doi.org/10.1128/jcm.29.2.297-301.1991

**O'Connell CM, Ferone ME.** *Chlamydia trachomatis* Genital Infections. Microb Cell. 2016 Sep 5;3(9):390–403. https://doi.org/10.15698/mic2016.09.525

**R Core Team.** A language and environment for statistical computing. Vienna (Austria): R Foundation for Statistical Computing; 2022 [cited 2022 Mar 1]. Available from https://www.R-project.org

**Ravel J, Gajer P, Abdo Z, Schneider GM, Koenig SS, McCulle SL, Karlebach S, Gorle R, Russell J, Tacket CO, et al.** Vaginal microbiome of reproductive-age women. Proc Natl Acad Sci USA. 2011 Mar 15;108(Suppl 1):4680–4687. https://doi.org/10.1073/pnas.1002611107

**Schwebke JR, Desmond R.** A randomized trial of metronidazole in asymptomatic bacterial vaginosis to prevent the acquisition of sexually transmitted diseases. Am J Obstet Gynecol. 2007 Jun;196(6):517.e1–517.e6. https://doi.org/10.1016/j.ajog.2007.02.048

**Vallor AC, Antonio MA, Hawes SE, Hillier SL.** Factors associated with acquisition of, or persistent colonization by, vaginal lactobacilli: Role of hydrogen peroxide production. J Infect Dis. 2001 Dec 1; 184(11):1431–1436. https://doi.org/10.1086/324445

**Wang X.** Firth logistic regression for rare variant association tests. Front Genet. 2014 Jun 19;5:187. https://doi.org/10.3389/fgene.2014.00187

**Watts DH, Fazzari M, Minkoff H, Hillier SL, Sha B, Glesby M, Levine AM, Burk R, Palefsky JM, Moxley M, et al.** Effects of bacterial vaginosis and other genital infections on the natural history of human papillomavirus infection in HIV-1-infected and high-risk HIV-1-uninfected women. J Infect Dis. 2005 Apr 1;191(7):1129–1139. https://doi.org/10.1086/427777

**Witkin SS, Linhares IM.** Why do lactobacilli dominate the human vaginal microbiota? BJOG. 2017 Mar;124(4):606–611. https://doi.org/10.1111/1471-0528.14390

**Yamazaki T, Matsumoto M, Matsuo J, Abe K, Minami K, Yamaguchi H.** Frequency of *Chlamydia trachomatis* in *Ureaplasma*-positive healthy women attending their first prenatal visit in a community hospital in Sapporo, Japan. BMC Infect Dis. 2012 Apr 2;12:82. https://doi.org/10.1186/1471-2334-12-82

ORIGINAL PAPER
Polish Journal of Microbiology
2022, Vol. 71, No 4, 519–528
https://doi.org/10.33073/pjm-2022-046

# The Emergence of Colistin- and Imipenem-Associated Multidrug Resistance in *Escherichia coli* Isolates from Retail Meat

BENSON CHUKS IWERIEBOR[1]*, OLIVIA SOCHI EGBULE[2] and LARRY C. OBI[1]

[1]School of Science and Technology, Sefako Makgatho Health Sciences University, Ga-Rankuwa, South Africa
[2]Department of Microbiology, Delta State University, Abraka, Nigeria

Submitted 15 July 2022, accepted 19 September 2022, published online 28 November 2022

Abstract

To determine the prevalence of *Escherichia coli* and their drug resistance profiles in fresh pork sold at two retail outlets (open-air market and closed retail stores) in Alice, South Africa. Retail meat samples (n = 176) collected from four shops (two from open-air markets and two from closed stores) were analyzed by conventional biochemical and PCR-based molecular confirmatory tests. The confirmed isolates were profiled for antimicrobial susceptibility to a panel of 12 commercial antibiotics: tetracycline, ampicillin, sulphamethoxazole trimethoprim, erythromycin, gentamycin, colistin sulphate, cefotaxime, chloramphenicol, norfloxacin, ciprofloxacin, cefuroxime, and imipenem. Colistin, ampicillin, and erythromycin resistance genes were profiled with the gene-specific primers. Multidrug resistance (MDR) and the association of imipenem and colistin in the MDR profile were determined. A total of 68 (39.08%) *E. coli* isolates were confirmed by PCR analysis. Resistance was most common to erythromycin (100%), followed by cefotaxime (95.58%), ampicillin (88.23%), cefuroxime (88.23%), trimethoprim-sulphamethoxazole (88.23%), and tetracycline (60.29%). Overall, 27/68 (39.70%) were MDR (≥3antibiotics classes). MDR *E. coli* isolates associated with imipenem resistance (50.00%) and colistin resistance (33.82%) were detected. The resistance genes were detected among the isolates though not in all the phenotypically resistant isolates. The detection of colistin resistance among MDR *E. coli* isolates from retail meat is troubling as the drug is a last resort antibiotic. Overall, the epidemiological implications of the findings are of public health importance.

Keywords: *Escherichia coli*, pork, multiple antibiotic resistance, susceptibility, retail outlet, colistin resistance, imipenem resistance

## Introduction

Foodborne pathogens from animal sources account for most of the foodborne illnesses each year. Poor hygienic practices are a major contributing factor in most developing countries of Africa, with contaminated raw meat as a leading source of foodborne illness. Raw meats are available in the open air, retail shops, and abattoirs. Microbial contamination of food can therefore transpire at numerous phases across the food chain, which includes production, slaughtering, distribution, and retail marketing (Elhadi 2014). Foodborne diseases are burdensome and represent a significant world health problem. Globally, the microbiological safety of food is a growing public health challenge. By estimate, every year, 600 million, or nearly 1 in 10 people globally, become ill through the consumption of contaminated food. A total of 420,000 individuals out of this figure die, including 12,000 children who fall under 5 as reported by the World Health Organization's estimates on the global burden of foodborne diseases (WHO 2015). *Escherichia coli*, a member of intestinal microbiota, is potentially pathogenic organism for humans and animals (Bumunang et al. 2019). The presence of *E. coli* in meat indicates poor hygienic practices in abattoirs or retail outlets. Contaminated, uncooked or undercooked red meats are particularly important in transmitting these foodborne pathogens (Wang et al. 2012). Foods of animal origin have been implicated as a leading vehicle involved in foodborne diseases (Baek et al. 2009). Pork is a highly consumed red meat in the world (Joy et al. 2014; Grobbelaar et al. 2021), and Statista GmbH has projected that the global consumption will amount to around 127.2 million metric

* Corresponding author: B.C. Iweriebor, School of Science and Technology, Sefako Makgatho Health Sciences University, Ga-Rankuwa, South Africa; **e-mail: benvida2004@yahoo.com**

tons by 2029 (Grobbelaar et al. 2021). The pork consumption in South Africa was reported to increase from 3.5 kg (2000) to over 4.2 kg (Streicher 2012).

In South Africa, pork is partly responsible for around 16.3% of the gross value of agricultural production (Mohlatlole et al. 2013). To meet production goals, antimicrobial agents are vital for the prophylaxis and treatment of many diseases in pork production (Ström et al. 2018). The most frequently administered antimicrobial agents in pork production include colistin, third and fourth-generation cephalosporins, and carbapenems. Colistin, a member of the antimicrobial agents, referred to as polymyxins, is a mixture of polymyxin E1 and E2 that are pentacationic lipopeptides and are bactericidal in action. Colistin is active against a wide range of Gram-negative bacteria and has no activity against Gram-positive bacteria due to the absence of an outer membrane. It is used in both human and veterinary medicine. However, it is only an empiric drug in treating infections with multidrug-resistant, extensively drug-resistant, and pan drug-resistant bacteria in humans (Magiorakos et al. 2012). In veterinary medicine, it is commonly used to treat food-producing animals from chicken to pigs, claves, cattle, cows, meat, and milk-producing sheep, goats, and rabbits. It is also used in aquaculture for the prevention and treatment of infections attributed to members of *Enterobacteriaceae* and other Gram-negative bacteria and used for growth promotion.

Imipenem is a beta-lactam antibiotic of the carbapenems class with a broad spectrum of activity. The mechanism of action involves the inactivation of the penicillin-binding proteins (PBP), thereby resulting in cell wall lysis or inhibition of its formation. They bind to a specific PBP (PBP-1) that results in more rapid lysis compared to other beta-lactams, thus resulting in higher bactericidal activity and a more prolonged post-antibiotic effect. Carbapenems have a broad spectrum of activity and are among the most active of all antibiotics. Their spectrum includes Gram-negative bacilli, including Enterobacteriaceae and Pseudomonas aeruginosa. Antibiotic resistance is one of the biggest threats to global health, food security, and development today (WHO 2020). Antibiotic resistance may develop naturally, but antibiotic misuse by humans and animal husbandry is accelerating the process. Currently, a growing number of infections are becoming harder to treat as the antibiotics used to treat them have become less effective. The consequences of antibiotic resistance lead to more extended hospital stays, higher medical costs, and increased mortality. There are four fundamental mechanisms of antimicrobial resistance: (i) enzymatic degradation of antibacterial drugs, (ii) alteration in the bacterial proteins that are antimicrobial targets, (iii) changes in membrane permeability to antibiotics, and (iv) intrinsic resistance caused by an absence of drug's target in the organism. Antibiotic resistance can be either plasmid-mediated or maintained on the bacterial chromosome.

Generally, resistance to colistin could be due to acquired resistance in which a once naturally susceptible organism modifies its cell surface, such as altering its lipopolysaccharide structure. Other known resistance mechanisms include capsular polysaccharide shedding, thus resulting in the trapping or binding of polymyxin or colistin, as in *Klebsiella pneumoniae*. In organisms such as *Acinetobacter baumannii*, there are two known mechanisms of resistance to colistin, which include loss of lipopolysaccharide production and the modification of the system that allows bacteria to respond to environmental conditions, which ultimately results in lipid modification and membrane permeability. The second most adopted mechanism is transferable colistin resistance mediated by a plasmid-coded gene, *mcr*. Currently, there are many variants of the gene since the first identification of the *mcr-1* gene in *E. coli* isolates from food animals and their meat in China between 2011 and 2014 and in *E. coli* and *K. pneumoniae* isolates collected in 2014 from humans in China (Liu et al. 2016; Skov and Monnet 2016).

The location of colistin resistance genes on transferable plasmids has resulted in the widespread dissemination of colistin resistance in various strains recovered from different sources (Aminov 2011; Popowska 2012). It leads to the development of multiple co-resistance or cross-resistance in bacteria (Gwida and El-Gohary 2015; Hoelzer et al. 2017). It affects both pathogenic bacteria and healthy microbiota, with the latter serving as a potential reservoir of resistance genes for pathogens. Multidrug-resistant pathogens can be transferred through the food chain weakening the potency of antimicrobials administered during infections (Brunelle et al. 2013). Thus, the widespread antibiotic resistance among foodborne pathogens undermines the successful treatment of infectious diseases (Yao et al. 2016) as antibiotics are rendered ineffective due to resistance leading to frequent treatment failures (Poirel et al. 2016). Most colistin-resistant positive isolates carry different resistance genes, including carbapenemase (Yao et al. 2016; Poirel et al. 2016) and other resistance genes (Turlej-Rogacka et al. 2018).

The evolution of carbapenem resistance has become rampant in Gram-negative bacteria, especially in intensive care units (ICUs), where the selective pressure exerted by antibiotics on bacterial populations is strong. This development is mediated by mutations or insertion sequences (ISs) that inactivate the gene coding for porin OprD, the specific portal of entry for carbapenems into these organisms. The reduced outer membrane permeability that results from OprD loss

usually causes an increase in the MICs of all the carbapenem molecules, including imipenem, meropenem, and doripenem (Fournier et al. 2013). In addition to this very prevalent mechanism, carbapenem-resistant bacteria may acquire numerous foreign genes encoding different classes of β-lactamases that are capable of hydrolyzing carbapenems to varying degrees. Similarly, there is an ever-growing number of bacterial isolates producing metallo-β-lactamase (MBL) (class B) that have been reported from many countries in recent years, indicating that these enzymes could become the predominant cause of carbapenem resistance in no distant future (Fournier et al. 2013).

Although colistin-resistant isolates are emerging and have been found in Africa, data on multidrug-resistant isolates exhibiting carbapenem and colistin resistance is scarce. Additionally, there is a dearth of data as regards the prevalence of multiple resistant *E. coli* contaminating pork in Eastern Cape, South Africa. Here we present data on multidrug-resistant *E. coli* isolates.

## Experimental

### Materials and Methods

**Sample collection.** The study was conducted in Alice. Alice is situated in the Eastern Cape, the "livestock" province of South Africa, which has about 46% goats, 28% sheep, 20% pigs, and 21% cattle (Caine et al. 2014). Alice was selected based on the meat consumption rate by this area's inhabitants. One hundred eighty raw pork samples were randomly purchased from open-air markets (Shops A and B) and closed retail stores (Shops C and D) located in Alice. The samples were individually packed in sterile plastic bags, marked, and then transported in cooler boxes with ice parks (4°C) to the University of Fort Hare Microbiology Laboratory for immediate processing. The study was carried out between May 2018 and October 2018.

**Isolation of presumptive organisms.** The modified method described by Bersisa et al. (2019) was adopted to isolate bacteria. Briefly, the raw meat samples were swabbed with a sterile cotton swab, and each swab sample was used to inoculate chromogenic agar plate (Merck, South Africa), and then the plates were incubated at 37°C for 48 h. About two to three separate distinct colonies were picked and were selectively plated onto chromocult tryptone bile X-glucuronide agar (TBX agar; Merck, South Africa), incubated aerobically at 37°C for 24 h. Each deep blue colony was selectively picked as presumptive *E. coli* isolate into LB broth and incubated for 24 h at 37°C. These presumptive isolates were stored at –80°C in 25% glycerol until further analyses.

**DNA extraction.** Genomic DNA of the presumptive *E. coli* isolates was prepared by the method earlier reported by Iweriebor et al. (2015). Briefly, the presumptive isolates in glycerol stock were resuscitated overnight in LB broth, from which 2 ml was centrifuged at 10,000 rpm. The supernatant was discarded, the pellet resuspended in nuclease free water, boiled at 100°C, and the resultant supernatant was used as DNA template in all the PCR assays.

**Molecular identification of presumptive *E. coli* by PCR.** Isolates considered as presumptive *E. coli* were confirmed by PCR using the *uid*A oligonucleotide primer (Inqaba Biotech, South Africa) and the details of the sequences are as follows: F: 5'-AAAACGGCAAGAAAAAGCAG-3' and R: 5'-ACGGTGGTTAACAGTCTTGCG-3' (Tsai et al. 1993). Each PCR was performed as previously described by Iweriebor et al. (2015), followed by gel electrophoresis on 1.5% agarose and documented in a gel documentation system. *E. coli* ATCC® 25922™ reference strain served as a positive control in this study.

**Determination of antimicrobial susceptibility of the isolates.** Antimicrobial susceptibility patterns of the confirmed *E. coli* isolates were performed on Mueller-Hinton agar (MHA) plates (Oxoid CM337), as previously reported by Bauer et al. (1966). About four to five *E. coli* colonies of an 18-hour-old culture were selected with a sterile wire loop and after that inoculated into 0.8% NaCl suspension in a micro-centrifuge tube, gently vortexed, and adjusted to a turbidity equivalent to 0.5 McFarland standard (Amri and Juma 2016). One hundred microliters of the standardized bacterial culture was then evenly spread on the entire surface of the MHA plates using a sterile cotton swab and allowed to dry for 10 min before placing the antibiotic discs. The plates were incubated at 37°C for 24 h and after that read according to CLSI guidelines (CLSI 2016). The list of antibiotics tested includes the following: tetracycline (30 µg), ampicillin (10 µg), sulphamethoxazole-trimethoprim (25 µg), erythromycin (15 µg), chloramphenicol (10 µg), cefuroxime (30 µg), gentamycin (10 µg), norfloxacin (10 µg), ciprofloxacin (5 µg), colistin sulphate (10 µg), cefotaxime (30 µg), and imipenem (10 µg). Isolates that were resistant to colistin by the disc diffusion method were then tested by the broth dilution method as recommended by the CLSI (2016). CLSI guidelines (CLSI 2016) recommended clinical resistance breakpoint for colistin as greater than or equal to ≥ 2 µg/ml. The isolates were then screened for *mcr*-1, *bla*TEM, and *erm*B by PCR, as previously described by Liu et al. (2016) and Iweriebor et al. (2015) while the other resistance determinants were not profiled.

**Multidrug resistance phenotype and multiple antibiotic resistance index.** The isolate which showed resistance to three or more classes of the antibiotics

Table I
Isolation and identification of *Escherichia coli*.

| Shop | Location of shop | Samples collected | Presumptive isolates | Positive isolates | % |
|---|---|---|---|---|---|
| A | Open-air market | 58 | 58 | 28 | 48.28 |
| B | Open-air market | 33 | 31 | 18 | 58.06 |
| C | Closed store | 43 | 43 | 8 | 18.60 |
| D | Closed store | 42 | 42 | 14 | 33.33 |
| Total | | 176 | 174 | 68 | 39.08 |

tested was considered to be a multidrug-resistant. The MDR patterns of the isolates were recorded according to the protocol earlier described by Ateba et al. (2008). The Multiple Antibiotic Resistance Index (MARI) was calculated using the mathematical expression: MARI = x/y, where 'x' stands for the total number of antibiotics to which resistance was observed in an individual isolate and 'y' stands for the total number of antibiotics against which an individual isolate was tested.

## Results

**Prevalence of *E. coli*.** From the 180 pork samples randomly collected from open-air markets and closed retail stores (Shop A to D) located in Alice, South Africa, 174 presumptive isolates were obtained through preliminary screening with the selective culture medium. Among the samples collected, shop A samples had the highest number of *E. coli* isolates, followed by shop B. These shops were located in open-air market. The percentage prevalence of *E. coli* isolates from shops C and D were lower (Table I).

**Molecular identification of presumptive *E. coli* isolates.** A total of 68 (39.08%) of the 174 presumptive isolates were confirmed as *E. coli* (Table I). Fig. 1 below shows the gel image representation of some of the confirmed isolates.

**Susceptibility patterns of *E. coli* isolates.** *E. coli* isolates from retail pork displayed resistance most frequently to erythromycin (100%; 68/68), cefotaxime (95.58% 65/68), ampicillin (88.23%; 60/68), cefuroxime (88.23%; 60/68), trimethoprim-sulphamethoxazole (88.23%; 60/68), and tetracycline (60.29%; 41/68). Lower resistance was observed against imipenem (50.00%; 34/68) and colistin (33.82%; 23/68). Notably, the resistance of *E. coli* isolates to ciprofloxacin (2.94%; 2/68) and norfloxacin (1.47%; 1/68) was lower than 5%. The susceptibility patterns of the isolates obtained in this study are shown in Fig. 2. Isolates showing resistance to at least three antibiotics of different classes were classified as multidrug-resistant. All isolates showing intermediate resistance were regarded as resistant. Genetic profiling for the *mrc*-1, *bla*TEM, and *erm*B resistance genes showed positive results as some of the phenotypic resistant isolates were positive for the genes profiled, as shown in Fig. 3–5. The frequencies of the profiled resistance genes among the isolates were as follow; *mrc*-1 11/23 (47%), *bla*TEM 13/34 (38%), and *erm*B 15/68 (22%).

**Multiple antibiotic resistance phenotypes and index.** This study characterized the antimicrobial resistance phenotype in *E. coli* isolates from retail stores and open-air markets. It was observed that 39.70% (27/68) of the study isolates were MDR, and 92.59% (25/27) of *E. coli* MDR isolates were resistant to cefotaxime – a third-generation cephalosporin. *E. coli* MDR isolates resistance to imipenem, a carbapenem used in this study and colistin was observed. The MDR pattern (Table II) indicated that the majority of

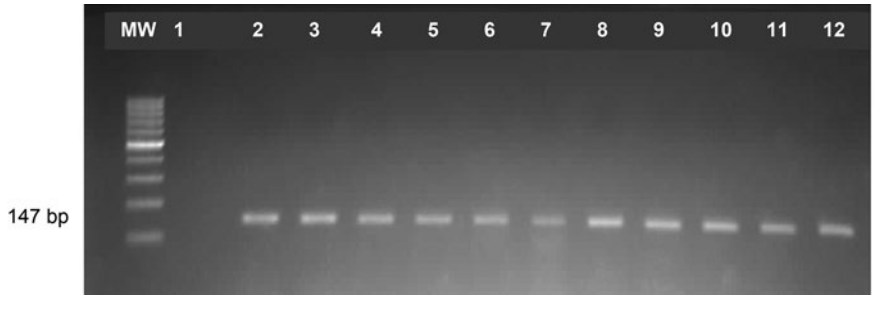


Fig. 1. Agarose gel electrophoresis for *Escherichia coli* identification.
Line M – 100 bp ladder, Line 1 – negative control, Line 2 – *E. coli* ATCC® 25922™ as a positive control, Lines 3–12 – the 147 bp PCR amplification product for *E. coli* isolates.

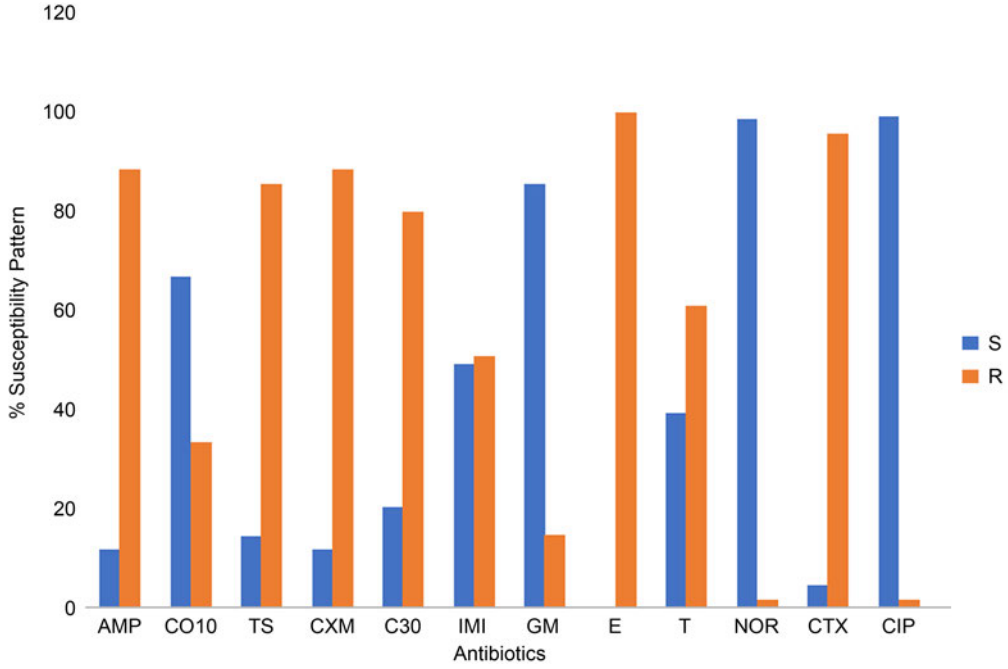


Fig. 2. The sensitivity pattern of *Escherichia coli* isolates against antibiotics.
AMP – ampicillin, CO10 – colistin sulphate, TS – trimethoprim-sulphamethoxazole, CXM – cefuroxime, E – erythromycin, C30 – chloramphenicol, IMI – imipenem, GM – gentamycin, T – tetracycline, NOR – norfloxacin, CTX – cefotaxime, CIP – ciprofloxacin, S – susceptible, R – resistant, I – intermediate

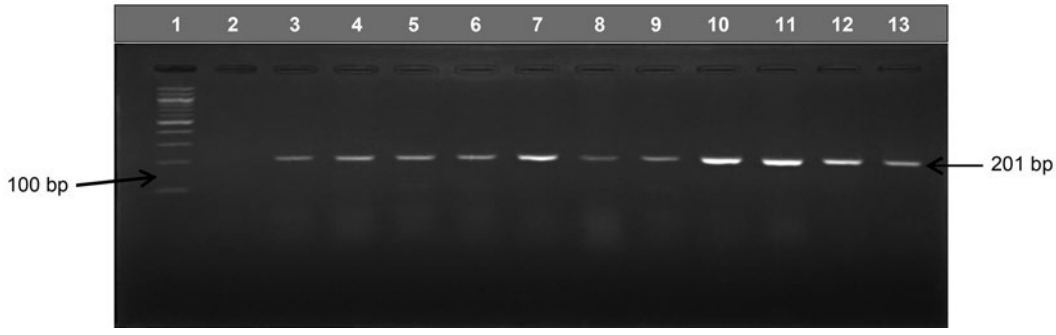


Fig. 3. Electrophoresis of *mrc-1* gene amplification among *Escherichia coli* isolates.
Line 1 – 100 bp ladder, Line 2 – negative control, Line 3–13 – positive isolates

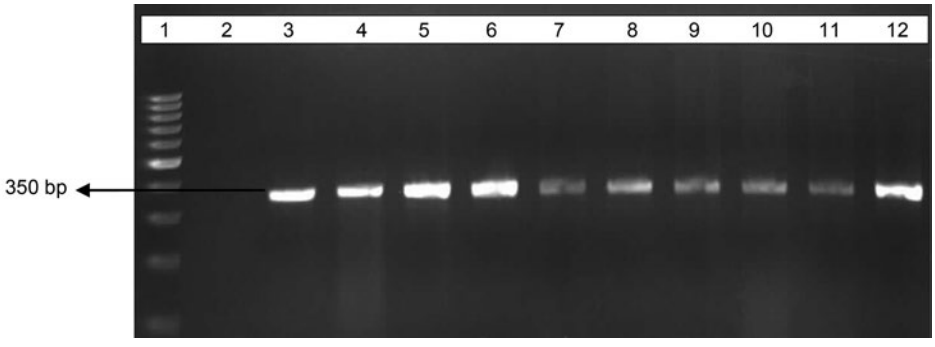


Fig. 4. Electrophoresis of the *erm*B gene amplification product (350 bp) in *Escherichia coli* isolates.
Line 1 – 100 bp DNA ladder, Line 2 – negative control, Lines 3–12 – the *erm*B-resistant *E. coli* isolates

the tested *E. coli* isolates demonstrated multiple antibiotic resistance against three to nine antibiotics. The lowest MDR rate was exhibited by 14.81% (4/27) of the isolates against three antibiotics, while 7.41% (2/27) exhibited the highest MDR rates against nine antibiotics. About 33.33% (9/27) of MDR *E. coli*

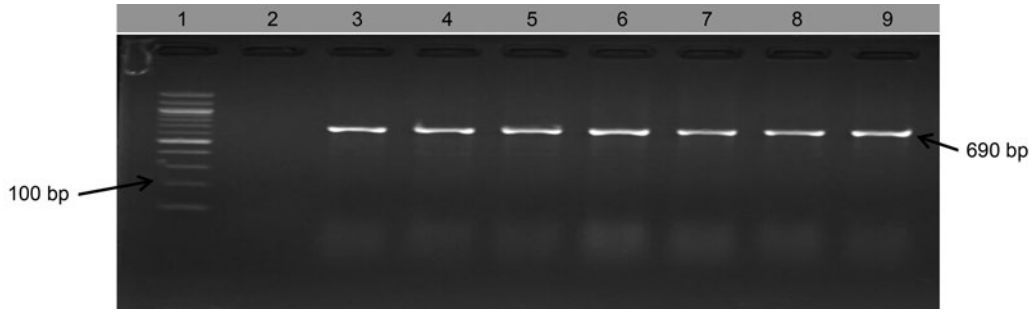


Fig. 5. Gel electrophoresis of the PCR product (690 bp) amplified with *bla*TEM primers for the detection of β-lactam-resistant *Escherichia coli* isolates.
Line 1 – DNA ladder, Line 2 – negative control, Lines 3–9 – β-lactam-resistant *E. coli* isolates

isolates were resistant to imipenem, while 29.62% (8/27) were resistant to colistin. Both imipenem resistant MDR and non-imipenem resistant MDR *E. coli* isolates were colistin-resistant (Table II and III). The MARI ranged between 0.25 and 0.75, with the average being 0.48.

Table II
Antibiotic resistance patterns and the Multiple Antibiotic Resistance Index (MARI) of the confirmed *E. coli* isolates.

| MDR phenotype | Number of antimicrobials | MARI |
|---|---|---|
| CTX-T-E | 3 | 0.25 |
| CTX-E-C30 | 3 | 0.25 |
| CTX-AMP-E | 3 | 0.25 |
| CTX-CXM-E | 3 | 0.25 |
| TS-GM-E-CO10 | 4 | 0.33 |
| CTX-CXM-AMP-E | 4 | 0.33 |
| AMP-T-TS-C30-E | 5 | 0.42 |
| CTX-CXM-T-TS-E | 5 | 0.42 |
| CTX-CXM-AMP-TS-E | 5 | 0.42 |
| CTX-CXM-AMP-T-E | 5 | 0.42 |
| CTX-CXM-TS-CO10-E | 5 | 0.42 |
| CTX-TS-E-IMI-CIP | 5 | 0.42 |
| CTX-CXM-AMP-T-E-C30 | 6 | 0.50 |
| CTX-CXM-AMP-TS-CO10-E | 6 | 0.50 |
| CTX-CXM-AMP-T-TS-E | 6 | 0.50 |
| CTX-CXM-AMP-TS-IMI-E | 6 | 0.50 |
| CTX-CXM-AMP-IMI-CO10-E | 6 | 0.50 |
| CTX-CXM-AMP-TS-IMI-E | 6 | 0.50 |
| CTX-CXM-AMP-TS-C30-GM | 6 | 0.50 |
| CTX-CXM-AMP-T-TS-C30-E | 7 | 0.58 |
| CTX-CXM-AMP-TS-IMI-E | 6 | 0.50 |
| CTX-CXM-AMP-T-TS-C30-IMI-E | 8 | 0.66 |
| CTX-CXM-AMP-T-TS-C30-CO10-E | 8 | 0.66 |
| CTX-CXM-AMP-T-TS-C30-GM-CO10 | 8 | 0.66 |
| CTX-AMP-T-TS-E-C30-IMI-NOR | 8 | 0.66 |
| CTX-CXM-AMP-T-TS-C30-IMI-CO10-E | 9 | 0.75 |
| CTX-CXM-AMP-TS-C30-IMI-GM-CO10-E | 9 | 0.75 |

MDR – indicates resistance to three or more classes of antibiotics, AMP – ampicillin, C30 – chloramphenicol, CIP – ciprofloxacin, CO10 – colistin sulphate, CTX – cefotaxime, CXM – cefuroxime, E – erythromycin, GM – gentamycin, IMI – imipenem, NOR – norfloxacin, T – tetracycline, TS – trimethoprim-sulphamethoxazole

Table III
Colistin and imipenem resistance patterns among the isolates.

| Colistin- and imipenem-resistant isolates (CO10+/IMP+) | Colistin-resistant and imipenem-sensitive isolates (CO10+/IMP–) | Colistin-sensitive and imipenem-resistant isolates (CO10–/IMP+) |
|---|---|---|
| CTX-CXM-AMP-TS-C30-IMI-GM-CO10-E | CTX-CXM-AMP-T-TS-C30-GM-CO10 | CTX-AMP-T-TS-E-C30-IMI-NOR |
| CTX-CXM-AMP-T-TS-C30-IMI-CO10-E | CTX-CXM-AMP-T-TS-C30-CO10-E | CTX-CXM-AMP-T-TS-E-C30-IMI-E |
| CTX-CXM-AMP-IMI-CO10-E | TS-GM-E-CO10 | CTX-CXM-AMP-TS-IMI-E |
| | CTX-CXM-TS-CO10-E | CTX-CXM-AMP-TS-E |
| | CTX-CXM-AMP-TS-CO10-E | CTX-TS-E-IMI-CIP |

AMP – ampicillin, C30 – chloramphenicol, CIP – ciprofloxacin, CO10 – colistin sulphate, CTX – cefotaxime, CXM – cefuroxime, E – erythromycin, GM – gentamycin, IMI – imipenem, NOR – norfloxacin, T – tetracycline, TS – trimethoprim-sulphamethoxazole

## Discussion

The overall aim of the study was to determine MDR in *E. coli* isolated from pork sold in some retail outlets in Alice, South Africa, and depict the association of colistin and imipenem in the MDR profile. Furthermore, we determined the antimicrobial susceptibility of the isolates to other antimicrobial agents. The 39.1% prevalence of *E. coli* reported in this study is lower than in some previous studies in South Africa (Tanih et al. 2015; Jaja et al. 2020) and other countries (Xia 2010; Reddy 2017). However, a similar prevalence figure as obtained in this study was observed by Pires et al. (2020). The variation in the prevalence of *E. coli* is partly related to the method of isolation and identification. Whereas some studies identified *E. coli* with conventional bacteriological and biochemical tests, others included PCR-based molecular confirmatory tests. The presence of this bacteria in pork indicates a possible breakdown of hygiene at the different stages of the food processing and distribution chain or a lack of proper storage of the meat, as microbial contamination of food has been reported at numerous stages along the food chain distribution (Elhadi 2014). *E. coli* is a member of the microbiota of the gastrointestinal tract and can cross-contaminate meat when the content of the gastrointestinal tract bursts during slaughter. Various poor handling and unhygienic practices were observed, especially amongst retailers in the open-air market, accounting for a higher prevalence of *E. coli*. Knives for cutting meat were not washed intermittently; meats were displayed on the improperly cleaned table and were exposed to houseflies. Adzitey (2016) observed similar unhygienic practices in handling meat in Ghana and Fukuda et al. (2019) observed a relatively high proportion of flies harboring antibiotic-resistant *E. coli* and transferring resistance genes in Thailand. All these are potential sources of cross-contamination and routes of spread of infections with food-borne pathogens to humans; it also raises food safety concerns for humans, who are the ultimate consumers. Increased emergence of *E. coli* isolates with varying MDR phenotypes is a growing problem in South Africa and other developing countries. About 39% of *E. coli* isolates in this study were MDR. The MDR *E. coli* isolates showing resistance to imipenem and colistin were 33% and 29%, respectively. This implies a movement toward a pan drug resistance because colistin is the last resort antibiotic for treating infections caused by carbapenem-resistant *Enterobacteriaceae* (Liu et al. 2016). Some reports have shown colistin and carbapenem resistance genes to be located on transferable plasmids and transferred via conjugation (Fukuda et al. 2019). The emergence of resistance to antimicrobial agents such as colistin is a troubling development and public health threat, primarily as colistin is known to have a wide range of activities against the majority of the *Enterobacteriaceae* family (Liu et al. 2016; Dandachi et al. 2018). More so, besides colistin, there are few or no alternative antimicrobial agents for treating bacterial infections. Therefore, there is a need to monitor the use of colistin in the human health sector and animal husbandry (Hao et al. 2014). Currently, colistin has displaced aminoglycosides (WHO 2012; Bialvaei and Samadi Kafil 2015), and it is now considered a critically important antibiotic for human medicine despite its known high toxicity (Huang et al. 2010).

Reports have documented the occasional human use of colistin in China due to its efficacy in treating carbapenemase-producing *Enterobacteriaceae* infections (Hu et al. 2012; Zhang et al. 2015). However, in this study, the *mcr-1* resistance gene was detected in some but not all isolates with phenotypic resistance to colistin. The most probable reason for this could be that other variants of the *mcr* gene were responsible for the observed resistance or that other acquired resistance mechanisms other than the transferable *mcr* are attributable. In addition to the MDR phenotypes exhibiting co-resistance to a carbapenem and colistin, multiple resistances to other antibiotics classes were observed. Two other resistance determinants were present in the isolates phenotypically resistant to

ampicillin and erythromycin. High resistance rates among the isolates were observed against ampicillin, erythromycin, tetracycline, and trimethoprim-sulphamethoxazole. It may have resulted from their frequent use in animal husbandry, especially on the farms where the animals were raised. Sobhy et al. (2020) and Henton et al. (2011) have reported that farmers commonly use tetracycline and ampicillin as growth promoters or to prevent animal diseases. Iwu et al. (2016), in a study, carried out within the same locality where the pork was sold also reported a high level of resistance to tetracycline by *E. coli* isolated from swine. Their result was linked with farmers' reliance on tetracycline due to its availability, cost-effectiveness, and broad-spectrum activity. The habitual use of trimethoprim-sulphamethoxazole for treating infections such as respiratory infections in farm animals has been reported (Reuben and Owuna 2013) and could be linked to high resistance.

*E. coli* isolates exhibited the MARI of 0.25–0.75 in this study. It is also comparable with the MARI of 0.2–0.7 reported by Iwu et al. (2016) and 0.2–0.75 reported by Matyar (2012). Studies carried out by Adzitey et al. (2020) revealed a lower MARI of 0.13–0.1 in *E. coli*. The MARI observed in this study suggests the broad use of antibiotics in the swine herds from which the pork was derived, thus indicating that pork could serve as a high-risk source of multidrug-resistant organisms to humans in the study area. The occurrence of this MDR phenotype in *E. coli* is of pressing contemporary concern (Harris et al. 2015), and therefore, stresses the importance of reducing the prevalence of *E. coli* and associated resistant genes in animal husbandry through stringent regulation of antimicrobial usage in veterinary medicine.

## Conclusions

In summary, the prevalence of *E. coli* isolates from retailed pork indicates fecal contamination at slaughter and processing. It calls for better hygiene practices at all stages of pork processing and highlights the importance of consumer awareness of safe pork handling and cooking. Furthermore, the association of imipenem and colistin resistance in the MDR profile is disturbing. Therefore, all unauthorized use of antibiotics, especially last resort antibiotics, should be discouraged where MDR has evolved. Therefore, the public should be educated on the perils of indiscriminate use of antimicrobial drugs. All unauthorized use of antibiotics should be discouraged. In contrast, prudent usage of antibiotics approved for veterinary use should be adopted to stem the rising trend of drug resistance among pathogenic bacteria of animal origin.

**ORCID**
Benson Chuks Iweriebor https://orcid.org/0000-0002-2621-6462

**Acknowledgments**
Authors acknowledge the shop owners who willingly allowed sample collections from their shops.

**Author contributions**
BCI and OSE conceptualized the study, BCI collected and analyzed the samples, BCI and OSE analyzed the results, OSE helped in writing and critiquing the manuscript, CLO provided funding and proofread the manuscript.

**Funding**
Funding was provided by NRF with grant number D400 UCGD.

**Conflict of interest**
The authors do not report any financial or personal connections with other persons or organizations, which might negatively affect the contents of this publication and/or claim authorship rights to this publication.

## Literature

**Adzitey F, Assoah-Peprah P, Teye GA, Somboro AM, Kumalo HM, Amoako DG.** Prevalence and antimicrobial resistance of *Escherichia coli* isolated from various meat types in the Tamale Metropolis of Ghana. Int J Food Sci. 2020 Nov 12;2020:8877196. https://doi.org/10.1155/2020/8877196

**Adzitey F.** The prevention and control of bacterial foodborne hazards in meats and meat products – an overview. J Meat Sci Technol. 2016;4(1):1–10.

**Aminov RI.** Horizontal gene exchange in environmental microbiota. Front Microbiol. 2011;2:158. https://doi.org/10.3389/fmicb.2011.00158

**Amri E, Juma S.** Evaluation of antimicrobial activity and qualitative phytochemical screening of solvent extracts of *Dalbergia melanoxylon* (Guill. and Perr.). Int J Curr Microbiol Appl Sci. 2016 Jul 15;5(7):412–423. https://doi.org/10.20546/ijcmas.2016.507.045

**Ateba CN, Mbewe M, Bezuidenhout CC.** Prevalence of *Escherichia coli* O157 strains in cattle, pigs and humans in North West province, South Africa. S Afr J Sci. 2008;104(1–2):7–8.

**Baek E, Lee D, Jang S, An H, Kim M, Kim K, Lee K, Ha N.** Antibiotic resistance and assessment of food-borne pathogenic bacteria in frozen foods. Arch Pharm Res. 2009 Dec;32(12):1749–1757. https://doi.org/10.1007/s12272-009-2213-y

**Bauer AW, Kirby WMM, Sherris JC, Turck M.** Antibiotic susceptibility testing by a standardized single disk method. Am J Clin Pathol. 1966 Apr 01;45(4_ts):493–496. https://doi.org/10.1093/ajcp/45.4_ts.493

**Bersisa A, Tulu D, Negera C.** Investigation of bacteriological quality of meat from abattoir and butcher shops in Bishoftu, Central Ethiopia. Int J Microbiol. 2019 May 02;2019:6416803. https://doi.org/10.1155/2019/6416803

**Bialvaei AZ, Samadi Kafil H.** Colistin, mechanisms and prevalence of resistance. Curr Med Res Opin. 2015 Apr 03;31(4):707–721. https://doi.org/10.1185/03007995.2015.1018989

**Brunelle BW, Bearson SMD, Bearson BL.** Tetracycline accelerates the temporally-regulated invasion response in specific isolates of multidrug-resistant *Salmonella enterica* serovar Typhimurium. BMC Microbiol. 2013;13(1):202. https://doi.org/10.1186/1471-2180-13-202

**Bumunang EW, McAllister TA, Zaheer R, Ortega Polo R, Stanford K, King R, Niu YD, Ateba CN.** Characterization of Non-O157 *Escherichia coli* from cattle faecal samples in the North-West Province of South Africa. Microorganisms. 2019 Aug 20;7(8):272. https://doi.org/10.3390/microorganisms7080272

**Caine LA, Nwodo U, Okoh A, Ndip R, Green E.** Occurrence of virulence genes associated with diarrheagenic *Escherichia coli* isolated from raw cow's milk from two commercial dairy farms in the Eastern Cape Province, South Africa. Int J Environ Res Public Health. 2014 Nov 18;11(11):11950–11963. https://doi.org/10.3390/ijerph111111950

**CLSI.** Methods for dilution antimicrobial susceptibility tests for bacteria that grow aerobically. Approved standard: M7-A6, 14th ed. Wayne (USA): Clinical and Laboratory Standards Institute; 2016.

**Dandachi I, Chabou S, Daoud Z, Rolain JM.** Prevalence and emergence of extended-spectrum cephalosporin-, carbapenem- and colistin-resistant gram-negative bacteria of animal origin in the Mediterranean basin. Front Microbiol. 2018 Sep 28;9:2299. https://doi.org/10.3389/fmicb.2018.02299

**Elhadi N**. Prevalence and antimicrobial resistance of *Salmonella* spp. in raw retail froze imported freshwater fish to Eastern Province of Saudi Arabia. Asian Pac J Trop Biomed. 2014 Mar;4(3):234–238. https://doi.org/10.1016/S2221-1691(14)60237-9

**Fournier D, Richardot C, Müller E, Robert-Nicoud M, Llanes C, Plésiat P, Jeannot K.** Complexity of resistance mechanisms to imipenem in intensive care unit strains of *Pseudomonas aeruginosa*. J Antimicrob Chemother. 2013 Aug;68(8):1772–1780. https://doi.org/10.1093/jac/dkt098

**Fukuda A, Usui M, Okamura M, Dong-Liang H, Tamura Y.** Role of flies in the maintenance of antimicrobial resistance in farm environments. Microb Drug Resist. 2019 Jan;25(1):127–132. https://doi.org/10.1089/mdr.2017.0371

**Grobbelaar W, Verma A, Shukla VK.** Analyzing human robotic interaction in the food industry. J Phys Conf Ser. 2021 Jan 01; 1714(1):012032. https://doi.org/10.1088/1742-6596/1714/1/012032

**Gwida M, El-Gohary A.** Prevalence and characterization of antibiotic resistance food borne pathogens isolated from locally produced chicken raw meat and their handlers. J Dairy Vet Anim Res. 2015;2(6):238-244. https://doi.org/10.15406/jdvar.2015.02.00062

**Hao H, Cheng G, Iqbal Z, Ai X, Hussain HI, Huang L, Dai M, Wang Y, Liu Z, Yuan Z.** Benefits and risks of antimicrobial use in food-producing animals. Front Microbiol. 2014 Jun 12;5:288. https://doi.org/10.3389/fmicb.2014.00288

**Harris P, Paterson D, Rogers B.** Facing the challenge of multidrug-resistant Gram-negative bacilli in Australia. Med J Aust. 2015 Mar; 202(5):243–246. https://doi.org/10.5694/mja14.01257

**Henton MM, Eagar HA, Swan GE, van Vuuren M.** Part VI. Antibiotic management and resistance in livestock production. S Afr Med J. 2011 Jul 28;101(8 Pt 2):583–586.

**Hoelzer K, Wong N, Thomas J, Talkington K, Jungman E, Coukell A.** Antimicrobial drug use in food-producing animals and associated human health risks: what, and how strong, is the evidence? BMC Vet Res. 2017 Dec;13(1):211. https://doi.org/10.1186/s12917-017-1131-3

**Hu F, Chen S, Xu X, Guo Y, Liu Y, Zhu D, Zhang Y.** Emergence of carbapenem-resistant clinical *Enterobacteriaceae* isolates from a teaching hospital in Shanghai, China. J Med Microbiol. 2012 Jan 01;61(1):132–136. https://doi.org/10.1099/jmm.0.036483-0

**Huang J, Tang YQ, Sun JY.** Intravenous colistin sulfate: A rarely used form of polymyxin E for the treatment of severe multidrug-resistant Gram-negative bacterial infections. Scand J Infect Dis. 2010 Jan;42(4):260–265. https://doi.org/10.3109/00365540903490018

**Iweriebor BC, Iwu CJ, Obi LC, Nwodo UU, Okoh AI.** Multiple antibiotic resistances among Shiga toxin producing *Escherichia coli* O157 in feces of dairy cattle farms in Eastern Cape of South Africa. BMC Microbiol. 2015 Dec;15(1):213. https://doi.org/10.1186/s12866-015-0553-y

**Iwu CJ, Iweriebor BC, Obi LC, Okoh AI.** Occurrence of non-O157 Shiga toxin-producing *Escherichia coli* in two commercial swine farms in the Eastern Cape Province, South Africa. Comp Immunol Microbiol Infect Dis. 2016 Feb;44:48–53. https://doi.org/10.1016/j.cimid.2015.12.004

**Jaja IF, Oguttu J, Jaja CJI, Green E.** Prevalence and distribution of antimicrobial resistance determinants of *Escherichia coli* isolates obtained from meat in South Africa. PLoS One. 2020 May 26;15(5):e0216914. https://doi.org/10.1371/journal.pone.0216914

**Joy SR, Li X, Snow DD, Gilley JE, Woodbury B, Bartelt-Hunt SL.** Fate of antimicrobials and antimicrobial resistance genes in simulated swine manure storage. Sci Total Environ. 2014 May;481:69–74. https://doi.org/10.1016/j.scitotenv.2014.02.027

**Liu YY, Wang Y, Walsh TR, Yi LX, Zhang R, Spencer J, Doi Y, Tian G, Dong B, Huang X, et al.** Emergence of plasmid-mediated colistin resistance mechanism MCR-1 in animals and human beings in China: a microbiological and molecular biological study. Lancet Infect Dis. 2016 Feb;16(2):161–168. https://doi.org/10.1016/S1473-3099(15)00424-7

**Magiorakos AP, Srinivasan A, Carey RB, Carmeli Y, Falagas ME, Giske CG, Harbarth S, Hindler JF, Kahlmeter G, Olsson-Liljequist B, et al.** Multidrug-resistant, extensively drug-resistant and pandrug-resistant bacteria: an international expert proposal for interim standard definitions for acquired resistance. Clin Microbiol Infect. 2012 Mar;18(3):268–281. https://doi.org/10.1111/j.1469-0691.2011.03570.x

**Matyar F.** Antibiotic and heavy metal resistance in bacteria isolated from the Eastern Mediterranean Sea coast. Bull Environ Contam Toxicol. 2012 Sep;89(3):551–556. https://doi.org/10.1007/s00128-012-0726-4

**Mohlatlole RP, Madoroba E, Muchadeyi FC, Chimonyo M, Kanengoni AT, Dzomba EF.** Virulence profiles of enterotoxigenic, Shiga toxin and enteroaggregative *Escherichia coli* in South African pigs. Trop Anim Health Prod. 2013 Aug;45(6):1399–1405. https://doi.org/10.1007/s11250-013-0377-4

**Pires AFA, Stover J, Kukielka E, Haghani V, Aminabadi P, de MELO RAMOS THAIS, Jay-Russell MT.** *Salmonella* and *Escherichia coli* prevalence in meat and produce sold at farmers' markets in Northern California. J Food Prot. 2020 Nov 01;83(11):1934–1940. https://doi.org/10.4315/JFP-20-079

**Poirel L, Kieffer N, Liassine N, Thanh D, Nordmann P.** Plasmid-mediated carbapenem and colistin resistance in a clinical isolate of *Escherichia coli*. Lancet Infect Dis. 2016 Mar;16(3):281. https://doi.org/10.1016/S1473-3099(16)00006-2

**Popowska M, Rzeczycka M, Miernik A, Krawczyk-Balska A, Walsh F, Duffy B.** Influence of soil use on prevalence of tetracycline, streptomycin, and erythromycin resistance and associated resistance genes. Antimicrob Agents Chemother. 2012 Mar;56(3):1434–1443. https://doi.org/10.1128/AAC.05766-11

**Reddy V.** Molecular characterization of *Escherichia coli* from pork meat by whole cell protein finger printing. J Pure Appl Microbiol. 2017 Dec 30;11(4):2045–2049. https://doi.org/10.22207/JPAM.11.4.49

**Reuben RC, Owuna G.** Antimicrobial resistance patterns of *Escherichia Coli* O157: H7 from Nigerian fermented milk samples in Nasarawa State, Nigeria. Int J Pharm Sci Invent. 2013;2(3):38–44.

**Skov RL, Monnet DL.** Plasmid-mediated colistin resistance (*mcr-1* gene): three months later, the story unfolds. Euro Surveill. 2016 Mar 03; 21(9):30155.https://doi.org/10.2807/1560-7917.ES.2016.21.9.30155

**Sobhy NM, Yousef SGA, Aboubakr HA, Nisar M, Nagaraja KV, Mor SK, Valeris-Chacin RJ, Goyal SM.** Virulence factors and antibiograms of *Escherichia coli* isolated from diarrheic calves of

Egyptian cattle and water buffaloes. PLoS One. 2020 May 11;15(5): e0232890. https://doi.org/10.1371/journal.pone.0232890

**Streicher S.** Varkbedryf in SA uitersgesond. Cape Town (South Africa): Landbouweekblad; 2012. p. 59–60.

**Ström G, Boqvist S, Albihn A, Fernström LL, Andersson Djurfeldt A, Sokerya S, Sothyra T, Magnusson U.** Antimicrobials in small-scale urban pig farming in a lower middle-income country – arbitrary use and high resistance levels. Antimicrob Resist Infect Control. 2018 Dec;7(1):35. https://doi.org/10.1186/s13756-018-0328-y

**Tanih NF, Sekwadi E, Ndip RN, Bessong PO.** Detection of pathogenic *Escherichia coli* and *Staphylococcus aureus* from cattle and pigs slaughtered in abattoirs in Vhembe District, South Africa. Scientific World Journal. 2015;2015:1–8. https://doi.org/10.1155/2015/195972

**Tsai YL, Palmer CJ, Sangermano LR.** Detection of *Escherichia coli* in sewage and sludge by polymerase chain reaction. Appl Environ Microbiol. 1993 Feb;59(2):353–357. https://doi.org/10.1128/aem.59.2.353-357.1993

**Turlej-Rogacka A, Xavier BB, Janssens L, Lammens C, Zarkotou O, Pournaras S, Goossens H, Malhotra-Kumar S.** Evaluation of colistin stability in agar and comparison of four methods for MIC testing of colistin. Eur J Clin Microbiol Infect Dis. 2018 Feb; 37(2):345–353. https://doi.org/10.1007/s10096-017-3140-3

**Wang H, McENTIRE JC, Zhang L, Li X, Doyle MP.** The transfer of antibiotic resistance from food to humans: facts, implications and future directions. Rev Sci Tech. 2012 Apr;31(1):249–260. https://doi.org/10.20506/rst.31.1.2117

**WHO.** Antibiotic resistance [Internet]. Geneva (Switzerland): World Health Organization; 2020 [cited 2022 Sep 6]. Available from https://www.who.int/news-room/fact-sheets/detail/antibiotic-resistance

**WHO.** Critically important antimicrobials for human medicine [Internet]. Geneva (Switzerland): World Health Organization; 2012 [cited 2021 Dec 10]. Available from https://www.who.int/publications/i/item/9789241515528

**WHO.** WHO estimates of the global burden of foodborne diseases: foodborne disease burden epidemiology reference group 2007–2015. Geneva (Switzerland): World Health Organization; 2015 [cited 2021 Dec 15]. Available from https://apps.who.int/iris/handle/10665/199350

**Yao X, Doi Y, Lv L, Liu JH.** Carbapenem-resistant and colistin-resistant *Escherichia coli* co-producing NDM-9 and MCR-1. Lancet Infect Dis. 2016;16(3):288–289. https://doi.org/10.1016/S1473-3099(16)00057-8

**Zhang S, Zhu X, Wu Q, Zhang J, Xu X, Li H.** Prevalence and characterization of *Escherichia coli* O157 and O157:H7 in retail fresh raw meat in South China. Ann Microbiol. 2015 Dec;65(4):1993–1999. https://doi.org/10.1007/s13213-015-1037-x

**Xia X, Meng J, McDermott PF, Ayers S, Blickenstaff K, Tran TT, Abbott J, Zheng J, Zhao S.** Presence and characterization of Shiga toxin-producing *Escherichia coli* and other potentially diarrheagenic *E. coli* strains in retail meats. Appl Environ Microbiol. 2010 Mar 15;76(6):1709–1717. https://doi.org/10.1128/AEM.01968-09

ORIGINAL PAPER
Polish Journal of Microbiology
2022, Vol. 71, No 4, 529–538
https://doi.org/10.33073/pjm-2022-047

# Production and Quantification of Virulence Factors in *Malassezia* Species

INÈS HADRICH[1, 2, 3]*, NAHED KHEMEKHEM[1, 2], SOUROUR NEJI[1, 2], HOUAIDA TRABLESI[1, 2], AMIN ILAHI[1], HAYET SELLAMI[1, 2], FATTOUMA MAKNI[1, 2] and ALI AYADI[1, 2]

[1] Laboratory of Fungal and Parasitic Molecular Biology, School of Medicine, University of Sfax, Sfax, Tunisia
[2] Laboratory of Parasitology – Mycology, UH Habib Bourguiba, Sfax, Tunisia
[3] Faculty of Science, University of Gabes, Gabes, Tunisia

Submitted 12 July 2022, accepted 20 September 2022, published online 6 December 2022

Abstract

Seventy-seven strains of *Malassezia* were included in this study. Biofilm and hydrolytic enzyme production were studied by using specific solid media. The Real-Time reverse transcriptase qPCR method was applied to determine the overexpression of genes encoding the extracellular enzymes. All included *Malassezia* species produced biofilms. No statistically significant difference was observed between *Malassezia* species in biofilm formation ($p = 0.567$). All *Malassezia* species produced lipase, and 95% of *Malassezia globosa* showed a strong enzymatic activity ($Pz = 0.55 \pm 0.02$). A statistically significant difference was observed between the mean keratinase indices of *Malassezia slooffiae* and the other *Malassezia* species ($p = 0.005$). The overexpression of one or more genes was observed in 100% of strains isolated from patients with folliculitis, 87.5% – with pityriasis versicolor, and 57.14% of the control group isolates. A statistically significant difference in the lipase gene expression ($p = 0.042$) was between the strains from patients with folliculitis and the control group. This investigation provides more information about the frequency of the production of the major enzymes considered virulence factors of *Malassezia* species. Interestingly, the overexpression of one or more genes was observed in strains isolated from patients with *Malassezia* disorders.

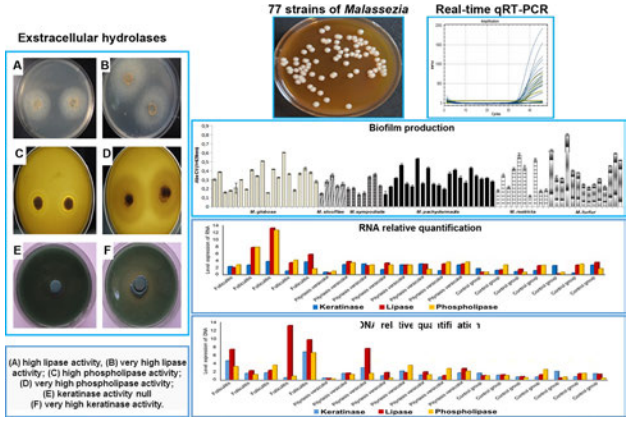


K e y w o r d s: *Malassezia*, Real-Time qRT-PCR, virulence factors, extracellular hydrolases, biofilm

## Introduction

*Malassezia* species, members of the human healthy skin microbiota, may cause a wide range of cutaneous and systemic diseases in predisposed individuals. Thus, they exist at the interface between commensal and pathogen. Their interaction with the human immune system is of great interest, despite being members of the indigenous cutaneous microbial population (Pedrosa et al. 2014).

When the skin's physical, chemical, or immunological mechanisms are altered, these yeasts can become pathogenic (Nardoni et al. 2005; Ashbee 2007; Bond 2010; Shokri et al. 2010; Gaitanis et al. 2012). Classic skin diseases caused by *Malassezia* yeasts include pityriasis versicolor (PV), seborrheic dermatitis, and *Malassezia* folliculitis.

Particular features of *Malassezia* organisms, such as its non-autoaggregation behavior and a very high lipolytic enzyme activity, may play an important role in the pathogenicity of parenteral lipid emulsion *Malassezia* related species (Kaneko et al. 2012).

Recently, the role of *Malassezia* lipases and phospholipases as pathogenicity mechanisms in seborrheic

* Corresponding author: I. Hadrich, Laboratory of Fungal and Parasitic Molecular Biology, School of Medicine, University of Sfax, Sfax, Tunisia; Laboratory of Parasitology – Mycology, UH Habib Bourguiba, Sfax, Tunisia; Faculty of Science, University of Gabes, Gabes, Tunisia; **e-mail: ineshadrich@yahoo.fr**

dermatitis was enhanced by demonstrating significantly increased lipase gene expression (Patiño-Uzcátegui et al. 2011). This finding was also supported by the in vitro induction of phospholipase activity of *Malassezia* seborrheic dermatitis isolates by β-endorphin, another putative virulence factor increased in inflammatory skin conditions (Vlachos et al. 2013).

Among keratinophilic microorganisms, *Malassezia* species can digest keratin, and it plays an important role in their growth and development.

A further health threat these pathogens impose is their propensity to develop biofilm on the skin and at the surface of indwelling medical devices. Biofilm represents a serious medical problem because it promotes resistance to antifungal drugs and acts as a reservoir for seeding infectious organisms at distant places (Cannizzo et al. 2007).

The present study aimed to quantify biofilm production and investigate the extracellular secretion of lipase, phospholipase, and keratinase for six *Malassezia* species by using microbiological and Real-Time reverse transcriptase qPCR methods. In addition, we examined whether virulence factors inherent in the organisms themselves might have clinical significance.

## Experimental

### Materials and Methods

**Isolates.** Seventy-seven strains of *Malassezia* were included in the study: 20 *Malassezia globosa*, 10 *Malassezia restricta*, 14 *Malassezia furfur*, 7 *Malassezia sympodialis,* 5 *Malassezia slooffiae*, and 21 *Malassezia pachydermatis.* They were collected from patients with *Malassezia* folliculitis (12), from babies in a neonatal intensive care unit (20), pityriasis versicolor (10). As a comparison, a group of healthy subjects, 35 healthy individuals with no skin diseases and without any known underlying disease, were also included in this study. Samples were collected from healthy subjects' backs, faces, and napes. These strains were identified by Real-Time qPCR using a specific hydrolysis probe as previously described (Ilahi et al. 2017).

**Evaluation of biofilm formation by crystal violet staining (CVS).** Biofilm formation by *Malassezia* species was assessed using crystal violet staining (CVS), as reported previously, with some modifications (Jin et al. 2003). The strains were cultured on Dixon agar at 32°C for three days. Thus, the culture was suspended in Dixon Liquid. The suspension (150 µl) was adjusted to match turbidity comparable to that of the 0.5 McFarland standard ($10^6$ CFU/ml), and 200 µl of Dixon Liquid were placed into selected wells of 96-well polystyrene microtiter plates (Kartell S.p.A., Italy). The plate was then incubated at 32°C on a shaker at 120 rpm. At 24 h, 200 µl of sterile Dixon Liquid was added and incubated for 48 h under the same conditions. Subsequently, the medium was removed, and each well was washed with sterile ultra-pure water.

For fixation of the biofilm, 200 µl of absolute methanol (15 min) were added and removed. The polystyrene microtiter plates were kept at room temperature for drying, and 200 µl of crystal violet (CV) (1% v/v) was added to each well and incubated for 5 min. Then, multiple washing with ultra-pure water was done until complete elimination of CV and finally, 200 µl of acetic acid was added.

A microtiter plate reader (Bio-Tek Synergy HT, Portugal) at 620 nm was used to read each well's absorbance. The control absorbance values (containing no cells) were subtracted from the values for the test wells to eliminate spurious results due to background interference. Data were recorded as arithmetic means of absorbance values. Experiments were repeated as part of three independent assays, and we calculated the means of three repeats (Abs mean).

**Evaluation of phospholipase production.** The production of phospholipase was assessed using the egg-yolk plate method. Briefly, the isolates were incubated in Dixon agar. Thus, the culture was suspended in Dixon Liquid. Ten microliters of yeast suspension prepared from a fresh culture ($10^6$ cells/ml determined through densitometry) were spot inoculated in triplicate onto the medium and incubated at 32°C for 10 days. The formation of precipitation zones surrounding the colonies was considered an indication of enzyme production. The diameter of the colony (*a*) and the diameter of the precipitation zone plus the diameter of the colony (*b*) were measured. The phospholipase index was designated as Pz = a/b, as described by Coutinho and Paula (Coutinho and Paula 2000; Machado et al. 2010). According to this definition, low Pz values mean high enzymatic production; inversely, high Pz values indicate low enzymatic production. The enzymatic activity was scored into four categories: Pz of 1.0 indicated no enzymatic activity (null); Pz between 0.99 and 0.90 indicated weak enzymatic activity; Pz between 0.89 and 0.70 corresponded to high activity, and low Pz values ≤ 0.69 mean very high enzymatic activities.

**Evaluation of lipase production**. The strains were inoculated in triplicate on agar plates containing Tween® 80 as substrate (Bacto™ Peptone 10 g; sodium chloride 5 g; calcium chloride 0.1 g; agar 20 g; Tween® 80 20% 50 ml; water 950 ml) and incubated for seven days at 32°C. Precipitation halo and colony size were measured.

Degradation intensity was gauged by the ratio between colony diameter and precipitation halo (Pz). Pz coefficients were grouped into five classes: deficient

Table I
The sequences of primers and probes used in RT-qPCR for gene expression studies in 20 *Malassezia globosa* isolates.

| Enzymes | Names | Sequences |
|---|---|---|
| Keratinase | KerF | 5'-ACGTCATGCTCAGATTGCAG-3' |
| | KerR | 5'-GACTTCCGCGAAGAACAAAG-3' |
| | KerP | 5'-FAM-CACAATTGCTCCCGATACCT-MGB |
| Lipase | LipF | 5'-ACCCAACATTTGCTTCGTTC-3' |
| | LipR | 5'-TCAATTATCAATGGTCGCGA-3' |
| | LipP | 5'-FAM-CCTTGGTGGTCGTCAAAGTT-MGB |
| Phospholipase | PhosF | 5'-AACTGGTGGATTTGCTGACC-3' |
| | PhosR | 5'-CTTTACGGGTCCAAGGTGAA-3' |
| | PhosP | 5'-FAM-CCGTGTGCCATTCTACATTG-MGB |
| Actin | ActF | 5'-CTCTCCTTGTACGCCTCTGG-3' |
| | ActR | 5'-TTGACAAGATGCTCCGTCAG-3' |
| | ActP | 5'-TET-GTATTGTGCTGGACTCGGGT-MGB |

group: Pz between 0.9 and 1, low group: Pz between 0.89–0.8, high group: Pz between 0.79–0.70; and very high group: Pz less than 0.69 or null (Pz = 1).

**Evaluation of keratinase production.** Keratin substrate (KS) was extracted from white chicken feathers. Ten grams of feathers were heated in 200 ml of DMSO (dimethylsulfoxide) for 2 hours at 100°C. The solution was precipitated for soluble keratin by using two volumes of cold acetone for one volume of the protein. Then, the caseous precipitate of keratin was suspended in 0.1 M of phosphate buffer. Afterward, soluble keratin was added to the solid medium at a concentration of 0.06%. The solid medium was inoculated with a micropipette by injecting 10 µl of standard suspension into the center of the Petri plate, and then incubated at 32°C. Control plates contained medium without keratin. The formation of precipitate zones around the colonies indicated keratinase production, and the zone was examined and measured. Pz coefficients were grouped into five classes as it was described for lipase activity.

**Virulence gene expression.** An RT-qPCR assay was newly developed to explore the virulence gene expression of 20 *M. globosa* isolates. The levels of mRNA and DNA copies keratinase (MGL_2332), lipase (LIP1 (MGL_0797)), phospholipase (MGL_3326), and the actin reference gene (ACT1) were measured.

The primers and probes were designed using Primer3 software (http://bioinfo.ut.ee/primer3-0.4.0), verified by using sequence manipulation suite software (http://bioinformatics.org/sms2) and were summarized in Table I.

Cellular lysates were prepared from cells grown in culture in Dixon medium (reference) and lipase, keratinase, and phospholipase medium to mid-log phase using proteinase K (Qiagen®, Germany).

RNA was extracted from cellular lysates using the RNeasy Mini Kit (Qiagen®, Germany) according to the manufacturers' instruction, and treated with DNase (Promega, USA).

For cDNA synthesis, 2.5 µl of total RNA was used as a template, and subsequent reverse transcription was performed using the PrimeScript RT Reagent Kit (Perfect Real Time) from TaKaRa (Shiga, Japan), following the manufacturer's instructions.

The reaction mixture (20 µl) for the TaqMan assay contained 10 µl TaqMan Universal PCR Master Mix (Applied Biosystems, UK), 20 pmol of forward and reverse primers, 7 pmol of hydrolysis probe, and 1 µl of the template (extracted DNA or cDNA). The thermal conditions were as follows: initial holding stage at 50°C for 2 min and 95°C for 10 min, followed by 50 cycles at 95°C for 15 s and a final step at 54°C for 1 min. All reactions were performed in triplicate in 48-well reaction plates using a CFX 96 Real-Time System (Bio-Rad, USA) according to the MIQE guideline (available at: http://clinchem.aaccjnls.org/content/55/4/611).

Fold changes in the target gene expression were then normalized to the reference gene via the published comparative 2-ΔΔCq method according to the formula: RQ = 2 – (Cq target – Cq reference) tested – (Cq target – Cq reference) control (VanGuilder et al. 2008). Reference control was the isolate (TN371, KU597270) cultured in Dixon medium (keratinase (null), lipase (low), and phospholipase (low)). An expression change of 2.5 times or an increase in gene copy number was considered as a gene overexpression.

**Statistical analysis.** Statistical analyses were performed using IBM SPSS software (version 20.0; IBM SPSS Inc., USA). Categorical variables were compared using the $\chi^2$ or Fisher's exact test and continuous variables by the ANOVA test. A $p$-value of 0.05 was

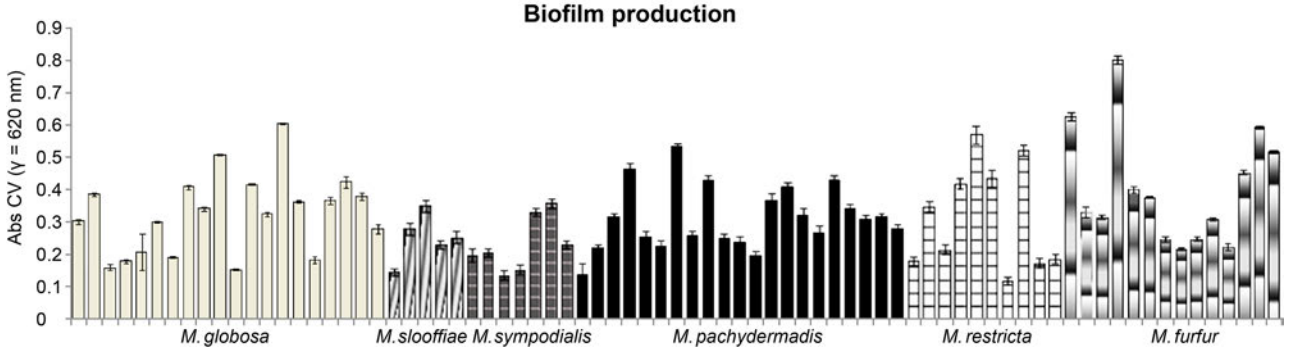


Fig. 1. Different *Malassezia* species biofilm quantification after crystal violet staining (Abs CV). Error bars represent a standard deviation.

considered significant. Pearson's correlation coefficient ($r$) was calculated to measure the correlation between different virulence factors. Where the value was equal to 1, it meant a perfect positive correlation, the value $r = 0$ meant no correlation, and the value of –1 meant a perfect negative correlation.

## Results

**Biofilm formation.** All *Malassezia* species formed biofilm (Fig. 1). The biofilm formation was estimated in triplicate, and an average was calculated for each isolate (Fig. 1). The absorbance for crystal violet after biofilm staining was as follows: 0.322 ± 0.01 for *M. globosa*, 0.336 ± 0.01 for *M. furfur*, 0.336 ± 0.02 for *M. restricta*, 0.349 ± 0.02 for *M. pachydermatis*, 0.256 ± 0.02 for *M. slooffiae*, and 0.235 ± 0.02 for *M. sympodialis* (Table II).

No statistically significant difference was observed between *Malassezia* species in biofilm formation ($p = 0.567$). Strains collected from neonates had the highest biofilm production (Abs mean = 0.396 ± 0.02), followed by strains from folliculitis (Abs mean = 0.342 ± ± 0.01), and pityriasis versicolor (Abs mean = 0.313 ± 0.02). However, there was no statistically significant association between the biofilm-forming ability and the clinical origin of the isolates ($p = 0.570$). Strains isolated from the control group formed biofilms to a lesser degree (Abs mean = 0.291 ± 0.02) (Table II). Furthermore, we noted that the total biofilm biomass formed in vitro by *Malassezia* isolates from patients was higher than those formed by *Malassezia* healthy skin isolates ($p = 0.02$).

**Lipase activity.** All *Malassezia* species displayed lipase activity (Fig. 2). Nineteen isolates of *M. globosa* (95%) (Pz = 0.55 ± 0.02) and five isolates of *M. sympodialis* (71.43%) (Pz = 0.54 ± 0.02) showed a very high enzymatic activity (Table III).

Strains isolated from pityriasis versicolor showed very high activity with Pz values between 0,28 and 0.36 (Table IV). Nevertheless, no statistically significant difference was observed between the mean lipase indices for different *Malassezia* species inducing different pathologies ($p = 0.356$).

However, a statistically significant difference was noted in lipase activity between *M. globosa* isolates from pityriasis versicolor and healthy skin ($p = 0.001$).

**Phospholipase activity.** All isolates of *M. furfur*, *M. globosa*, *M. sympodialis*, *M. slooffiae* and *M. pachydermatis* included in this study demonstrated a high

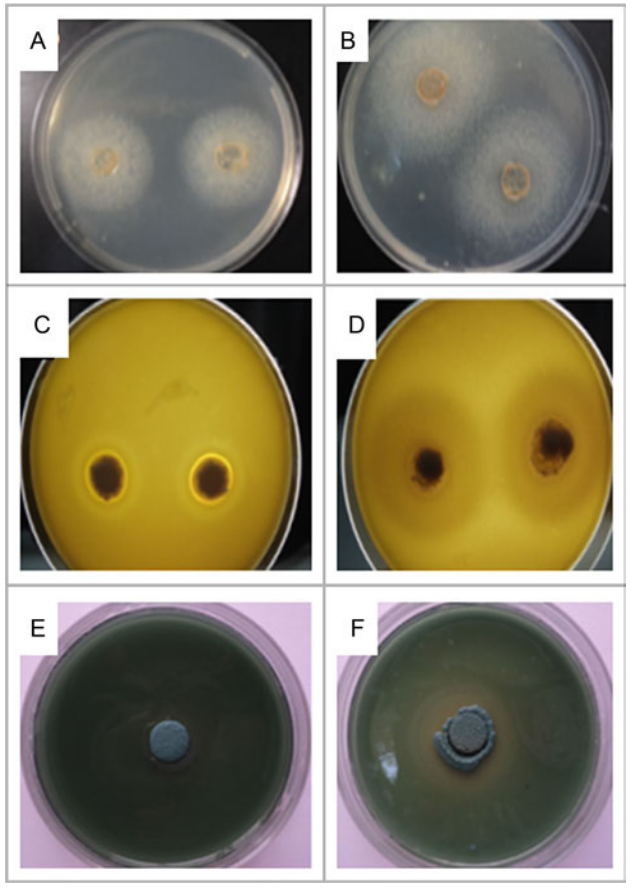


Fig. 2. *Malassezia* species colonies of A) high lipase activity, B) very high lipase activity, C) high phospholipase activity, D) very high phospholipase activity, E) keratinase activity null, F) very high keratinase activity.

Table II
Biofilm production by *Malassezia* species isolated from different clinical sites.

| Groups | *Malassezia globosa* | | *Malassezia restricta* | | *Malassezia furfur* | | *Malassezia sympodialis* | | *Malassezia slooffiae* | | *Malassezia pachydermatis* | | Total |
|---|---|---|---|---|---|---|---|---|---|---|---|---|---|
| | Mean Abs ± SD | Range | Mean Abs ± SD | Range | Mean Abs ± SD | Range | Mean Abs ± SD | Range | Mean Abs ± SD | Range | Mean Abs ± SD | Range | Mean Abs ± SD |
| Folliculitis (N = 12) | 0.321 ± 0.01 | 0.155–0.41 | 0.366 ± 0.01 | 0.301–0.398 | 0.339 ± 0.01 | 0.317–0.594 | 0 | | 0 | | 0 | | 0.342 ± 0.01 |
| Neonates group (N = 20) | 0 | 0 | | 0.433 ± 0.02 | | 0 | | 0 | | 0.361 ± 0.02 | 0.30–0.54 | 0.396 ± 0.02 | |
| Pityriasis versicolor (N = 10) | 0.317 ± 0.01 | 0.16–0.604 | 0.306 ± 0.02 | | 0.316 ± 0.02 | | 0 | | 0 | | 0 | | 0.313 ± 0.02 |
| Control group (N = 35) | 0.328 ± 0.01 | 0.18–0.51 | 0.338 ± 0.02 | 0.12–0.311 | 0.255 ± 0.02 | 0.12–0.311 | 0.235 ± 0.02 | 0.137–0.361 | 0.256 ± 0.02 | 0.167–0.331 | 0.336 ± 0.02 | 0.22–0.44 | 0.291 ± 0.02 |
| Total | 0.322 ± 0.01 | 0.155–0.604 | 0.336 ± 0.02 | 0.12–0.572 | 0.336 ± 0.02 | 0.12–0.594 | 0.235 ± 0.02 | 0.137–0.362 | 0.256 ± 0.03 | 0.167–0.332 | 0.349 ± 0.02 | 0.22–0.54 | |

N – number of tested isolates; SD – standard deviation

Table III
Level of phospholipase, lipase, and keratinase production by *Malassezia* species.

| | Phospholipase activity number of isolates (rate of isolates) | | | | Lipase activity number of isolates (rate of isolates) | | | Keratinase activity number of isolates (rate of isolates) | | | |
|---|---|---|---|---|---|---|---|---|---|---|---|
| | Mean (Pz) ± SD | very high n (%) | high n (%) | Nul n (%) | Mean (Pz) ± SD | very high n (%) | high n (%) | Mean (Pz) ± SD | very high n (%) | high n (%) | null |
| *Malassezia globosa* (N = 20 ) | 0.64 ± 0.03 | 9 (45) | 11 (55) | 0 (0) | 0.55 ± 0.02 | 19 (95) | 1 (5) | 0.65 ± 0.02 | 10 (50) | 6 (30) | 4 (20) |
| *Malassezia restricta* (N = 10) | 0.76 ± 0.02 | 0 (0) | 7 (70) | 3 (30) | 0.36 ± 0.03 | 10 (100) | 0 (0) | 0.69 ± 0.02 | 0 (0) | 2 (20) | 8 (80) |
| *Malassezia furfur* (N = 14) | 0.64 ± 0.02 | 2 (14.29) | 12 (85.71) | 0 (0) | 0.45 ± 0.03 | 14 (100) | 0 (0) | 0.67 ± 0.02 | 1 (7.15) | 6 (42.85) | 7 (50) |
| *Malassezia sympodialis* (N = 7) | 0.67 ± 0.02 | 1 (14.29) | 6 (85.71) | 0 (0) | 0.54 ± 0.02 | 5 (71.43) | 2 (28.57) | 0.62 ± 0.03 | 1 (14.3) | 3 (42.85) | 3 (42.85) |
| *Malassezia slooffiae* (N = 5) | 0.64 ± 0.02 | 2 (40) | 3 (60) | 0 (0) | 0.4 ± 0.04 | 5 (100) | 0 (0) | 0.67 ± 0.02 | 2 (40) | 3 (60) | 0 (0) |
| *Malassezia pachydermatis* (N = 21) | 0.64 ± 0.03 | 9 (42.86) | 12 (57.14) | 0 (0) | 0.31 ± 0.02 | 21 (100) | 0 (0) | 0.68 ± 0.02 | 3 (14.29) | 8 (38.5) | 10 (47.66) |
| Total | 0.66 ± 0.02 | 23 (29.87) | 51 (66.23) | 3 (3.9) | 0.48 ± 0.02 | 74 (91.1) | 3 (3.9) | 0.66 ± 0.02 | 17 (22.08) | 28 (36.36) | 32 (41.56) |

N – number of tested isolates
n – number of isolates with positive activity for the corresponding hydrolytic enzyme
SD – standard deviation

Table IV
Enzymatic activities of *Malassezia* species isolated from different clinical sites.

| | | Folliculitis (N = 12) | Neonates group (N = 20) | Pityriasis versicolor (N = 10) | Control group (N = 35) |
|---|---|---|---|---|---|
| Phospholipase activity Mean (Pz) ± SD | *Malassezia globosa* (N = 20) | 0.69 ± 0.01 (5/12) | – (0/20) | 0.74 ± 0.02 (8/10) | 0.73 ± 0.02 (7/35) |
| | *Malassezia restrict* (N = 10) | 0.67 ± 0.01 (1/12) | – (0/20) | 0.8 ± 0.02 (1/10) | 0.83 ± 0.02 (8/35) |
| | *Malassezia furfur* (N = 14) | 0.74 ± 0.01 (6/12) | 0.70 ± 0.02 (1/20) | 0.69 ± 0.02 (1/10) | 0.71 ± 0.01 (6/35) |
| | *Malassezia sympodialis* (N = 7) | – (0/12) | – (0/20) | – (0/10) | 0.78 ± 0.02 (7/35) |
| | *Malassezia slooffiae* (N = 5) | 0 (0/12) | – (0/20) | – (0/10) | 0.77 ± 0.02 (5/35) |
| | *Malassezia pachydermatis*(N = 21) | 0 (0/12) | 0.66 ± 0.02 (19/20) | – (0/10) | 0.79 ± 0.01 (2/35) |
| | Total | 0.70 ± 0.01 | 0.68 ± 0.02 | 0.74 ± 0.02 | 0.77 ± 0.02 |
| Lipase activity Mean (Pz) ± SD | *Malassezia globosa* (N = 20) | 0.36 ± 0.01 (5/12) | – (0/20) | 0.36 ± 0.02 (8/10) | 0.38 ± 0.02 (7/35) |
| | *Malassezia restricta* (N = 10) | 0.37 ± 0.01 (1/12) | – (0/20) | 0.32 ± 0.02 (1/10) | 0.36 ± 0.02 (8/35) |
| | *Malassezia furfur* (N = 14) | 0.32 ± 0.02 (6/12) | 0.39 ± 0.02 (1/20) | 0.28 ± 0.01 (1/10) | 0.36 ± 0.02 (6/35) |
| | *Malassezia sympodialis* (N = 7) | – (0/12) | – (0/20) | – (0/10) | 0.48 ± 0.02 (7/35) |
| | *Malassezia slooffiae* (N = 5) | – (0/12) | – (0/20) | – (0/10) | 0.4 ± 0.01 (5/35) |
| | *Malassezia pachydermatis* (N = 21) | – (0/12) | 0.31 ± 0.01 (19/20) | – (0/10) | 0.38 ± 0.02 (2/35) |
| | Total | 0.35 ± 0.02 | 0.35 ± 0.02 | 0.32 ± 0.02 | 0.39 ± 0.02 |
| Keratinase activity Mean (Pz) ± SD | *Malassezia globosa* (N = 20) | 0.75 ± 0.02 (5/12) | – (0/20) | 0.62 ± 0.02 (8/10) | 0.85 ± 0.02 (7/35) |
| | *Malassezia restricta* (N = 10) | 1 (1/12) | – (0/20) | 0.65 ± 0.02 (1/10) | 1 (8/35) |
| | *Malassezia furfur* (N = 14) | 0.82 ± 0.02 (6/12) | 0.53 ± 0.02 (1/20) | 0.65 ± 0.02 (1/10) | 0.96 ± 0.02 (6/35) |
| | *Malassezia sympodialis* (N = 7) | – (0/12) | – (0/20) | – (0/10) | 0.84 ± 0.02 (7/35) |
| | *Malassezia slooffiae* (N = 5) | – (0/12) | – (0/20) | – (0/10) | 0.8 ± 0.02 (5/35) |
| | *Malassezia pachydermatis* (N = 21) | – (0/12) | 0.85 ± 0.02 (19/20) | – (0/10) | 0.79 ± 0.02 (2/35) |
| | Total | 0.86 ± 0.02 | 0.69 ± 0.02 | 0.64 ± 0.02 | 0.873 ± 0.02 |

N – number of tested isolates; SD – standard deviation

or very high phospholipase activity (Fig. 2). However, only 70% of the *M. restricta* isolates showed high activity (Table III). A high activity level with Pz values (0.66 ± 0.02) was found in 95% of isolates from neonates (Table IV).

No statistically significant difference was observed between the mean phospholipase production of *Malassezia* species inducing different pathologies ($p = 0.65$). However, a statistically significant difference between pityriasis versicolor isolates and healthy skin isolates was noted for *M. globosa* phospholipase activity ($p = 0.001$).

**Keratinase activity.** The Pz values for the keratinase activity of *Malassezia* isolates ranged from 0.33 to 0.91. All *M. slooffiae* strains showed positive keratinase activity (Fig. 2), and 40% were shown to be very high producers (Table III).

Sixteen isolates of *M. globosa* (80%) (Pz = 0.65 ± 0.02), four isolates of *M. sympodialis* (57.15%) (Pz = 0.62 ± 0.03), seven isolates of *M. furfur* (50%) (Pz = 0.67 ± 0.02), two isolates of *M. restricta* (20%) (Pz = 0.69 ± 0.02), and 11 isolates *M. pachydermatis* (52.29%) (Pz = 0.68 ± 0.02) showed keratinase activity (Table III).

A statistically significant difference was observed between the mean keratinase indices of *M. slooffiae* and the other *Malassezia* species ($p = 0.005$). In addition, a statistically significant difference between *M. globosa* isolates from pityriasis versicolor and healthy skin was noted for keratinase activity ($p = 0.001$).

A positive correlation between secretion of keratinase and phospholipase ($r = 0.31$, $p < 0.001$) was also observed.

**Expression of keratinase, lipases, and phospholipases of *M. globosa*.** RT-qPCR was used for the quantitative study on the expression and copy number of three genes (encoding keratinase, lipase, and phospholipase) responsible for the virulence of 20 *M. globosa* strains collected from patients with folliculitis (5), pityriasis versicolor (8), and a control group (7). Their expression was compared to the ACT1 gene and the isolates (TN371, KU597270) cultured in the Dixon medium. The overexpression of one or more genes was observed in 5/5 (100%) of strains isolated from patients with folliculitis, in 7/8 (87.5%) from pityriasis versicolor isolates, and in 3/7 (42.85%) control group isolates (Table V). The increase in expression of keratinase varied from 0.81 to 3.52 folds and the increase of lipase varied from 1.84 to 12.99 folds in folliculitis strains. The phospholipase's highest expression level was 12.4 folds in the S3 isolate collected from folliculitis (Table V). Upregulation of the enzyme expression was noted in strains

Table V
Relative quantification of gene expression and keratinase, lipase, and phospholipase genes copy number in 20 *Malassezia globosa* strains.

| ID | Clinical sites | RNA relative quantification | | | DNA relative quantification | | |
|---|---|---|---|---|---|---|---|
| | | Keratinase | Lipase | Phospholipase | Keratinase | Lipase | Phospholipase |
| S1 | Folliculitis | 2.11 | 1.84 | **2.59** | **4.43** | **7.22** | **3.06** |
| S2 | Folliculitis | **2.52** | **7.51** | **7.57** | 1.36 | 2.04 | 1.08 |
| S3 | Folliculitis | **3.52** | **12.99** | **12.40** | 1.50 | 2.12 | **3.36** |
| S4 | Folliculitis | 0.81 | **3.20** | **3.91** | 0.32 | **12.98** | 0.69 |
| S5 | Folliculitis | **3.40** | **5.55** | 1.48 | **6.58** | **9.57** | **6.36** |
| S6 | Pityriasis versicolor | 0.49 | 0.31 | 0.78 | 0.29 | 0.21 | 0.02 |
| S7 | Pityriasis versicolor | **2.65** | **3.52** | **3.17** | 1.35 | 1.46 | 1.10 |
| S8 | Pityriasis versicolor | **2.82** | 2.35 | **2.54** | **2.79** | **7.43** | 1.34 |
| S9 | Pityriasis versicolor | 1.25 | **3.10** | **2.53** | 0.77 | 1.60 | 0.24 |
| S10 | Pityriasis versicolor | **2.57** | **2.55** | **2.52** | 1.96 | 1.56 | **3.33** |
| S11 | Pityriasis versicolor | **2.84** | **2.75** | 1.32 | 0.97 | 1.74 | 1.03 |
| S12 | Pityriasis versicolor | 0.96 | **2.86** | **3.37** | 0.46 | 0.86 | **2.56** |
| S13 | Pityriasis versicolor | **2.55** | **2.86** | **3.38** | 1.50 | **2.58** | 1.88 |
| S14 | Control group | 1.53 | 0.53 | 0.56 | 1.42 | 0.82 | 0.75 |
| S15 | Control group | 1.04 | 1.19 | **2.55** | 0.92 | 1.05 | 0.86 |
| S16 | Control group | 0.67 | 1.36 | 0.48 | 0.50 | 0.61 | 0.32 |
| S17 | Control group | 0.94 | 2.37 | 2.43 | 0.50 | 1.06 | 2.33 |
| S18 | Control group | 2.36 | 0.07 | 0.48 | 1.87 | 0.26 | 0.49 |
| S19 | Control group | 0.24 | **2.52** | **2.80** | 0.56 | 1.31 | 1.39 |
| S20 | Control group | **2.51** | **3.30** | 1.50 | 1.31 | 1.18 | 0.27 |

collected from the control group as follows: lipase in only one isolate; and keratinase and phospholipase in two isolates. A statistically significant difference in the lipase gene expression ($p = 0.042$) was observed in the strains collected from patients with folliculitis compared to the group control. The overproduction of three genes was observed in five strains (S2, S3, S7, S10, and S13). The overexpression of the keratinase, lipase, and phospholipase genes was associated with an increased copy number of the corresponding genes in eight strains of *M. globosa* (Table V).

In addition, correlation analysis with Pearson's coefficient revealed a statistically significant positive association between the production of the enzymes and the expression of their genes: keratinase ($r = 0.881$, $p < 0.0001$), lipase ($r = 0.530$, $p = 0.016$), and phospholipase ($r = 0.754$, $p = 0.0001$).

## Discussion

In the present study, we examined multiple virulence factors, such as extracellular secreted hydrolytic enzymes and biofilm development which contribute to the ability of *Malassezia* species to colonize host tissues and cause disease. However, only a few studies focused on virulence factors' expression and pathogenesis of the *Malassezia* species. Our results demonstrated that all *Malassezia species* included in our study, like many other fungal and bacterial species, produced biofilms (Davey and O'Toole 2000).

A better knowledge of the mechanisms of antifungal drug resistance may lead to developing novel therapies for biofilm-based diseases. Multiple mechanisms have been proposed for the biofilm resistance (Mukherjee and Chandra 2004). Metabolic quiescence has been proposed as a mechanism of antimicrobial resistance in biofilm bacteria (Mah and O'Toole 2001) and fungi (Mukherjee and Chandra 2004). However, our data revealed that CVS staining showed biofilm cells to be active in our *Malassezia* species, in line with previous data for *Candida albicans* and *Candida parapsilosis* (Kuhn et al. 2002). Therefore, biofilm production is unlikely to significantly promote the antifungal resistance of *Malassezia* species (Mukherjee and Chandra 2004). Biofilm production has been studied only for *M. furfur* (Simonetti et al. 2016; Angiolella et al. 2018) and *M. pachydermatis* (Figueredo et al. 2012). Angiolella et al. (2018) demonstrated that biofilm adherence and hydrophobicity are virulence factors in *M. furfur*. Also, these studies showed that *M. pachydermatis* strains from dogs with or without skin lesions can form

a biofilm with variable quantity and structures, which are likely to be strain-dependent (Figueredo et al. 2012).

In our study, we showed that all *Malassezia* species produced lipase, and 95% of *M. globosa* showed a very high enzymatic activity. Lipases catalyze the hydrolysis of ester bonds of triacylglycerols, resulting in the release of fatty acids. In almost all organisms, lipases play essential roles in lipid metabolism, including digestion, transport, and processing of dietary lipids. Lipases also play essential roles in the virulence of skin-associated lipophilic fungal pathogens such as *Malassezia* spp. The gene that encodes lipase in *M. furfur*, *M. pachydermatis*, and *M. globosa* has been identified, and the recent genome sequencing efforts have revealed at least 14 lipase-encoding genes in *M. globosa* (Figueredo et al. 2012). Juntachai et al. (2009) suggested that lipase may be a pathogenic factor in *Malassezia* skin disease and explained why *M. globosa* is an important pathogenic species in several human skin diseases despite its slow rate of growth (Jin et al. 2003). We showed a high lipase activity from *M. globosa* strains isolated from pityriasis versicolor. In the previous studies, *M. globosa*, one of the most frequently isolated *Malassezia* spp. from patients with dandruff and seborrheic dermatitis, displayed extracellular lipase activity (Plotkin et al. 1996; DeAngelis et al. 2007; Vlachos et al. 2013).

Phospholipase activity exhibited by pathogenic microorganisms is another virulence factor that permits hydrolyzing one or more ester linkages in glycerophospholipids, releasing free fatty acids. In this study, all strains could express phospholipase except for *M. restricta*. Only 70% of isolates of this species were phospholipase producers. Additionally, we noted a high phospholipase activity for *Malassezia* isolates recovered from neonates. This virulence factor intrinsic to *Malassezia* yeasts has been discussed in association with the pathogenesis of seborrheic dermatitis. The increased level of production of phospholipase has been shown only for pathogenic *M. pachydermatis* strains (Cannizzo et al. 2007).

Current information on phospholipases in *Malassezia* spp. is limited. Juntachai et al. (2009) detected extracellular phospholipase activities in *M. furfur*, *M. pachydermatis*, *M. slooffiae*, *M. sympodialis*, *M. globosa*, *M. restricta*, and *M. obtusa*. However, enzyme activity was higher only in *M. pachydermatis* (Juntachai et al. 2009). The ability to express enzymes not only varied among different species of *Malassezia* but also differed among the strains of the same species isolated from different clinical manifestations. We showed a statistically significant difference in *M. globosa* phospholipase activity between pityriasis versicolor isolates and healthy skin isolates. The production of *Malassezia* phospholipases on the skin could result in the removal of epidermal lipids, disruption of the epidermal barrier function, and the development of seborrheic dermatitis when sebum production is constitutionally decreased (Cannizzo et al. 2007).

Keratinases are proteolytic enzymes in nature. They mainly attack the disulfide bond of the keratin substrate (Böckle et al. 1995; Gupta and Ramnani 2006). As previously reported, the dermatophytes and non-dermatophytes species were both keratinase producers capable of damaging the keratinized structure of the skin (Yu et al. 1971; Takiuchi et al. 1984; Gupta and Ramnani 2006). In our study, all *M. slooffiae* isolates were keratinase producers. However, only half of *M. furfur* had positive enzymatic activity. Peyton et al. found that *M. furfur* can degrade keratin (Gupta and Ramnani 2006; Peyton et al. 2012). However, Gupta and Ramnani (2006) reported a lack of keratinase activity of *M. furfur.*

Our study found a positive correlation between the secretion of keratinase and phospholipase. These virulence factors appear to act synergistically to contribute to the virulence of *Malassezia* strains. The high enzymatic activity shown in our *Malassezia* isolates could be responsible for this yeast changing from a commensal to a pathogenic status.

*Malassezia* isolates from patients with different pathologies had an enzymatic activity ($p = 0.001$) and biofilm biomass ($p = 0.02$) significantly higher than those isolated from healthy individuals. This observation suggests that the enzymatic activity of *Malassezia* may play a role in the onset of skin lesions. Others confirm these results (Pini and Faggi 2011; Angiolella et al. 2018).

The genome sequencing data revealed that *M. globosa* possesses the genes encoding for 14 lipases and nine phospholipases. Among them, four lipases (MGL_3878, MGL_3507 MGL_0799, and MGL_0798) and two phospholipases (MGL_4252 and MGL_3326) were expressed on human scalps (Xu et al. 2007). Based on the activity and expression levels of *MgLip2* in *M. globosa*, the Lip lipase family appears to have the highest impact on the pathogenicity of *M. globosa* (Sommer et al. 2016; Lan et al. 2017). Few studies were carried out to analyze the expression of lipases and phospholipases of the fungus (Brunke and Hube 2006). However, to our knowledge, no information is currently available for the expression of keratinase. In our study, the RT-qPCR analysis of the expression and copy number of these genes in 20 *M. globosa* isolates showed the overexpression of one or more genes in 5/5 isolates from folliculitis and 7/8 from pityriasis versicolor. The phospholipase's highest expression level was 12.4 folds by the isolates collected from folliculitis.

Moreover, we noted a statistically significant difference in the lipase gene expression ($p = 0.042$) that was higher in the strains collected from patients with folliculitis compared to the control group. These data

imply a possible role of lipase in the host environment to produce free fatty acids for the fungus. The concurrent overproduction of three genes was observed in five strains isolated from patients with folliculitis and pityriasis versicolor. However, overexpression was noted in only two control group cases, suggesting that these enzymes play an important role in the pathogenicity of *Malassezia* disorder inducing a transition from colonization to infection. Interestingly, further studies evaluated the expression of lipases and phospholipases of *M. restricta* in patients with seborrheic dermatitis and suggested that the most of the patients' isolates expressed these enzymes (Lee et al. 2013).

Moreover, Patiño-Uzcátegui et al. (2011) found a significantly higher expression of *Mgl0797*, *Mgl0798*, and *Mflip1* virulence genes in seborrheic dermatitis HIV patients. They concluded that lipases may be related to developing seborrheic dermatitis and could be considered virulence factors.

In the study of Aghaei Gharehbolagh et al. (2018), RT-PCR was used to investigate the contribution of the *MGL_3741* gene to the pathogenicity of *M. globosa* in pityriasis versicolor. These authors revealed that this gene can be related to the yeast's pathogenicity and is a candidate for the new antifungal search for a better treatment of pityriasis versicolor (Aghaei Gharehbolagh et al. 2018). However, further studies are still needed to determine its role.

This investigation provides more information about the production frequency of the significant enzymes considered virulence factors of *Malassezia* species. Interestingly, the overexpression of one or more genes was observed in strains isolated from patients with the *Malassezia* disorder. These data emphasize the role of lipase and phospholipase in the pathogenicity of this fungus and suggest that these enzymes can act synergistically in *Malassezia*-induced pathologies.

**Acknowledgments**

This research was funded by the Ministry of Higher Education and Scientific Research, Tunisia.

**Conflict of interest**

The authors do not report any financial or personal connections with other persons or organizations, which might negatively affect the contents of this publication and/or claim authorship rights to this publication.

## Literature

**Aghaei Gharehbolagh S, Kordbacheh P, Hashemi SJ, Daie Ghazvini R, Asgari Y, Agha Kuchak Afshari S, Seyedmousavi S, Rezaie S.** *MGL_3741* gene contributes to pathogenicity of *Malassezia globosa* in pityriasis versicolor. Mycoses. 2018 Dec;61(12):938–944. https://doi.org/10.1111/myc.12840

**Angiolella L, Leone C, Rojas F, Mussin J, de Los Angeles Sosa M, Giusiano G.** Biofilm, adherence, and hydrophobicity as virulence factors in *Malassezia furfur*. Med Mycol. 2018 Jan 1;56(1):110–116. https://doi.org/10.1093/mmy/myx014

**Ashbee HR.** Update on the genus *Malassezia*. Med Mycol. 2007 Jun; 45(4):287–303. https://doi.org/10.1080/13693780701191373

**Böckle B, Galunsky B, Müller R.** Characterization of a keratinolytic serine proteinase from *Streptomyces pactum* DSM 40530. Appl Environ Microbiol. 1995 Oct;61(10):3705–3710. https://doi.org/10.1128/aem.61.10.3705-3710.1995

**Bond R.** Superficial veterinary mycoses. Clin Dermatol. 2010 Mar 4;28(2):226–236. https://doi.org/10.1016/j.clindermatol.2009.12.012

**Brunke S, Hube B.** *MfLIP1*, a gene encoding an extracellular lipase of the lipid-dependent fungus *Malassezia furfur*. Microbiology (Reading). 2006 Feb;152(2):547–554. https://doi.org/10.1099/mic.0.28501-0

**Cannizzo FT, Eraso E, Ezkurra PA, Villar-Vidal M, Bollo E, Castellá G, Cabañes FJ, Vidotto V, Quindós G.** Biofilm development by clinical isolates of *Malassezia pachydermatis*. Med Mycol. 2007 Jun;45(4):357–361. https://doi.org/10.1080/13693780701225767

**Coutinho SD, Paula CR.** Proteinase, phospholipase, hyaluronidase and chondroitin-sulphatase production by *Malassezia pachydermatis*. Med Mycol. 2000 Feb;38(1):73–76. https://doi.org/10.1080/mmy.38.1.73.76

**Davey ME, O'Toole GA.** Microbial biofilms: from ecology to molecular genetics. Microbiol Mol Biol Rev. 2000 Dec;64(4):847–867. https://doi.org/10.1128/MMBR.64.4.847-867.2000

**DeAngelis YM, Saunders CW, Johnstone KR, Reeder NL, Coleman CG, Kaczvinsky JR Jr, Gale C, Walter R, Mekel M, Lacey MP, et al.** Isolation and expression of a *Malassezia globosa* lipase gene, *LIP1*. J Invest Dermatol. 2007 Sep;127(9):2138–2146. https://doi.org/10.1038/sj.jid.5700844

**Figueredo LA, Cafarchia C, Desantis S, Otranto D.** Biofilm formation of *Malassezia pachydermatis* from dogs. Vet Microbiol. 2012 Nov 9; 60(1–2):126–131. https://doi.org/10.1016/j.vetmic.2012.05.012

**Gaitanis G, Magiatis P, Hantschke M, Bassukas ID, Velegraki A.** The *Malassezia* genus in skin and systemic diseases. Clin Microbiol Rev. 2012 Jan;25(1):106–141. https://doi.org/10.1128/CMR.00021-11

**Gupta R, Ramnani P.** Microbial keratinases and their prospective applications: an overview. Appl Microbiol Biotechnol. 2006 Mar;70(1):21–33. https://doi.org/10.1007/s00253-005-0239-8

**Ilahi A, Hadrich I, Neji S, Trabelsi H, Makni F, Ayadi A.** Real-Time PCR identification of six *Malassezia* species. Curr Microbiol. 2017 Jun;74(6):671–677. https://doi.org/10.1007/s00284-017-1237-7

**Jin Y, Yip HK, Samaranayake YH, Yau JY, Samaranayake LP.** Biofilm-forming ability of *Candida albicans* is unlikely to contribute to high levels of oral yeast carriage in cases of human immunodeficiency virus infection. J Clin Microbiol. 2003 Jul;41(7):2961–2967. https://doi.org/10.1128/JCM.41.7.2961-2967.2003

**Juntachai W, Oura T, Murayama SY, Kajiwara S.** The lipolytic enzymes activities of *Malassezia* species. Med Mycol. 2009;47(5): 477–484. https://doi.org/10.1080/13693780802314825

**Kaneko T, Murotani M, Ohkusu K, Sugita T, Makimura K.** Genetic and biological features of catheter-associated *Malassezia furfur* from hospitalized adults. Med Mycol. 2012 Jan;50(1):74–80. https://doi.org/10.3109/13693786.2011.584913

**Kuhn DM, Chandra J, Mukherjee PK, Ghannoum MA.** Comparison of biofilms formed by *Candida albicans* and *Candida parapsilosis* on bioprosthetic surfaces. Infect Immun. 2002 Feb;70(2):878–888. https://doi.org/10.1128/IAI.70.2.878-888.2002

**Lan D, Xu H, Xu J, Dubin G, Liu J, Iqbal Khan F, Wang Y.** *Malassezia globosa Mg*MDL2 lipase: Crystal structure and rational modification of substrate specificity. Biochem Biophys Res Commun. 2017 Jun 24;488(2):259–265. https://doi.org/10.1016/j.bbrc.2017.04.103

**Lee YW, Lee SY, Lee Y, Jung WH.** Evaluation of expression of lipases and phospholipases of *Malassezia restricta* in patients with seborrheic dermatitis. Ann Dermatol. 2013 Aug;25(3):310–314. https://doi.org/10.5021/ad.2013.25.3.310

**Machado ML, Cafarchia C, Otranto D, Ferreira RR, Bianchi SP, Latrofa MS, Parisi A, Ferreiro L.** Genetic variability and phospholipase production of *Malassezia pachydermatis* isolated from dogs with diverse grades of skin lesions. Med Mycol. 2010 Sep;48(6):889–892. https://doi.org/10.3109/13693780903532080

**Mah TF, O'Toole GA.** Mechanisms of biofilm resistance to antimicrobial agents. Trends Microbiol. 2001 Jan;9(1):34–39. https://doi.org/10.1016/s0966-842x(00)01913-2

**Mukherjee PK, Chandra J.** *Candida* biofilm resistance. Drug Resist Updat. 2004 Aug–Oct;7(4–5):301–309. https://doi.org/10.1016/j.drup.2004.09.002

**Nardoni S, Mancianti F, Rum A, Corazza M.** Isolation of *Malassezia* species from healthy cats and cats with otitis. J Feline Med Surg. 2005 Jun;7(3):141–145. https://doi.org/10.1016/j.jfms.2004.07.005

**Patiño-Uzcátegui A, Amado Y, Cepero de García M, Chaves D, Tabima J, Motta A, Cárdenas M, Bernal A, Restrepo S, Celis A.** Virulence gene expression in *Malassezia* spp. from individuals with seborrheic dermatitis. J Invest Dermatol. 2011 Oct;131(10):2134–2136. https://doi.org/10.1038/jid.2011.178

**Pedrosa AF, Lisboa C, Gonçalves Rodrigues A.** *Malassezia* infections: A medical conundrum. J Am Acad Dermatol. 2014 Jul;71(1):170–176. https://doi.org/10.1016/j.jaad.2013.12.022

**Peyton CC, Keys T, Tomblyn S, Burmeister D, Beumer JH, Holleran JL, Sirintrapun J, Washburn S, Hodges SJ.** Halofuginone infused keratin hydrogel attenuates adhesions in a rodent cecal abrasion model. J Surg Res. 2012 Dec;178(2):545–552. https://doi.org/10.1016/j.jss.2012.07.053

**Pini G, Faggi E.** Extracellular phospholipase activity of *Malassezia* strains isolated from individuals with and without dermatological disease. Rev Iberoam Micol. 2011 Oct–Dec;28(4):179–182. https://doi.org/10.1016/j.riam.2011.05.002

**Plotkin LI, Squiquera L, Mathov I, Galimberti R, Leoni J.** Characterization of the lipase activity of *Malassezia furfur*. J Med Vet Mycol. 1996 Jan–Feb;34(1):43–48. https://doi.org/10.1080/02681219680000071

**Shokri H, Khosravi A, Rad M, Jamshidi S.** Occurrence of *Malassezia* species in Persian and domestic short hair cats with and without otitis externa. J Vet Med Sci. 2010 Mar;72(3):293–296. https://doi.org/10.1292/jvms.09-0421

**Simonetti G, Tocci N, Valletta A, Brasili E, D'Auria FD, Idoux A, Pasqua G.** *In vitro* antifungal activity of extracts obtained from *Hypericum perforatum* adventitious roots cultured in a mist bioreactor against planktonic cells and biofilm of *Malassezia furfur*. Nat Prod Res. 2016;30(5):544–550. https://doi.org/10.1080/14786419.2015.1028059

**Sommer B, Overy DP, Haltli B, Kerr RG.** Secreted lipases from *Malassezia globosa*: recombinant expression and determination of their substrate specificities. Microbiology (Reading). 2016 Jul; 162(7): 1069–1079. https://doi.org/10.1099/mic.0.000299

**Takiuchi I, Sei Y, Takagi H, Negi M.** Partial characterization of the extracellular keratinase from *Microsporum canis*. Sabouraudia. 1984 May;22(3):219–224. https://doi.org/10.1080/00362178485380351

**VanGuilder HD, Vrana KE, Freeman WM.** Twenty-five years of quantitative PCR for gene expression analysis. Biotechniques. 2008 Apr;44(5):619–626. https://doi.org/10.2144/000112776

**Vlachos Ch, Gaitanis G, Alexopoulos EC, Papadopoulou C, Bassukas ID.** Phospholipase activity after beta-endorphin exposure discriminates *Malassezia* strains isolated from healthy and seborrhoeic dermatitis skin. J Eur Acad Dermatol Venereol. 2013 Dec; 27(12):1575–1578. https://doi.org/10.1111/j.1468-3083.2012.04638.x

**Xu J, Saunders CW, Hu P, Grant RA, Boekhout T, Kuramae EE, Kronstad JW, Deangelis YM, Reeder NL, Johnstone KR, et al.** Dandruff-associated *Malassezia* genomes reveal convergent and divergent virulence traits shared with plant and human fungal pathogens. Proc Natl Acad Sci U S A. 2007 Nov 20;104(47):18730–18735. https://doi.org/10.1073/pnas.0706756104

**Yu RJ, Harmon SR, Grappel SF, Blank F.** Two cell-bound keratinases of *Trichophyton mentagrophytes*. J Invest Dermatol. 1971 Jan; 56(1):27–32. https://doi.org/10.1111/1523-1747.ep12291869

ORIGINAL PAPER
Polish Journal of Microbiology
2022, Vol. 71, No 4, 539–551
https://doi.org/10.33073/pjm-2022-049

# Ciliated Peritrichous Protozoa in a Tezontle-Packed Sequencing Batch Reactor as Potential Indicators of Water Quality

ANDREA M. RIVAS-CASTILLO[1], ANTONIO A. GARCIA-BARRERA[2], ARISTEO GARRIDO-HERNANDEZ[2], FRANCISCO J. MARTINEZ-VALDEZ[2], MARIA S. CRUZ-ROMERO[2] and MARIBEL QUEZADA-CRUZ[2]*

[1] Universidad Tecnológica de la Zona Metropolitana del Valle de Mexico, Tizayuca, México
[2] Laboratory of Environmental Technology, Universidad Tecnológica de Tecámac, Tecámac, México

Submitted 29 June 2022, accepted 2 October 2022, published online 12 December 2022

Abstract

The presence of colonial and solitary ciliated peritrichous protozoa was determined in a Sequencing Batch Reactor system filled with tezontle, a volcanic rock, economic, and abundant material that can be found in some parts of the world, like Mexico. The presence of these protozoa was related to the removal efficiencies of organic matter. Also, two novel staining techniques are proposed for staining both colonial and solitary peritrichous protozoa. The results show that tezontle promotes the growth of solitary and colonial ciliated peritrichous protozoa, which, once identified, could be used as indicators of the efficiency of the wastewater treatment process. Additionally, the staining techniques established in the current study allowed the precise observation of protozoan nuclei. They can represent a useful complementary methodology for identifying protozoan species present in water treatment processes, along with the already existing identification techniques. The number and variety of protozoa found in the system may be considered potential bioindicators of water quality during biological treatments.

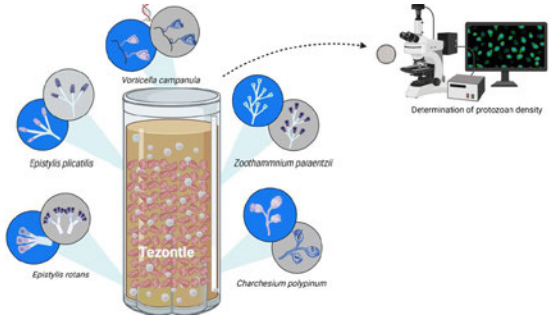


K e y w o r d s: peritrichous protozoa, sessile ciliates, Sequencing Batch Reactor (SBR), tezontle, protozoan staining techniques

## Introduction

The biological systems of wastewater treatment involve microorganisms that include mainly bacteria, protozoa, rotifers, and in some cases, fungi. Bacteria play a fundamental role in the degradation of organic matter, while protozoa perform the function of purifying effluents by consuming particulate (suspended) material that remains after bacterial degradation. That is, protozoa are efficient in purifying of wastewater due to their ability to act as predators that feed on dispersed bacteria (Rakshit et al. 2014). Also, it has been demonstrated that protozoa indirectly influence the clarification of effluents by forming flocs, increasing bacterial activity, contributing directly to the secretion of exopolymer substances, and participating in the development of the structure and biological activity of the flocs (Papadimitriou et al. 2010). It has also been documented that the appearance, abundance, and diversity of protozoa are related to the chemical conditions of the systems, like the presence of toxic substances, oxygen load, etc. Physical conditions also influence the characteristics of the protozoan community, such as the type of packaging (if used) for support purposes. Support materials may be synthetic or natural (Yáñez-Ocampo et al. 2011; Dzionek et al. 2016) and may serve as elements for the retention of suspended particles (mechanic effect) and to underpin microbial activity (biochemical and microbiological effects) (Liu et al. 2015). Some authors have stated that, in contrast

* Corresponding author: M. Quezada-Cruz, Laboratory of Environmental Technology, Universidad Tecnológica de Tecámac, Tecámac, México; **e-mail: mquezadac@uttecamac.edu.mx**

to synthetic materials like plastics, ceramic, and diatomaceous earth, the tezontle is a low-cost material that may be less costly and easier to manipulate than the former ones (Yáñez-Ocampo et al. 2011). Tezontle is a natural, economic, and abundant (in some parts of the world) volcanic rock commonly used in Mexico as a construction material, which presents a characteristic reddish color due to the presence of Fe ions (Dzionek et al. 2017). Specifically in Mexico, this rock is abundantly produced in the proximities of the volcanic belt of Central Mexico, composed of $SiO_2$ (60%), $Al_2O_3$ (12%), MgO (8%), $Fe_2O_3$ (5%), CaO (4%), $Na_2O$ (3%), and other oxides at low concentrations (Acevedo-Davila et al. 2007). Protozoa are related to the efficiencies of wastewater treatment facilities. For example, the presence of the protozoan *Euglena* spp. in treatment systems is related to $Cr^{6+}$ (20 μg/ml) and $Pb^{2+}$ (30 μg/ml) tolerance (Rehnam 2011). Peritrichous protozoa like *Vorticella* spp., *Epistylis* spp., and *Opercularia* spp. show resistance to hydrocarbons present in residual waters (Kachieng'a and Momba 2018). Protozoan number and diversity differ between continuous and Sequencing Batch Reactors (SBR), or between aerobic and anaerobic conditions (Ogleni et al. 2010; Papadimitriou et al. 2010; Pérez-Uz et al. 2010). An SBR is a system of activated sludge for wastewater treatment, and it has been successfully used to treat both municipal and industrial wastewater. In this system, the wastewater is used to fill a single batch reactor, and the water is treated to remove the non-desirable components, and both are finally discharged. The homogenization, aeration, and clarification can be achieved using a single batch reactor. Two or more discontinuous reactors in a specific operational order can be used to optimize the system's yield (EPA 1999). The efficiency of the SBR is evaluated with determinations such as organic material, total solids, suspended solids, and the presence of pathogens and parasites, among others.

The most representative protozoa in SBR are *Arcella* spp. and *Difflugia* spp. from the amoeba group, *Didinium* spp. (ciliated free-living protozoa), *Aspidisca* spp. (walking ciliate), *Peranema* spp. (flagellate species), and sessile ciliates, such as *Carchesium* spp., *Epistylis* spp., and *Vorticella* spp., are considered indicators of the excellent quality of activated sludges (Ogleni et al. 2010). Sessile protozoa are those adhered or attached by a peduncle, stalk, or lorica to sediment, other organisms, or even the interior of a lorica. Mucus secretion plays an important role in adhesion capability (Arndt et al. 2003). For protozoan identification, it is important to evaluate their size, the shapes of the zoids and nucleus, and their movements, among other characteristics.

Due to the importance of protozoa for wastewater treatment systems, many studies have focused on their identification to a species level. Different staining methods are used to fulfill this task, such as the pyridinated silver carbonate or protargol methods or even molecular techniques, which can be more time-consuming and expensive. Nevertheless, sometimes protozoa can be only identified at a genus level with these staining methologies (Azovsky and Mazei 2018) due mainly to the low nuclei definition achieved, causing easy confusion among species (Robertson et al. 2019). Besides, some protozoan species can resist the stains used in conventional techniques. These facts indicate that establishing novel, quick, and accurate techniques may be helpful. The present study assessed the relationship between the density and diversity of peritrichous protozoa with water quality in the SBR with tezontle as a packaging material.

Additionally, two new and effective nuclei staining techniques for identifying solitary and peritrichous protozoa were proposed. The first used Morrison's fixative, Freitas mordant, and Delafield's hematoxylin (MFD), and the second one employed only Freitas mordant and Delafield's hematoxylin (FD). It could complement the traditional techniques used for this purpose. A molecular approach for protozoan identification was also performed to validate the staining techniques established.

## Experimental

### Materials and Methods

**Sequencing Batch Reactor.** Tezontle stones with a mean particle size of 2–2.5 cm were used as fillers in an automatic SBR. The inoculum (bacteria and protozoa) and the wastewater used to feed the reactor were obtained from the municipal activated sludge treatment plant (Tecamac, State of Mexico). Protozoan samples, once taken, were preserved under aerated conditions with over 2 mg/l of oxygen, and oxygen concentration was kept higher than 2.3 mg/l during experimentation. The environmental temperature oscillated from 22–26°C, and the pH of the residual water was adjusted to 7.6 with 0.1N HCl solution. The system functioned with typical cycles: feeding, aeration-reaction, sedimentation, and discharge, with corresponding times of 1 min, 23 h, 20 min, and 1 min. The hydraulic retention time was 23 h, and the volumes of wastewater and tezontle were 1.8 and 2 l, respectively.

**Physicochemical analyses.** Chemical oxygen demand (COD) and total solids (TS) were determined following the standard methods of water analyses (Baird et al. 2017). These two parameters were assessed to determine the efficiency of the reactor and their relationship with the density and diversity of protozoa. pH and temperature were determined in situ; pH was measured using a potentiometer (HANNA Instruments, model pH 211; USA), while the temperature was

measured with a Branan mercury thermometer. These parameters were determined in both the influent and the effluent during the 60 days.

**Analysis of the packaging material (Tezontle).** The density of tezontle was calculated by Archimedes' principle. First, dried tezontle stones were weighed, then again weighed when submerged in distilled water at 22°C. Tezontle density was calculated using the following equation:

$$\rho_{tez} = \frac{M_d}{M_d - M_w} \rho_{pwz} \quad (1)$$

where: $\rho_{tez}$ is the tezontle density, $M_d$ is the mass of the dried tezontle, $M_w$ is the mass of the tezontle submerged in water, and $\rho_{wz}$ is the density of distilled water at 22°C.

The scanning electron microscopy (SEM) images of tezontle stones were recorded using a JCM-6000 Plus NeoScope operating under a low accelerating voltage (5 kV). The dried tezontle, without further preparation, was placed on the sample holder of the microscope.

**Staining techniques.** Two novel staining techniques were developed to observe peritrichous protozoan nuclei, both colonial and solitary, and complement the traditional techniques of protozoan identification. The first used Morrison's fixative, Freitas mordant, and Delafield's hematoxylin (MFD), and the second one employed only Freitas mordant and Delafield's hematoxylin (FD). This latter dye was prepared as indicated by Beltran et al. (2014) with a modification: the addition of 80 ml of methyl alcohol and 80 ml of glycerol. Metazoans' identification was achieved with the help of Baird et al. (2017) based on morphological observations.

For MFD, Morrison's Fixative was added to a 25-µl sample (previously dried for 2 hours) and let stand for 6 min. After this time, the sample was rinsed with a moderate water flow, and it was drained and entirely dried by slightly pressing the sample with absorbent paper. Once totally dried, the sample was covered with Freitas' Mordant and let stand for 5 min. Afterward, the sample was rinsed and dried in the same way. The sample was then covered with Delafield's hematoxylin for 5 min and subsequently rinsed. A drop of water was added and spread over the sample to prevent the zoids from becoming dehydrated. After staining, the sample was observed under the optic microscope at 20× or 40×, as specified for each case.

In the FD technique, 0.5% hydrochloric acid was added to the sample (pre-dried for 2 hours), covering it for 6 min. After this time, it was rinsed with moderate water flow. Afterward, the sample was drained and dried entirely by slightly pressing the sample with absorbent paper. Once completely dried, the sample was covered with Freitas' Mordant and let stand for 5 min, subsequently rinsed and dried in the same way. The sample was covered with Delafield's hematoxylin for 6 min; then, it was rinsed, drained, and a drop of water was added and spread over the sample to prevent it from drying. Then, protozoa were observed through the microscope under the same conditions described above. Both FMD and FD staining techniques were repeated at least six times for each specimen to ensure reproducibility.

**Assessment of protozoan density.** To determine the density and diversity of protozoa in the SBR, tezontle samples were taken at the beginning and the end of the experimentation period (after 60 days); the assessment was independently performed twice, taking two replicates in each repetition.

Each sample consisted of the biomass scrapped from two tezontle stones using for this purpose a sterilized brush. Samples were homogenized, adding 50 ml of wastewater and shaking them for 2 min. 25-µl samples were taken with an automatic micropipette (Socorex, Switzerland) to quantify the density of both protozoa and metazoans. Afterward, the samples were observed in-fresh for cell counting using a Neubauer chamber (in triplicate) and observed for a period no longer than 3 h (Dubber and Gray 2009), using a clear-field microscope Ni-U NIKON® (USA) with 40× and 100× objectives.

Samples were observed in vivo using MFD and FD techniques (permanent preparations) to determine protozoan diversity in the SBR. To this end, the different organelles and structures (cilia, flagella, zoids, peduncles, and nuclei) were highlighted by right-field microscopy and Nomarski (DIC, Differential Interference Contrast) techniques using a Ni-U NIKON® (USA) microscope. Species were identified according to Isac et al. (2008), Lynn (2010), and Küppers et al. (2020). As for rotifers, genera were identified according to their movement and morphology, following Baird et al. (2017).

**Molecular approach for protozoan identification.** The *Vorticella campanula*'s identity was confirmed by using a conserved region of the ITS 18S rRNA, for which total RNA was extracted by the TRIZOL reagent technique (Sigma Aldrich). The RNA obtained was reconstituted with RNAase-free water, aliquoted in Eppendorf tubes at a concentration of 50 µg/µl, and stored at –70°C. For amplification, an RT-PCR was developed using a Sensicript™ Reverse Transcription Kit (QIAGEN) and a Taq PCR Core Kit (QIAGEN), using the set of primers designed to identify the conserved region within the ITS 18S of the microorganism, which is VCS302 3'-ACGGCTACCACATCTACGG-5' and the VCA103 5'-GTGCAAAACCGTCAATTCCT-3'. Amplification was effected using the following protocol: reverse transcription at 37°C for 60 min; PCR at 94°C for 4 min, followed by 30 cycles of 60 s at 94°C, 30 s at 55°C and 60 s at 74°C, and a final extension at 74°C for 10 min. The RT-PCR product was visualized by electrophoresis on a 1.2% agarose gel and quantified by spectrophotometry.

The amplicons were extracted from the agarose gel, purified directly using a QIAquick Gel Extraction Kit (QIAGEN, Germany), and sequenced automatically using the dideoxynucleotide chain-termination method.

The phylogenetic analysis was performed using data from the entire ITS 18S regions obtained from GenBank. Sequences were aligned using CLUSTALX and adjusted with the BIOEDIT v.7.0.9 (Sun et al. 2013). The aligned matrix was analyzed by using three methods: maximum likelihood (ML), neighbor-joining (NJ), and maximum parsimony (MP). The analysis was performed with MEGA X (Kumar et al. 2016) and Modeltest 3.7 (Posada and Crandall 1998), using the GTR + I and GTR + G model, and Kimura of 2-parameters with a 1,000 bootstrap (Liao et al. 2018).

**Statistical analysis.** Each experiment was replicated to obtain protozoan density, and the results were analyzed using R software. To determine the difference between the total densities of the sessile ciliated protozoan species present in the different replicates, a Student's *t*-test was performed ($p = 0.01$). An ANOVA was performed to evaluate the difference between the densities of each species ($p = 0.01$). To corroborate these significant differences between the densities, data was analyzed by a Tukey test ($p = 0.01$). Also, a multivariate analysis was conducted (Principal Components Analysis, PCA) to statistically analyze the results, using the Statgraphic Plus v.5.1 software (Statgraphics Technologies Inc., USA); this analysis allowed the detection of the relationship between the density of each protozoan species with the operating time of the reactor.

## Results

**Establishment of protozoan staining techniques.** Two different protocols were assessed to establish novel, quick, and accurate techniques that may be useful for identifying solitary and colonial peritrichous protozoa. To this end, protozoan samples were taken from the facilities of a municipal activated sludge treatment plant in Tecamac, State of Mexico. First, Fig. 1 shows a colony of peritrichous protozoa in fresh (Fig. 1a) and stained with the Harris Hematoxylin traditional technique (Fig. 1b). It was observed that nuclei could not be distinguished, and only dark spots could be seen. Therefore, it was corroborated that using conventional staining protocols, it is difficult to determine protozoan species. In contrast, there are examples of protozoan samples in fresh (Fig. 1c and 1e) and stained with MFD (Fig. 1f and 1h) and FD (Fig. 1d and 1g) protocols. In the first technique, MFD, the cell body was stained intensively. In contrast, while the nucleus was stained in lighter shades than the rest of the zoid, so the size, shape, and position of the macronucleus can be distinguished (Fig. 1f and 1), which allowed the identification of the species *Epistylis plicatilis*. On the other hand, the FD technique (Fig. 1d) allowed the dyed of the macronucleus in a stronger color. At the same time, the rest of the zoid was dyed in lighter shades, also allowing the identification of *E. plicatilis*.

**Identification of protozoan species in the SBR.** Identifying colonial peritrichous protozoa is not easy, as training is necessary regarding microscopical and specific staining techniques; furthermore, long-lasting fixing and preserving methods for free-living protozoa are still required, as was indicated by Küppers et al. (2020). Using the MFD and FD protocols described above, the colonial and solitary peritrichous protozoan species present in the SBR were detected: *Zoothamnium paraentzii*, *E. plicatilis*, *V. campanula*, *Epistylis*

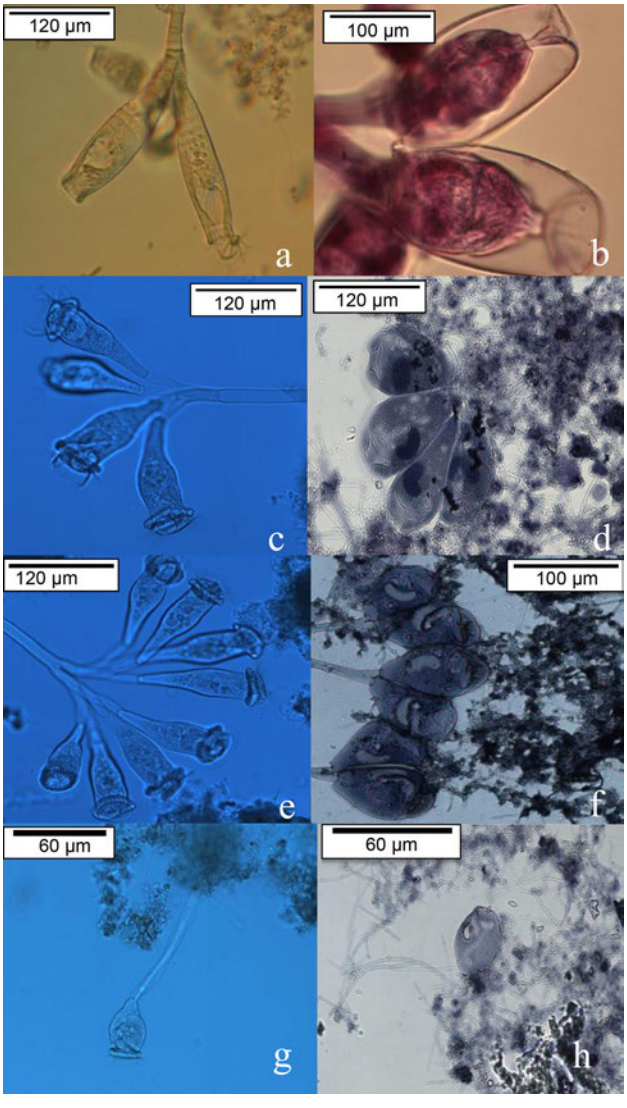


Fig. 1. Micrographs of colonial peritrichous protozoa.
a) Fresh sample and b) stained with Harris hematoxylin technique at 40x; c) 4-zoid fresh colony using Nomarski technique and d) FD staining at 40x; e) 8-zoid fresh colony using Nomarski technique and f) the MFD staining at 40x; and g) fresh samples of *Vorticella campanula* and h) stained with the MFD technique ("J" shaped nucleus) at 20x magnification.

Table I
The density of peritrichous protozoa (peritrichous protozoa $\times 10^3$/ml).

| Time (days) | *Zoothamnium paraentzii* | *Epistylis plicatilis* | *Vorticella campanula* | *Epistylis rotans* | *Charchesium polypinum* | *Vorticella convallaria* | *Vorticella aquadulcis* | Total density ($\times 10^3$ protozoa/ml) |
|---|---|---|---|---|---|---|---|---|
| 1 | 11 | 8 | 10 | 7 | 33 | 1.5 | 1 | 72 |
| 10 | 142 | 34 | 57 | 47 | 17 | 2 | 2 | 299 |
| 20 | 267 | 34 | 57 | 47 | 17 | 2 | 2 | 425 |
| 30 | 220 | 92 | 96 | 76 | 11 | 5 | 2 | 500 |
| 40 | 244 | 63 | 76 | 61 | 14 | 3 | 2 | 462 |
| 60 | 232 | 77 | 86 | 68 | 12 | 4 | 2 | 481 |

*rotans*, *Carchesium polypinum*, *Vorticella convallaria*, and *Vorticella aquadulcis*. Other genera of protozoa, different from ciliated peritrichous, were identified by their morphology and movement as *Cyclidium* sp., *Colpidium* sp., *Litonotus* sp., *Paramecium* sp., *Chilodonela* sp., *Aspidisca* sp., *Euplotes* sp., *Euglypha* sp., and *Centropyxis* sp. Metazoans such as *Philodina* sp., *Rotaria rotatoria*, and *Chaetonotus* sp. were identified based on their morphology.

Micrographs included as supplementary material (Fig. S1–S6) present some protozoan species identified in the SBR by MFD and FD techniques. In *V. campanula*, stained using the MFD technique (Fig. 1g and 1 h), it presents very wide inverted bell-shaped zoids, with measures of 50–157 μm for the zoid, 35–100 μm for the peristomal width and peduncles of 250–350 μm long.

*V. campanula* is abundant in the SBR system and tolerant to some heavy metals. Therefore, this species is essential for degrading some toxic compounds (Vilas-Boas et al. 2020). It is also subsequently used to complement, by a molecular approach, the precision of staining techniques for identifying the protozoan species. To this end, the ITS 18S region of this protozoan sample was amplified and aligned (Table SI). A phylogenetic analysis was performed (Fig. 2) using the procedures described in Materials and Methods. The identity percentage of the aligned region (98.5%), and the phylogenetic analysis indicated on *V. campanula*, and the strain was codified as *V. campanula* 01mex. Since protozoa are commonly found in consortia, it is important to mention that it may be challenging to isolate strains and subsequently perform molecular biology techniques for their identification. Even though, the identification of the *V. campanula* 01mex specimen by a molecular approach was successfully achieved in the current study as a complement to the staining methods proposed.

**Protozoan density and SBR efficiency.** Table I shows the density and diversity of protozoa found during the 60 days of SBR functioning. The highest densities of sessile ciliates were found for the species *Z. paraentzii*, *E. plicatilis*, *V. campanula*, *E. rotans*, and *Carchesium polypinum* with maximum values of $244 \times 10^3$ protozoa/ml, $92 \times 10^3$/ml, $96 \times 10^3$/ml, $76 \times 10^3$/ml, and $33 \times 10^3$/ml respectively. *V. convallaria* and *Vorticella aquadulcis* were detected at low density: $5 \times 10^3$ and $2 \times 10^3$ protozoa/ml, respectively. The densities of other relevant microorganisms related to water quality were also assessed and are as follows: *Euglypha* sp. and *Centropyxis* sp. from the amoebae group were present at the constant density (a maximum of $4.5 \times 10^4$ amoebae/ml). The behavior of the free-swimming ciliated protozoa, like *Cyclidium* sp., *Colpidium* sp., *Litonotus* sp., *Paramecium* sp., and *Chilodonella* sp. was different, as their density remained of up to $4.1 \times 10^4$ of free-swimming ciliates/ml. Metazoans, considered good indicators of treatment quality in activated sludge systems, were also identified and it was *Philodina* sp., *R. rotatoria*, and *Chaetonotus* sp. Regarding the density of total protozoa (ciliated sessile, free-swimming, and amoebae), two consecutive stages were observed; an adaptation stage followed by a stabilization one (Fig. 3), as the total density of the sessile protozoa increased steadily from day 1 to day 20. After day 20 and up to day 60, the protozoan density remained constant. The *t*-test analysis showed no significant differences when comparing the total densities of peritrichous protozoa between the two independent experiments. Additionally, ANOVA and Tukey analyses demonstrated the significant differences between the densities of the diverse protozoan species (Table II). The density

Table II
The mean abundance of peritrichous protozoan species.

| Species | Average density (protozoa $\times 10^3$/ml) |
|---|---|
| *Zoothamnium paraentzii* | 185.79[a] |
| *Epistylis plicatilis* | 51.18[b] |
| *Vorticella campanula* | 63.56[b] |
| *Epistylis rotans* | 50.79[b] |
| *Charchesium polypinun* | 17.31[c] |
| *Vorticella convallaria* | 2.85[d] |
| *Vorticella acuadulcis* | 1.64[d] |

[a–d] – lower-case letters represent groups of data that were significantly different by the Tukey's test ($\alpha = 0.01$)

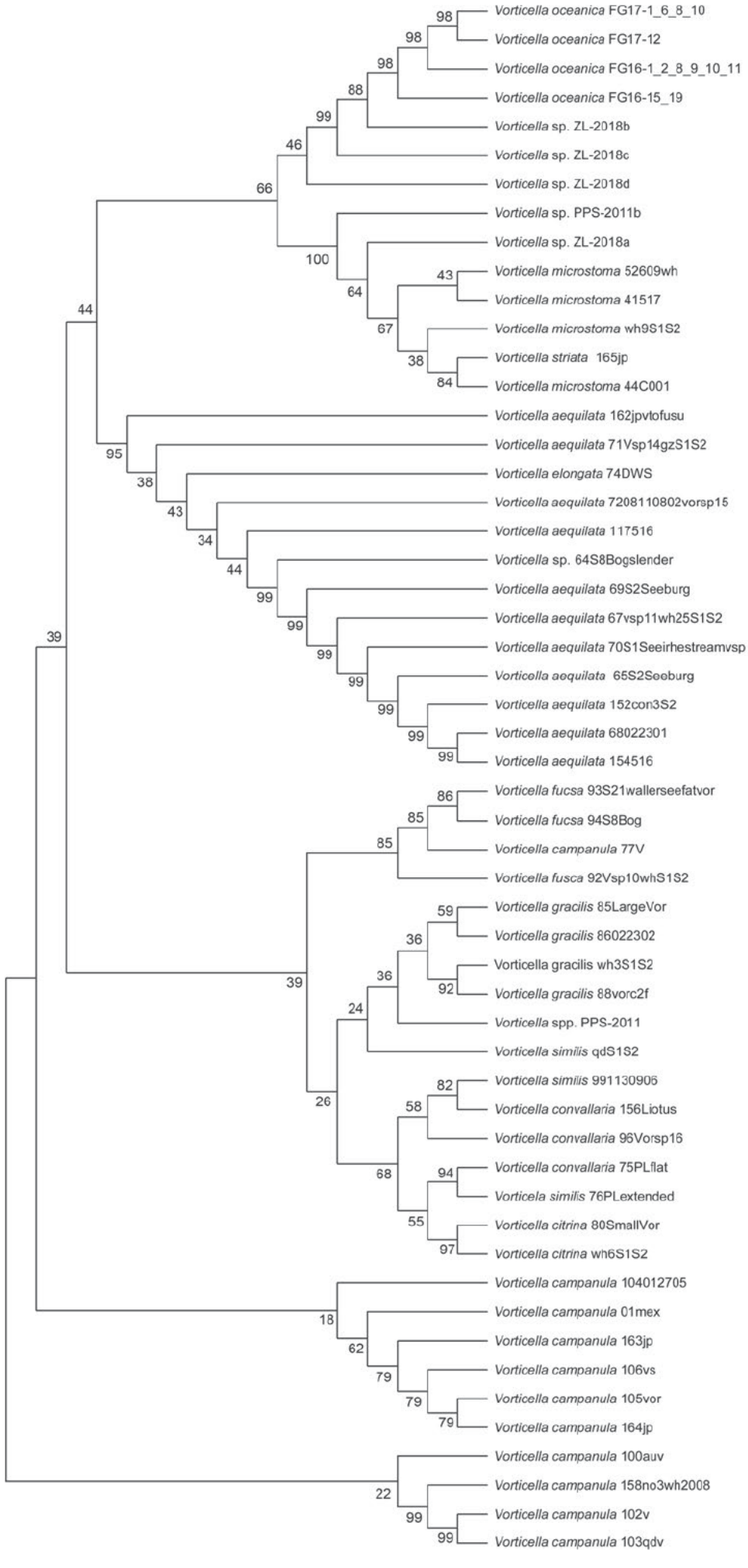


Fig. 2. Identification of *Vorticella campanula* 01mex by a phylogenetic analysis based on its ITS 18S rRNA sequence.

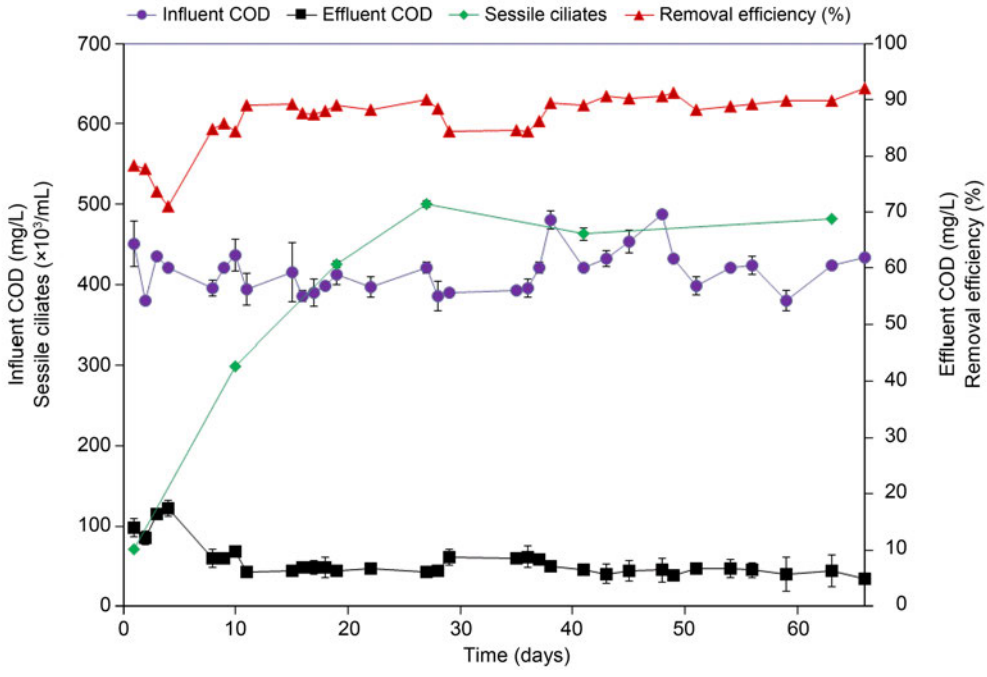


Fig. 3. Relationship between protozoan density and COD in the SBR.
Protozoa density; Influent COD; Effluent COD; Removal efficiency (%).

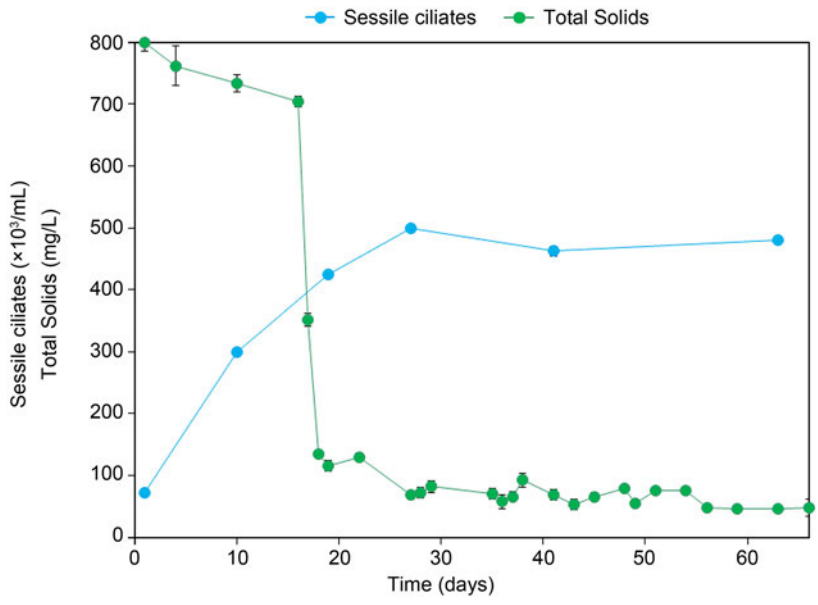


Fig. 4. Behavior of sessile ciliates with respect to the concentration of total solids.

of *Z. paraentzii* was the highest, while the densities of *E. plicatilis*, *V. campanula*, *V. convallaria*, and *Vorticella aquadulcis* were similar. Since the COD is indicative of the effluent quality and the efficiency of the removal of organic matter, the COD concentrations were measured in the influent and effluent (Fig. 3). They were in the ranges of 377–480 mg/l, and 38–122 mg/l, for days 10 to 60, respectively. During the first stage (days 1–20), protozoa/ml densities of $7.2 \times 10^3$ to $4.25 \times 10^5$ were obtained, with COD average removal efficiencies of 83.5%. In the second stage (days 21–60), the maximum density obtained was $5{,}0 \times 10^5$ protozoa/ml, with a mean removal efficiency of 88.7%. In the stabilization stage, efficiency percentages increased from 84.27 to 91.93%, while the protozoan density remained nearly constant ($4.63–5.0 \times 10^3$/ml).

The density of the sessile ciliates and total suspended solids (TSS) in the effluent were determined (Fig. 4), since suspended solids indirectly quantify the organic matter and the number of microorganisms

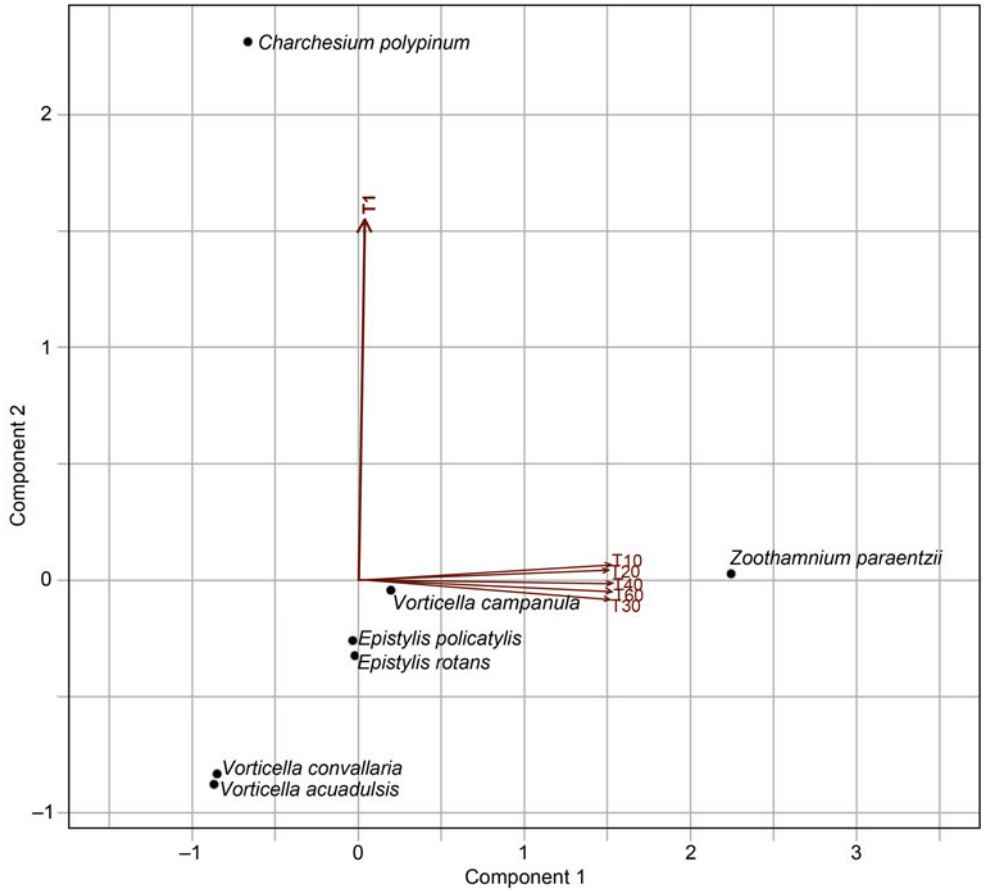


Fig. 5. Principal Component Analysis (PCA): relationship between the abundance of protozoa and other microorganisms, time, and removal percentage. Axes 1 and 2 account for 54.9% and 22.1% of the total variation presented, respectively.

(bacteria, protozoa, rotifers, and algae in some cases) in the effluent. A decrease in the TSS concentration suggests a decrease in the number of microorganisms and enhances water quality by diminishing the floating solids. At the beginning of the process (day 1), the TSS concentration in the effluent was higher than 700 mg/l. On the other hand, concentrations decreased to the range of 46–96 mg/l during the stabilization stage.

**Principal Component Analysis (PCA).** A PCA analysis was performed to determine the relationship between the functioning time of the reactor and the densities of diverse species of colonial and solitary peritrichous protozoa (Fig. 5). The first component of the PCA explains 80% of the data obtained, while the second one explains the 17%; thus, 97% of all the data obtained could be explained with these first two components. The analysis showed that *Z. paraentzii* had a strong correlation with the functioning time of the reactor. At the same time, species of colonial peritrichous protozoa like *V. campanula*, *E. plicatilis*, and *E. rotans* presented a moderate correlation with the functioning time of the reactor.

**Tezontle in the SBR.** The weight and porosity of tezontle were determined to assess the potential use of tezontle as supporting material (as a filler) in the SBR. The tezontle weight was calculated using Archimedes' principle, which provided a value of $2.537 \pm 0.060$ g/ml, with a porosity of $43.605 \pm 2.046$. Afterward, an SEM analysis of the tezontle was performed to observe its internal structure (Fig. 6). Tezontle showed a broad, porous diameter distribution (from tens to hundreds of micrometers) in the tezontle stone. Besides their size, the porous varied in shape and profundity among them.

## Discussion

Both staining techniques proposed in the present study seemed economical, efficient, and quick options for staining protozoan nuclei of biological wastewater treatment systems, which could represent a relevant tool for identifying these microorganisms. Besides, all the microorganisms found in the SBR system using these novel staining methods have been earlier found in the systems of good removal efficiencies (> 90%), as full-scale operations activated sludge treatment plants, rotating biological contactors, and wetlands (Ginoris et al. 2007; Papadimitriou et al. 2010). Metazoans are highly sensitive to physical, chemical, and operational conditions (Ginoris et al. 2007); the metazoan

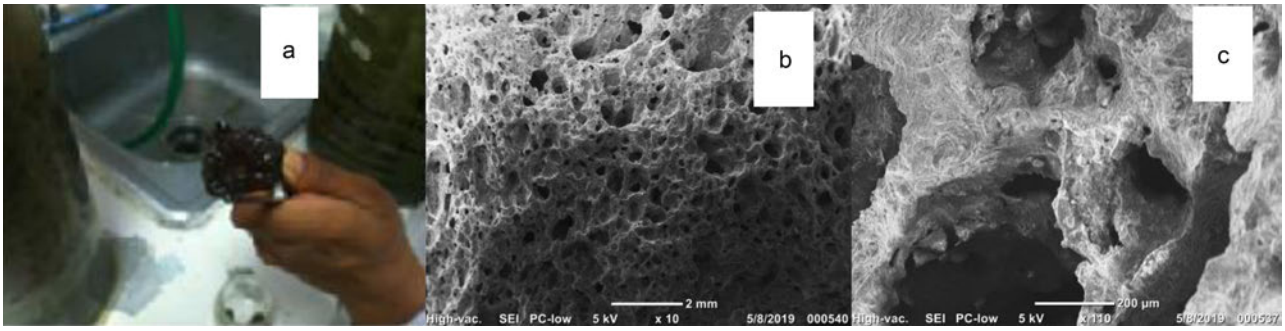


Fig. 6. Properties of tezontle as supporting material of the SBR. a) A piece of tezontle containing adhered peritrichous colonies; b) Scanning Electron Microscopy (SEM) of tezontle stones; c) closeup of tezontle pores.

identified *R. rotatoria* has been previously found in wetlands (Priya et al. 2007) and activated sludge systems (Ginoris et al. 2007).

As can be observed, *Z. paraentzii* (MFD technique) (Fig. S1) developed colonies with various zoids; in some cases, small colonies were shown, while other samples presented huge colonies with hundreds of zoids. A common dichotomous stalk connected the colonies, and the contractile spasmonema run uninterrupted throughout the colony, allowing contraction as a single unit. The body was highly variable in shape but usually elongated, measuring about 50–80 × 25–45 µm. The peristomial lip was single-layered, contractile vacuole apically located, and macronucleus generally C-shaped and horizontally oriented (Sun et al. 2005). It is important to note that the MFD staining technique proposed within this study is economical, quick, and allows the correct observation of the nucleus of *Z. paraentzii* for its identification. It represents a significant contribution, as in previous studies, only macronuclei drawings could be observed; other staining methods do not allow clear nuclei observations, so the identification of this microorganism could only be made at the genus level (Isac et al. 2008; Lynn 2010). This staining technique allows for obtaining permanent samples.

The MFD technique also allowed identifying *E. plicatilis* (Fig. 1d and Fig. S2); colonial ciliated protozoa with branching peduncles and without contractile capability (without myonema), whose zooids had a peristomial lip. They had dichotomous ramification colonies of up to 2–3 mm, with malleus-shaped zoids ranging from 70–90 mm, with nonhollow peduncle and horseshoe-shaped transversal macronucleus. It has been reported that the ciliated *Epistylis* spp. was related to the stabilization of activated sludge systems that work well with optimal loading (Isac et al. 2008).

On the other hand, the FD staining technique allowed *Carchesium polypinum* staining (Fig. S3) and, in agreement to Isac et al. (2008), its colony presented bell-shaped zoids, with independent and spiral contraction, peduncle without septa and with visible discontinuous spasmonema, dichotomous branches, and marked peristomal lip. The zoids' width was 46 µm, with a length of 72 µm. The colony showed a horseshoe-shaped macronucleus located at the top of the zoid. This kind of protozoa indicates that the sludge system of the plant is in optimal aeration conditions and has a high biological quality (Isac et al. 2008). Besides, nuclei of telotroch larvae were also efficiently stained with the proposed techniques: MFD and FD (Fig. S4). It is known that a telotroch is a mobile form that disperses when peritrichous protozoa divide. After the telotroch chooses a site, it begins to secrete a stalk from the scapula at the aboral pole of the body (Bradbury 1994).

The FD technique allowed the nuclei staining of *V. aquadulcis* (Fig. S5), which had an inverted cup-shaped zoid; this was a sessile organism with a contractile vacuole located in the upper part of the body, and its very elongated macronucleus was "C" shaped. This organism measured 55 µm long and 35 µm wide, and the diameter of the peristomatic lip was 30 µm (Isac et al. 2008; Lynn 2010). The FD staining technique also allowed the identification of *V. convallaria* (Fig. S6), which had a flared shape and a peristomial lip, with a width equal to or greater than that of the zoid, a fine and elongated peduncle (100–500 µm), a macronucleus in the form of "J", and a contractile vacuole in the anterior third of the cell (Isac et al. 2008). This microorganism is also related to transitory conditions (unstable or colonization), indicating nitrification absence in biological reactors (Martín-Cereceda et al. 2001). *V. campanula* is commonly associated with low organic loads (Isac et al. 2008, Küppers et al. 2020). It has been reported that the genus *Vorticella* has substantial environmental importance, like in the degradation of petroleum hydrocarbons in wastewater (Kachieng'a and Momba 2018), and the tolerance to heavy metals (Vilas-Boas et al. 2020).

The genus *Z. paraentzii* was also found to be one of the most abundant species in some phases of the process. Similar results were found in rotating biological contactors and activated sludge systems (Martín-Cereceda et al. 2002). This behavior is very interesting because tezontle conditions may have allowed the

growth of protozoa that are difficult to grow in the laboratory or have relevant biotechnological potential. Thus, this system could serve to grow colonial and solitary peritrichous ciliated protozoa, such as *Vorticella* sp. and *Epistylis* sp. that currently degrade hydrocarbons (Kachieng'a and Momba 2018), or some ciliated protozoa that may be used for the bioremediation of waters contaminated with heavy metals (Kumar et al. 2017; Vilas-Boas et al. 2020). Madoni (2010) mentioned that in a plant of activated sludge with an appropriate operation, the protozoan community is dominated by peritrichous specimens (*Vorticella* spp., *Carchesium* spp., *Zoothamnium* spp., *Epistylis* spp.) and hypotricks (*Aspidisca* spp., *Euplotes* spp.). In the case of amoeba, the genus *Euglypha* sp. was the most abundant, being these amoebae associated with good effluent quality (Ginoris et al. 2007). Additionally, the presence of the metazoan *Philodina* sp. is interesting because it has been reported that it is a rotifer that secretes polymeric extracellular substances that act as promoters of bacterial growth (Kachieng'a and Momba 2018).

The results regarding protozoan densities indicate an adaptation stage of the sessile protozoa. They could reflect one of the relevant advantages that tezontle may have: its porous structure, which seemed to allow the establishment of a microbial consortium. These results agree with those obtained from real-scale systems, such as wetlands, SBR, and activated sludge processes with advanced nitrogen-reducing systems (Papadimitriou et al. 2010). Besides, it has been reported that some protozoa are present in wastewater treatment systems, especially in activated sludge operations, rotating biological contactors, percolating filters, wetlands, and coastal areas (Ogleni et al. 2010; Papadimitriou et al. 2010; Charpentier 2014).

Overall, the results observed in the SBR system support previous reports that the most common protozoa in wastewater treatment systems are flagellates, free- swimming ciliates, crawling and sessiles, including the genera *Paramecium* sp., *Colpidium* sp., *Peranema* sp., *Tetrahymena* sp., *Euplotes* sp., *Aspidisca* sp., *Trachelophyllum* sp., *Vorticella* sp., *Epistylis* sp., *Difflugia* sp., *Arcella* sp., *Zoothamnium* sp., and *Carchesium* sp., among others (Ginoris et al. 2007; Canals et al. 2017). The observations also suggest a relationship between protozoan density and COD removal efficiencies in the SBR. During the growth stage, the removal efficiencies increased progressively from 71.02% to 89.08%, and the protozoan density increased from $7.2 \times 10^4$ protozoa/ml to $4.81 \times 10^5$ protozoa/ml. These results agree with those obtained by Priya et al. (2007) in continuously stirred anaerobic reactors that the density of ciliated protozoa was strongly related to the COD removal. The pH of the influent remained constant at 7.5 (data not shown), which is the same value reported by other researchers, such as Martín-Cereceda et al. (2001), who worked with a system of rotating biological contactors. They found species like *Zoothamnium* sp., *Vorticella* sp., *Epistylis* sp., *Euplotes* sp., and *Opercularia* sp. In the present study, the SBR worked in a range of 22–26°C throughout the experimentation, allowing bacteria and protozoa to grow.

Notably, the pH values and temperature were adequate with the metabolism of protozoa, thus promoting the correct functioning of the reactor. This observed behavior is logical since the sessile ciliated protozoa are bacterial and organic matter predators, so it can be inferred that when protozoan density increases, they feed on bacteria, and therefore TSS will diminish. This behavior is consistent with the fact that most protozoa were sessile attached to the support material (tezontle). Li et al. (2013) mentioned that *Vorticella* spp. and some rotifers are linked to the ingestion of fine particles, which positively affects the reduction of suspended solids. Also, the observed correlation in the PCA could be related to sessile protozoan stalks, which may have led to a better adhesion to the tezontle; these microorganisms may have had better adaptation opportunities and hence, presented an increase in their abundance. Besides, the PCA confirmed that free-living protozoa, amoebas, and metazoans (rotifers) always occurred in low abundance, indicating that they had no chance of survival compared to sessile protozoa (with stalk). Papadimitriou et al. (2010) stated that protozoan abundance could be used as a bioindicator of the treatment efficiency in constructed wetlands. In this regard, the present study elucidated a similar conclusion.

In addition, it is suggested that a greater abundance and diversity of protozoa may correlate with the effluent's good quality. It has also been mentioned that a correlation between the phosphorus and the rates of removal of total coliforms was observed in the presence of increased protozoan taxa, while the removal of the organic load and the inorganic nitrogen increased in the case of high protozoan diversity in the soil/water interface. Some authors have pointed out that each group of protozoa is associated with different factors influencing the process. For example, the ciliate group is related to good organic matter removal, while the flagellates are closely related to nitrogen elimination (Papadimitriou et al. 2010). The present study considers the high densities of the sessile protozoa (*E. rotans*, *E. plicatilis*, *Z. paraentzii*, *C. polypinum*, and *O. coarctata*) as high-quality effluent indicators (Li et al. 2017).

Additionally, the quick identification of the species present in the system (the proposed MFD and FD staining techniques) led determining the relationship between the presence of specific protozoan species and some system conditions, such as the quality of the effluent, removal efficiencies, and amount of organic matter. Previously, Li et al. (2017) also obtained a moderate

correlation between all protozoan communities and environmental parameters, such as the concentrations of ammonia nitrogen ($NH^{4+}$-N), total nitrogen (TN), total phosphorus (TP), and COD. Additionally, Xu et al. (2014) mentioned that the biofilms formed by the spatial patterns of the ciliated communities were significantly correlated with environmental variables, especially COD and nutrients, in coastal waters.

Concerning the support material used in this study, the "tezontle" word is derived from the Nahuatl "teztzontli", where "tezt" means stone and "zontli" means hair. Tezontle is a volcanic stone native to the State of Morelos, Mexico, which has a water retention capacity of 12.91–43.3%. In addition, its high porosity provides a large contact surface area, so it can be used as a substrate for many applications; the viability for the establishment of micro-bacterial colonies in tezontle stone due to its micropores has been previously reported (Liu et al. 2015). Besides, tezontle has good absorption properties and high mechanical resistance (Yáñez-Ocampo et al. 2011), which may be relevant for the region in which the study took place because Mexico has large tezontle deposits. The material could be used as a natural, environmental-friendly, and economic support for different wastewater treatment systems. Based on its characteristics, it may allow the adherence of protozoa, which may serve as indicators of different conditions in water treatment systems, besides promoting good removal efficiencies of organic and particulate matter (bacteria). The results obtained about the density and porosity of tezontle match very well with the density and porosity ranges reported before for this material (2.93 g/ml) (Li et al. 2017) and 55.5% (Rodríguez-Díaz et al. 2013), respectively. These characteristics are very important in absorption applications, as they represent the surface area and confirm that the tezontle's porosity might have been strongly related to the adhesion of the peritrichous ciliated protozoa. Also, it has been previously reported that tezontle mainly comprises of iron, aluminum, and silicon oxides, representing more than 70 wt % of its composition. It also contains magnesium, calcium, and sodium oxides (around 30 wt %). Kachieng'a and Momba (2018) obtained more than 90% of COD removal after 20 days, This percentage was obtained due to their sessile and free nature and the interaction among the protozoan isolates (consortium).

On the other hand, Nacheva et al. (2008) observed more than 95% biodegradation (COD removal) when activated carbon and tezontle were used as biofilm supports in anaerobic biofilters. Specifically, more than 95% biodegradation was obtained with both support materials at organic loads lower than 1.7 $kg/m^3 \times d$ in tezontle, and with loads of up to 13.3 $kg/m^3 \times d$ in granulated activated carbon. In the present research, the density of the colonial and solitary peritrichous ciliates was much higher than that of free-living ciliates during the process. It suggests that the silicon oxide contained in the tezontle promotes good conditions for the growth of sessile ciliates. Some organisms, from protists to sponges, employ silicon sources to build internal or external skeletons and/or scale structures (Perry et al. 2003; Foissner et al. 2009). Moreover, according to Foissner et al. (2009), silicon granulates regulate light perception and are a protective mechanism against mechanical stress and protozoan predation.

Some studies show the suitability of using packaging materials (known as carriers) to immobilize microorganisms to obtain high removal efficiencies of water contaminants; such materials include tezontle, bagasse, sawdust, coconut fiber, and cotton fiber, among others. However, these packaging materials have been mainly used with bacteria, algae, and fungi but not with protozoa (Dzionek et al. 2016). In contrast to publications on the association of bacteria and algae with substrates, knowledge about the behavior of protozoa associated with substrates is scarce, although protozoa occur in high numbers in biofilms (Arndt et al. 2003). It has been mentioned that packaging materials for wastewater treatment purposes should possess specific characteristics present in tezontle, like being insoluble, non-toxic (for the system and the environment), accessible, economical, stable, and appropriate for regeneration. The matrices used for adsorption or attachment should be of high porosity to ensure the high contact area, as has been determined for tezontle. Besides, for wastewater treatment processes, packaging materials must have high mechanical resistance, as they can be exposed to diverse types of physical stress factors (Dzionek et al. 2016).

Thus, the activity of protozoa in the present study seems to be influenced by the presence of the tezontle. On one side, this substrate has the appropriate characteristics (theoretically and experimentally established) to be used as a suitable packaging material. On the other side, protozoa, as the sessile pedunculated ones, survive on various substrates like solid-air (soil grains, rocks), water-air, or solid-water (stones, macrophytes, animals, leaf litter, etc.) (Arndt et al. 2003). The protozoa's capability to adhere, colonize substrates, or temporally separate from biofilms provides them with clear advantages because food concentration (bacteria, algae, and other protists) may be significantly higher than in the surrounding water, and biofilms can serve as a refuge against predation (Arndt et al. 2003).

The proposed nuclei staining techniques for colonial and solitary peritrichous ciliated protozoa were simple, fast, and economical. Both techniques seem reproducible and reliable, allowing the observation of well-defined nuclei in all the cases evaluated and identifying the most abundant species that colonized tezontle in

the system. On the other hand, tezontle is an economical, natural, and abundant material in Mexico; it has a large number of pores and, therefore, a large surface area that allowed good adhesion of bacteria and peritrichous protozoa, consequently obtaining good removal efficiencies of organic matter (91.93%). Therefore, the present work confirmed that tezontle is an economical material with favorable composition and porosity for the abundant growth of solitary and colonial peritrichous ciliated protozoa, indicators of the excellent quality of treated wastewater.

The protozoan species that grew in the system could later be used to degrade toxic compounds, such as hydrocarbons or metals. Ciliated protozoa with peduncles, like *Z. paraentzii*, *E. plicatilis*, *V. campanula*, and *E. rotans*, showed a moderate to strong relationship with the functioning time of the reactor, which allowed the obtention of high removal efficiencies of both organic matter and suspended bacteria. The novel FMD and FD staining techniques highlighted the nuclei in all solitary and colonial peritrichous protozoa. It helped to identify them at the species level; therefore, they could be used for protozoan identification or as complementary techniques to those already existing for staining nuclei of species resistant to other dyes.

**ORCID**
Andrea M. Rivas-Castillo https://orcid.org/0000-0001-9710-2975
Antonio A. Garcia-Barrera https://orcid.org/0000-0003-2192-1725
Aristeo Garrido-Hernandez https://orcid.org/0000-0002-3706-7327
Francisco J. Martinez-Valdez https://orcid.org/0000-0002-1640-5577
Maria S. Cruz-Romero https://orcid.org/0000-0002-9164-7832
Maribel Quezada-Cruz https://orcid.org/0000-0003-0839-0421

**Acknowledgments**

The authors thank the CCAI (Industry-Academy Cooperation Center) at the Technological University of Tecamac for the technical support with the SEM. They also thank Margarita Reyes Santos (UNAM), Victoria Enciso Tenorio for the technical support provided. Additionally, the authors thank Luz Mariana Maciel Montes and Evelin Guadalupe Galvan Martinez for standardizing the staining techniques. Finally, thanks are given to Brandon Daniel Perez Garcia for the elaboration of the graphical abstract. The Ministry of Public Education financed this work through PRODEP-/103.5/13/7345.

**Conflict of interest**

The authors do not report any financial or personal connections with other persons or organizations, which might negatively affect the contents of this publication and/or claim authorship rights to this publication.

## Literature

**Acevedo-Davila J, Torres-Trevino LM, Lauren Y, Gómez Z.** Tezontle aggregate substitute optimization in building blocks mixture. Paper presented at: Electronics, Robotics and Automotive Mechanics Conference (CERMA 2007); 2007 September 25–28; Cuernavaca, Mexico. p. 307–311. https://doi.org/10.1109/cerma.2007.4367704

**Arndt H, Schmidt-Denter K, Auer B, Weitere M.** Protozoans and biofilms. In: Krumbein WE, Paterson DM, Zavarzin GA, editors. Fossil and recent biofilms. Dordrecht (Netherlands): Springer; 2003. p. 173–189. https://doi.org/10.1007/978-94-017-0193-8_10

**Baird RB, Eaton AD, Rice EW.** Standard methods for the examination of water and wastewater. Washington DC (United States): American Public Health Association; 2017. p. 2–68–10–17.

**Azovsky AI, Mazei YA.** Diversity and distribution of free-living ciliates from high-arctic Kara Sea sediments. Protist 2018 Apr; 169(2):141–157. https://doi.org/10.1016/j.protis.2018.01.001

**Beltran FME, Otarola MJ, Tarqui KT.** [Laboratory procedures for feces diagnosis] (in Spanish). In: Zavaleta Martinez-Vargas A, editor. [Manual of laboratory procedures for the diagnosis of intestinal parasites in humans] (in Spanish). Lima (Peru): National Institute of Health; 2014. p. 9–35.

**Bradbury PC.** Ciliates of fish. In: Kreier JP, editor. Parasitic protozoa. Massachusetts (USA): Elsevier; 1994. p. 81115.

**Canals O, Massana R, Riera JL, Balagué V, Salvadó H.** Microeukaryote community in a partial nitritation reactor prior to anammox and an insight into the potential of ciliates as performance bioindicators. N Biotechnol. 2018 Jul 25;43:3–12. https://doi.org/10.1016/j.nbt.2017.05.003

**Charpentier J.** [Treatment of residual waters with activated sludges] (in Spanish). Buenos Aires (Argentina): National Institute of Industrial Technology; 2014. p. 1–43.

**Dubber D, Gray NF.** Enumeration of protozoan ciliates in activated sludge: Determination of replicate number using probability. Water Res. 2009 Aug;43(14):3443–3452. https://doi.org/10.1016/j.watres.2009.05.006

**Dzionek A, Wojcieszynka D, Guzik U.** Natural carriers in bioremediation: A review. Electron J Biotechnol. 2016 Sep;23:28–36. https://doi.org/10.1016/j.ejbt.2016.07.003

**EPA.** Wastewater, technology fact sheet: sequencing batch reactor. Office of Water, Washington DC (USA): United States Environmental Protection Agency; 1999 [cited 2022 Apr 29]. Available from https://www3.epa.gov/npdes/pubs/sbr_new.pdf

**Foissner W, Weissenbacher B, Krautgartner WD, Lütz-Meindl U.** A cover of glass: first report of biomineralized silicon in a ciliate, *Maryna umbrellata* (Ciliophora: Colpodea). J Eukaryot Microbiol. 2009 Nov–Dec;56(6):519–530. https://doi.org/10.1111/j.1550-7408.2009.00431.x

**Ginoris YP, Amaral AL, Nicolau A, Coelho MA, Ferreira EC.** Development of an image analysis procedure for identifying protozoa and metazoa typical of activated sludge system. Water Res. 2007 Jun;41(12):2581–2589. https://doi.org/10.1016/j.watres.2007.02.006

**Isac L, Rodriguez E, Salas L, Fernández N.** [Atlas of protists and metazoans present in activated sludge] (in Spanish). Paper presented at: Jornada Internacional de Tratamiento y Reutilización en Aguas Residuales; 2008 June 5; Sevilla, Spain. p. 1–76.

**Kachieng'a L, Momba MNB.** The synergistic effect of a consortium of protozoan isolates (*Paramecium* sp , *Vorticella* sp., *Epistylis* sp. and *Opercularia* sp.) on the biodegradation of petroleum hydrocarbons in wastewater. J Environ Chem Eng. 2018 Aug;6(4):4820–4827. https://doi.org/10.1016/j.jece.2018.07.005

**Kumar N, Saini R, Chaudhary K, Bansal M, Kanika, Pandey N.** Correlation between toxic stress by heavy metal toxicants and periphytic protozoan colonization rates. Int J Adv Res. 2017 May;5(5): 529–534. https://doi.org/10.21474/IJAR01/4140

**Kumar S, Stecher G, Tamura K.** MEGA7: Molecular Evolutionary Genetics Analysis Version 7.0 for Bigger Datasets. Mol Biol Evol. 2016 Jul;33(7):1870-1874. https://doi.org/10.1093/molbev/msw054

**Küppers GC, Kosakyan A, Siemensma F, Claps MC, da Silva Paiva T, Fernández LD, Burdman L, Krashevska V, Lara E, Damborenea C.**

Protozoa. In: Thorp JH and Rogers CD, editors. Amsterdam (Netherlands): Elsevier; 2020. p. 9–77.
https://doi.org/10.1016/B978-0-12-804225-0.00002-2
**Li J, Ma L, Wei S, Horn H.** Aerobic granules dwelling vorticella and rotifers in an SBR fed with domestic wastewater. Sep Purif Technol. 2013 June;110:127–131. https://doi.org/10.1016/j.seppur.2013.03.022
**Li YD, Chen Y, Wang L, Yao L, Pan XM, Lee DJ.** Pollution tolerant protozoa in polluted wetland. Bioresour Technol. 2017 Sep;240: 115–122. https://doi.org/10.1016/j.biortech.2017.02.051
**Liao CC, Shin JW, Chen LR, Huang LLH, Lin WC.** First molecular identification of *Vorticella* sp. from freshwater shrimps in Tainan, Taiwan. Int J Parasitol Parasites Wildl. 2018 Oct 11;7(3):415–422. https://doi.org/10.1016/j.ijppaw.2018.10.002
**Liu J, Chen S, Ding J, Xiao Y, Han H, Zhong G.** Sugarcane bagasse as support for immobilization of *Bacillus pumilus* HZ-2 and its use in bioremediation of mesotrione-contaminated soils. Appl Microbiol Biotechnol. 2015 Dec;99(24):10839–10851.
https://doi.org/10.1007/s00253-015-6935-0
**Lynn DH.** Phylum CILIOPHORA – conjugating, ciliated protists with nuclear dualism. In: Lynn DH, editor. The ciliated protozoa. Dordrecht (Netherlands): Springer; 2010. p. 89–120.
https://doi.org/10.1007/978-1-4020-8239-9_4
**Madoni P.** Protozoa in wastewater treatment processes: A minireview. Ital J Zool. 2010 Mar;78(1):3–11.
https://doi.org/10.1080/11250000903373797
**Martín-Cereceda M, Pérez-Uz B, Serrano S, Guinea A.** Dynamics of protozoan and metazoan communities in a full scale wastewater treatment plant by rotating biological contactors. Microbiol Res. 2001;156(3):225–238. https://doi.org/10.1078/0944-5013-00105
**Martín-Cereceda M, Zamora J, Pérez-Uz B, Guinea A.** Ciliate communities of rotating biological contactor biofilms: A multivariate approach. Syst Appl Microbiol. 2002 Aug;25(2):301–313.
https://doi.org/10.1078/0723-2020-00090
**Nacheva PM, Moeller Chávez G, Bustos C, Garzón Zúñiga MA, Hornelas Orozco Y.** Comparison of bioreactors with different kinds of submerged packed beds for domestic wastewater treatment. Water Sci Technol. 2008;58(1):29–36.
https://doi.org/10.2166/wst.2008.321
**Ogleni N, Topaloglu D, Dere T, Ileri R.** Microbiological investigation of activated sludge in sequencing batch bioreactor for urban wastewater treatment. J Sci Ind Res. 2010 Aug;69(8):643–646.
**Papadimitriou CA, Papatheodoulou A, Takavakoglou V, Zdragas A, Samaras P, Sakellaropoulos GP, Lazaridou M, Zalidis G.** Investigation of protozoa as indicators of wastewater treatment efficiency in constructed wetlands. Desalination 2010 Jan;250(1):378–382. https://doi.org/10.1016/j.desal.2009.09.060
**Pérez-Uz B, Arregui L, Calvo P, Salvadó H, Fernández N, Rodríguez E, Zornoza A, Serrano S.** Assessment of plausible bioindicators for plant performance in advanced wastewater treatment systems. Water Res. 2010 Sep;44(17):5059–5069.
https://doi.org/10.1016/j.watres.2010.07.024
**Perry CC, Belton D, Shafran K.** Studies of biosilicas; structural aspects, chemical principles, model studies and the future. In: Müller WEG, editor. Silicon Biomineralization. Progress in Molecular and Subcellular Biology. Berlin, Heidelberg (Germany); Springer: 2003(33). p. 269–299. https://doi.org/10.1007/978-3-642-55486-5_11
**Posada D, Crandall KA.** MODELTEST: testing the model of DNA substitution. Bioinformatics. 1998;14(9):817–818.
https://doi.org/10.1093/bioinformatics/14.9.817
**Priya M, Haridas A, Manilal VB.** Involvement of protozoa in anaerobic wastewater treatment process. Water Res. 2007 Dec;41(20): 4639–4645. https://doi.org/10.1016/j.watres.2007.06.047
**Rakshit D, Biswas SN, Sarkar SK, Bhattacharya BD, Godhantaraman N, Satpathy KK.** easonal variations in species composition, abundance, biomass and production rate of tintinnids (Ciliata: Protozoa) along the Hooghly (Ganges) River Estuary, India: A multivariate approach. Environ Monit Assess. 2014 May;186(5):3063–3078.
https://doi.org/10.1007/s10661-013-3601-9
**Rehnam A.** Heavy metals uptake by *Euglena proxima* isolated from tannery effluents and its potential use in wastewater treatment. Russ J Ecol. 2011 Jan;42:44–49.
https://doi.org/10.1134/S1067413611010085
**Robertson LJ, Clark CG, Debenham JJ, Dubey JP, Kváč M, Li J, Ponce-Gordo F, Ryan U, Schares G, Su C, et al.** Are molecular tools clarifying or confusing our understanding of the public health threat from zoonotic enteric protozoa in wildlife? Int J Parasitol Parasites Wildl. 2019 Feb 13;9:323–341.
https://doi.org/10.1016/j.ijppaw.2019.01.010
**Rodríguez-Díaz E, Salcedo-Pérez E, Rodríguez-Macias R, González-Eguiarte DR, Mena-Munguía S.** [Tezontle reuse: effect on physical properties and tomato *(Lycopersicon esculentum* Mill) production] (in Spanish). Terra Latinoam. 2013 Oct;31(4):275–284.
http://www.scielo.org.mx/scielo.php?script=sci_arttext&pid=S0187-57792013000500275&lng=es&nrm=iso
**Sun P, Ji D, Song W.** Notes on a new marine peritrichous ciliate (Ciliophora: Peritrichida), *Zoothamnium xuianum* n. sp., with redescription of *Z. paraentzii* Song, 1991 from northern China. Zootaxa 2005 Nov;1075(1):41–53. https://doi.org/10.11646/zootaxa.1075.1.2
**Sun P, Clamp JC, Xu D, Huang B, Shin MK, Turner F**. An ITS-based phylogenetic framework for the genus *Vorticella*: finding the molecular and morphological gaps in a taxonomically difficult group. Proc Biol Sci. 2013 Oct 2;280(1771):20131177.
https://doi.org/10.1098/rspb.2013.1177
**Vilas-Boas JA, Cardoso SJ, Senra MVX, Rico A, Dias RJP.** Ciliates as model organisms for the ecotoxicological risk assessment of heavy metals: A meta-analysis. Ecotoxicol Environ Saf. 2020 Aug;199: 110669. https://doi.org/10.1016/j.ecoenv.2020.110669
**Yáñez-Ocampo G, Sánchez-Salinas E, Ortiz-Hernández ML.** Removal of methyl parathion and tetrachlorvinphos by a bacterial consortium immobilized on tezontle-packed up-flow reactor. Biodegradation. 2011 Nov;22(6):1203–1213.
https://doi.org/10.1007/s10532-011-9475-z
**Xu H, Zhang W, Jiang Y.** Do early colonization patterns of periphytic ciliate fauna reveal environmental quality status in coastal waters? Environ Sci Pollut Res Int. 2014;21(11):7097–7112.
https://doi.org/10.1007/s11356-014-2615-3

Supplementary materials are available on the journal's website.

ORIGINAL PAPER
Polish Journal of Microbiology
2022, Vol. 71, No 4, 553–562
https://doi.org/10.33073/pjm-2022-051

# *In vivo* Efficacy of *Bacillus velezensis* Isolated from Korean Gochang Bokbunja Vinegar against Carbapenem-Resistant *Klebsiella pneumoniae* Infections

FATEMEH GHORBANIAN[1, 2#], HOONHEE SEO[1, 2#], HANIEH TAJDOZIAN[1, 2], YOUNGKYOUNG LEE[1, 2], MD ABDUR RAHIM[1, 2], SUKYUNG KIM[2], IL-YUN JUNG[3], SAEBIM LEE[1, 2] and HO-YEON SONG[1, 2*]

[1] Department of Microbiology and Immunology, School of Medicine, Soonchunhyang University, Cheonan, Chungnam, Republic of Korea
[2] Probiotics Microbiome Convergence Center, Soonchunhyang University, Asan, Chungnam, Republic of Korea
[3] Korea Balsamic Vinegar Association, Gochang, Jeonbuk, Republic of Korea

Submitted 9 September 2022, accepted 3 November 2022, published online 12 December 2022

Abstract

Outbreaks of carbapenem-resistant *Enterobacteriaceae* (CRE), especially *Klebsiella pneumoniae* (CRKP), are commonly reported as severe infections in hospitals and long-term care settings, and their occurrence is increasing globally. Conventional antibiotics used for treating CRE have become ineffective due to resistance development. Furthermore, their safety issues restrict their availability and use for CRE treatment. Therefore, developing new drugs different from existing drugs to combat this deadly menace is urgently needed. Probiotics can be a potential option in this context, as probiotics' efficacy against a variety of infectious illnesses has already been well established. Here, we report the effect of the *Bacillus velezensis* strain isolated from Gochang Bokbunja vinegar in Korea on CRE infection using two mouse models. Data showed that pretreatment with *B. velezensis* significantly reduced body weight loss and mortality of CRKP-infected mice in the preventive model. The oral administration of *B. velezensis* in a therapeutic model also decreased the mortality and illness severity in CRKP-infected mice. Moreover, a two-week oral acute toxicity assay in guinea pigs did not reveal any aberrant clinical signs. Our findings demonstrate the potential effectiveness of our candidate probiotic strain, *B. velezensis*, against CRKP, suggesting that it could be used as an antimicrobial agent for treating CRKP-related infections.

Keywords: *Bacillus velezensis*, *Klebsiella pneumoniae*, carbapenem-resistant *Enterobacteriaceae* (CRE), Gochang Bokbunja vinegar, probiotics

## Introduction

Antimicrobial resistance has been considered one of the biggest threats to human health globally (Sulis et al. 2022). According to a recent report published in 2022, 4.95 million deaths were associated with antimicrobial resistance in 2019, including 1.27 million deaths directly attributable to antimicrobial resistance (Murray et al. 2022). To make matters worse, resistance to carbapenem, the preferred last resort drug for treating multidrug-resistant bacterial infections was first reported in *Enterobacteriaceae* strains in the early 1990s. These carbapenemase-producing isolates have spread worldwide, causing a global health crisis (Potter et al. 2016; Lutgring 2019). According to the Center for Disease Control and Prevention (CDC) report, in 2017, 13,100 carbapenem-resistant *Enterobacteriaceae* (CRE) infections were estimated among hospitalized patients, which resulted in 1,100 deaths in the USA (CDC 2019).

Meanwhile, *Klebsiella pneumoniae* is the species that causes the most cases of CRE infections (Logan and Weinstein 2017). It caused more than 55,700 deaths

# Fatemeh Ghorbanian and Hoonhee Seo contribute equally to this work and are co-first authors.

* Corresponding author: H.-Y. Song, Department of Microbiology and Immunology, School of Medicine, Soonchunhyang University, Cheonan, Chungnam, Republic of Korea; Probiotics Microbiome Convergence Center, Soonchunhyang University, Asan, Chungnam, Republic of Korea; **e-mail: songmic@sch.ac.kr**

worldwide in 2019 (Murray et al. 2022). As such, with the significant increase in the use of carbapenems in clinical practice today, the evolution of carbapenem-resistant bacteria has become a significant concern (Sheu et al. 2019). Although standards for treating CRE infections are being developed in response to this human threat, problems due to resistance, treatment failure, and toxicity still exist (Tilahun et al. 2021). Therefore, new and effective anti-CRE medicines are desperately needed.

According to the Food and Agriculture Organization (FAO)/ World Health Organization (WHO), probiotics are 'live microorganisms which, when administered in adequate amounts, confer a health benefit on the host' (FAO/WHO 2001). As reported by many studies, probiotics have many functions, including providing nutrients, modifying biological activities, preventing pathogenic microorganisms, boosting immune responses, and enhancing growth (Oelschlaeger 2010). Some reports have shown the effects of probiotics against different diseases, such as necrotizing enterocolitis (Patel and Underwood 2018), acute infectious diarrhea (Allen et al. 2010), antibiotic-associated diarrhea (Kopacz and Phadtare 2022), metabolic disorders (Li et al. 2021a), and autoimmune diseases (De Luca and Shoenfeld 2019). Furthermore, probiotics could play an essential role in acute infectious diseases, namely: tuberculosis (Rahim et al. 2022), acquired immunodeficiency syndrome (AIDS) (Ceccarelli et al. 2019), *Pseudomonas aeruginosa* infection (Huang et al. 2020), and COVID-19 (coronavirus disease 2019) (Anwar et al. 2021). Probiotics have been extensively studied to treat various diseases, including infectious ones. Thus, the application of probiotics is considered valuable for treating CRE infections. This study aimed to determine the impact of a *Bacillus velezensis* strain isolated from Gochang Bokbunja vinegar in Korea on carbapenem-resistant *Klebsiella pneumoniae* (CRKP) infection.

## Experimental

### Materials and Methods

**CRKP.** CRKP was collected from the Pathogenic Resource Bank at Soonchunghyng University Hospital (Tajdozian et al. 2021). It was cultured in MacConkey broth (BD Difco, USA) and incubated at 37C for 18 h. Next, bacterial growth was determined using a spectrophotometer (DR 1900, HACH, USA), and optical density at 600 nm ($OD_{600\ nm}$) was adjusted to 1.0. After that, the bacterial number was enumerated through a colony-forming unit (CFU) assay. For further uses, stock culture in 60% glycerol was prepared and kept at –80°C.

**Isolation and identification of a probiotic strain from naturally fermented vinegar.** The candidate probiotic was obtained from naturally 14-days-fermented Gochang Bokbunja vinegar from Gochang County, North Jeolla Province, South Korea. Upon receiving the samples, they were streaked onto an MRS agar (BD Difco, USA) plate and incubated at 37°C for 24 h. After that, single colonies were picked and subcultured in MRS broth (BD Difco, USA). After incubating in a shaking incubator overnight at 37°C under aerobic conditions, bacterial growth was determined using the spectrophotometer. Stock in 60% glycerol was prepared and stored at –80°C for further use. This probiotic strain was sent to a company (Biofact Co, Korea) for 16S rRNA sequencing and species identification.

**Biochemical tests.** A biochemical test was conducted using an API 50CH kit (bioMerieux, France) to observe the carbohydrate fermentation pattern of the probiotic strain compared to other reference strains. The candidate probiotic strain was cultured on an MRS agar plate. A single colony was then picked and mixed with 1 ml suspension medium. After that, the suspension turbidity was determined using 2 McFarland, and 0.1 ml of this suspension was diluted in 10 ml of CHB medium (bioMerieux, France). Next, the strip was removed from the API kit and placed in a tray. The final prepared bacterial suspension was transferred into the strip's wells and incubated at 37°C for 48 h. Subsequently, color change in each well was observed, and an identification table was prepared as (+/–).

**Quantitative RT-PCR assay.** qRT-PCR is a well-established and robust approach for detecting and quantifying microorganisms (Kralik and Ricchi 2017). Thus, qRT-PCR was performed to identify the isolated strain. Genomic DNA was extracted from the isolated candidate probiotic strain using the QIAamp DNA Mini Kit (QIAGEN, Germany). Genomic DNAs were also extracted from *B. velezensis* KCTC 13417, *Bacillus amyloliquefaciens* KCTC 3002, *Bacillus subtilis* KCTC 3135, and *Bacillus lichenoformis* KCTC 1659. They were obtained from the Korean Collection for Type Cultures (KCTC) as reference organisms to help us to distinguish closely related species in the *Bacillus* genus. Extracted DNA was then diluted to run qRT-PCR using species-specific primers (Kwon et al. 2009; Huang et al. 2017a; Dunlap 2019; Bahuguna et al. 2020). A primer for the macrolactin gene was used to distinguish between *B. velezensis* and *B. amyloliquefaciens* (Fan et al. 2018; Li et al. 2021b). The used primers are listed in Table SI. We performed qRT-PCR in a final volume of 20 µl consisting of 10 µl of SYBER Green Supermix (BIO-RAD, USA), 4 µl nuclease-free water, 5 µl of genomic DNA, and 0.5 µl each of forward and reverse primers. Amplification used the following thermal cycling steps: an initial DNA denaturation step at 95°C for 3 min, followed

by 39 cycles of 10 s at 95°C for denaturation, 10 s at 55°C for annealing, and 30 s at 72°C for extension.

**Cultivation of *B. velezensis* using a lab-scale fermenter based on food-grade media.** We used food-grade medium (FGM) to cultivate our strain as an anti-CRE therapeutic agent that could be developed in the future. FGM was used for cultivation because this strain could grow well in this medium. In addition, FGM is safe for human consumption, and it is composed of glucose, yeast peptone, Tween 80, and magnesium sulfate based on an MRS medium (Table SII). The pH of the optimized FGM was 7.5. We adjusted its pH to 6.3 using 6 N HCl. Before growing in a fermenter system, the strain was cultivated in 30 ml FGM. After incubation at 37°C for 18 h, the OD and pH of the culture broth were checked with a spectrophotometer and a pH meter (Mettler-Toledo, Switzerland), respectively, every 2 h during the incubation period. After confirming the bacterial growth and the pH, the probiotic strain was grown in a lab-scale fermenter system (FMT-ST-S07, Fermentec, South Korea). The fermenter was first filled up with 2 l of FGM. The FGM-filled fermenter was then autoclaved at 121°C for 15 minutes. After that, when the medium reached the optimal temperature, 1.0% of probiotic culture was aseptically added into the fermenter system and fermented at 37°C for 10 h using a fermenter impeller. After incubation, the culture was recovered in a sterile container, centrifuged, washed, and resuspended with the culture supernatant at $1.5 \times 10^9$ CFU/200 µl for each mouse of the therapeutic model. FGM-cultured probiotics were used in the treatment model, but MRS-cultured probiotics were used in the prevention model and toxicity tests.

**Investigation of the effect of *B. velezensis* in a CRKP-infected mouse model.** In this study, preventive and therapeutic models were applied to evaluate the effectiveness of probiotics in a CRKP-infected mouse model, and 9-week-old female BALB/c mice (Dooyeol Biotech, Korea) were used. The prevention model was used to see preventive effects by administering probiotics before infection. In the treatment model, probiotics were administered the day after inducing infection to see the therapeutic effect. At the time of treatment with probiotics in both models, the probiotic-treatment group received *B. velezensis*. However, the infection and control groups received distilled water through oral gavage for making the same treatment condition. In both models, gastric neutralization was induced by oral administration of sodium bicarbonate ($NaHCO_3$) to increase animal severity through the increased intestinal reach of live pathogens (Czuprynski and Faith 2002). In addition, cyclophosphamide was intraperitoneally injected 3 days before infection to induce neutropenia (Pan et al. 2015). 5-Fluorouracil (5-FU) was also administered intraperitoneally to induce additional immunosuppression (VanderVeen et al. 2020). Disease severity score, body weight, and survival of mice were checked in both models during the experimental period.

We examined the preventive effect of our candidate probiotic strain, *B. velezensis*, in CRKP-infected BALB/c mice. The probiotic strain was administered at $1.5 \times 10^9$ CFU/mouse in 200 µl daily as a single dose by oral gavage for three days before infection. Cyclophosphamide (Sigma Aldrich, USA) at 450 mg/kg (200 µl) was also injected intraperitoneally three days before infection. Three days after neutropenia, infection was induced twice per week through oral administration at a dose level of $6.7 \times 10^9$ CFU/200 µl/mouse on day 0 and $9 \times 10^9$ CFU/200 µl/mouse on days 2, 10, and 12. $NaHCO_3$ (0.2 M, 200 µl) (Sigma Aldrich, USA) was administered along with the infection. 5-FU (50 mg/kg, 200 µl) (Sigma Aldrich, USA) was administered intraperitoneally on days 13 and 15 after inducing infection.

We investigated the therapeutic potential of our candidate probiotic strain, *B. velezensis*, in CRKP-infected BALB/c mice. In the therapeutic mouse model, 200 µl of cyclophosphamide (450 mg/kg) was injected intraperitoneally three days before infection. Infection was then induced by oral administration of 200 µl CRKP at $9 \times 10^9$ CFU/mouse on days 0, 2, and 6 with pretreatment of $NaHCO_3$ (0.2 M, 200 µl). Mice were treated with *B. velezensis* at $1.5 \times 10^9$ CFU/200 µl/mouse twice the next day after the infection treatment. They were intraperitoneally injected on days 10 and 14 with one dose of 5-FU (50 mg/kg, 200 µl).

**Evaluation of repeated oral acute toxicity of probiotics in guinea pigs.** A 2-week repeated oral acute toxicity evaluation of probiotics in guinea pigs was performed according to a previous report (Lee et al. 2021). Adult male guinea pigs (weight range 1,000 to 1,280 g) were used and administered orally, and sterile water was used as the vehicle. In the case of the treatment group, probiotics ($2 \times 10^8$ CFU/ml/200 µl) were administered once a day, and clinical symptoms, mortality, and weight changes were observed over the entire period.

**Review of animal experiment ethics.** All animal experiments were conducted in a biosafety level 2 facility (LML 20–591) of Soonchunhyang University, according to the Ministry of Food and Drug Safety (Registration, MFDS, No. 657). This study's animal experiments protocol was approved by the Institutional Animal Care and Use Committee (IACUC) of Soonchunhyang University.

## Results

**Identification based on 16S rRNA gene sequencing.** The 16S rRNA gene sequencing analysis was done for the isolated strain (Table I). The result was compared to sequences stored in the National Center for

Table I
Identification of isolated bacterial strain based on 16S rRNA gene sequence analysis.

| NCBI references | Organisms | Length | Score | Identities | Gaps |
|---|---|---|---|---|---|
| NR_075005.2 | *Bacillus velezensis* strain FZB42 | 1,550 | 2,728 bits (1,477) | 1,492/1,499 (99%) | 2/1,499 (0%) |
| NR_116240.1 | *Bacillus velezensis* strain CBMB205 | 1,445 | 2,615 bits (1,416) | 1,427/1,432 (99%) | 2/1,432 (0%) |
| NR_112685.1 | *Bacillus amyloliquefaciens* strain NBRC 15535 | 1,475 | 2,699 bits (1,461) | 1,470/1,475 (99%) | 0/1,475 (0%) |
| NR_041455.1 | *Bacillus amyloliquefaciens* strain NBRC 15535 | 1,472 | 2,697 bits (1,460) | 1,468/1,472 (99%) | 0/1,472 (0%) |
| NR_102783.2 | *Bacillus subtilis* subsp. *subtilis* strain 168 | 1,550 | 2712 bits (1,468) | 1,489/1,499 (99%) | 2/1,499 (0%) |
| NR_118996.1 | *Bacillus licheniformis* strain DSM 13 | 1,545 | 2,579 bits (1,396) | 1,466/1,500 (98%) | 4/1,500 (0%) |
| NR_116023.1 | *Bacillus licheniformis* strain BCRC 11702 | 1,468 | 2,545 bits (1,378) | 1,439/1,469 (98%) | 2/1,469 (0%) |

Biotechnology Information (NCBI) databases. The 16S rRNA gene sequencing of the probiotic strain shared 99% sequence identities with 16S rRNA gene sequences of *B. velezensis* strain FZB42, *B. velezensis* strain CBMB205, *B. amyloliquefaciens* strain NBRC 15535, and *B. subtilis* subsp. *subtilis* strain 168. It also shared 98% sequence identities with *B. licheniformis* strain DSM 13 and *B. licheniformis* strain BCRC 11702. These findings suggest that the isolated strain belongs to the *Bacillus* genus.

**Carbon utilization assay of the isolated probiotic strain by API kit.** To identify and characterize phenotypes of the probiotic strain, biochemical characterization was performed using an API 50CH Biochemical Kit. Utilization patterns of carbon sources of the isolated probiotic strain were compared with *B. velezensis* KCTC 13417, *B. amyloliquefaciens* KCTC 3002, and *B. lichenoformis* KCTC 1659, obtained from KCTC. Results are shown in Table II. The candidate strain showed carbon source utilization patterns more similar to *B. velezensis* than to *B. licheniformis* and *B. amyloliquefaciens* but showed some differences with the KCTC *B. velezensis*.

**Identification of isolated probiotic strain by qRT-PCR assay.** The qRT-PCR assay was conducted to identify the candidate probiotic strain using species-specific primer sets (Table III). We analyzed the resulting threshold cycle ($C_t$ value). We found that the *B. velezenesis*-specific primer was specific for both *B. velezensis* KCTC 13417 and our candidate probiotic strain, but it could not detect other closely related species. We used a *B. amyloliquefaciens*-specific primer and observed amplification result for *B. amyloliquefaciens* KCTC 3002, *B. velezensis* KCTC 13417, and the candidate probiotic strain. We found that this primer could not work specifically. Therefore, to distinguish between *B. amyloliquefaciens* and *B. velezensis*, we ran the PCR using a macrolactin-specific primer. Macrolactin is a gene cluster detected only in *B. velezensis* (Fan et al. 2017). After running the PCR using a macrolactin-specific primer, we noticed the amplification cycle of *B. velezensis* KCTC 13417 and our candidate probiotic strain but not *B. amyloliquefaciens* KCTC 3002. This result strongly proves that our candidate probiotic strain is *B. velezensis*. Species-specific primers for *B. lichenoformis* and *B. subtilis* showed the amplification for *B. lichenoformis* KCTC 1659 and *B. subtilis* KCTC 3135, respectively, while they did not show the amplification for other strains. These results confirm that our isolated probiotic strain is *B. velezensis*.

**Cultivation using lab-scale fermenter and FGM.** The probiotic strain was cultivated in FGM. Bacterial growth and pH were checked every 2 h (Fig. 1). Fig. 1a shows the growth curve of our candidate probiotic strain. Its OD reached 0.8 after 10 h of incubation. The pH of the broth culture was also checked. We noticed a reduction of pH after 2 h of incubation. It continued to

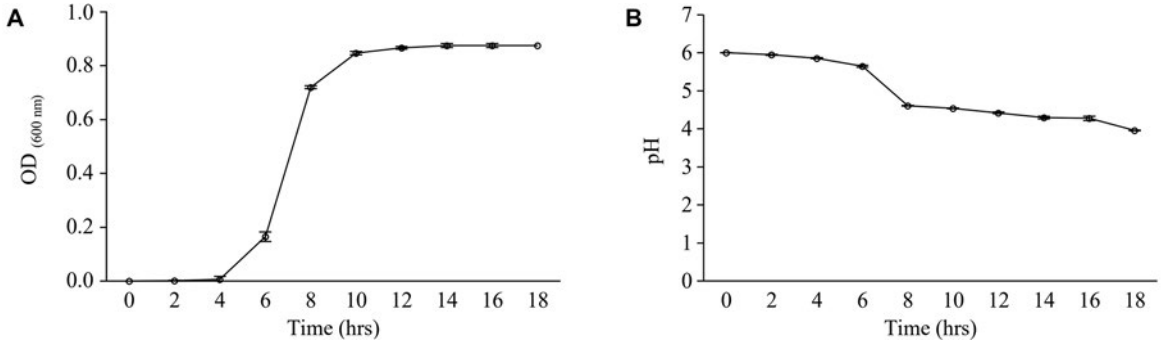


Fig. 1. Bacterial growth and pH measurement in food grade medium with time. The probiotic strain was inoculated and cultivated. Its A) growth and B) pH were checked every 2 h.

Table II
The ability of the candidate probiotic strain to dehydrate carbon sources.

| No. | Type of test | Candidate strain | | *Bacillus velezensis* KCTC 13417 | | *Bacillus amyloliquefaciens* KCTC 3002 | | *Bacillus licheniformis* KCTC 1659 | |
|---|---|---|---|---|---|---|---|---|---|
| | | 24 h | 48 h | 24 h | 48 h | 24 h | 48 h | 24 h | 48 h |
| 0 | Control | – | – | – | – | – | – | – | – |
| 1 | Glycerol | + | + | + | + | + | – | + | + |
| 2 | Erythritol | – | – | – | – | – | – | – | – |
| 3 | D-arabinose | – | – | – | – | – | – | – | – |
| 4 | L-arabinose | – | + | + | + | + | + | – | + |
| 5 | D-ribose | + | + | + | + | + | + | + | + |
| 6 | D-xylose | – | + | + | + | + | + | – | – |
| 7 | L-xylose | – | – | – | – | – | – | – | – |
| 8 | D-adonite | – | – | – | – | – | – | – | – |
| 9 | Methyl-βD-xylopyranoside | – | – | – | – | – | – | – | – |
| 10 | D-galactose | + | + | + | + | – | – | – | – |
| 11 | D-glucose | + | + | + | + | + | – | + | – |
| 12 | D-fructose | + | + | + | + | + | – | + | – |
| 13 | D-mannose | + | + | + | + | + | – | + | – |
| 14 | L-sorbose | – | – | – | + | – | – | – | – |
| 15 | L-rhamnose | + | + | + | + | – | – | – | – |
| 16 | Dulcitol | – | – | – | – | – | – | – | – |
| 17 | Inocitol | + | + | + | + | + | + | – | – |
| 18 | D-mannitol | + | + | + | + | + | – | + | – |
| 19 | D-sorbito | + | + | + | + | + | – | + | + |
| 20 | Methyl-αD-mannopyranoside | – | – | – | – | – | – | – | – |
| 21 | Methyl-αD-glucopyranoside | – | + | + | + | + | + | + | + |
| 22 | N-acetylglucosamine | + | + | – | – | + | – | + | – |
| 23 | Amygdaline | + | + | + | + | – | + | + | – |
| 24 | Arbutine | + | + | + | + | + | – | + | – |
| 25 | Esculine | + | + | + | + | + | + | + | + |
| 26 | Salicin | + | + | + | – | + | + | + | – |
| 27 | D-Cellibiose | + | + | + | + | + | + | + | + |
| 28 | D-Maltose | + | + | + | + | + | + | + | + |
| 29 | D-Lactose | + | + | – | – | + | + | + | + |
| 30 | D-Melibiose | – | + | – | + | + | + | – | + |
| 31 | D-Sacharose | + | + | + | – | + | + | + | – |
| 32 | D-Trehalose | + | + | + | + | + | + | – | – |
| 33 | Inulin | – | – | – | + | – | – | – | – |
| 34 | D-Melezitose | + | – | – | – | – | – | – | – |
| 35 | D-Raffinose | + | + | + | + | + | + | + | + |
| 36 | Amidon | + | + | + | – | + | – | + | – |
| 37 | Glycogen | – | + | + | – | + | – | + | – |
| 38 | Xylitol | – | – | – | – | – | – | – | – |
| 39 | Gentibiose | + | – | – | – | – | – | + | – |
| 40 | D-Turanose | – | – | + | + | – | – | + | + |
| 41 | D-Lyxose | – | – | – | – | – | – | – | – |
| 42 | D-Tagatose | + | + | + | – | – | – | – | – |
| 42 | D-Fucose | – | – | – | – | – | – | – | – |
| 44 | L-Fucose | – | – | – | – | – | – | – | – |
| 45 | D-arabitol | – | – | – | – | – | – | – | – |
| 46 | L-arabitol | – | – | – | – | – | – | – | – |
| 47 | Potassium gluconate | + | – | – | – | – | – | – | – |
| 48 | Potassium 2 ketogluconate | – | – | – | – | – | – | – | – |
| 49 | Potassium 5 ketogluconate | – | – | – | – | – | – | – | – |

(+) – positive reaction (yellow) (No. 25: black); (–) – negative reaction (red)

Table III
Identification of the isolated bacterial strain by qRT-PCR.

| Species-specific primer for- | Oligo name | Amplification results | | | | |
|---|---|---|---|---|---|---|
| | | Candidate probiotic strain | *B. velezensis* KCTC 13417 | *B. amyloliquefaciens* KCTC 3002 | *B. subtilis* KCTC 3135 | *B. licheniformis* KCTC 1659 |
| *Bacillus velezensis* | Bvel | + | + | – | – | – |
| *Bacillus subtilis* | YtcP | – | – | – | + | – |
| *Bacillus amyloliquefaciens* | spBamyphes | + | + | + | – | – |
| *Bacillus licheniformis* | Blich | – | – | – | – | + |
| Macrolactin | Mln | + | + | – | – | – |

(+) – amplification, (–) – no amplification

reduce slowly until 18 h (Fig. 1b). We cultured our strain in the lab-scale fermenter system based on these results.

**Evaluation of the preventive effect of *B. velezensis* in CRKP-infected mice.** The preventive effect of our candidate strain was evaluated (Fig. 2). Throughout the test phase, the body weights of untreated mice decreased significantly more compared to the mice treated with *B. velezensis* (Fig. 2a). Body weight reduction rate was 8.4% for the treated group on days 18 and 20. In contrast, it was 35.8% for the untreated group. Illness severity scores of the probiotic-treated group and infection group were observed from day 0 to day 21 (Fig. 2b). The group not treated with probiotics increased steadily throughout the experiment and then increased more rapidly at 2 to 3 weeks but to a lesser extent in the probiotic-treated group. The survival rates of mice in both groups are shown in (Fig. 2c). The untreated group showed a survival rate of 60% on day 20, and finally, all mice died on day 21, whereas 80% of mice survived in the treated group until the end of the experiment. Fig. 2d shows the images of mice in different groups. After finishing the experiment, we found that all mice in the infection group without probiotic treatment died (left image), whereas mice in the probiotic-treatment group were healthy (right image). These results showed a preventive effect of our candidate probiotic strain against CRKP infection in a mouse model.

**Evaluation of the therapeutic effect of *B. velezensis* on CRKP-infected mice.** Therapeutic effects of *B. velezensis* on lethal CRKP-infected mice were evaluated (Fig. 3). On days 13 and 18, the untreated group lost 29.5% of their body weight. In contrast, the treated

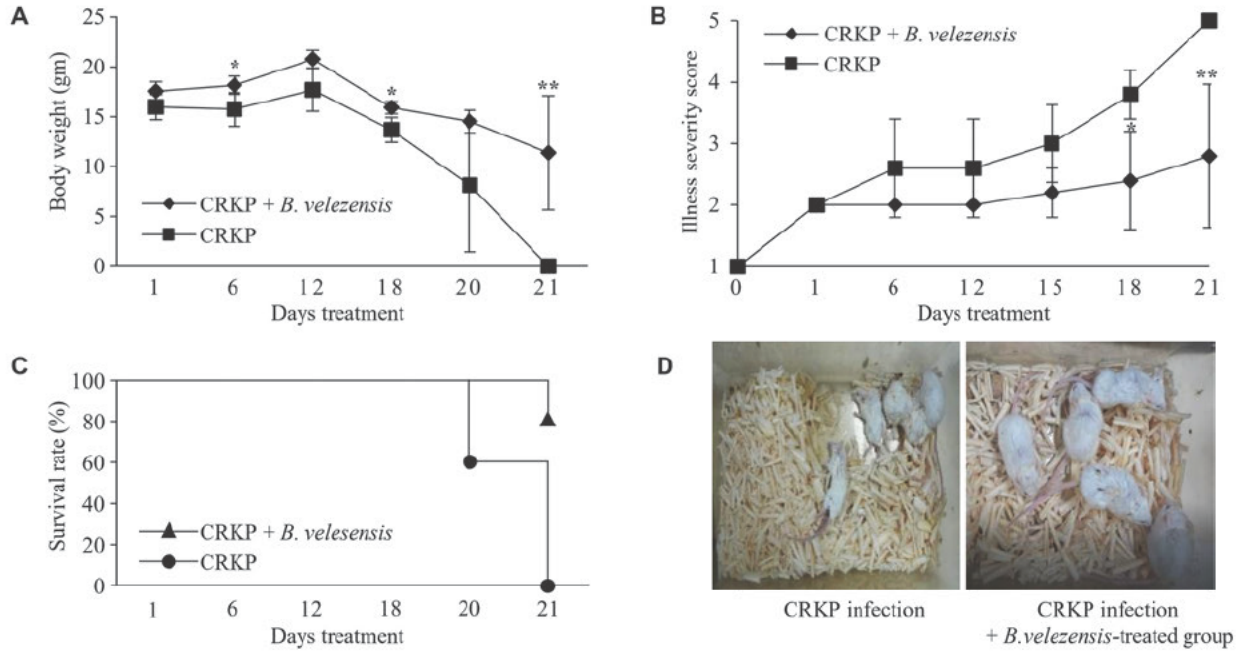


Fig. 2. Effect of *B. velezensis* on a clinical isolate of CRKP in the preventive infection murine model.
A) Body weight and B) illness severity were observed during the experimental period. Illness severity score was evaluated as (1 – healthy, 2 – minimally ill, 3 – moderately ill, 4 – severely ill, 5 – dead). C) Survival rate was observed during the entire experimental period. D) CRKP treated group (left image), CRKP + *B. velezensis* treated group (right image).
Statistical significance with the control was analyzed using unpaired Student's *t*-test (*** $p<0.001$; ** $p<0.01$; * $p<0.05$).

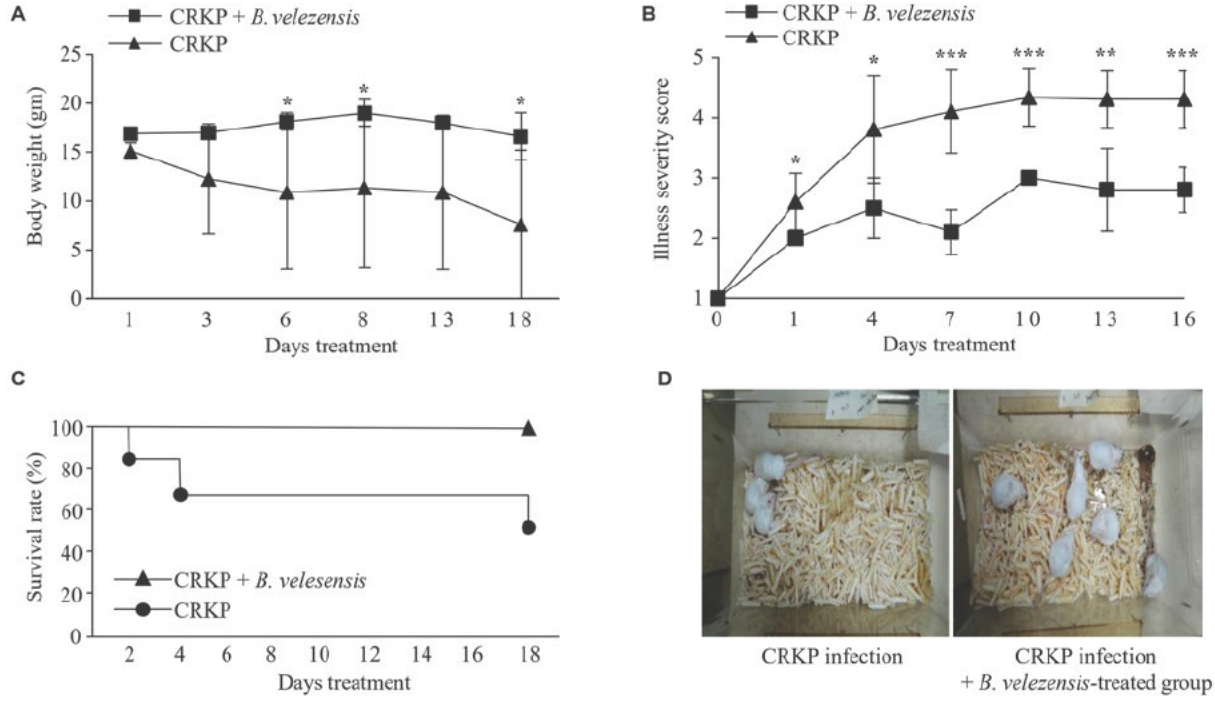


Fig. 3. Effect of *B. velezensis* on a clinical isolate of CRKP in a therapeutic infection murine model.

A) Body weight, B) severity of illness, and C) survival rate were observed during the experimental period. Illness severity score was evaluated (1 – healthy, 2 – minimally ill, 3 – moderately ill, 4 – severely ill, 5 – dead). D) CRKP treated group (left image), and CRKP + *B. velezensis* treated group (right image). Statistical significance with the control was analyzed using unpaired Student's *t*-test (*** $p < 0.001$; ** $p < 0.01$; * $p < 0.05$).

group showed insignificant body-weight reduction (Fig. 3a). The severity of illness was measured for both the probiotic-treated group and the infection group from day 0 to day 20 (Fig. 3b). We observed a variation in sickness scores between the groups. The survival rate of mice was determined for both groups (Fig. 3c). The untreated group's survival rate had decreased to 50.2%, whereas all mice remained alive in the treated group. Fig. 3d shows images of mice after CRKP infection. The infection group developed sickness and eventually died (left image), while mice with probiotic treatment were healthy (right image).

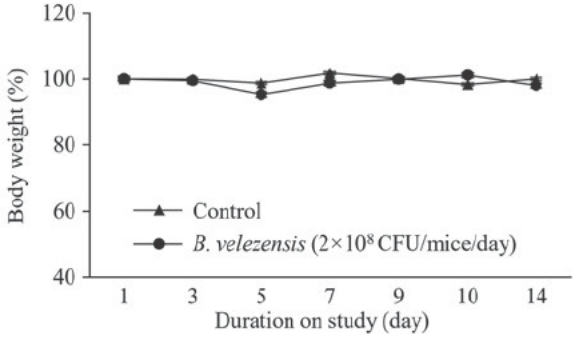


Fig. 4. Two-week repeated oral dose toxicity test of *B. velezensis* using guinea pigs. The body weights of guinea pigs were measured on days 1, 3, 5, 7, 9, 10, and 14. The candidate probiotic was orally administered at $2 \times 10^8$ CFU/mice/day at 200 µl per animal once a day, every day, for 2 weeks.

**Acute oral dose toxicity of *B. velezensis*.** Acute oral toxicity of *B. velezensis* was evaluated using guinea pigs through oral administration for two weeks. No significant variations in body weight were observed between the groups (Fig. 4). Additionally, unusual clinical symptoms or death in guinea pigs treated with *B. velezensis* were not observed (Table SIII).

## Discussion

CRKP strains are causing a significant public health concern across the globe because of their capacity to spread quickly in the hospital setting with a high mortality rate and their extensive antimicrobial resistance characteristics (Brink 2019). Currently, infections with CRE have a limited number of therapeutic options, which have been utilized rarely due to concerns about their effectiveness and toxicity (Morrill et al. 2015). Therefore, new anti-CRE drug agents that differ from existing drug regimens are desperately needed. Under such circumstances, probiotics can be a potential option as their effectiveness against different infectious diseases has already been well established.

Several human studies have recently reported the effectiveness of probiotics for various gut-related diseases, such as necrotizing enterocolitis and antibiotic-associated diarrhea (Cremonini et al. 2002; AlFaleh and

Anabrees 2014). Besides, probiotics can help maintain intestinal barrier integrity (Hemert et al. 2013). Moreover, probiotic administration can protect and enhance the gut microbiota of mice by improving the number of beneficial bacteria while decreasing the number of pathogenic bacteria (Li et al. 2019). With this background, our research team is interested in using probiotics to counter the threat to human health caused by CRE infections.

Our research team isolated various probiotic strains, such as *Bacillus*, during a vinegar microbiome study, and the *Bacillus* genus was applied to the CRE infection treatment study. Vinegar has long been considered fermented food for its many health benefits, including its antioxidant activity, ability to improve hypercholesterolemia, prevent metabolic syndromes, and regulate the gut immune system (Urtasun et al. 2020; Sui et al. 2021;). However, *in vivo* effects of probiotics isolated from vinegar on CRKP infection have not been reported yet. Here we report the efficacy of a probiotic strain isolated from Gochang Bokbunja vinegar against CRKP infections.

The strain discovered in the vinegar was confirmed as *B. velezensis* through 16S rRNA gene sequencing analysis and additional species-specific PCR. It was judged to be a new strain as it showed a different carbon use pattern from the existing standard *B. velezensis* strain. As a result of additional efficacy evaluation *in vivo*, this candidate probiotic strain's prophylactic and therapeutic efficacies were confirmed, similar to a recent study (Tajdozian et al. 2021) showing the infection prevention and therapeutic effect of probiotics in a mouse model. Such effects are believed to be related to their diverse ability to adhere to epithelial surfaces and induce immunological responses (Wagner et al. 1997). Moreover, it has recently been reported that *Bacillus* treatment might have a solid immunostimulatory effect on the host to defend against infections (Plaza-Diaz et al. 2014; Mazaya et al. 2015; Suva et al. 2016). According to the results of related studies on *B. velezensis* as a candidate strain in this study, *B. velezensis* naturally produces various antibiotic compounds such as bacteriocins, short-chain fatty acids, and organic acids that can protect the gastrointestinal tract from diseases (Lee et al. 2019). There have also been claims that the administration of *B. velezensis* in animals can increase intestinal *Lactobacillus* and *Ruminococcus* and decrease *Acinetobacter* and that the effectiveness of *B. velezensis* on CRE might be related to this phenomenon (Li et al. 2019).

Probiotics are classified as Generally Regarded as Safe (GRAS) by the United States Food and Drug Administration (FDA) (Martín and Langella 2019). Probiotics have been used for a long time, and their safety has been established. These findings allow their usage as food or supplements from a scientific perspective (Martín and Langella 2019). Although probiotics are commonly considered safe (Williams 2010), some strains can cause bacteremia and septicemia (Kulkarni 2019). In consideration of these safety issues, a repeated two-week oral acute toxicity test was performed using guinea pigs. No abnormal clinical symptoms, weight loss, or animal death were observed during the experiment period.

Concerning safety, this study used probiotic strains cultured in FGM. FGM is one medium allowed to come into direct contact with foods, and it does not cause any hazards or change the taste and flavor, making it suitable for human consumption (Sawatari et al. 2006). Besides, FGM is less expensive and easier for bulk production; therefore, many *in vivo* studies rely on FGM (Huang et al. 2016; 2017b).

Many studies have found that the gastrointestinal tract's stability and beneficial bacterial population enhance the host's immune system and antioxidant capacity and prevent the spread of pathogenic bacteria in the gut (Khalid et al. 2021; Li et al. 2019). Moreover, according to a report, the probiotic strain *B. velezensis* can also generate secondary metabolites such as polyketides, lipopeptides, and peptides that have antibacterial properties (Ye et al. 2018). However, here, the in-depth mechanism of action based on the metabolite mentioned above and pathology studies to support the effectiveness of this probiotic strain remains a limitation.

## Conclusions

In summary, in this study, a new probiotic strain, the *B. velezensis* strain, was isolated from Korean Gochang Bokbunja fermented vinegar. Its efficacy against CRKP infections was confirmed *in vivo*. Results of this study suggest the potential for developing *B. velezensis* as a live biotherapeutic agent for CRKP-associated infections. To develop CRKP therapeutics, extensive and in-depth research is required, including extensive animal efficacy investigations, GLP toxicity studies, clinical trials, and research regarding synergistic effects with existing drugs.

**ORCID**
Ho-Yeon Song https://orcid.org/0000-0003-4429-1383

**Acknowledgments**

Financial support for this study was provided by a grant (No. 2021040D288) from the Gochang Bokbunja vinegar Research Project through the Gochang Agricultural Technology Center, funded by Gochang County, Republic of Korea. This work was also supported by the Technology Innovation Program (20018499), funded By the Ministry of Trade, Industry & Energy (MOTIE, Korea). This research was also supported by the Soonchunhyang University Research Fund. Moreover, we would like to thank the officials of Gochang-gun, the vinegar farmers in the Gochang area,

and the PMC researchers at Soonchunhyang University. We would also like to thank Uhjin Song, M.D., for his medical advice and English proofreading of the manuscript.

**Conflict of interest**

The authors do not report any financial or personal connections with other persons or organizations, which might negatively affect the contents of this publication and/or claim authorship rights to this publication.

## Literature

**AlFaleh K, Anabrees J.** Probiotics for prevention of necrotizing enterocolitis in preterm infants. Evid Based Child Health. 2014; 9(3):584–671. https://doi.org/10.1002/ebch.1976

**Allen SJ, Martinez EG, Gregorio GV, Dans LF.** Probiotics for treating acute infectious diarrhoea. Cochrane Database Syst Rev. 2010; (11):CD003048. https://doi.org/10.1002/14651858.CD003048.pub3

**Anwar F, Altayb HN, Al-Abbasi FA, Al-Malki AL, Kamal MA, Kumar V.** Antiviral effects of probiotic metabolites on COVID-19. J Biomol Struct Dyn. 2021;39(11):4175–4184. https://doi.org/10.1080/07391102.2020.1775123

**Bahuguna A, Joe A, Kumar V, Lee JS, Kim SY, Moon JY, Cho SK, Cho H, Kim M.** Study on the identification methods for effective microorganisms in commercially available organic agriculture materials. Microorganisms. 2020;8(10):1568. https://doi.org/10.3390/microorganisms8101568

**Brink AJ.** Epidemiology of carbapenem-resistant Gram-negative infections globally. Curr Opin Infect Dis. 2019;32(6):609–616. https://doi.org/10.1097/QCO.0000000000000608

**CDC.** Antibiotic resistance threats in the united states. Atlanta (USA): U.S. Department of Health and Human Services, Centers for Disease Control and Prevention; 2019 [cited 2022 Aug 01]. Available from http://www.cdc.gov/drugresistance/Biggest-Threats.html

**Ceccarelli G, Statzu M, Santinelli L, Pinacchio C, Bitossi C, Cavallari EN, Vullo V, Scagnolari C, d'Ettorre G.** Challenges in the management of hiv infection: update on the role of probiotic supplementation as a possible complementary therapeutic strategy for cART treated people living with HIV/AIDS. Expert Opin Biol Ther. 2019;19(9):949–965. https://doi.org/10.1080/14712598.2019.1638907

**Cremonini F, Di Caro S, Santarelli L, Gabrielli M, Candelli M, Nista EC, Lupascu A, Gasbarrini G, Gasbarrini A.** Probiotics in antibiotic-associated diarrhoea. Dig Liver Dis. 2002;34:S78–S80. https://doi.org/10.1016/S1590-8658(02)80171-2

**Czuprynski C, Faith N.** Sodium bicarbonate enhances the severity of infection in neutropenic mice orally inoculated with *Listeria monocytogenes* EGD. Clin Vaccine Immunol. 2002;9(2):477–481. https://doi.org/10.1128/CDLI.9.2.477-481.2002

**De Luca F, Shoenfeld Y.** The microbiome in autoimmune diseases. Clin Exp Immunol. 2019;195(1):74–85. https://doi.org/10.1111/cei.13158

**Dunlap CA.** Taxonomy of registered *Bacillus* spp. strains used as plant pathogen antagonists. Biol Control. 2019;134:82–86. https://doi.org/10.1016/j.biocontrol.2019.04.011

**Fan B, Blom J, Klenk H-P, Borriss R.** *Bacillus amyloliquefaciens*, *Bacillus velezensis*, and *Bacillus siamensis* form an "operational group *B. amyloliquefaciens*" within the *B. subtilis* species complex. Front Microbiol. 2017;8:22. https://doi.org/10.3389/fmicb.2017.00022

**Fan B, Wang C, Song X, Ding X, Wu L, Wu H, Gao X, Borriss R.** *Bacillus velezensis* FZB42 in 2018: the Gram-positive model strain for plant growth promotion and biocontrol. Front Microbiol. 2018; 9:2491. https://doi.org/10.3389/fmicb.2018.02491

**FAO/WHO.** Report of a joint FAO/WHO expert consultation on evaluation of health and nutritional properties of probiotics in food including powder milk with live lactic acid bacteria. Cordoba (Argentina): World Health Organization/Food and Agriculture Organization of the United Nations; 2001.

**Huang CH, Huang L, Chang MT, Wu CP.** Use of novel specific primers targeted to *pheS* and *tuf* gene for species and subspecies identification and differentiation of the *Bacillus subtilis* subsp. *subtilis*, *Bacillus amyloliquefaciens* and *Bacillus licheniformis*. Afr J Microbiol Res. 2017a;11(7):264–270. https://doi.org/10.5897/AJMR2017.8434

**Huang FC, Lu YT, Liao YH.** Beneficial effect of probiotics on *Pseudomonas aeruginosa*-infected intestinal epithelial cells through inflammatory IL-8 and antimicrobial peptide human beta-defensin-2 modulation. Innate Immun. 2020;26(7):592–600. https://doi.org/10.1177/1753425920959410

**Huang S, Cauty C, Dolivet A, Le Loir Y, Chen XD, Schuck P, Jan G, Jeantet R.** Double use of highly concentrated sweet whey to improve the biomass production and viability of spray-dried probiotic bacteria. J Funct Foods. 2016;23:453–463. https://doi.org/10.1016/j.jff.2016.02.050

**Huang S, Vignolles M-L, Chen XD, Le Loir Y, Jan G, Schuck P, Jeantet R.** Spray drying of probiotics and other food-grade bacteria: a review. Trends Food Sci Technol. 2017b;63:1–17. https://doi.org/10.1016/j.tifs.2017.02.007

**Khalid F, Khalid A, Fu Y, Hu Q, Zheng Y, Khan S, Wang Z.** Potential of *Bacillus velezensis* as a probiotic in animal feed: a review. J Microbiol. 2021;59(7):627–633. https://doi.org/10.1007/s12275-021-1161-1

**Kopacz K, Phadtare S.** Probiotics for the prevention of antibiotic-associated diarrhea. Healthcare. 2022;10(8):1450. https://doi.org/10.3390/healthcare10081450

**Kralik P, Ricchi M.** A basic guide to real time PCR in microbial diagnostics: definitions, parameters, and everything. Front Microbiol. 2017;8:108. https://doi.org/10.3389/fmicb.2017.00108

**Kulkarni RP.** Probiotics leap from gut to blood. Sci Transl Med. 2019;11(521):eaaz9763. https://doi.org/10.1126/scitranslmed.aaz9763

**Kwon GH, Lee HA, Park JY, Kim JS, Lim J, Park CS, Kwon DY, Kim YS, Kim JH.** Development of a RAPD-PCR method for identification of *Bacillus* species isolated from Cheonggukjang. Int J Food Microbiol. 2009;129(3):282–287. https://doi.org/10.1016/j.ijfoodmicro.2008.12.013

**Lee NK, Kim WS, Paik HD.** *Bacillus* strains as human probiotics: characterization, safety, microbiome, and probiotic carrier. Food Sci Biotechnol. 2019;28(5):1297–1305. https://doi.org/10.1007/s10068-019-00691-9

**Lee Y, Seo H, Kim S, Rahim MDA, Yoon Y, Jung J, Lee S, Beom Ryu C, Song HY.** Activity of *Lactobacillus crispatus* isolated from vaginal microbiota against *Mycobacterium tuberculosis*. J Microbiol. 2021;59(11):1019–1030. https://doi.org/10.1007/s12275-021-1332-0

**Li A, Wang Y, Pei L, Mehmood K, Li K, Qamar H, Iqbal M, Waqas M, Liu J, Li J.** Influence of dietary supplementation with *Bacillus velezensis* on intestinal microbial diversity of mice. Microb Pathog. 2019; 136:103671. https://doi.org/10.1016/j.micpath.2019.103671

**Li HY, Zhou DD, Gan RY, Huang SY, Zhao CN, Shang A, Xu XY, Li HB.** Effects and mechanisms of probiotics, prebiotics, synbiotics, and postbiotics on metabolic diseases targeting gut microbiota: a narrative review. Nutrients. 2021a;13(9):3211. https://doi.org/10.3390/nu13093211

**Li S, He P, Fan H, Liu L, Yin K, Yang B, Li Y, Huang SM, Li X, Zheng SJ.** A real-time fluorescent reverse transcription quantitative PCR assay for rapid detection of genetic markers' expression associated with fusarium wilt of banana biocontrol activities in *Bacillus*. J Fungi (Basel). 2021b;7(5):353. https://doi.org/10.3390/jof7050353

**Logan LK, Weinstein RA.** The epidemiology of carbapenem-resistant *Enterobacteriaceae*: the impact and evolution of a global menace. J Infect Dis. 2017;215(suppl_1):S28–S36. https://doi.org/10.1093/infdis/jiw282

**Lutgring JD.** Carbapenem-resistant *Enterobacteriaceae*: an emerging bacterial threat. Semin Diagn Pathol. 2019;36(3):182–186. https://doi.org/10.1053/j.semdp.2019.04.011

**Martín R, Langella P.** Emerging health concepts in the probiotics field: streamlining the definitions. Front Microbiol. 2019;10:1047. https://doi.org/10.3389/fmicb.2019.01047

**Mazaya B, Hamzawy MA, Khalil MA, Tawkol WM, Sabit H.** Immunomodulatory and antimicrobial efficacy of Lactobacilli against enteropathogenic infection of Salmonella typhi: *in-vitro* and *in-vivo* study. Int J Immunopathol Pharmacol. 2015;28(4):469–478. https://doi.org/10.1177/0394632015592099

**Morrill HJ, Pogue JM, Kaye KS, LaPlante KL.** Treatment options for carbapenem-resistant *Enterobacteriaceae* infections. Open Forum Infect Dis. 2015;2(2):ofv050. https://doi.org/10.1093/ofid/ofv050

**Murray CJ, Ikuta KS, Sharara F, Swetschinski L, Aguilar GR, Gray A, Han C, Bisignano C, Rao P, Wool E, et al.** Global burden of bacterial antimicrobial resistance in 2019: a systematic analysis. Lancet. 2022;399(10325):629–655. https://doi.org/10.1016/S0140-6736(21)02724-0

**Oelschlaeger TA.** Mechanisms of probiotic actions – a review. Int J Med Microbiol. 2010;300(1):57–62. https://doi.org/10.1016/j.ijmm.2009.08.005

**Pan YJ, Lin TL, Lin YT, Su PA, Chen CT, Hsieh PF, Hsu CR, Chen CC, Hsieh YC, Wang JT.** Identification of capsular types in carbapenem-resistant *Klebsiella pneumoniae* strains by *wzc* sequencing and implications for capsule depolymerase treatment. Antimicrob Agents Chemother. 2015;59(2):1038–1047. https://doi.org/10.1128/AAC.03560-14

**Patel RM, Underwood MA.** Probiotics and necrotizing enterocolitis. Semin Pediatr Surg. 2018;27(1):39–46. https://doi.org/10.1053/j.sempedsurg.2017.11.008

**Plaza-Diaz J, Gomez-Llorente C, Fontana L, Gil A.** Modulation of immunity and inflammatory gene expression in the gut, in inflammatory diseases of the gut and in the liver by probiotics. World J Gastroenterol. 2014;20(42):15632. https://doi.org/10.3748/wjg.v20.i42.15632

**Potter RF, D'Souza AW, Dantas G.** The rapid spread of carbapenem-resistant *Enterobacteriaceae*. Drug Resist Updat. 2016;29:30–46. https://doi.org/10.1016/j.drup.2016.09.002

**Rahim MA, Seo H, Kim S, Tajdozian H, Barman I, Lee Y, Lee S, Song HY.** *In vitro* anti-tuberculosis effect of probiotic *Lacticaseibacillus rhamnosus* PMC203 isolated from vaginal microbiota. Sci Rep. 2022;12:8290. https://doi.org/10.1038/s41598-022-12413-z

**Sawatari Y, Hirano T, Yokota A.** Development of food grade media for the preparation of *Lactobacillus plantarum* starter culture. J Gen Appl Microbiol. 2006;52(6):349–356. https://doi.org/10.2323/jgam.52.349

**Sheu CC, Chang YT, Lin SY, Chen YH, Hsueh PR.** Infections caused by carbapenem-resistant *Enterobacteriaceae*: an update on therapeutic options. Front Microbiol. 2019;10:80. https://doi.org/10.3389/fmicb.2019.00080

**Sui Y, Liu J, Liu Y, Wang Y, Xiao Y, Gao B, Zhu D.** *In vitro* probiotic characterization of *Lactobacillus* strains from fermented tangerine vinegar and their cholesterol degradation activity. Food Biosci. 2021; 39:100843. https://doi.org/10.1016/j.fbio.2020.100843

**Sulis G, Sayood S, Gandra S.** Antimicrobial resistance in low-and middle-income countries: current status and future directions. Expert Rev Anti Infect Ther. 2022;20(2):147–160. https://doi.org/10.1080/14787210.2021.1951705

**Suva MA, Sureja VP, Kheni DB.** Novel insight on probiotic *Bacillus subtilis*: mechanism of action and clinical applications. J Curr Res Sci Med 2016;2(2):65–72. https://doi.org/10.4103/2455-3069.198381

**Tajdozian H, Seo H, Kim S, Rahim MA, Lee S, Song HY.** Efficacy of *Lactobacillus fermentum* isolated from the vagina of a healthy woman against carbapenem-resistant *Klebsiella* infections *in vivo*. J Microbiol Biotechnol. 2021;31(10):1383–1392. https://doi.org/10.4014/jmb.2103.03014

**Tilahun M, Kassa Y, Gedefie A, Ashagire M.** Emerging carbapenem-resistant *Enterobacteriaceae* infection, its epidemiology and novel treatment options: a review. Infect Drug Resist. 2021;14: 4363–4374. https://doi.org/10.2147/IDR.S337611

**Urtasun R, Díaz-Gómez J, Araña M, Pajares MJ, Oneca M, Torre P, Jiménez M, Munilla G, Barajas M, Encío I.** A combination of apple vinegar drink with *Bacillus coagulans* ameliorates high fat diet-induced body weight gain, insulin resistance and hepatic steatosis. Nutrients. 2020;12(9):2504. https://doi.org/10.3390/nu12092504

**Hemert S, Verwer J, Schütz B.** Clinical studies evaluating effects of probiotics on parameters of intestinal barrier function. Adv Microbiol. 2013;3(2):212–221. https://doi.org/10.4236/aim.2013.32032

**VanderVeen BN, Sougiannis AT, Velazquez KT, Carson JA, Fan D, Murphy EA.** The acute effects of 5 fluorouracil on skeletal muscle resident and infiltrating immune cells in mice. Front Physiol. 2020; 11:593468. https://doi.org/10.3389/fphys.2020.593468

**Wagner RD, Warner T, Roberts L, Farmer J, Balish E.** Colonization of congenitally immunodeficient mice with probiotic bacteria. Infect Immun. 1997;65(8):3345–3351. https://doi.org/10.1128/iai.65.8.3345-3351.1997

**Williams NT.** Probiotics. Am J Health Syst Pharm. 2010;67(6): 449–458. https://doi.org/10.2146/ajhp090168

**Ye M, Tang X, Yang R, Zhang H, Li F, Tao F, Li F, Wang Z.** Characteristics and application of a novel species of *Bacillus*: *Bacillus velezensis*. ACS Chem Biol. 2018;13(3):500–505. https://doi.org/10.1021/acschembio.7b00874

Supplementary materials are available on the journal's website.

ORIGINAL PAPER
Polish Journal of Microbiology
2022, Vol. 71, No 4, 563–575
https://doi.org/10.33073/pjm-2022-052

# Isolation, Identification, and Fermentation Medium Optimization of a Caproic Acid-Producing *Enterococcus casseliflavus* Strain from Pit Mud of Chinese Strong Flavor Baijiu Ecosystem

HAO LUO[1#], TAO LI[3#], JIA ZHENG[2], KAIZHENG ZHANG[1], ZONGWEI QIAO[2], HUIBO LUO[1] and WEI ZOU[1*]

[1] College of Bioengineering, Sichuan University of Science and Engineering, Yibin, China
[2] Wuliangye Yibin Co. Ltd., Yibin, China
[3] Sichuan Vocational College of Chemical Technology, Luzhou, China

Submitted 19 September 2022, accepted 11 November 2022, published online 19 December 2022

Abstract

Caproic acid is the precursor material of ethyl hexanoate, a representative flavor substance in strong flavor baijiu (SFB). Increasing the content of caproic acid in SFB helps to improve its quality. In the present study, caproic acid-producing bacteria from the pit mud of an SFB ecosystem were isolated, purified, and characterized. Strain BF-1 with the highest caproic acid yield (0.88 g/l) was selected. The morphological and molecular identification analysis showed that strain BF-1 was *Enterococcus casseliflavus*. The genome of *E. casseliflavus* BF-1 was sequenced and was found to be 2,968,377 bp in length with 3,270 open reading frames (ORFs). The caproic acid biosynthesis pathway in *E. casseliflavus* BF-1 was predicted based on the KAAS annotation. The virulence factors in the genome of strain BF-1 were annotated, which showed that *E. casseliflavus* BF-1 is safe at the genetic level. After adding essential nutrients based on the KAAS annotation, the optimum medium conditions for acid production by strain BF-1 were obtained by performing orthogonal experiments. The caproic acid yield of strain BF-1 reached 3.03 g/l, which was 3.44-fold higher than the initial yield. The optimized fermentation of caproic acid production by BF-1 was reported for the first time. The strain could be further used to regulate the ecosystem in baijiu production to improve its quality.

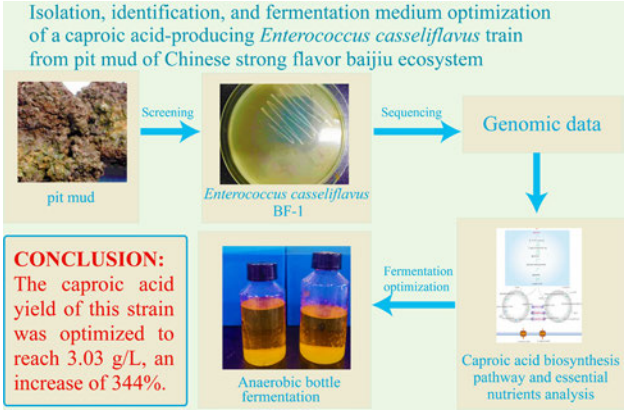


K e y w o r d s: baijiu, caproic acid, *Enterococcus casseliflavus*, genome sequencing, fermentation optimization

## Introduction

Strong flavor baijiu (SFB), a traditional Chinese distilled liquor, contains more than 1,300 different flavor compounds (Ji et al. 2017; Zou et al. 2018). Among these compounds, ethyl hexanoate is the primary flavoring substance of SFB, and its content can directly affect the quality of SFB (Hong et al. 2020). Caproic acid, also known as hexanoic acid, is a common carboxylic acid that can be used as a precursor for producing liquid fuels and synthetic chemicals such as food and animal feed additives (Van Immerseel et al. 2004; Nabi et al. 2006; Serhan et al. 2016). Caproic acid-producing bacteria (CPB) are generally considered the most critical functional microorganisms in an SFB ecosystem (Liu and Sun 2018). The isolation, screening, identification, and culture of CPB are important to improve the quantity and quality of CPB in pit mud (Wang et al. 2019; Zhao et al. 2019; Tian et al. 2020). In addition to the SFB ecosystem, CPB have been isolated from different ecological niches such as anaerobic digestion sludge (Kim et al. 2015), the rumen of cattle and sheep (Weimer

# Hao Luo and Tao Li contributed equally to this study.

* Corresponding author: Wei Zou, College of Bioengineering, Sichuan University of Science and Engineering, Yibin, China; **e-mail: weizou1985@163.com**

and Stevenson 2012), and silt (Gildemyn et al. 2017). The oxygen demands of different strains of CPB during the production of caproic acid are not consistent. Most of the reported CPBs are anaerobic species, including members of *Clostridium* (Weimer and Stevenson 2012), *Bacillus* (Zhao et al. 2012), *Ruminococcaceae* (Zhu et al. 2015), and *Megasphaera* (Kim et al. 2018). They can accumulate caproic acid by using ethanol, lactic acid, glucose, and D-galactitol as the main carbon source (Wang et al. 2020).

In the present study, a new strain of *Enterococcus casseliflavus* (strain BF-1) with high caproic acid yield was isolated from the pit mud of an SFB ecosystem. *E. casseliflavus* has potential probiotic effects on growth performance, immunity, and disease resistance (Akbari et al. 2021). In this study, the whole genome of *E. casseliflavus* BF-1 was sequenced and annotated. The safety of the strain at the genetic level and the caproic acid biosynthesis pathway were analyzed. We verified the essential nutrients of *E. casseliflavus* BF-1 synthesis defect through single-omission growth experiments and added essential nutrients to the fermentation medium to improve the yield of caproic acid. The results showed that this strain could be further used as a reinforced inoculum in the SFB production process.

## Experimental

### Materials and Methods

**Isolation and screening of caproic acid-producing bacteria.** A five-point sampling method was used to collect pit mud samples from an SFB factory in Anhui, China. Next, 5 g of pit mud was put into a 150 ml triangular flask containing 45 ml of sterile water. After adequate mud dispersion, the pit mud extract was shaken well, and 10% of the extract was inoculated into an enrichment medium (EM). The composition of the EM was as follows (per 1,000 ml): sodium acetate 15 g, yeast extract 10 g, $MgSO_4 \cdot 7H_2O$ 0.2 g, $KH_2PO_4$ 7 g, $K_2HPO_4$ 7 g, $(NH_4)_2SO_4$ 0.5 g, L-cysteine 0.5 g, ethanol 20 ml, pH 7.0. The extract was cultured at 35°C for four days. Then, 200 µl of the pit mud culture solution was pipetted and spread on a solid agar plate. The plates were incubated under anaerobic conditions at 35°C until the colonies grew. A single colony on the agar plate was selected and subcultured three times on the solid medium.

The single colony was inoculated into 100 ml EM, incubated anaerobically at 35°C for 12 h, and cultured for two generations to obtain a seed liquid. The seed liquid was inoculated into the fermentation medium with 5% inoculation volume, and the fermentation was performed under an anaerobic static culture condition at 35°C for 10 days. The caproic acid yield of each experimental batch was estimated by the $CuSO_4$ staining method. The yield was higher when the color was darker (Zhong and Xie 2004). The strain with the highest caproic acid yield was used for further analysis.

**Morphological identification and 16S rDNA sequence analysis.** The isolated strains with the highest caproic acid yield were selected. The physiological and biochemical characteristics of the selected representative strains were studied using Bergey's Manual of Determinative Bacteriology (Ceddia et al. 1980). First, the bacterial morphological shape and staining pattern was observed under a microscope (Motic MLC-150, Motic China Group Co., Ltd., China). The genomic DNA was extracted from the CPB strains using the bacterial genomic DNA rapid extraction kit (Tiangen Biochemical Technology (Beijing) Co., Ltd., China). The extracted DNA was used as a template for PCR amplification with universal primers 27F (5'-AGAGTTTGATCCTGGCTCAG-3') and 1492R (5'-CTACGGCTACCTTGTTACGA-3'). The amplified products were sent to Nanjing Parsono Biology Company (China) for sequencing. The sequences were spliced by the basic local alignment search tool (BLAST) program available at the National Centre for Biotechnology Information (NCBI) database and compared with the data available in the NCBI 16S rDNA database to obtain the homologous sequence showing the most remarkable similarity with the sequence of the species to be tested. The phylogenetic tree was constructed by MEGA 5.0 software by using the neighbor-joining (NJ) method (Kumar et al. 2016).

**Whole genome sequencing and annotation.** The genome of strain BF-1 was sequenced by Shanghai Personal Biotechnology Co., Ltd. (China). A 400-bp insert library was prepared using the TruSeq™ DNA Sample Prep Kit (Illumina Inc., USA). Sequencing was performed on the HiSeq™ 2000 sequencing system (Illumina Inc., USA) with a 200-cycle paired-end configuration at the National Laboratory of Genomics for Biodiversity (LANGEBIO), Irapuato, Guanajuato, Mexico. A5-miseq (Coil et al. 2014) and SPAdes (Bankevich et al. 2012) were used to assemble the sequencing data of the removed joint sequence from scratch to construct the contig and scaffold. The assembly results were evaluated and compared, the SPAdes results were finally selected, and Pilon software was used for base correction (Walker et al. 2014). Libraries with different indices were multiplexed and loaded using an Illumina HiSeq instrument according to the manufacturer's instructions. GeneMarkS was used to predict the protein-coding genes of the bacterial genome (Blake and Cohen 2001). tRNAscan-SE was used to predict tRNA genes in the whole genome (Lowe and Eddy 1997), and Barrnap was used to predict rRNA genes. The other noncoding

RNAs were mainly predicted by comparing them with the rfam database (Kalvari et al. 2018). Genes were annotated by the NCBI Prokaryotic Genome Annotation Pipeline (Tatusova et al. 2016). Metabolic pathways were annotated using the KAAS (Moriya et al. 2007). Clusters of Orthologous Groups of proteins (COG) annotation was performed using eggNOG-mapper for assigning the COG category to the genes (Szklarczyk et al. 2019). Virulence factor prediction was performed using VFanalyzer available in the virulence factor database (VFDB) (Qin et al. 2012).

**Culture medium optimization.** ***Selection of carbon source.*** Sodium acetate, glucose, lactose, galactose, fructose, mannose, and soluble starch were selected as carbon sources, and 2% of each carbon source was added to the fermentation medium. The yield of caproic acid was detected after anaerobic culture at 35°C for 10 days. Based on caproic acid yield, the best carbon source was selected, and it was added at the concentration of 1.0%, 2.0%, 3.0%, 4.0%, and 5.0% to the fermentation medium. The yield of caproic acid was then determined after 10 days of anaerobic culture.

***Screening for nitrogen source.*** Ammonium chloride, sodium nitrate, urea, peptone, beef extract, and yeast extract were selected as nitrogen sources in the fermentation medium. The yield of caproic acid was analyzed after the addition of each nitrogen source under anaerobic culture at 35°C for 10 days. The best nitrogen source was determined and added to the fermentation medium at the concentration of 0.5%, 1.0%, 1.5%, 2.0%, 3.0%, and 4.0%. The yield of caproic acid was estimated after anaerobic culture for 10 days.

***Screening for inorganic salts and growth factors.*** In single-omission experiments, the cell growth was monitored when each vitamin or amino acid was separately left out of the medium. The selected optimal carbon source and nitrogen source were used in the culture medium, and inorganic salts ($MgSO_4 \cdot 7H_2O$, $KH_2PO_4$, $K_2HPO_4$, and $(NH_4)_2SO_4$) and nutrients (L-cysteine, biotin, and ethanol) were added separately to the medium. The yield of caproic acid was estimated after anaerobic culture for 10 days, and the correlation between various inorganic salts and growth factors for the acid production of *E. casseliflavus* BF-1 was obtained. Their final concentration was optimized based on the effect of various inorganic salts and growth factors on the caproic acid production of *E. casseliflavus* BF-1.

***Orthogonal experiment.*** Four-level orthogonal experiments (Table I) were conducted on four factors (glucose, yeast extract, sodium acetate, and alcohol) with a strong influence on caproic acid production by single-factor optimization fermentation. The results of some single-factor optimization trials showed little difference in the yield of caproic acid between the four levels; hence, a 4-factor 4-level orthogonal experiment was considered to estimate the optimal fermentation conditions of the strain more efficiently. Under the optimum conditions obtained from the single factor optimization results, the strain was fermented and cultured, and the optimal acid production conditions of the strain were determined based on the yield of caproic acid as the investigation index.

Table I
Orthogonal experiment of four factors and four levels.

| Level | Factor A (glucose g/l) | Factor B (yeast extract g/l) | Factor C (sodium acetate g/l) | Factor D (ethanol %) |
|---|---|---|---|---|
| 1 | 10 | 10 | 2 | 1 |
| 2 | 20 | 20 | 4 | 2 |
| 3 | 30 | 30 | 6 | 3 |
| 4 | 40 | 40 | 8 | 4 |

**Qualitative and quantitative analysis of caproic acid.** The caproic acid content in the fermentation broth was determined by gas chromatography-mass spectrometry (GC-MS). The fermented broth was centrifuged at 10,000 × *g* for 20 min, and the supernatant was passed through a 0.22-μm organic phase filter membrane and collected in an electropolished (EP) pipe. One milliliter of the filtered supernatant was injected into the bottle for testing. In online detection, the sample was first separated in G.C. The separated metabolites were ionized into ion fragments of different sizes through the ion source and then further separated by MS. Finally, the separated ions reached the detector and hit the surface of the detector. Different metabolites formed electrical signals of different intensities. The GC conditions were as follows: column, db-wax UI column (30 m) × 0.25 mm, 0.25 μm; temperature, programmed at 40°C with a holding time for 1 min and increased to 150°C at 20°C/min and then increased to 250°C at 10°C for 2 min; split ratio, 30 : 1; carrier gas, helium; flow rate, 1 ml/min; flow rate for $H_2$, 40 ml/min; flow rate for $O_2$, 300 ml/min; and detector, flame ionization detector (FID). The MS conditions were as follows: electron ionization (EI) source, transmission line temperature 250°C, electron energy 70 EV, photomultiplier tube voltage 350 V, mass scanning range 30–350 amu. For qualitative and quantitative analyses, the MS data obtained by the GC-MS analysis were searched in the 17 standard libraries of the National Institute of Standards and Technology (NIST), and the content of caproic acid in the fermentation broth was determined using the standard external method. The standard external method is a quantitative method that uses the pure components to be measured as the reference material. It compares the response signal of the reference material to the response signal of the components to be measured in the sample. The method is simple and does

not require a correction factor. The components can be quantified regardless of whether other components in the sample are peaked or not.

**Data processing.** Origin was used to process the experimental data and draw graphs. IBM SPSS Statistics (version R24.0.0.0) was used to conduct variance analysis between the experimental groups. A *p*-value of $< 0.05$ was considered to be statistically significant.

## Results and Discussion

**Screening of caproic acid-producing strains.** A total of 41 strains were screened from pit mud, and among these strains, 19 strains showed the ability to produce caproic acid (Fig. 1). Strain BF-1 showed the highest yield of caproic acid (0.88 g/l). Therefore, strain BF-1 was selected for further studies.

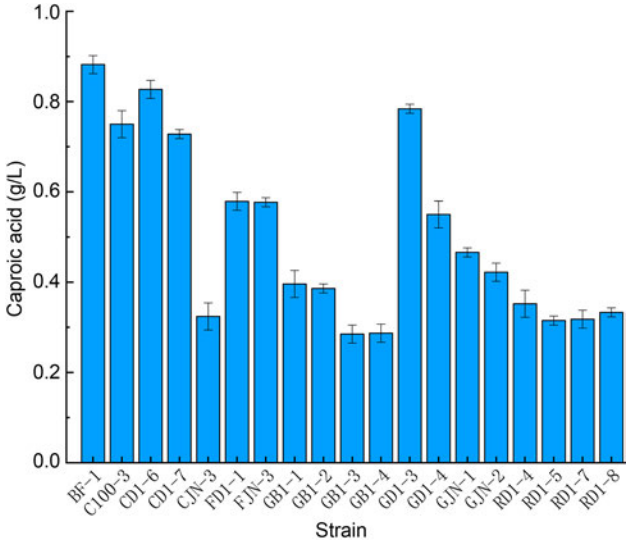


Fig. 1. The yield of caproic acid of different isolated strains.

**Physiological characteristics and phylogenetic classification of strain BF-1.** Strain BF-1 grew well on sodium acetate solid medium, with large, smooth, milky white, protuberant, and round colonies; the cells were non-spore-forming Gram-positive cocci (Fig. 2a and 2b). The results for VP test, gelatin hydrolysis, glycerol test, and nitrate reduction test were negative, while those for MR test; starch hydrolysis; and tests of growth using lactose, sucrose, raffinose, mannitol, fructose, stachyose, cellobiose, xylose, galactose, glycerol, and mannose as the sole carbon source were positive (Table II).

Based on the physiological, biochemical, and 16S rDNA sequence analyses (Fig. 2c), strain BF-1 was classified as *E. casseliflavus*. A physiological tree was then constructed based on the alignment of the 16S rDNA of strain BF-1 with other 16S rDNA sequences in the GenBank database. The results revealed that strain BF-1 was closest to *E. casseliflavus* FDAARGOS 1120 and similarity is 100 %. Therefore, strain BF-1 was designated as *E. casseliflavus* BF-1. It is the first study to report that *E. casseliflavus* is a caproic acid producer (Yuan et al. 2022).

Table II
Results of physiological and biochemical experiments.

| BF-1strain | | | |
|---|---|---|---|
| Voges-Proskauer test | – | Mannitol | + |
| MRtest | + | Fructose | + |
| Gelatin hydrolysis | – | Stachyose | + |
| Starch hydrolysis | + | Cellobiose | + |
| Nitrate reduction | – | Xylose | + |
| Lactose | + | Galactose | + |
| Sucrose | + | Glycerin | – |
| Raffinose | + | Mannose | + |

**Genome properties of *E. casseliflavus* BF-1.** ***Genome assembly and annotation of E. casseliflavus BF-1.*** To understand the physiological and metabolic characteristics of *E. casseliflavus* BF-1, we sequenced and annotated its genome (Table III). The contig total sequence length was 3,383,020 bp, and the contig N50 was 372,495 bp. The scaffold N50 was 570,209 bp. The *E. casseliflavus* genome is 2,968,377 bp in length, has a GC content of 43.52%, and contains 3,270 coding sequences, three rRNA genes, and 53 tRNA genes. The nucleotide sequence of *E. casseliflavus* BF-1 is deposited in the NCBI database under the accession number PRJNA759370.

Table III
Basic characteristics of the genome of strain BF-1.

| Features | BF-1 |
|---|---|
| Read-Num | 8,697,842 bp |
| HQ reads | 8,663,546 bp |
| Genome size | 2,968,377 bp |
| G + C content | 43.52% |
| ORF number | 3270 |
| ORF density | 0.967 genes per kb |
| ORF average length | 907,76 bp |
| Intergenetic region length | 414,643 bp |
| Coding percentage | 87.74% |
| rRNA | 3 |
| tRNA | 53 |
| ncRNA | 113 |
| Q value | 40 |
| Q20-rate | 98.84 |
| Q30-rate | 95.83 |
| Contig N50 | 372,495 bp |
| Scaffold N50 | 570,209 bp |
| Contig total sequence length | 3,383,020 bp |
| Scaffold total sequence length | 3,383,020 bp |

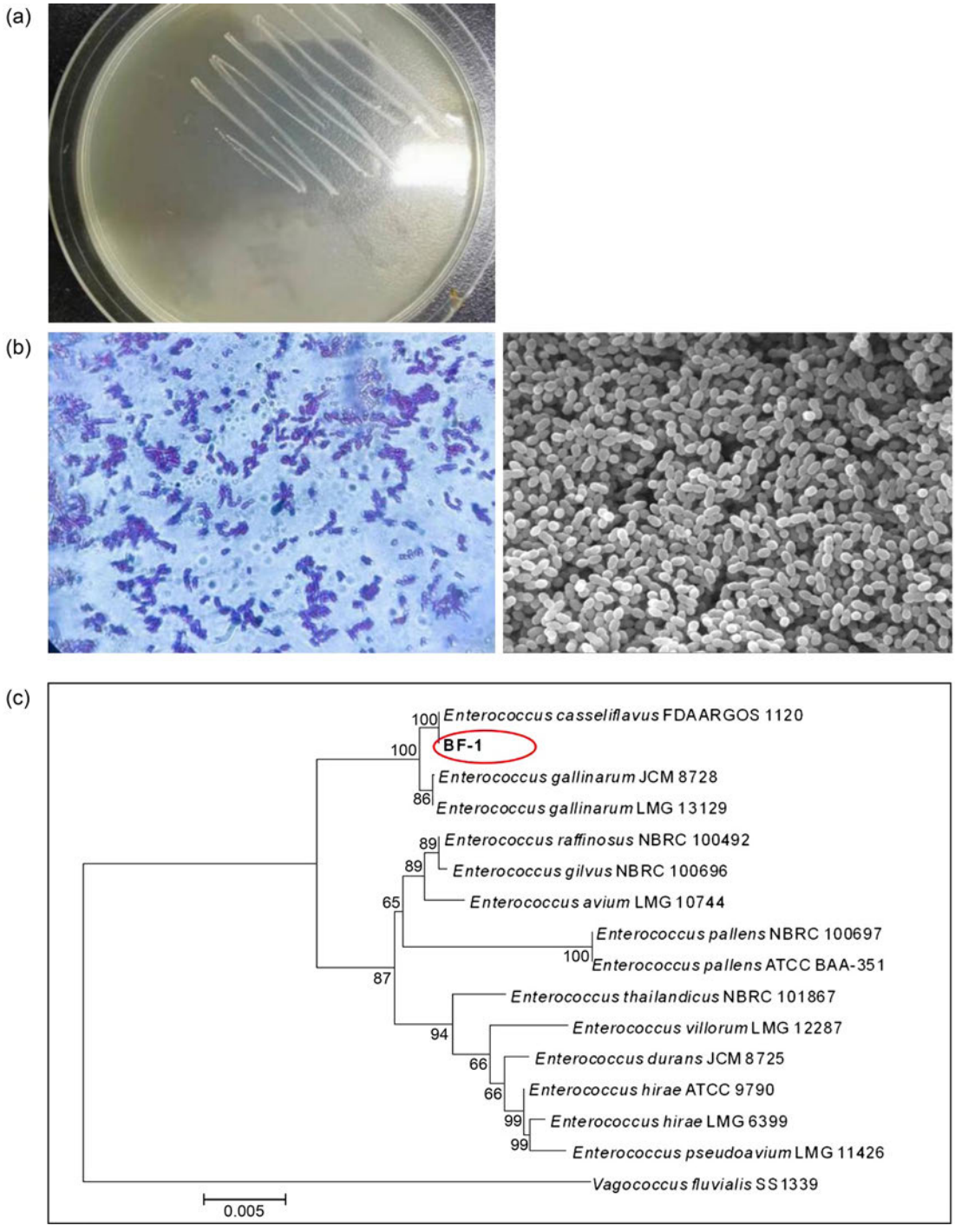


Fig. 2. Morphological and phylogenetic characteristics of the F6 strain.
a) Colony morphology of strain BF-1, b) Gram staining and SEM image showing the coccoid shape of the BF-1 strain, c) phylogenetic analysis of strain BF-1 based on BLAST results.

For the COG annotation (Fig. 3a), a total of 2,819 genes were assigned with COG terms, which account for 85.8% of the total genes in *E. casseliflavus* BF-1. Function unknown (S) was the largest category (24.76%). Apart from S, carbohydrate transport and metabolism (G) and transcription (K) were the most prominent groups, accounting for 13.4% and 9.5%, respectively. According to the KAAS annotation, a total of 3,155 genes were assigned with KO terms. The largest three metabolic pathway categories in the genome of strain BF-1 were carbohydrate metabolism (428), amino acid metabolism (187), and energy metabolism (124) (Fig. 3b).

***Caproic acid biosynthesis pathway analysis.*** According to the KAAS annotation, we constructed the metabolic pathway of caproic acid in *E. casseliflavus* BF-1 according to the KAAS annotation. The process of synthesizing caproic acid from glucose by *E. casseliflavus* BF-1 is divided into three steps (Fig. 4): (1) *E. casseliflavus*

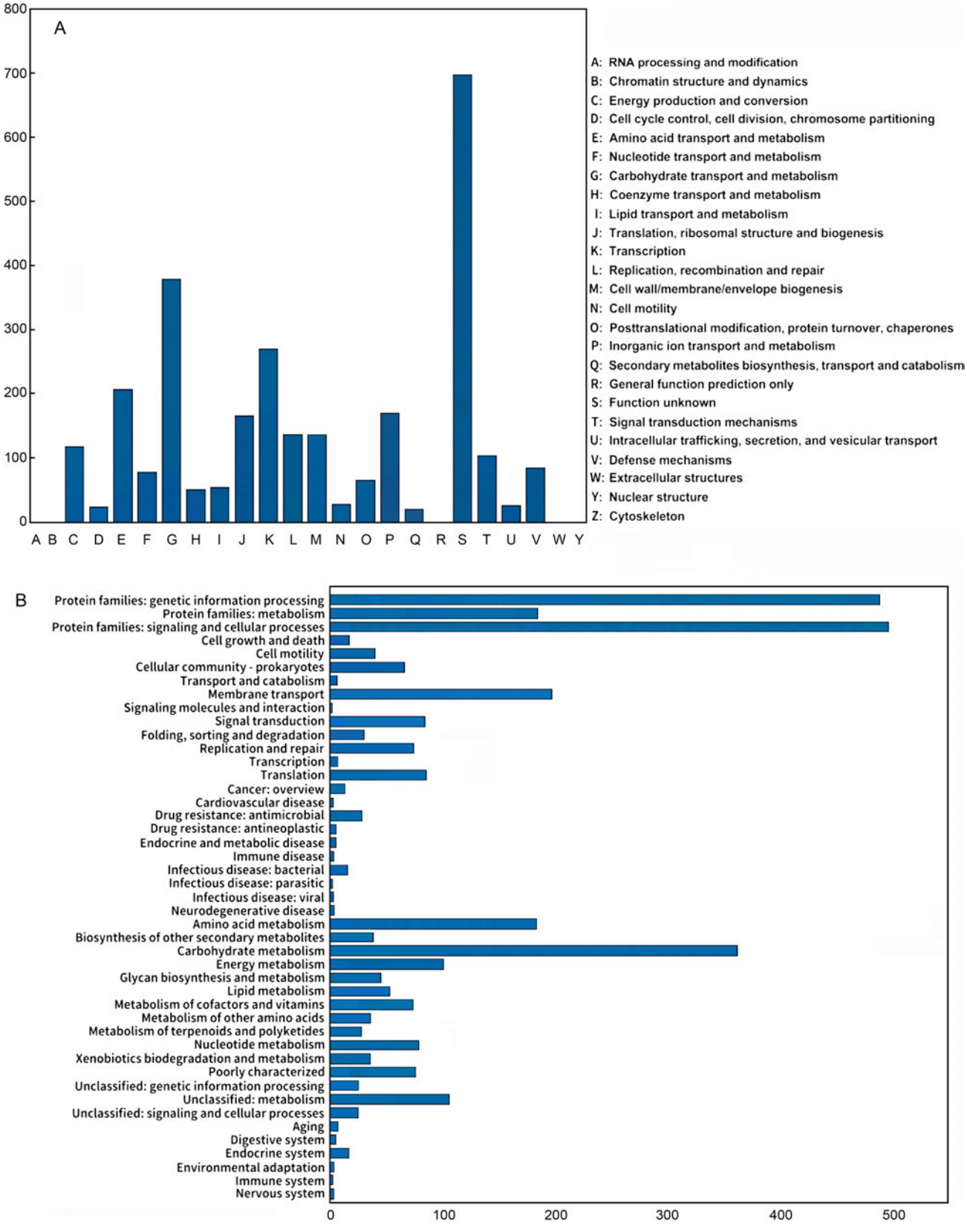


Fig. 3. Genome annotation of strain BF-1.
A) COG functional gene classification, B) KEGG functional gene classification.

BF-1 produces acetyl CoA through pyruvic acid by pyruvate ferredoxin oxidoreductase (porA); (2) Acetyl CoA is converted to butyl CoA under the action of NADH, $FADH_2$, and CoA, and butyl CoA was converted to butyric acid and acetyl CoA under the action of acetic acid and CoA transferase; and (3) Hexanoyl

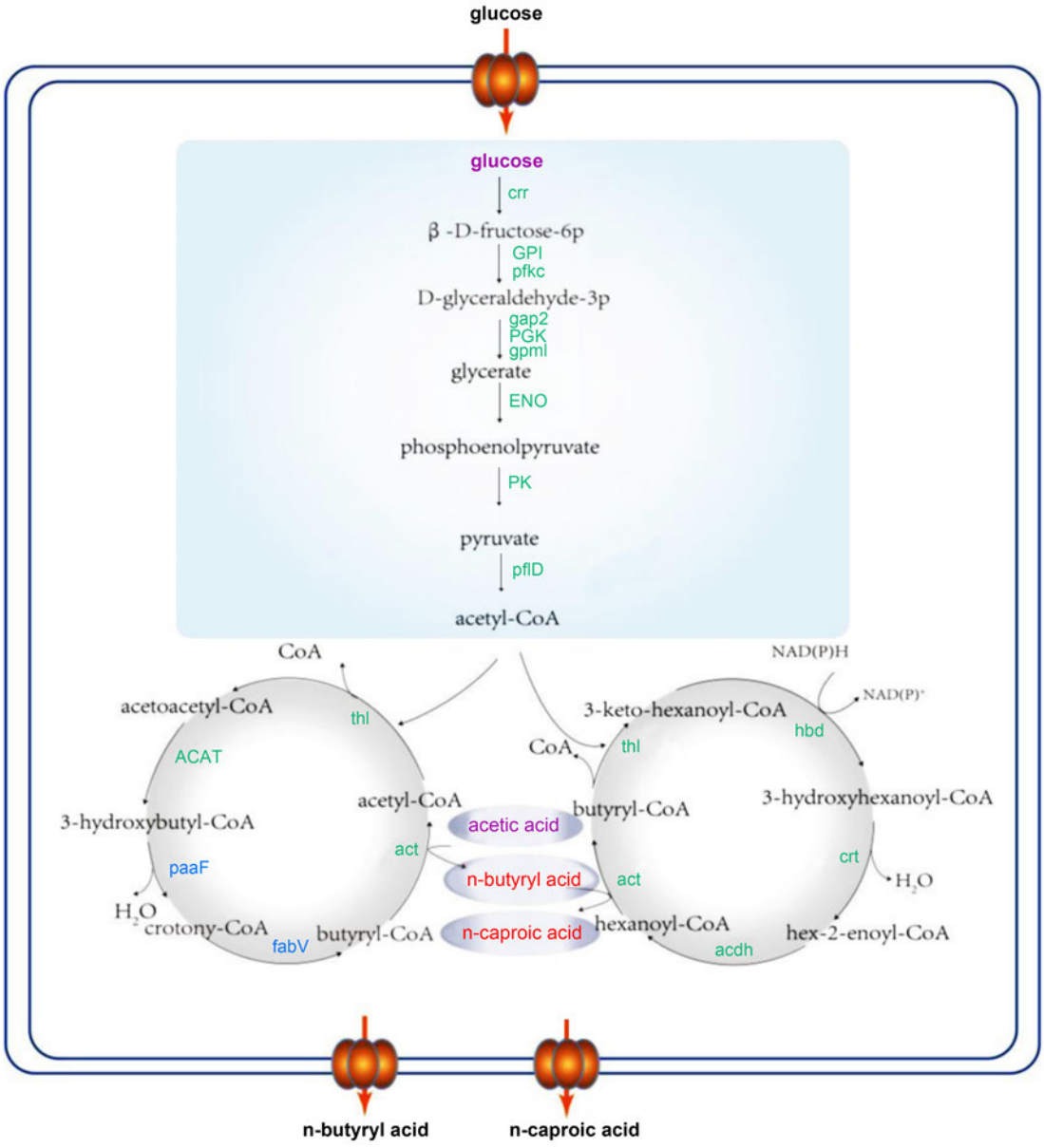


Fig. 4. Caproic acid production pathway of strain BF-1. Substrates are shown in purple, products are shown in red, annotated genes are shown in green, and non-annotated genes are shown in blue.

CoA and butyric acid are converted into caproic acid and butyryl CoA through CoA transferase. Because acyl CoA transferase has a wide range of catalytic activities, it has been speculated that hexanoyl CoA may also directly react with acetic acid to synthesize caproic acid. The main enzymes involved in (1) and (3) are completely annotated. In contrast enoyl-CoA hydratase (paaF) and crotonyl-CoA(ccrA) reductase involved in (2) are not annotated, which indicates the inability of this strain to synthesize crotonyl-CoA and butanoyl-CoA. It contradicts the experimental result that caproic acid was produced by strain BF-1. There are two explanations for this contradiction: (i) the existence of other non-annotated functional enzymes and (ii) the substitution of other spectral enzymes. It is also possible that 3-hydroxybutyryl-CoA dehydrogenase may replace enoyl-CoA hydratase and glutaconyl-CoA decarboxylase subunit alpha may replace crotonyl-CoA due to their wide use of substrates.

***Biosynthesis and transport of amino acids and vitamins.*** According to the KAAS annotation, *E. casseliflavus* BF-1 cannot synthesize four amino acids (cysteine, methionine, tyrosine, and phenylalanine) and four vitamins (niacin, pantothenate, biotin and folic acid) (Supplementary materials). However, *E. casseliflavus* BF-1 cells can transport these amino acids and vitamins into their cell membrane through ATP-binding cassette (ABC) transporters (Supplementary materials).

***Prediction of virulence factors.*** The virulence factors in the genome of strain BF-1 were annotated by VFanalyzer in VFDB (Table IV). Among all the potential virulence factors of *Enterococcus*, experimental results have

Table IV
The occurrence of virulence factor encoding genes in the strain BF-1 genome.

| Related genes | VFclass |
|---|---|
| *ebpA*, *ebpC*, *srtC*, *efaA*, *slrA* | Adherence |
| *cpsA*, *cpsB*, *cpsJ* | Antiphagocytosis |
| *bopD* | Biofilm formation |
| – | Toxin |
| – | Exoenzyme |
| *ctpV* | Copper up take |
| *capD*, *cps4I*, *cpsY* | Immune evasion |
| *htrA*/*degP* | Protease |
| *cheY* | Regulation |

shown that toxins, exoenzymes, and antiphagocytosis proteins are pathogenic factors (Zischka et al. 2012). The genome of strain BF-1 does not contain the genes virulent toxins and exoenzymes, although it contains the genes (*cpsA*, *cpsB*, and *cpsJ*) antiphagocytic proteins. The latter operon, however, needs a complete gene cluster (*cpsA*, *cpsB*, *cpsC*, *cpsD*, *cpsE*, *cpsF*, *cpsG*, *cpsH*, *cpsI*, *cpsJ*, and *cpsK*), or else it cannot form a capsule (Thurlow et al. 2009). Therefore, *E. casseliflavus* BF-1 is safe at the genetic level and could be further used in regulating baijiu microbial ecosystem.

**Verification of *E. casseliflavus* BF-1 defection.** In order to verify the results of KAAS annotation, we carried out the single-omission growth experiments experiment of *E. casseliflavus*. The results are shown in Fig. 5. L-cysteine, L-methionine, L-tyrosine, L-phenylalanine, niacin, pantothenate, biotin, and folic acid were subtracted from the CDM. The $OD_{600nm}$ of *E. casseliflavus* BF-1 decreased to 24%, 18%, 30%, 21%, 20%, 88%, 24%, and 42%, respectively. It is confirmed that *E. casseliflavus* BF-1 has defects in synthesizing the above eight nutrients. In this case, the synthesis of biofilm, nucleic acid, and protein of BF-1 would be affected, which could further influence the energy metabolism, oxygen stress resistance, and the growth of bacteria. However, *E. casseliflavus* BF-1 cells can transport these nutrients into the cell through ATP-binding cassette (ABC) transporters (Additional File 1). BF-1 can assimilate these nutrients for growth by adding the missing nutrients to the medium.

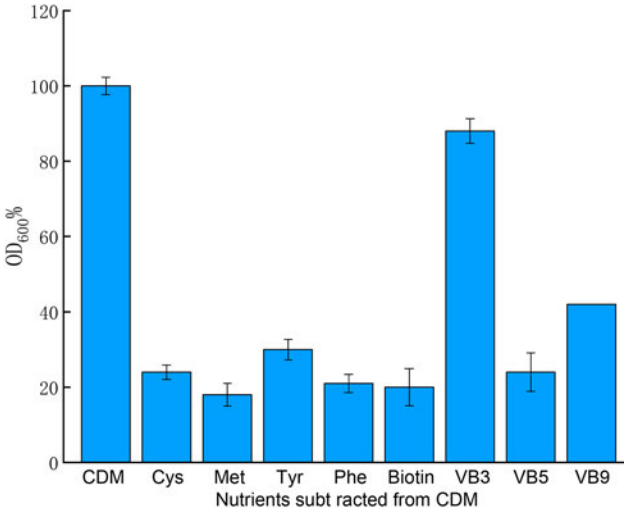


Fig. 5. Single-omission growth experiments based on CDM.

**Optimization of medium for caproic acid production based on KAAS annotation.** In different carbon sources conditions, the best carbon source for caproic acid production in strain BF-1 was glucose, followed by sodium acetate and mannose (Fig. 6a). Strain BF-1 did not use starch to produce caproic acid. As shown in Fig. 6c, the optimum concentration of glucose added was 2%. Yeast extract as a nitrogen source was found to significantly promote the production of caproic acid by *E. casseliflavus* BF-1. Yeast extract was therefore selected as a nitrogen source for the growth of *E. casseliflavus* BF-1 (Christ and Blank 2019). As shown in Fig. 6d, the optimal concentration of yeast extract added was 2.0%. *E. casseliflavus* BF-1 showed weak caproic acid production when using an inorganic nitrogen source (Fig. 6b).

Based on a single-omission growth experiment, we confirmed that *E. casseliflavus* BF-1 has defects in synthesizing eight nutrients. Because organic nitrogen source contains many complex nutritional components and rich bioactive substances, we added essential nutrients to the fermentation medium to explore its effects on the growth and acid production of *E. casseliflavus* BF-1.

We added L-cysteine, L-methionine, L-tyrosine, L-phenylalanine, niacin, pantothenate, biotin, and folic acid to the fermentation medium (L-cysteine was removed from the control). In the medium supplemented with L-cysteine and biotin, the $OD_{600nm}$ and yield of caproic acid of *E. casseliflavus* BF-1 increased significantly compared with the control. The $OD_{600nm}$ of *E. casseliflavus* BF-1 increased by 10.1% and 10.5%, respectively, after 10 days of fermentation (Fig. 7a). The yield of caproic acid increased by 6.1% and 13.1%, respectively (Fig. 7b). The nutrients in yeast extract were complex. For the sake of cost, only L-cysteine and biotin were added in the subsequent optimization experiment. Based on Fig. 8a–8h, we determined the value of each factor when the yield of caproic acid reached the maximum: sodium acetate 6 g/l, $MgSO_4 \cdot 7H_2O$ 0.25 g/l, $KH_2PO_4$ 6 g/l, $K_2HPO_4$ 8 g/l, $(NH_4)_2SO_4$ 1 g/l, L-cysteine 0.6 g/l, biotin 0.002 g/l, and ethanol at a concentration of 2%.

**Orthogonal experiment.** Based on the results of single factor optimization experiment, an $L_{16}$ ($4^4$) orthogonal experiment was designed to study further the interaction between four factors, namely A: glucose addition, B: yeast extract addition, C: sodium acetate

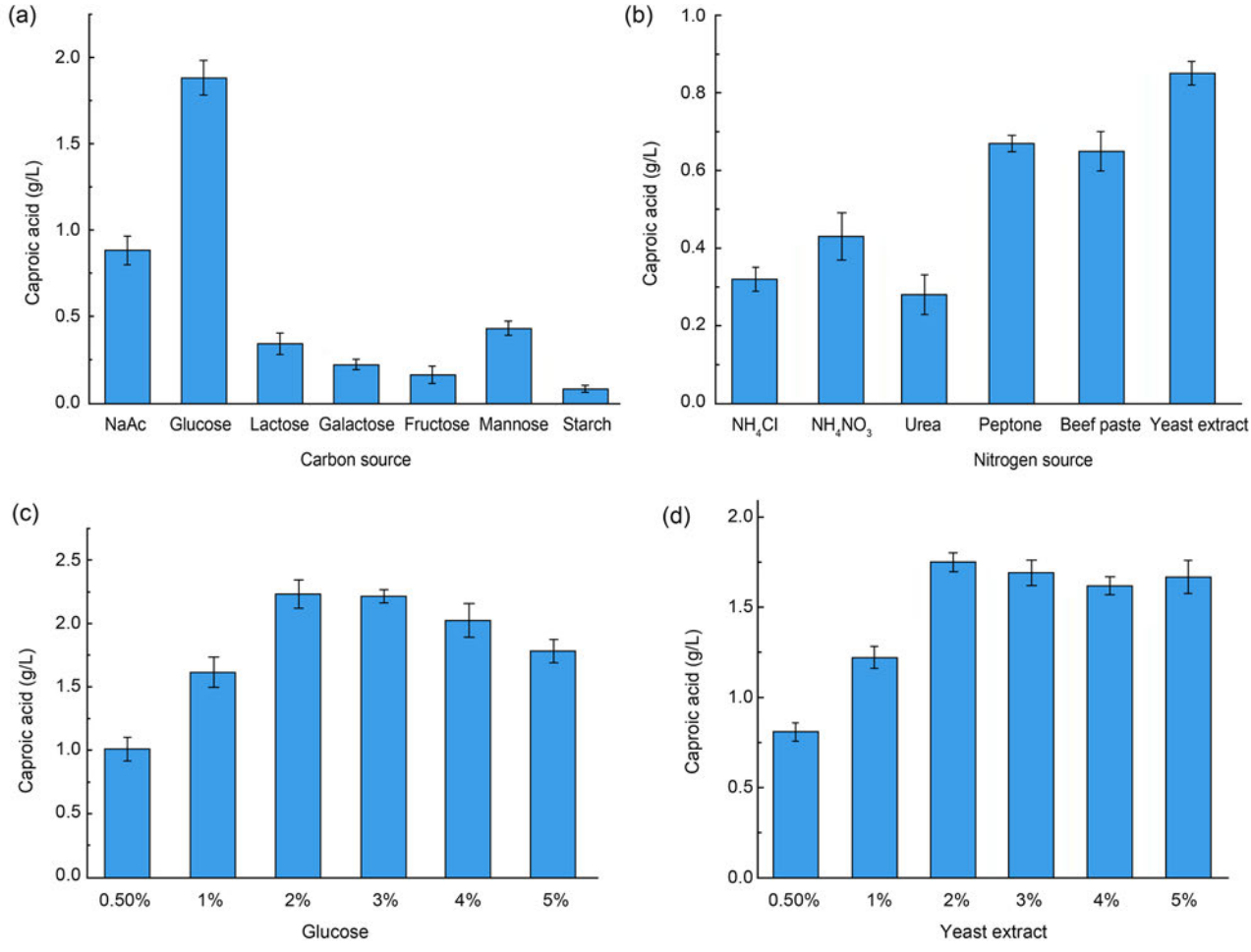


Fig. 6. Effects of adding carbon and nitrogen compounds on caproic acid yield of strain BF-1.
a) Effects of different carbon sources, b) effects of different nitrogen sources, c) effect of glucose addition, d) effect of yeast extract addition.

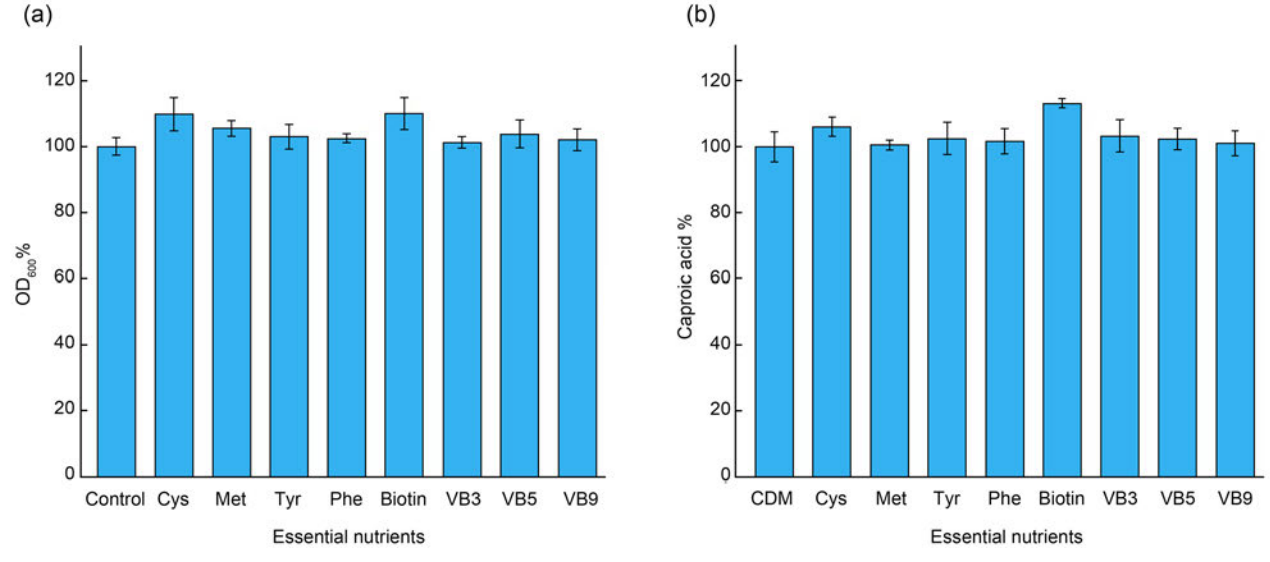


Fig. 7. Effect of supplying essential nutrients to the fermentation medium on the cell growth and caproic acid production by *E. casseliflavus* BF-1 strain.

addition, and D: ethanol addition, and four factors and four levels. The results of the orthogonal experiment are shown in Table III. According to the experimental results (Table V), the Kn value and R-value were calculated. The best fermentation scheme was as follows: $A_2B_2C_4D_1$, i.e., glucose 20 g/l, yeast extract 20 g/l, sodium

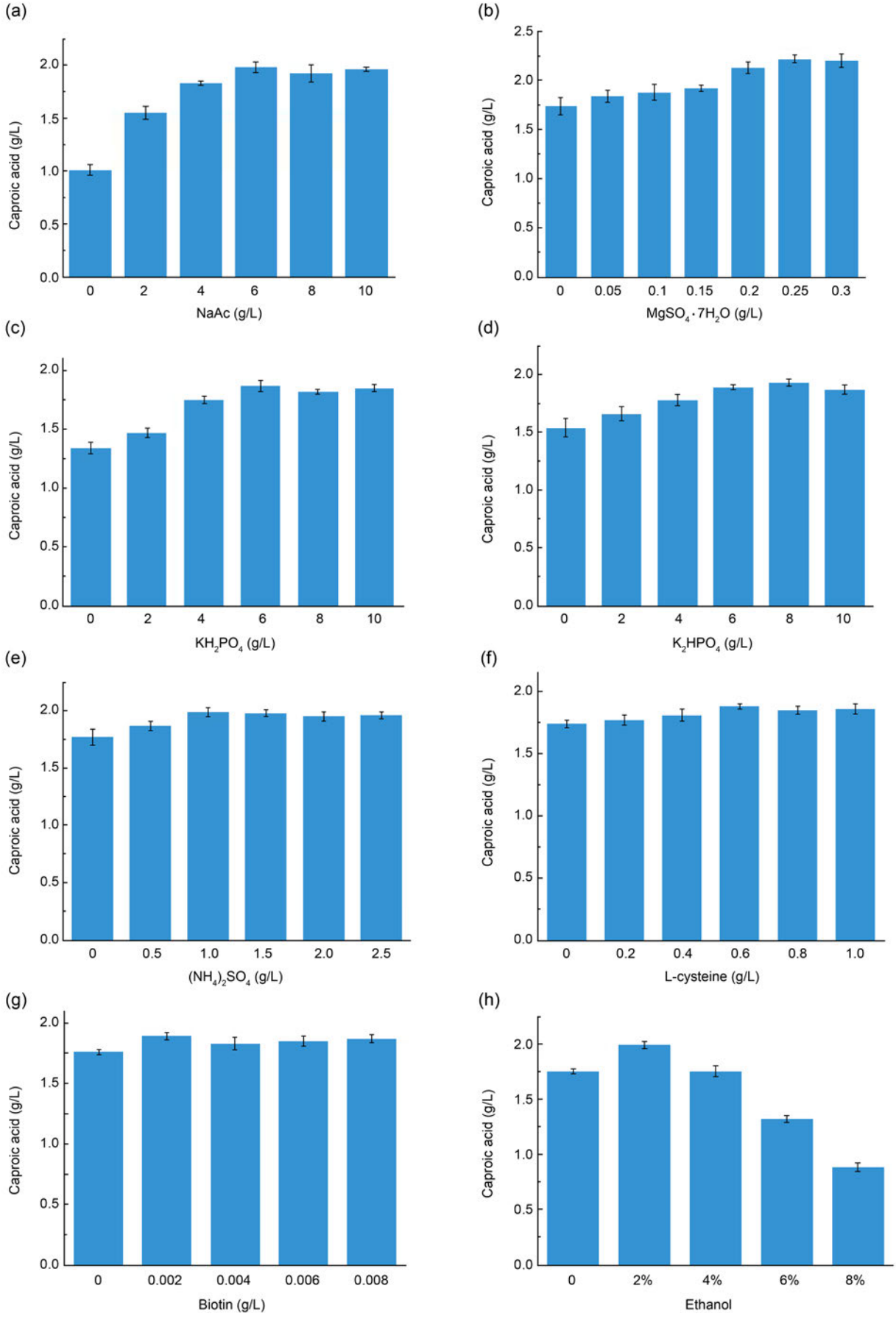


Fig. 8. Effect of adding of inorganic salts and growth factors on caproic acid production by strain BF-1.
a) Sodium acetate, b) $MgSO_4 \cdot 7H_2O$, c) $KH_2PO_4$, d) $K_2HPO_4$, e) $(NH_4)_2SO_4$, f) L-cysteine, g) biotin, h) ethanol.

Table V
Results of $L_{16}$ ($4^4$) orthogonal experiment.

| | Glucose | Yeast extract | Sodium acetate | Ethanol | Caproic acid production (g/l) |
|---|---|---|---|---|---|
| | 1 | 1 | 1 | 1 | 1.76 |
| | 1 | 2 | 2 | 2 | 1.99 |
| | 1 | 3 | 3 | 3 | 1.81 |
| | 1 | 4 | 4 | 4 | 1.63 |
| | 2 | 1 | 2 | 3 | 2.33 |
| | 2 | 2 | 1 | 4 | 2.22 |
| | 2 | 3 | 4 | 1 | 2.79 |
| | 2 | 4 | 3 | 2 | 1.96 |
| | 3 | 1 | 3 | 4 | 1.87 |
| | 3 | 2 | 4 | 3 | 2.43 |
| | 3 | 3 | 1 | 2 | 2.12 |
| | 3 | 4 | 2 | 1 | 1.96 |
| | 4 | 1 | 4 | 2 | 2.44 |
| | 4 | 2 | 3 | 1 | 2.56 |
| | 4 | 3 | 2 | 4 | 2.08 |
| | 4 | 4 | 1 | 3 | 1.56 |
| $K_1$ | 1.798 | 2.1 | 1.915 | 2.268 | |
| $K_2$ | 2.325 | 2.3 | 2.09 | 2.127 | |
| $K_3$ | 2.095 | 2.22 | 2.05 | 2.033 | |
| $K_4$ | 2.16 | 1.777 | 2.322 | 1.95 | |
| R | 0.527 | 0.523 | 0.407 | 0.318 | |

acetate 8 g/l, and ethanol added at a concentration of 1%; A was found to be the most significant factor. The results of the variance analysis of the orthogonal experiment are shown in Table VI. From these results, it can be concluded that glucose, yeast extract, and sodium acetate significantly impacted on the test results, and glucose had the most significant impact on caproic acid production of *E. casseliflavus* BF-1 strain ($p = 0.013$).

The following optimum medium conditions for acid production by strain BF-1 were obtained by the orthogonal experiment: glucose 20 g/l, yeast extract 20 g/l, sodium acetate 8 g/l, ethanol 1%, $MgSO_4 \cdot 7H_2O$ 0.25 g/l, $KH_2PO_4$ 6 g/l, $K_2HPO_4$ 8 g/l, $(NH_4)_2SO_4$ 1 g/l, L-cysteine 0.6 g/l, and biotin 0.002 g/l. The yield of caproic acid was 3.03 g/l after fermentation for 10 days at initial pH 7 and 35°C, which was 3.44-fold of that before optimization. The caproic acid yield of BF-1 was higher than those of most caproic acid bacteria (Zhao et al. 2012; Hu et al. 2015; Dobritsa et al. 2017; Gou et al. 2020). *E. casseliflavus* BF-1 could be further used as an enhanced inoculum during the SFB production to increase the yield of ethyl hexanoate. In addition, *E. casseliflavus* BF-1 could be applied in pit mud maintenance, artificial pit mud preparation, and esterification liquid production.

## Conclusion

CPB is a crucial functional group in an SFB ecosystem, as they affect the content of caproic acid and ethyl hexanoate in SFB. The present study is the first to report caproic acid production of *E. casseliflavus* BF-1. The genomic analysis confirmed that this strain is not pathogenic. After adding the predicted essential nutrients based on the KAAS annotation, the optimum medium conditions for the acid production of strain BF-1 were glucose 20 g/l, yeast extract 20 g/l, sodium acetate 8 g/l, ethanol 1%, $MgSO_4 \cdot 7H_2O$ 0.25 g/l, $KH_2PO_4$ 6 g/l, $K_2HPO_4$ 8 g/l, $(NH_4)_2SO_4$ 1 g/l, L-cysteine 0.6 g/l, and biotin 0.002 g/l by orthogonal experiment, and the yield of caproic acid reached 3.03 g/l. Strain BF-1 screened in this study can be used for the daily maintenance of pit mud and the rapid culture of artificial pit mud, which can improve the maintenance effect of pit mud, shorten the aging cycle of artificial pit mud, and reduce production cost. This strain can also be used in future animal feed and other fields.

Table VI
Variance analysis of the strain BF-1 orthogonal experiment.

| Variance source | Sum of squares | Freedom | Mean square | *F*-value | *p*-value | Significance |
|---|---|---|---|---|---|---|
| Correction model | 1.766[a] | 12 | 0.147 | 14.537 | 0.025 | |
| Intercept | 70.183 | 1 | 70.183 | 6,933.032 | 0.000 | |
| Factor A | 0.583 | 3 | 0.194 | 19.182 | 0.018 | * |
| Factor B | 0.616 | 3 | 0.205 | 20.268 | 0.017 | * |
| Factor C | 0.345 | 3 | 0.115 | 11.354 | 0.038 | * |
| Factor D | 0.223 | 3 | 0.074 | 7.342 | 0.068 | – |
| Error | 0.030 | 3 | 0.010 | | | |
| Total | 71.979 | 16 | | | | |
| Corrected total | 1.796 | 15 | | | | |

[a] – R square = 0.983 (adjusted R square = 0.915)
* – significance

**ORCID**
Wei Zou https://orcid.org/0000-0002-6335-8785

**Acknowledgments**

We thank International Science Editing (http://www.internationalscienceediting.com) for editing this manuscript.

**Author contributions**

Conceptualization: Wei Zou; methodology: Hao Luo and Tao Li; formal analysis: Hao Luo, Tao Li, Jia Zheng, Kaizheng Zhang, and Zongwei Qiao; writing, review, and editing: Hao Luo, Tao Li, Huibo Luo, and Wei Zou; supervision: Huibo Luo and Wei Zou. All authors read and approved the final manuscript.

**Funding**

This work was supported by grants from the Cooperation Project of Wuliangye Group Co., Ltd. and Sichuan University of Science & Engineering, China (CXY2019ZR011), Sichuan University of Science & Engineering (Item No. 2020RC36), and Sichuan Academician (Expert) Workstation of Solid-State Brewing (2017YSGZZ03).

**Conflict of interest**

The authors do not report any financial or personal connections with other persons or organizations, which might negatively affect the contents of this publication and/or claim authorship rights to this publication.

## Literature

**Akbari H, Shekrabi SPH, Soltani M, Mehrgan MS.** Effects of potential probiotic *Enterococcus casseliflavus* (EC-001) on growth performance, immunity, and resistance to *Aeromonas hydrophila* infection in common carp (*Cyprinus carpio*). Probiotics Antimicrob Proteins. 2021 Oct;13(5):1316–1325. https://doi.org/10.1007/s12602-021-09771-x

**Bankevich A, Nurk S, Antipov D, Gurevich AA, Dvorkin M, Kulikov AS, Lesin VM, Nikolenko SI, Pham S, Prjibelski AD, et al.** SPAdes: A new genome assembly algorithm and its applications to single-cell sequencing. J Comput Biol. 2012 May;19(5):455–477. https://doi.org/10.1089/cmb.2012.0021

**Blake JD, Cohen FE.** Pairwise sequence alignment below the twilight zone. J Mol Biol. 2001 Mar 23;307(2):721–735. https://doi.org/10.1006/jmbi.2001.4495

**Ceddia T, Mancini A, Marinucci MC.** [A new ICSB classification of *Staphylococci* stocks previously classified according to Bergey's Manual of Determinative Bacteriology] (in Italian). Boll Soc Ital Biol Sper. 1980 Jul 15;56(13):1409–1413.

**Christ JJ, Blank LM.** *Saccharomyces cerevisiae* containing 28% polyphosphate and production of a polyphosphate-rich yeast extract thereof. FEMS Yeast Res. 2019 May 1;19(3):foz011. https://doi.org/10.1093/femsyr/foz011

**Coil D, Jospin G, Darling AE.** A5-miseq: an updated pipeline to assemble microbial genomes from Illumina MiSeq data. Bioinformatics. 2015 Feb 15;31(4):587–589. https://doi.org/10.1093/bioinformatics/btu661

**Dobritsa AP, Kutumbaka KK, Werner K, Wiedmann M, Asmus A, Samadpour M.** *Clostridium tepidum* sp. nov., a close relative of *Clostridium sporogenes* and *Clostridium botulinum* Group I. Int J Syst Evol Microbiol. 2017 Jul;67(7):2317–2322. https://doi.org/10.1099/ijsem.0.001948

**Gildemyn S, Molitor B, Usack JG, Nguyen M, Rabaey K, Angenent LT.** Upgrading syngas fermentation effluent using *Clostridium kluyveri* in a continuous fermentation. Biotechnol Biofuels. 2017 Mar 29;10:83. https://doi.org/10.1186/s13068-017-0764-6

**Gou WJ, Tian Y, Kong XY, Wu FF, Fang F.** [Bacterial composition in pit mud of Yanghe liquor and identification of acid producing bacteria] (in Chinese). Microbiol. China. 2020 Jun:47(6):1651–1661. https://doi.org/10.13344/j.microbiol.china.190839

**Hong J, Tian W, Zhao D.** Research progress of trace components in sesame-aroma type of baijiu. Food Res Int. 2020 Nov;137:109695. https://doi.org/10.1016/j.foodres.2020.109695

**Hu XL, Du H, Xu Y.** Identification and quantification of the caproic acid-producing bacterium *Clostridium kluyveri* in the fermentation of pit mud used for Chinese strong-aroma type liquor production. Int J Food Microbiol. 2015 Dec 2;214:116–122. https://doi.org/10.1016/j.ijfoodmicro.2015.07.032

**Ji X, Xu Y, Mu XQ, Ge XY.** [Improvement of caproic acid production in the mixed culture of *Clostridium kluyveri* and *Saccharomyces cerevisiae*] (in Chinese). J Food Sci Biotechnol. 2017 Sep; 36(09): 922–926.

**Kalvari I, Argasinska J, Quinones-Olvera N, Nawrocki EP, Rivas E, Eddy SR, Bateman A, Finn RD, Petrov AI.** Rfam 13.0: shifting to a genome-centric resource for non-coding RNA families. Nucleic Acids Res. 2018 Jan 4;46(D1):D335–D342. https://doi.org/10.1093/nar/gkx1038

**Kim BC, Seung Jeon B, Kim S, Kim H, Um Y, Sang BI.** *Caproiciproducens galactitolivorans* gen. nov., sp. nov., a bacterium capable of producing caproic acid from galactitol, isolated from a wastewater treatment plant. Int J Syst Evol Microbiol. 2015 Dec; 65(Pt_12): 4902–4908. https://doi.org/10.1099/ijsem.0.000665

**Kim H, Jeon BS, Pandey A, Sang BI.** New coculture system of *Clostridium* spp. and *Megasphaera hexanoica* using submerged hollow-fiber membrane bioreactors for caproic acid production. Bioresour Technol. 2018 Dec;270:498–503. https://doi.org/10.1016/j.biortech.2018.09.033

**Kumar S, Stecher G, Tamura K.** MEGA7: Molecular Evolutionary Genetics Analysis Version 7.0 for bigger datasets. Mol Biol Evol. 2016 Jul;33(7):1870–1874. https://doi.org/10.1093/molbev/msw054

**Liu H, Sun B.** Effect of fermentation processing on the flavor of baijiu. J Agric Food Chem. 2018 Jun 6;66(22):5425–5432. https://doi.org/10.1021/acs.jafc.8b00692

**Lowe TM, Eddy SR.** tRNAscan-SE: A program for improved detection of transfer RNA genes in genomic sequence. Nucleic Acids Res. 1997 Mar 1;25(5):955–964. https://doi.org/10.1093/nar/25.5.955

**Moriya Y, Itoh M, Okuda S, Yoshizawa AC, Kanehisa M.** KAAS: an automatic genome annotation and pathway reconstruction server. Nucleic Acids Res. 2007 Jul;35(Suppl_2):W182–W185. https://doi.org/10.1093/nar/gkm321

**Nabi MN, Akhter MS, Zaglul Shahadat MM.** Improvement of engine emissions with conventional diesel fuel and diesel-biodiesel blends. Bioresour Technol. 2006 Feb;97(3):372–378. https://doi.org/10.1016/j.biortech.2005.03.013

**Qin X, Galloway-Peña JR, Sillanpaa J, Roh JH, Nallapareddy SR, Chowdhury S, Bourgogne A, Choudhury T, Muzny DM, Buhay CJ, et al.** Complete genome sequence of *Enterococcus faecium* strain TX16 and comparative genomic analysis of *Enterococcus faecium* genomes. BMC Microbiol. 2012 Jul 7;12:135. https://doi.org/10.1186/1471-2180-12-135

**Serhan M, Mattar J, Debs L.** Concentrated yogurt (Labneh) made of a mixture of goats' and cows' milk: physicochemical, microbiological and sensory analysis. Small Rumin Res. 2016 May;138:46–52. https://doi.org/10.1016/j.smallrumres.2016.04.003

**Szklarczyk D, Gable AL, Lyon D, Junge A, Wyder S, Huerta-Cepas J, Simonovic M, Doncheva NT, Morris JH, Bork P, et al.** STRING v11: protein-protein association networks with increased coverage, supporting functional discovery in genome-wide experimental datasets. Nucleic Acids Res. 2019 Jan 8;47(D1):D607–D613. https://doi.org/10.1093/nar/gky1131

**Tatusova T, DiCuccio M, Badretdin A, Chetvernin V, Nawrocki EP, Zaslavsky L, Lomsadze A, Pruitt KD, Borodovsky M, Ostell J.** NCBI prokaryotic genome annotation pipeline. Nucleic Acids Res. 2016 Aug 19;44(14):6614–6624.
https://doi.org/10.1093/nar/gkw569

**Thurlow LR, Thomas VC, Fleming SD, Hancock LE.** *Enterococcus faecalis* capsular polysaccharide serotypes C and D and their contributions to host innate immune evasion. Infect Immun. 2009 Dec; 77(12):5551–5557.
https://doi.org/10.1128/IAI.00576-09

**Tian N, Guo X, Wang M, Chen C, Cui H, Zhang L, Tang H.** Bacterial community diversity of shilixiang baijiu *Daqu* based on metagenomics. J Food Biochem. 2020 Jul 29:e13410.
https://doi.org/10.1111/jfbc.13410

**Van Immerseel F, De Buck J, Boyen F, Bohez L, Pasmans F, Volf J, Sevcik M, Rychlik I, Haesebrouck F, Ducatelle R.** Medium-chain fatty acids decrease colonization and invasion through *hilA* suppression shortly after infection of chickens with *Salmonella enterica* serovar Enteritidis. Appl Environ Microbiol. 2004 Jun;70(6):3582–3587.
https://doi.org/10.1128/AEM.70.6.3582-3587.2004

**Walker BJ, Abeel T, Shea T, Priest M, Abouelliel A, Sakthikumar S, Cuomo CA, Zeng Q, Wortman J, Young SK, et al.** Pilon: An integrated tool for comprehensive microbial variant detection and genome assembly improvement. PLoS One. 2014 Nov 19;9(11): e112963. https://doi.org/10.1371/journal.pone.0112963

**Wang MY, Yang JG, Zhao QS, Zhang KZ, Su C.** Research progress on flavor compounds and microorganisms of Maotai flavor baijiu. J Food Sci. 2019 Jan;84(1):6–18.
https://doi.org/10.1111/1750-3841.14409

**Wang Q, Zhang P, Bao S, Liang J, Wu Y, Chen N, Wang S, Cai Y.** Chain elongation performances with anaerobic fermentation liquid from sewage sludge with high total solid as electron acceptor. Bioresour Technol. 2020 Mar 14;306:123188.
https://doi.org/10.1016/j.biortech.2020.123188

**Weimer PJ, Stevenson DM.** Isolation, characterization, and quantification of *Clostridium kluyveri* from the bovine rumen. Appl Microbiol Biotechnol. 2012 Apr;94(2):461–466.
https://doi.org/10.1007/s00253-011-3751-z

**Yuan S, Jin Z, Ali A, Wang C, Liu J.** Caproic acid-producing bacteria in Chinese Baijiu Brewing. Front Microbiol. 2022 May 4; 13:883142.
https://doi.org/10.3389/fmicb.2022.883142

**Zhao H, Chang Y, Wang W, Ling HZ, Ping WX, Zhao ZC, Yang ZH.** [Isolation and identification of facultative anaerobic strains with high yield of hexanoic acid from Luzhou-flavor liquor pit mud] (in Chinese). Food Sci. 2012 Sep;33(05):177–182.

**Zhao T, Ni D, Hu G, Wang L, Chen S, Xu Y.** 6-(2-Formyl-5-methyl-1*H*-pyrrol-1-yl)hexanoic acid as a novel retronasal burnt aroma compound in soy sauce aroma-type Chinese Baijiu. J Agric Food Chem. 2019 Jul 17;67(28):7916–7925.
https://doi.org/10.1021/acs.jafc.9b02095

**Zhong Y, Xie YH.** [Method for determination of caproic acid content in caproic acid bacteria culture solution] (in Chinese). Liquor Mak Sci Technol. 2004 Apr;04:91–92.

**Zhu X, Tao Y, Liang C, Li X, Wei N, Zhang W, Zhou Y, Yang Y, Bo T.** The synthesis of *n*-caproate from lactate: a new efficient process for medium-chain carboxylates production. Sci Rep. 2015 Sep 25; 5:14360. https://doi.org/10.1038/srep14360

**Zischka M, Kuenne C, Blom J, Dabrowski PW, Linke B, Hain T, Nitsche A, Goesmann A, Larsen J, Jensen LB, et al.** Complete genome sequence of the porcine isolate *Enterococcus faecalis* D32. J Bacteriol. 2012 Oct;194(19):5490–5491.
https://doi.org/10.1128/JB.01298-12

**Zou W, Zhao C, Luo H.** Diversity and function of microbial community in Chinese strong-flavor baijiu ecosystem: A Review. Front Microbiol. 2018 Apr 9;9:671.
https://doi.org/10.3389/fmicb.2018.00671

Supplementary materials are available on the journal's website.

ORIGINAL PAPER
Polish Journal of Microbiology
2022, Vol. 71, No 4, 577–587
https://doi.org/10.33073/pjm-2022-053

# Omicron SARS-CoV-2 Variants in an *In Silico* Genomic Comparison Study with the Original Wuhan Strain and WHO-Recognized Variants of Concern

ELMUTUZ H. ELSSAIG[1, 2, 3], TARIG M.S. ALNOUR[1, 2, 3]*, MOHAMMAD FAHAD ULLAH[1, 2] and ELTAYIB H. AHMED-ABAKUR[1, 2, 3]

[1] Department of Medical Laboratory Technology (FAMS), University of Tabuk, Saudi Arabia
[2] Prince Fahd Bin Sultan Chair for Biomedical Research, University of Tabuk, Tabuk, Saudi Arabia
[3] Faculty of Medical Laboratory Science, Department of Microbiology and Immunology, Alzaiem Alazhari University, Khartoum Bahry, Sudan

Submitted 19 September 2022, accepted 12 November 2022, published online 19 December 2022

Abstract

This study aimed to determine the genetic alterations in the Omicron variants compared to other variants of concern (VOCs) to trace the evolutionary genetics of the SARS-CoV-2 variants responsible for the multiple COVID-19 waves globally. The present study is an *in silico* analysis determining the evolution of selected 11 VOCs compared to the original Wuhan strain. The variants included six Omicrons and one variant of Alpha, Beta, Delta, Gamma, and Mu. The pairwise alignment with the local alignment search tool of NCBI Nucleotide-BLAST and NCBI Protein-BLAST were used to determine the nucleotide base changes and corresponding amino acid changes in proteins, respectively. The genomic analysis revealed 210 nucleotide changes; most of these changes (127/210, 60.5%) were non-synonymous mutations that occurred mainly in the S gene (52/127, 40.1%). The remaining 10.5% (22/210) and 1.9% (4/210) of the mutations were frameshift deletions and frameshift insertions, respectively. The frameshift insertion (Ins22194T T22195G) led to frameshift deletion (Δ211N). Only four mutations (C241T, C3037T, C14408T, and A23403G) were shared among all the VOCs. The nucleotide changes among Omicron variants resulted in 61 amino acid changes, while the nucleotide changes in other VOCs showed 11 amino acid changes. The present study showed that most mutations (38/61, 62.3%) among Omicron variants occurred in the S gene; and 34.2% of them (13/38) occurred in the receptor-binding domain. The present study confirmed that most of mutations developed by Omicron variants occurred in the vaccine target gene (S gene).

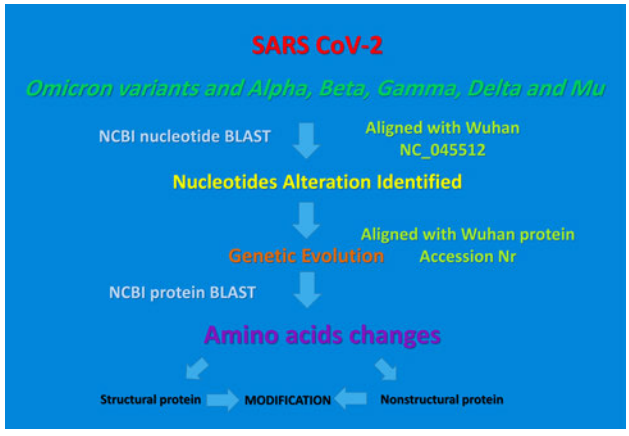


K e y w o r d s: *in silico*, Omicron, VOCs, Nucleotide-BLAST, Protein-BLAST

## Introduction

The COVID-19 pandemic, which started at the end of 2019, continues at the dawn of 2022, with an unprecedented vigor against humanity that was unheard of in recent times (Sofi et al. 2020). The global crisis demonstrated the loss of millions of human lives, and billions underwent a dreadful experience of economic, social, and psychological distress (Rudrapal et al. 2020). The healthcare systems across the world are exhausted and racing against time to save millions of SARS-CoV-2 -infected people. During this long pandemic, different

* Corresponding author: T.M.S. Alnour, Department of Medical Laboratory Technology (FAMS), University of Tabuk, Saudi Arabia; Prince Fahd Bin Sultan Chair for Biomedical Research, University of Tabuk, Tabuk, Saudi Arabia; Faculty of Medical Laboratory Science, Department of Microbiology and Immunology, Alzaiem Alazhari University, Khartoum Bahry, Sudan; **e-mail: telnour@ut.edu.sa; tarigms@yahoo.com**

parts of the world saw multiple waves of the disease that were driven by dominant variants originating through mutations in the original SARS-CoV-2 viral genome. Consequently, Alpha, Beta, Gamma, Kappa, Delta, Mu, IHU, and Omicron have originated as novel variants with the varying potential of virulence, transmissibility, and disease severity (Choi and Smith 2021; Karim and Karim 2021). The SARS-CoV-2, like other coronaviruses, possesses an enveloped genome of positive-sense single-stranded ~ 30 kb RNA with six open reading frames (Cao et al. 2021). The genome's two-thirds of length comprises 265 nucleotides 5'UTR, followed by 21,290 nucleotides long ORF1ab that encode poly-protein for 16 non-structural proteins. The other one-third at the 3' end has 229 nucleotide 3'UTR and several genes that encode surface, envelope, membrane, and nucleocapsid structural proteins such as 3,822 nucleotide-S, 228 nucleotide-E, 669 nucleotide-M, and 908 nucleotide-N, respectively. Six accessory proteins are encoded by 828 nucleotide ORF3a, 186 nucleotide ORF6, 366 nucleotide ORF7a, 132 nucleotide ORF7b, 193 nucleotide ORF8, and 117 nucleotide ORF10 genes. It is known that the viral genome is a hotspot of mutations with one of the highest mutation rates among all organisms.

Moreover, compared to DNA viruses, RNA viruses are more prone to mutations due to the low fidelity of RNA polymerase, resulting in higher rates of erroneous miss-incorporation of bases during replication. Some of these mutations might provide the endurance to the replicating virus that grants higher potential of transmission and pathogenicity, causing the emergence of a dominant variant associated with higher rates of infection, mortality, and evasiveness to the existing natural or vaccines elicited immunity. The Delta variant of SARS-CoV-2 (B.1.617.2) which was detected in India, exhibited characteristics that outweighed the previously existing Alpha and Kappa lineages, making it a dominant variant that was responsible for the calamitous second wave in India with devastating human sufferings and loss of lives (Adiga and Nayak 2021). Experimental evidence suggests that the Delta variant as compared to wild-type Wuhan-1, was less sensitive to neutralizing antibodies from the serum of recovered individuals (six-fold loss of efficacy), and vaccine-induced antibodies (eight-fold loss of efficacy), demonstrating a potential risk of infection due to a compromised vaccine efficacy even in the vaccinated population (Mlcochova et al. 2021).

Consequently, the Delta variant was observed to be associated with a longer period of infections, higher viral load, and higher rates of re-infections, emerging as a globally dominant variant driving 2$^{nd}$, 3$^{rd}$, and 4$^{th}$ waves of COVID-19 infections in many countries worldwide. Recently on November 25, 2021, another variant of concern named Omicron (B.1.1.529) was reported in South Africa, leaving the world apprehensive about the next course of COVID-19 disease and the efficacy of vaccines (Callaway 2021). Since then, the Omicron infection has been reported in fully vaccinated individuals, and the probability of higher transmission rates has also been suggested (Gu et al. 2021). The emergence of new variants with higher virulence downplays the containment strategies and increases the risk of greater harm to human lives. Studies characterizing the genetic diversity of such variants are therefore considered significant to tracing the course of the pandemic. In this study, we have characterized the genetic alterations in the variants of concern (VOC) including the Omicron variant which exhibits a continuous evolution of the heterogeneity in the viral genome (structural and non-structural genes) in comparison to the original Wuhan SARS-CoV-2 genome and other VOCs such as Alpha, Beta, Delta, Gamma, and Mu.

The novelty of our work can be assessed from the results wherein we have described the genetic variations in the whole genome of the Omicron SARS-CoV-2 variants as compared to other studies which focused only on the spike protein of the virus. It is also the first study wherein inter-variant genomic variations have been compared, tracing the genetic variations from the original Wuhan strain to variants of concern that emerged during different waves of COVID-19 globally.

## Experimental

### Materials and Methods

Our laboratory has been engaged in studies related to the genetic variations in SARS-CoV-2 over the last two years. This study is an *in silico* analysis of the evolutionary heterogeneity of selected variants of concern compared to the original Wuhan reference. The present study included six Omicron variants retrieved from GISAID database that were Omicron (EPI_ISL_6640916) from Botswana, Omicron (EPI_ISL_6647956) from South Africa, Omicron (EPI_ISL_6647957) from South Africa, Omicron (EPI_ISL_6647961) from South Africa, Omicron (EPI_ISL_7740798) from South Africa and Omicron (EPI_ISL_8182845) from South Africa plus five VOCs isolated from Japan and retrieved from GISAID database that were Alpha (EPI_ISL_6756515), Beta (EPI_ISL_5416540), Gamma (EPI_ISL_6228367), Delta (EPI_ISL_6832166) and Mu (EPI_ISL_4470504).

The sequences of SARS-CoV-2 of the original Wuhan variant were retrieved from NCBI COVID-19 Resource Repository (https://www.ncbi.nlm.nih.gov/genbank/sars-cov-2-seqs). The selected variants included complete genomic sequences aligned with the first

characterized isolate, the Wuhan strain from China (NC_045512.2) (Lu et al. 2020). The pairwise alignment with the local alignment search tool Nucleotide-BLAST (NCBI) was used to determine the nucleotide base changes and gene variation against Wuhan standard reference. Moreover, the NCBI Protein-BLAST was used to report the corresponding amino acid changes in the protein.

Evolutionary relationships: The Neighbor-Joining method was used to build a phylogenetic tree for understanding the evolutionary relationship of the evolving variants of SARS-CoV-2 using Molecular Evolutionary Genetics Analysis Software (MEGA 4), Philadelphia, USA (Saitou and Nei 1987). As reported in the results, the clustered taxa clad in the bootstrap test included 500 replicates, which are represented as a percentage of replicate trees shown close to the branches (Felsenstein 1985). The evolutionary distances were determined by the Maximum Composite Likelihood method (Tamura et al. 2004) showing the number of base substitutions/site units. This analysis involved a set of SARS-CoV-2 variants of concerns, including Beta, Gamma, Delta, Mu, and Omicron, along with the original Wuhan sequence. The FASTA sequence for each of the specimen variants retrieved from the database were selected, aligned, and phylogenetic association was obtained using the tools incorporated within the software. The analysis disregarded all the enigmatic positions with a pairwise deletion option for each sequence pair. A total of 29,903 positions representing the approximate length of the whole viral genome were present in the final dataset.

## Results

The multi-alignment analysis showed that Omicron variants have the lowest homology compared to the original strain; they exhibited homology ranging between 99.74 to 99.3% except for Omicron (EPI_ISL_8182845), which showed 99.84%, while the other VOCs showed homology ranging between 99.82 to 99.85%. The genomic analysis of the VOCs of SARS-CoV-2 (Alpha, Beta, Delta, Gamma, Mu, and Omicron variants) revealed 210 nucleotide changes. Most of these changes (127/210, 60.5%) were non-synonymous mutations that occurred mainly in the S gene (52/127, 40.1%) followed by ORF1a/b (43/127, 33.9%) and the N gene (11/127, 8.9%). The remaining 10.5% (22/210) and 1.9% (4/210) of the mutations were frameshift deletions and frameshift insertions, respectively (Table I).

The comparative analysis showed that only four mutations were common among all the VOCs; one silent mutation (C241T) on the 5'UTR region, one synonymous mutation in ORF1a/b (C3037T), one non-synonymous mutation in ORF1a/b (C14408T), which changed the amino acid (P4715L), and one non-synonymous mutation in the S gene (A23403G), which changed the amino acid (D614G).

The nucleotide changes among Omicron variants resulted in 61 amino acid changes, while the nucleotide changes in other VOCs of SARS-CoV-2 (Alpha, Beta, Delta, Gamma, and Mu) showed 11 amino acid changes (Table II, III, and IV). The present study exhibited that the majority of mutations (38/61, 62.3%) among Omicron variants occurred in the S gene, 34.2% (13/38) out of that occurred in the receptor-binding domain RBD (the RBD has involved 541–319 residues of the S1 subunit), as follows: G339D, S371L, S373P, **N440K**, **G446S**, **K417N**, **S477N**, **T478K**, **E484A**, **Q493R**, **G496S**, **Q498R**, **N501Y**. The mutations indicated with the bold font representing 69.2% (9/13) of the mutations in BDR were located in the receptor-binding motif (508aa–438aa).

The mutations among Omicron variants were categorized into three groups; the unique common mutations group which involved 50.8% (31/61) of the mutations (Table II); the unique non-common mutations

Table I
Distribution and type of mutations among variants of concern of SARS-CoV-2.

| Type of mutation | 3'UTR | ORF10 | N gene | ORF8 | ORF7b | ORF7a | ORF6 | M gene | E gene | ORF3 | S gene | ORF1 a/b | 5'UTR | Total |
|---|---|---|---|---|---|---|---|---|---|---|---|---|---|---|
| Non-coding | 2 | – | – | – | – | – | – | – | – | – | – | – | 3 | 5 |
| Non-synonymous | – | – | 11 | 6 | 1 | 3 | – | 4 | 2 | 5 | 52 | 43 | – | 127 |
| Synonymous | – | – | 5 | 1 | 1 | – | 1 | – | 1 | 2 | 4 | 36 | – | 51 |
| Frame shift/insertion | – | – | 1 | – | – | – | – | – | – | – | 3 | – | – | 4 |
| Frame shift/deletion | – | – | 4 | – | – | – | – | – | – | – | 15 | 3 | – | 22 |
| Nonsense | – | – | – | 1 | – | – | – | – | – | – | – | – | – | 1 |
| | 2 | | 21 | 8 | 2 | 3 | 1 | 4 | 3 | 7 | 74 | 82 | 3 | 210 |

Table II
The unique common mutations among Omicron variants.

| Nucleotide Mutation | Protein mutation | Type of mutation | Gene |
|---|---|---|---|
| A2832G | K856R | Nonsynonymous | ORF1a/b |
| 3T5386G | – | Synonymous | ORF1a/b |
| G8393A | A2710T | Nonsynonymous | ORF1a/b |
| C10449A | – | Synonymous | ORF1a/b |
| A11537G | I3758V | Nonsynonymous | ORF1a/b |
| C15240T | – | Synonymous | ORF1a/b |
| A18163G | I5968V | Nonsynonymous | ORF1a/b |
| Δ21762 ΔC<br>Δ21764 ΔA | A67V | Frameshift (deletion) | S gene |
| Δ21767–21769 ΔCAT | Δ69H | Frameshift (deletion) | S gene |
| Δ21770 ΔG | Δ70V | Frameshift (deletion) | S gene |
| Δ21987–21988 ΔGT | G142D | Frameshift (deletion) | S gene |
| Δ21989–21991 ΔGTT | Δ143V | Frameshift (deletion) | S gene |
| Δ21992–21994 ΔTAT | Δ144Y | Frameshift (deletion) | S gene |
| Δ21995 ΔG | Δ145Y | Frameshift (deletion) | S gene |
| G22578A | G339D | Nonsynonymous | S gene |
| C23202A | T547K | Nonsynonymous | S gene |
| C23525T | H655Y | Nonsynonymous | S gene |
| T23599G | N679K | Nonsynonymous | S gene |
| C23854A | N764K | Nonsynonymous | S gene |
| G23948T | D796Y | Nonsynonymous | S gene |
| C24130A | N856K | Nonsynonymous | S gene |
| A24424T | Q954H | Nonsynonymous | S gene |
| T24469A | N969K | Nonsynonymous | S gene |
| C25000T | – | Synonymous | S gene |
| C25584T | – | Synonymous | ORF3a |
| C26270T | T9I | Nonsynonymous | E gene |
| A26530G | D3G | Nonsynonymous | M gene |
| G26709A | A63T | Nonsynonymous | M gene |
| C28311T | P13L | Nonsynonymous | N gene |
| Δ28363–28364 ΔGA | – | Frameshift (deletion) | N gene |
| Δ28365–28367 ΔGAA | Δ31E | Frameshift (deletion) | N gene |
| Δ28368–28370 ΔCGC | Δ32R | Frameshift (deletion) | N gene |
| Δ28371 ΔA | Δ33S | Frameshift (deletion) | N gene |

group, which involved 31.1% (19/61) of the mutations (Table III), and the shared mutations group which involved 18.0% (11/61) of the mutations (Table IV). The unique common mutations characterized and differentiated Omicron variants from the other VOCs. These mutations were present only in Omicron variants, unique non-common mutations were also associated with Omicron variants but were absent in all variants, while the shared mutations existed in Omicron as well the other VOCs. Most of the unique common mutations 54.8% (17/31) were non-synonymous mutations, followed by 29% (9/31) frameshift deletions, which were observed in the S gene 55.6% (5/9) and in the N gene 44.4% (4/9) (Table II and Fig. 1).

Similarly, many unique non-common mutations (12/19, 63.2%) were non-synonymous. Some of them (3/19, 15.8%) were frameshift deletions and (1/19, 5.3%) frameshift insertions (Table III and Fig. 1). Interestingly the frameshift insertion (Ins22194, T22195G) led to frameshift deletion (Δ211N) (Table III and Fig. 1).

All Omicron variants showed frameshift deletions in the S and N genes and ORF1a/b except (EPI_ISL_6647956) variant, which did not show deletion in the ORF1a/b. All Omicron variants showed frameshift insertion in the S gene except (EPI_ISL_8182845) variant. The Alpha, Beta, and Gamma variants showed frameshift deletions in ORF1a/b, while the Mu variant showed frameshift insertion in the S gene.

Table III
The unique non-common mutations among Omicron variants.

| Nucleotide mutation | Protein mutation | Type of mutation | Gene | Comment |
|---|---|---|---|---|
| C24503T | L981F | Nonsynonymous | S gene | Not detected in (EPI-ISL-6640916) variant |
| Δ11283–1129 ΔGTTTGTCTG | Δ3674–3676 ΔLSG | Frameshift (deletion) | ORF1a/b | Not detected in variant (EPI_ISL_6647956) |
| C27807T | | Synonymous | ORF7b | Not detected in (EPI_ISL_8182845) variant |
| T13195C | | synonymous | ORF1a/b | Not detected in one (EPI_ISL_8182845) variant |
| Ins22194T T22195G | Δ211N | Frameshift (deletion) | S gene | |
| T22197G A22198C | L212I | Nonsynonymous | S gene | |
| INS22202–22203 AG INS22203–22204 CA T22204A INS22205 A | INS214–216 EPE | Frameshift (insertion) | S gene | |
| T22673C C22674T | S371L | Nonsynonymous | S gene | |
| T22882G | N440K | Nonsynonymous | S gene | |
| G22898A | G446S | Nonsynonymous | S gene | |
| T22679C | S373P | Nonsynonymous | S gene | |
| G22813T | K417N | Nonsynonymous | S gene | Not detected in one (EPI_ISL_8182845) variant |
| Δ6513–6515 ΔGTT | Δ2083 S L2084I | Frameshift (deletion) | ORF1a/b | Not detected in two variants (EPI-ISL-6640916 and EPI_ISL_6647956) |
| A27259C | | Synonymous | M gen | Not detected in two variants (EPI_ISL_6647956 and (EPI_ISL_8182845) |
| G22992A | S477N | Nonsynonymous | S gene | Not detected in three variants (EPI_ISL_6647956, EPI_ISL_6647957 and EPI_ISL_8182845) |
| A23013C | E484A | Nonsynonymous | S gene | |
| A23040G | Q493R | Nonsynonymous | S gene | |
| G23048A | G496S | Nonsynonymous | S gene | |
| A23055G | Q498R | Nonsynonymous | S gene | |

Table IV
Mutations shared between Omicron and other VOCs.

| Nucleotide mutation | Protein mutation | Type of mutation | Gene | Comment |
|---|---|---|---|---|
| Δ21767-21769 ΔCAT | Δ69H | Frameshift (deletion) | S gene | Shared with Alpha variant (EPI_ISL_6756515) |
| Δ21770 ΔG | Δ70V | Frameshift (deletion) | S gene | |
| C23525T | H655Y | Nonsynonymous | S gene | Shared with Gamma variant (EPI_ISL_6228367) |
| C10029T | T3255I | Nonsynonymous | ORF1a/b | Shared with Delta (EPI_ISL_6832166) and Mu (EPI_ISL_4470504) variants |
| C21846T | T95I | Nonsynonymous | S gene | |
| C23604A | P681H | Nonsynonymous | S gene | Shared with Alpha (EPI_ISL_6756515) and Mu (EPI_ISL_4470504) variants |
| G28881T | R203K | Nonsynonymous | N gene | Shared with Alpha (EPI_ISL_6756515) and Gamma (EPI_ISL_6228367) variants |
| G28882A | | Synonymous | N gene | |
| G28883C | G204R | Nonsynonymous | N gene | |
| C22995A | T478K | Nonsynonymous | S gene | Shared with Delta (EPI_ISL_6832166) variant |
| A23063T | N501Y | Nonsynonymous | S gene | Shared with Alpha (EPI_ISL_6756515), Beta (EPI_ISL_5416540), Gamma (EPI_ISL_6228367), Mu (EPI_ISL_4470504), variants |

Furthermore, 11 mutations were shared between Omicron variants and other VOCs (Alpha, Beta, Delta, Gamma, and Mu); 63.6% (7/11) of these mutations occurred on the S gene, 18.2% (2/11) were frameshift deletion (Δ21767-21769 ΔCAT (Δ69H) and Δ21770 ΔG (Δ70V)) that were shared with Alpha variant and three mutations in the N gene; G28881T (R203K), G28882A, G28883C (G204R) shared with Alpha (EPI_ISL_6756515) and Gamma (EPI_ISL_6228367) variants, one mutation occurred in ORF1a/b C10029T

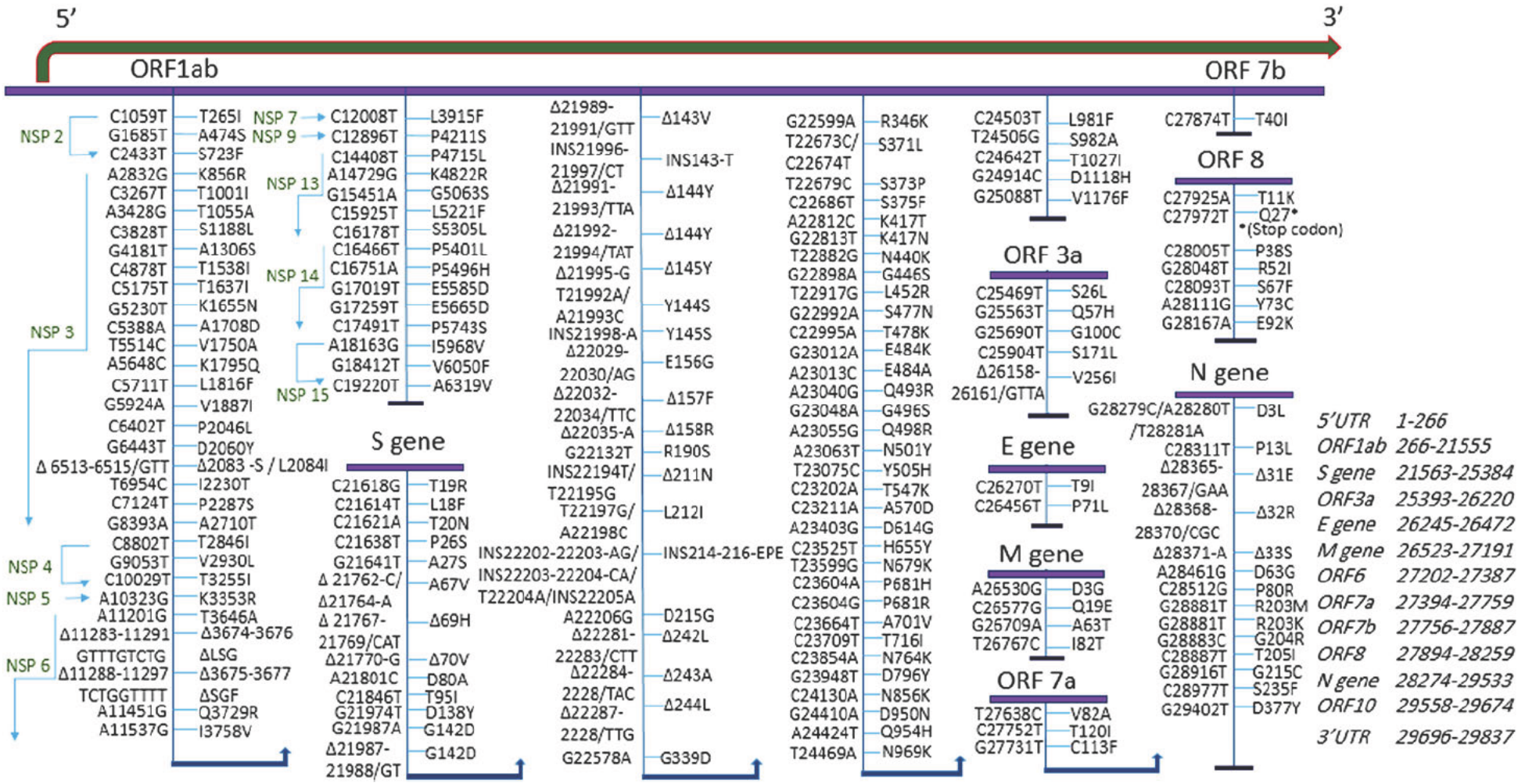


Fig. 1. The genomic landscape representing nucleotides changes for variants of concerns of SARS-CoV-2 and corresponding amino acid changes.

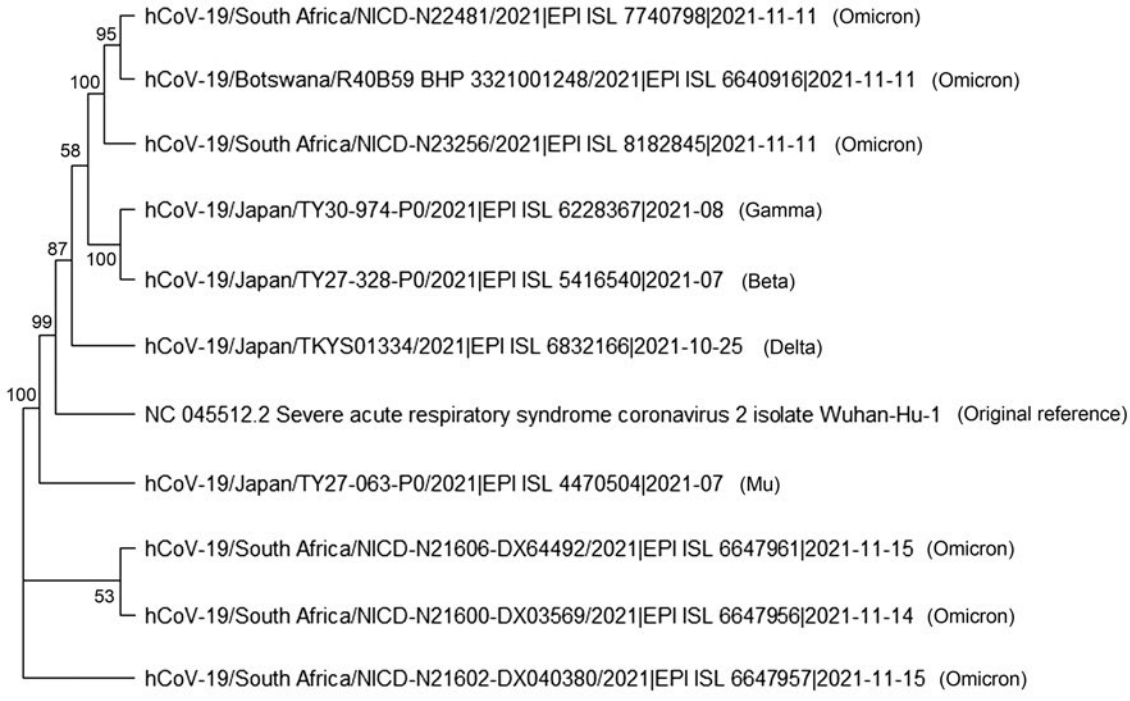


Fig. 2. Phylogenetic affiliation for variants of concerns of SARS-CoV-2.

(T3255I) shared with Delta (EPI_ISL_6832166) and Mu (EPI_ISL_4470504) variants. The mutation A23063T (N501Y) in the S gene was shared with Alpha (EPI_ISL_6756515), Beta (EPI_ISL_5416540), Gamma (EPI_ISL_6228367), Mu (EPI_ISL_4470504), and Omicron variants (EPI_ISL_8182845, EPI_ISL_6647961, EPI_ISL_7740798, EPI-ISL-6640916) (Table IV and Fig. 1).

A phylogenetic relationship between Omicron variants, Wuhan reference, and certain variants of concerns revealed two distinct clads of Omicron: one at the top and one at the bottom of the evolutionary tree (Fig. 2).

## Discussion

Omicron variants showed too many mutations compared to the previously evolved variants of concern (Kannan et al. 2021), which is why it has been described as a "worrying type". These mutations may alter the virus's conformation and affect the capacity for immune evasion, disease severity, and transmissibility (Zhang et al. 2021). However, the information about the Omicron variants is limited (Kannan et al. 2022).

The present study displayed that most of the mutations (60.5%) among the VOCs were non-synonymous mutations that occurred mainly in the S gene. This finding was contradictory to our earlier reports at the beginning of this pandemic, in which we found that most mutations occurred in ORF1a/b (Ahmed-Abakur and Alnour 2020). Several other authors stated that ORF1a/b was occupied with more than 60% of mutations (Khailany et al. 2020; Shishir et al. 2021). The recent reports approved that the principal mechanism of SARS-CoV-2 evolution is natural selection, so the heavy mutations in the S gene could be attributed to the breakthrough of the SARS-CoV-2 vaccine. Wang et al. 2021 proposed that vaccine breakthroughs will become a major mechanism of SARS-CoV-2 evolution as most of the population is either infected or vaccinated.

Our study showed 61 amino acid mutations among Omicron variants; 31 of 61 (50.8%) were unique common mutations, 19 of 61 (31.1%) were unique non-common mutations, and 11 of 61 (18%) were shared mutations. These results reflected a high occurrence of mutations among the Omicron variants under the study compared to the most published reports that indicated 47 to 58 mutations in Omicron variants (Jia et al. 2022; Poudel et al. 2022; Tan et al. 2022; Thakur and Ratho 2022). Kannan et al. (2022) studied the unique features of the Omicron variant and reported 46 mutations, 23 of which were unique to the Omicron variant. Jia et al. (2022) and Kannan et al. (2022) mentioned that some Omicron signature mutations might not be present in some variants, similar to our finding concerning the unique non-common mutations.

The present study showed that only four common mutations were present in all the VOCs; one silent mutation (C241T) in the 5'UTR region, one synonymous mutation (C3037T) in ORF1, one non-synonymous mutation in ORF1a/b (C14408T) which changed the amino acid (P4715L), and one non-synonymous mutation in the S gene (A23403G) changing the amino acid

(D614G). These findings showed the importance and role of these four mutations. We propose that they have become part of each circulating variant of SARS-CoV-2. Although the mutations (C241T) and (C3037T) do not affect protein structure or function, they may support the virus to cloak itself within the host or affect transmission. The (C14408T) might influence the replication rate; it altered the amino acid in RNA-dependent RNA polymerase (Ahmed-Abakur et al. 2022). The (D614G) mutation occurred in the S2 domain, which is important for the fusion of the spike protein with the host cell membrane, thus may increase the infectivity and spread of the virus (Callaway 2021; Quarleri et al. 2022). Corresponding to this finding, Korber et al. (2020) reported that SARS-CoV-2 carrying the mutation D614G has become the dominant form. However, many reports showed the co-existence of C241T, C3037T, C14408T, and A23403G (Ahmed-Abakur et al. 2022; Kandeel et al. 2022; Kumar et al. 2022).

Our study showed 14 frameshift deletions (nine in the unique common mutations group, three in the unique non-common mutations group, and two in the shared mutations group) and two frameshift insertions. A higher number of deletions and insertions were reported by Tan et al. (2022), who characterized the first two cases of the Omicron variant in China. They showed 39 deletions and nine insertions. The CDC (2021) stated that the Omicron variant (B.1.1.529) has one tiny insertion and three small deletions in the spike glycoprotein Δ69-70 Δ143-145, Δ211 (28). The previously mentioned frameshift affected five amino acids that were Δ69H, Δ70V, Δ143V, Δ144Y, and Δ145Y. In addition to these deletions, our study pointed out nine frameshift deletions more: three in the S gene (A67V, G142D, and Δ211N), four in the N gene (Δ31E, Δ32R, Δ33S, and one synonymous), and two in ORF1a/b (Δ3674-3676 ΔLSG and Δ2083S L2084I). Thakur and Ratho (2022) reported that the deletions at positions H69- and V70- result in failure of the S-gene target. Recently, some studies proposed that the SARS-CoV-2 spike protein insertion sequences may be derived from either host or other coronaviruses. These findings might have subsequently affected the viral entry and failure of antibodies to deactivate this variant (Kannan et al. 2022).

The present study exhibited heavy mutations in the S gene compared to the previous studies; several authors figured out 30–32 mutations in the S gene of Omicron variants, one minor insertion, and three deletions (Karim and Karim 2021; Zhang et al. 2021; Gao et al. 2022; Gowrisankar et al. 2022; Kumar et al 2022;). However, our study showed that 34.2% (13/38) of the mutations in the S gene occurred in the receptor-binding domain (RBD). This site (RBD) is important for the entry of SARS-CoV-2, represents the binding site to the host receptor (ACE2), and is the main target of antibodies and therapeutics agents (Hu et al. 2022). Therefore, mutations at this site mainly affected the transmission, efficiency of the available vaccine, and treatment. In alignment with our findings, Zhang et al. (2021) mentioned that Q498R, Q493K, G496S, S477N, G446S, N440K, S375F, S373P, S371, and G339D were the new mutations in the RBD of Omicron variants. They concluded that the mutation on the receptor-binding motif leads to conformational changes that may potentiate the ability of immune evasion. Also, Lupala et al. 2022 found that most of the mutations on RBD were located at the RBD-ACE2 interface. Subsequently, these mutations alter the electrostatic charges at the interface which affects the binding of neutralizing antibodies and medications targeting the interface (Zhang et al. 2021; Mohapatra et al. 2022; Saxena et al. 2022). The modification at the RBD-ACE2 interface increases the binding through increasing buried solvent accessible surface area and enhancing the hydrogen bonding interaction (Lupala et al. 2022). Similarly, Andreata-Santos et al. (2022) stated that the mutations G142D and P681H corresponded to vital regions targeted by neutralizing antibodies. Kannan et al. (2021) reported that N501Y, Q493R, E484A, and T478K were the vital mutations in the RBM. The mutation T478K was also found in Delta variants, and it was linked to infections of vaccinated people (Zhang et al. 2021). Likewise, the mutation in 484 was observed in Gamma and Beta variants and associated with the reinfection with the Gamma variant (Kannan et al. 2021), where the glutamic acid is replaced by lysine (E484K). Interestingly, in the Omicron variant, it is replaced by alanine (E484A). The mutation E484A might modify the interaction between human angiotensin-converting hACE2 and RBD. The mutation N501Y was detected earlier in the Gamma, Beta, and Alpha variants and was recognized as having a strong affinity to hACE2 (CDC 2021).

However, Karim and Karim (2021) reported that most Omicron mutations' effects are unknown, leading to uncertainty about how these mutation combinations could affect the response to natural and acquired immunity. Poudel et al. (2022) mentioned that only twelve mutations were studied in the past, and it is early to realize the new mutations and how they affect the virus behavior.

The mutations in the ORF1a/b gene in the present study were almost matched with the results by Thakur and Ratho (2022), who reported that the mutations in ORF1a/b compromise the cell's capability to destroy viral components and therefore assist in the evasion of innate immunity. The mutations in the E gene in our study were in alignment with Saxena et al. (2022) and Kannan et al. (2021). Opposite to our results for the M gene, numerous reports showed two non-synony-

mous mutations (D3G and Q19E) and one synonymous mutation (A63T) (Kannan et al. 2021; Saxena et al. 2022; Thakur and Ratho 2022). The changings in the N gene in our study matched with Kannan et al. (2021), Saxena et al. (2022), and Thakur and Ratho (2022), concerning the non-synonymous mutations (P13L, N: R203K, and N: G204R). Moreover, Saxena et al. (2022) showed one deletion (Δ31-33). In addition to the previous mutations, we pointed out four frameshift deletions (Δ28363-28364 ΔGA, Δ31E, Δ32R, Δ33S), and one synonymous G28882A.

Our study showed that 11 mutations were shared between Omicron and other VOCs; N501Y was the most common mutation; it appeared in Omicron, Alpha, Beta, Gamma, and Mu. T3255I and T95I were shared with Delta, Mu, and Omicron. The deletions Δ69H and Δ70V were observed in Alpha and Omicron variants. T478K appeared in Omicron and Delta. R203K, G204R, and the synonymous mutation G28882A were found in Alpha, Gamma, and Omicron variants. However, numerous other mutations have been reported by other authors, such as Lys38Arg, SΔ1265, Leu1266Ile, Ala1892Thr, Thr492Ile, Phe132His, Δ105-107, Ile189Val, Pro323Leu NSP14-Ile42Val (Saxena et al. 2022). P3395H, S3675-, G3676- (Thakur and Ratho 2022). T492I, P314L, P323L (Kannan et al. 2021). L141F, R346K, V367F 5 L455, P499, A475 and F486 (Yi et al.2020).

The phylogenetic tree in our study showed two distinct clads of Omicron; one at the top and one at the bottom. Such a pattern is as arduous to explain as the Omicron origin and its higher number of mutations within a limited time frame compared to the original SARS-CoV-2 and its other variants. Nonetheless, the three sub-lineages of Omicron have been reported to be sufficiently distinct (Mahase 2022). It might be presumed that the Omicron has originated from an early lineage of wild-type SARS-CoV-2 and subsequently, its sub-lineages evolved independently in an unmonitored environment which was not traced in the reservoir population somewhere in the world until it became dominant with the steady weakening of other VOCs due to herd, vaccine-induced or hybrid immunity (Mallapaty 2022). Moreover, a study by Wang and Cheng (2022) analyzed the sequence of Omicron variants in South Africa and reported two subclades based on the sequence of spike genes.

Indeed, the impact of this variant had been reported to be high as incidence of Omicron infections increased exponentially in various affected regions such as South Africa, United Kingdom, and USA, which in a short-span overtook the delta variant, thus implying that the variant was highly transmissible (Sharma et al. 2022). Interestingly, the variant emerged when the vaccine breakthrough was already achieved (Rauf et al. 2022). As mentioned, spike proteins which are the target of vaccine immunity were found to be heavily mutated in the variant. Various comparative studies emerged suggesting new approaches to target viral-host molecular interactions and evolve preventive strategies (Isidoro et al 2022; Vardhan and Sahoo 2022a; 2022b).

## Conclusions

The present study confirmed that the majority of mutations developed by Omicron variants occurred in the vaccine target gene (S gene) and most of the mutations in the receptor-binding domain occurred in the receptor-binding motif. Thus, we propose that the vaccine breakthrough has the potential to affect the genetic evolution of SARS-CoV-2.

## Future perspectives

The inevitable stress caused by the COVID-19 disease globally, with the loss of human lives, post-COVID-19 mental and physical health issues, and disturbing social cohesion and economic failure has been an unprecedented incidence in recent times. Henceforth in a short time, enormous experimental research and meta-analyses have brought forward a bulk of studies that facilitated the determination of viral genomic landscape, sources and mode of viral transmission, pathogenesis, preventive strategies, and acquired immunity through vaccines. Our study is a significant piece of work that has the potential to be used as a reference in the future for the evolutionary genetics of SARS-CoV-2 and relate to any further risk of emerging variants and abeyant COVID-19 waves.

**ORCID**
Elmutuz H. Elssaig https://orcid.org/0000-0003-3136-1899
Tarig M.S. Alnour https://orcid.org/0000-0001-5880-793X
Eltayib H. Ahmed-Abakur https://orcid.org/0000-0001-9496-7519

**Acknowledgments**
The authors acknowledge the resources at the Department of MLT – Faculty of Applied Medical Science, University of Tabuk.

**Author contributions**
The conception and design of the study was done by all authors, the second and third authors retrieved the data from NCBI. The first, second, and third authors analyzed the data while the fourth author arranged the results. The third and fourth authors wrote the manuscript whereas the rest of the authors revised it.

**Conflict of interest**
The authors do not report any financial or personal connections with other persons or organizations, which might negatively affect the contents of this publication and/or claim authorship rights to this publication.

## Literature


**Adiga R, Nayak V.** Emergence of novel SARS-CoV-2 variants in India: second wave. J Infect Dev Ctries. 2021 Nov;15(11):1578–1583. https://doi.org/10.3855/jidc.15484

**Ahmed-Abakur EH, Alnour TMS.** Genetic variations among SARS-CoV-2 strains isolated in China. Gene Rep. 2020 Dec;21:100925. https://doi.org/10.1016/j.genrep.2020.100925

**Ahmed-Abakur EH, Ullah MF, Elssaig EH, Alnour TMS.** *In-silico* genomic landscape characterization and evolution of SARS-CoV-2 variants isolated in India shows significant drift with high frequency of mutations. Saudi J Biol Sci. 2022 May;29(5):3494–3501. https://doi.org/10.1016/j.sjbs.2022.02.030

**Andreata-Santos R, Janini LMR, Durães-Carvalho R.** From Alpha to Omicron SARS-CoV-2 variants: what their evolutionary signatures can tell us? J Med Virol. 2022 May;94(5):1773–1776. https://doi.org/10.1002/jmv.27555

**Callaway E.** Beyond Omicron: what's next for COVID's viral evolution. Nature. 2021 Dec;600(7888):204–207. https://doi.org/10.1038/d41586-021-03619-8

**Cao C, Cai Z, Xiao X, Rao J, Chen J, Hu N, Yang M, Xing X, Wang Y, Li M, et al.** The architecture of the SARS-CoV-2 RNA genome inside virion. Nat Commun. 2021 Jun;12(1):3917. https://doi.org/10.1038/s41467-021-22785-x

**CDC.** Science brief: Omicron (B.1.1.529) variant [Internet]. Atlanta (USA): Centers for Disease Control and Prevention; 2021 [cited 2022 Mar 18]. Available from https://www.cdc gov/coronavirus/2019-ncov/science/science-briefs/scientific-brief-Omicron-variant.html

**Choi JY, Smith DM.** SARS-CoV-2 variants of concern. Yonsei Med J. 2021 Nov;62(11):961–968. https://doi.org/10.3349/ymj.2021.62.11.961

**Felsenstein J.** Confidence limits on phylogenies: an approach using the bootstrap. Evolution. 1985 Jul;39(4):783–791. https://doi.org/10.1111/j.1558-5646.1985.tb00420.x

**Gao SJ, Guo H, Luo G.** Omicron variant (B.1.1.529) of SARS-CoV-2, a global urgent public health alert! J Med Virol. 2022 Apr; 94(4): 1255–1256. https://doi.org/10.1002/jmv.27491

**Gowrisankar A, Priyanka TMC, Banerjee S.** Omicron: a mysterious variant of concern. Eur Phys J Plus. 2022;137(1):100. https://doi.org/10.1140/epjp/s13360-021-02321-y

**Gu H, Krishnan P, Ng DYM, Chang LDJ, Liu GYZ, Cheng SSM, Hui MMY, Fan MCY, Wan JHL, Lau LHK, et al.** Probable transmission of SARS-CoV-2 Omicron variant in quarantine hotel, Hong Kong, China, November 2021. Emerg Infect Dis. 2022 Feb; 28(2): 460–462. https://doi.org/10.3201/eid2802.212422

**Hu J, Peng P, Cao X, Wu K, Chen J, Wang K, Tang N, Huang AL.** Increased immune escape of the new SARS-CoV-2 variant of concern Omicron. Cell Mol Immunol. 2022 Feb;19(2):293–295. https://doi.org/10.1038/s41423-021-00836-z

**Isidoro C, Chiung-Fang Chang A, Sheen LY.** Natural products as a source of novel drugs for treating SARS-CoV2 infection. J Tradit Complement Med. 2022 Jan;12(1):1–5. https://doi.org/10.1016/j.jtcme.2022.02.001

**Jia H, Wang H, Cao L, Lai Z, Cheng Z, Chen Q, Liu T, Liu X, Wen Y, Xu C, et al.** Genetic analysis of a SARS-CoV-2 Omicron variant from a Chinese traveller returning from overseas. Emerg Microbes Infect. 2022 Dec;11(1):306–309. https://doi.org/10.1080/22221751.2022.2025747

**Kandeel M, Mohamed MEM, Abd El-Lateef HM, Venugopala KN, El-Beltagi HS.** Omicron variant genome evolution and phylogenetics. J Med Virol. 2022 Apr;94(4):1627–1632. https://doi.org/10.1002/jmv.27515

**Kannan S, Shaik Syed Ali P, Sheeza A.** Omicron (B.1.1.529) – variant of concern – molecular profile and epidemiology: a mini review. Eur Rev Med Pharmacol Sci. 2021 Dec;25(24):8019–8022. https://doi.org/10.26355/eurrev_202112_27653

**Kannan SR, Spratt AN, Sharma K, Chand HS, Byrareddy SN, Singh K.** Omicron SARS-CoV-2 variant: unique features and their impact on pre-existing antibodies. J Autoimmun. 2022 Jan;126: 102779. https://doi.org/10.1016/j.jaut.2021.102779

**Karim SSA, Karim QA**. Omicron SARS-CoV-2 variant: a new chapter in the COVID-19 pandemic. Lancet. 2021 Dec;398(10317): 2126–2128. https://doi.org/10.1016/S0140-6736(21)02758-6

**Khailany RA, Safdar M, Ozaslan M.** Genomic characterization of a novel SARS-CoV-2. Gene Rep. 2020 Jun;19:100682. https://doi.org/10.1016/j.genrep.2020.100682

**Korber B, Fischer WM, Gnanakaran S, Yoon H, Theiler J, Abfalterer W, Hengartner N, Giorgi EE, Bhattacharya T, Foley B, et al; Sheffield COVID-19 Genomics Group.** Tracking changes in SARS-CoV-2 spike: Evidence that D614G increases infectivity of the COVID-19 virus. Cell. 2020 Aug;182(4):812–827.e19. https://doi.org/10.1016/j.cell.2020.06.043

**Kumar S, Thambiraja TS, Karuppanan K, Subramaniam G.** Omicron and Delta variant of SARS-CoV-2: a comparative computational study of spike protein. J Med Virol. 2022 Apr;94(4):1641–1649. https://doi.org/10.1002/jmv.27526

**Lu R, Zhao X, Li J, Niu P, Yang B, Wu H, Wang W, Song H, Huang B, Zhu N, et al.** Genomic characterisation and epidemiology of 2019 novel coronavirus: implications for virus origins and receptor binding. Lancet. 2020 Feb;395(10224):565–574. https://doi.org/10.1016/S0140-6736(20)30251-8

**Lupala CS, Ye Y, Chen H, Su XD, Liu H.** Mutations on RBD of SARS-CoV-2 Omicron variant result in stronger binding to human ACE2 receptor. Biochem Biophys Res Commun. 2022 Jan;590:34–41. https://doi.org/10.1016/j.bbrc.2021.12.079

**Mahase E.** Covid-19: What do we know about omicron sublineages? BMJ. 2022 Feb;376:o358. https://doi.org/10.1136/bmj.o358

**Mallapaty S**. Where did Omicron come from? Three key theories. Nature. 2022 Feb;602(7895):26–28. https://doi.org/10.1038/d41586-022-00215-2

**Mlcochova P, Kemp SA, Dhar MS, Papa G, Meng B, Ferreira IATM, Datir R, Collier DA, Albecka A, Singh S, et al.; Indian SARS-CoV-2 Genomics Consortium (INSACOG); Genotype to Phenotype Japan (G2P-Japan) Consortium; CITIID-NIHR BioResource COVID-19 Collaboration.** SARS-CoV-2 B.1.617.2 Delta variant replication and immune evasion. Nature. 2021 Nov;599(7883): 114–119. https://doi.org/10.1038/s41586-021-03944-y

**Mohapatra RK, Sarangi AK, Kandi V, Azam M, Tiwari R, Dhama K.** Omicron (B.1.1.529 variant of SARS-CoV-2); an emerging threat: current global scenario. J Med Virol. 2022 May;94(5):1780–1783. https://doi.org/10.1002/jmv.27561

**Poudel S, Ishak A, Perez-Fernandez J, Garcia E, León-Figueroa DA, Romaní L, Bonilla-Aldana DK, Rodriguez-Morales AJ.** Highly mutated SARS-CoV-2 Omicron variant sparks significant concern among global experts – what is known so far? Travel Med Infect Dis. 2022 Jan-Feb;45:102234. https://doi.org/10.1016/j.tmaid.2021.102234

**Quarleri J, Galvan V, Delpino MV.** Omicron variant of the SARS-CoV-2: a quest to define the consequences of its high mutational load. Geroscience. 2022 Feb;44(1):53–56. https://doi.org/10.1007/s11357-021-00500-4

**Rauf A, Abu-Izneid T, Khalil AA, Hafeez N, Olatunde A, Rahman M, Semwal P, Al-Awthan YS, Bahattab OS, Khan IN, et al.** Nanoparticles in clinical trials of COVID-19: an update. Int J Surg. 2022 Aug;104:106818. https://doi.org/10.1016/j.ijsu.2022.106818

**Rudrapal M, Khairnar SJ, Borse LB, Jadhav AG.** Coronavirus Disease-2019 (COVID-19): an updated review. Drug Res (Stuttg). 2020 Sep;70(9):389–400. https://doi.org/10.1055/a-1217-2397

**Saitou N, Nei M.** The neighbor-joining method: a new method for reconstructing phylogenetic trees. Mol Biol Evol. 1987 Jul;4(4): 406–425. https://doi.org/10.1093/oxfordjournals.molbev.a040454

**Saxena SK, Kumar S, Ansari S, Paweska JT, Maurya VK, Tripathi AK, Abdel-Moneim AS.** Characterization of the novel SARS-CoV-2 Omicron (B.1.1.529) variant of concern and its global perspective. J Med Virol. 2022 Apr;94(4):1738–1744. https://doi.org/10.1002/jmv.27524

**Sharma V, Rai H, Gautam DNS, Prajapati PK, Sharma R.** Emerging evidence on Omicron (B.1.1.529) SARS-CoV-2 variant. J Med Virol. 2022 May;94(5):1876–1885. https://doi.org/10.1002/jmv.27626

**Shishir TA, Naser IB, Faruque SM.** *In silico* comparative genomics of SARS-CoV-2 to determine the source and diversity of the pathogen in Bangladesh. PLoS One. 2021 Jan;16(1):e0245584. https://doi.org/10.1371/journal.pone.0245584

**Sofi MS, Hamid A, Bhat SU.** SARS-CoV-2: A critical review of its history, pathogenesis, transmission, diagnosis and treatment. Biosaf Health. 2020 Dec;2(4):217–225. https://doi.org/10.1016/j.bsheal.2020.11.002

**Tamura K, Nei M, Kumar S.** Prospects for inferring very large phylogenies by using the neighbor-joining method. Proc Natl Acad Sci USA. 2004 Jul;101(30):11030–11035. https://doi.org/10.1073/pnas.0404206101

**Tan Z, Chen Z, Yu A, Li X, Feng Y, Zhao X, Xu W, Su X.** The first two imported cases of SARS-CoV-2 Omicron variant – Tianjin Municipality, China, December 13, 2021. China CDC Wkly. 2022 Jan; 4(4):76–77. https://doi.org/10.46234/ccdcw2021.266

**Thakur V, Ratho RK.** OMICRON (B.1.1.529): A new SARS-CoV-2 variant of concern mounting worldwide fear. J Med Virol. 2022 May; 94(5):1821–1824. https://doi.org/10.1002/jmv.27541

**Vardhan S, Sahoo SK.** Computational studies on the interaction of SARS-CoV-2 Omicron SGp RBD with human receptor ACE2, limonin and glycyrrhizic acid. Comput Biol Med. 2022a May; 144: 105367. https://doi.org/10.1016/j.compbiomed.2022.105367

**Vardhan S, Sahoo SK.** Exploring the therapeutic nature of limonoids and triterpenoids against SARS-CoV-2 by targeting nsp13, nsp14, and nsp15 through molecular docking and dynamics simulations. J Tradit Complement Med. 2022b Jan;12(1):44–54. https://doi.org/10.1016/j.jtcme.2021.12.002

**Wang L, Cheng G.** Sequence analysis of the emerging SARS-CoV-2 variant Omicron in South Africa. J Med Virol. 2022 Apr; 94(4): 1728–1733. https://doi.org/10.1002/jmv.27516

**Wang R, Chen J, Wei GW.** Mechanisms of SARS-CoV-2 evolution revealing vaccine-resistant mutations in Europe and America. J Phys Chem Lett. 2021 Dec;12(49):11850–11857. https://doi.org/10.1021/acs.jpclett.1c03380

**Yi C, Sun X, Ye J, Ding L, Liu M, Yang Z, Lu X, Zhang Y, Ma L, Gu W, et al.** Key residues of the receptor binding motif in the spike protein of SARS-CoV-2 that interact with ACE2 and neutralizing antibodies. Cell Mol Immunol. 2020 Jun;17(6):621–630. https://doi.org/10.1038/s41423-020-0458-z

**Zhang X, Wu S, Wu B, Yang Q, Chen A, Li Y, Zhang Y, Pan T, Zhang H, He X.** SARS-CoV-2 Omicron strain exhibits potent capabilities for immune evasion and viral entrance. Signal Transduct Target Ther. 2021 Dec;6(1):430. https://doi.org/10.1038/s41392-021-00852-5

Supplementary materials are available on the journal's website.

ORIGINAL PAPER
Polish Journal of Microbiology
2022, Vol. 71, No 4, 589–599
https://doi.org/10.33073/pjm-2022-048

# Molecular Characterization of *Aspergillus flavus* Strains Isolated from Animal Feeds

HADJER SABER[1], YAHIA CHEBLOUNE[2]* and ABDALLAH MOUSSAOUI[1]

[1] Laboratory of Plant Resources Valorization and Food Safety in Semi-Arid Areas of Southwestern Algeria, Department of Biology, University of Bechar, Bechar, Algeria
[2] USC 1450 INRAE/UGA Lentiviral Pathogenesis and Vaccination Laboratory, Department of Biology, University of Grenoble Alpes, Saint-Martin-d'Hères, France

Submitted 9 June 2022, accepted 21 September 2022, published online 19 December 2022

Abstract

Aflatoxin (AF)-producing fungi such as *Aspergillus flavus* commonly contaminate animal feeds, causing high economic losses. *A. flavus* is the most prevalent and produces AFB1, a potent mutagen, and carcinogen threatening human and animal health. *Aspergillaceae* is a large group of closely related fungi sharing number of morphological and genetic similarities that complicate the diagnosis of highly pathogenic strains. We used here morphological and molecular assays to characterize fungal isolates from animal feeds in Southwestern Algeria. These tools helped to identify 20 out of 30 *Aspergillus* strains, and 15 of them belonged to the *Aspergillus* section *Flavi*. Further analyses detected four out of 15 as belonging to *Aspergillus flavus-parasiticus* group. PCR targeting the AF genes' *aflR-aflS(J)* intergenic region amplified a single 674 bp amplicon in all four isolates. The amplicons were digested with a *Bgl*II endonuclease, and three specific fragments were observed for *A. flavus* but *A. parasitucus* lacked two typical fragments. Sequencing data of four amplicons confirmed the presence of the two *Bgl*II restriction sites yielding the three fragments, confirming that all four strains were *A. flavus*. In addition, this analysis illustrated the genetic variability within the *A. flavus* strains.

K e y w o r d s: *Aspergillus flavus*, *aflR-aflS(J)*, IGS, PCR-RFLP, diagnosis tools

## Introduction

*Aspergillus* producing AF from contaminated animal feed, a secondary metabolite, is a global problem with high economic impacts on animal and human health. Contaminations occur before harvest, and during the storage and distribution of seeds. In sub-Saharan Africa, the global agricultural loss associated with AF contamination was estimated at 40% of the global production, corresponding to $450 million (Gbashi et al. 2018). Aflatoxins refer to a family of over 18 related compounds, principally B1, B2, G1, and G2 (Ibrahim 2019), produced primarily by the closely related fungi, *Aspergillus flavus* and *Aspergillus parasiticus* (Rao et al. 2020). Aflatoxins are polyketide-derived secondary metabolites. *AflR* encodes a protein containing a zinc-finger binding domain that interacts with target sequence DNA (Lee et al. 2006). *AflS* encodes a costimulatory regulatory protein that enhances the transcription activity (Liao et al. 2020).

*A. flavus* and *A. parasiticus* are dominant species found in crops (Kim et al. 2017) that share morphological similarities and closely cluster in phylogeny (Godet and Munaut 2010). Thus, the distinction between these species is difficult because microscopic identification requires experts in filamentous fungi taxonomy (El Khoury et al. 2011). In addition, the morphological methods of identification are inaccurate because of close inter-species similarities. In contrast, molecular techniques save labor time and their sensitivity and specificity, provide distinct species closeness and distance estimations without sophisticated culture and further confirmation steps (Ahmad et al. 2010).

Recently, several molecular approaches have been used to differentiate among many *Aspergillus* species, including random amplified polymorphic DNA (RAPD)

* Corresponding author: Y. Cheboune, Lentiviral Pathogenesis and Vaccination Laboratory, PAVAL Lab., Department of Biology, University of Grenoble Alpes, Saint-Martin-d'Hères, France; **e-mail: yahia.cheboune@inrae.fr**

(Yin et al. 2009; Daghriri et al. 2018), amplified fragment length polymorphism (AFLP), with specific diagnostic PCR primers, polymorphic microsatellite marker analysis, microsatellite length polymorphism (Healy et al. 2004), and DNA sequencing (Nicholson et al. 1998).

The commonly used molecular approaches often target the analysis of the coding sequences for rRNA that contain both conserved and variable regions (Paterson 2006). Fungal rDNA operons have been shown to contain variability regions within genera (Levy et al. 2001). However, PCR-RFLP has been used to identify variations in DNA sequences, and it was shown to recognize closely related organisms using inter-phylogenetic relations (Zarrin and Erfaninejad 2016). This technique has been proven to be fast, sensitive, and reliable in determining the genetic variability among *A.* section *Flavi* species (Bagyalakshmi et al. 2007; Mohankumar et al. 2010; Lavkor 2020). Currently, there is a limited understanding of molecular variability among populations of *A. flavus* isolated from feed sources. Characterization of *A. flavus* requires an expert polyphasic approach to fully confirm its taxonomic status and develop an effective control strategy (Singh et al. 2018; Frisvad et al. 2019; Martinez-Miranda et al. 2019). Using molecular biology methods combined with morphology has revealed the diversity and genetic variability within the *A. flavus* species (Okoth et al. 2018).

In the present study, we used the PCR-RFLP targeting the *aflR-aflS(J)* intergenic spacer (IGS) of the AF biosynthesis cluster to complement the findings of the morphological characterization. The main objectives were to establish and assess the genetic relationships and variability patterns of *A. flavus* strains isolated from feeds in the southwestern Saharan region of Algeria using PCR and sequence analysis of the IGS region, followed by phylogenetic analysis.

## Experimental

### Materials and Methods

**Fungal isolates and morphological identification.** Thirty fungal isolates were obtained from various animal feeds. Out of these, twenty were identified as *Aspergillus*, and 15 out of 20 were identified as *A.* section *Flavi*. Samples were collected in the livestock feed manufacturing unit's storage facilities in Southwestern Algeria. As described earlier, the strains were isolated using Potato Dextrose Agar (PDA) (Pitt and Hocking 2009). Strains identification included macroscopic (colony color and morphology) and microscopic (head seriation, conidia morphology, and size) characteristics. The identification was performed according to the criteria defined for the taxonomic keys and guidelines for the Aspergillus genus (Pitt and Hocking 2009). All isolates were cultured on *Aspergillus flavus*/*parasiticus* agar (AFPA) (bacteriological peptone 10 g; yeast extract 20 g; ferric ammonium citrate 0.5 g; bacteriological agar 15 g; dichloran 2 mg (0.2% in ethanol, 1.0 ml); distilled water 1 l). One hundred microliters of spore suspension were inoculated in the center of 60 mm petri dishes and then incubated at 25°C for 48 h in the absence of light (Abriba et al. 2013; Hossain et al. 2018) as a particular growth condition for rapid identification of *Aspergillus* belonging to *A.* section *Flavi* (Pitt et al. 1983). At 48 h of culture on AFPA, the colonies of *A. flavus* and *A. parasiticus* strains appear with an orange color in the bottom of the culture, whereas the other species of *Aspergillus* section *Flavi* do not (Bothast and Fennell 1974; Hamsa and Ayres 1977; Pitt et al. 1983).

**Molecular identification of fungal strains.** Since the isolation and characterization by culture fail to differentiate between *A. parasiticus* and *A. flavus*, we used the molecular tools to perform this analysis.

**Culture preparation.** Fungal mycelia were produced by inoculating the fungal conidia with a glass Pasteur pipette in 250 ml Erlenmeyer flasks containing 150 ml Potato Dextrose Broth (PDB) and incubated for 48 hours at 25°C under orbital agitation at 150 rpm. Mycelia were harvested following filtration on 0.45 µm pore size filters and then snapped frozen into liquid nitrogen. Frozen mycelia were grounded into a fine powder using a mortar and pestle and then stored at –80°C until use.

**DNA extraction.** One hundred mg of powdered, frozen mycelia were transferred into a 1.5 ml microcentrifuge tube, thawed, and resuspended into 800 µl of DNA extraction buffer (100 mM TRIS-HCl (pH 7.4), 20 mM EDTA (pH 8.0), 1.4 mM NaCl, 2% sodium dodecyl sulfate) as described by (Lee et al. 2006). Subsequently, 10 µl of Proteinase K (20 mg/ml) was added, and the solution was incubated for 20 min at 60°C. The cell lysate was supplemented with 800 µl of phenol-chloroform-isoamyl alcohol (25/24/1, v/v/v) and then mixed by inversion until an emulsion was obtained. Following centrifugation for 5 min at 13,000 rpm at 20°C, the upper (aqueous) phase was transferred into a new microfuge tube. Four hundred microliters of chloroform/isoamyl alcohol (24:1) were added and mixed by inversion, and then the mixture was centrifuged for 10 min at 13,000 rpm at 4°C. The upper aqueous phase was transferred into a new microfuge tube and supplemented with 0.7 ml of cold 2-propanol for instant DNA precipitation. The precipitate was centrifuged for 10 min at 4°C, 13,000 rpm, and then the supernatant was discarded. The pellet was rinsed with 500 µl of 70% ethanol to remove residual salts. Following the last centrifugation at 13,000 rpm for 5 min at 4°C, ethanol was discarded, and the DNA pellet air dried. DNA pellet was then resuspended into 50 µl of sterile

ultrapure water. To remove the contaminant RNA, 5 µl of RNase (20 mg/ml) was added, incubated for 15 min at 37°C, and then heat-inactivated for 20 min at 70°C. The quality of DNA was checked following DNA separation by electrophoresis in a 0.8% agarose gel in TAE (40 mM Tris, 20 mM sodium acetate, and 1 mM EDTA, pH = 8.6) buffer and a high molecular weight marker. DNA concentration was measured at the optical density (OD) of 260 nm and the purity at 240 and 280 nm wavelengths using a UV spectrophotometer.

**Primers.** The non-coding intergenic sequences (IGS) that separate the *aflR* and *aflS(J)* genes of fungal ribosomal DNA operon were used as a target for PCR amplification to detect *A. flavus* and *A. parasiticus*. Sequences of the primers used were as follows: IGS-F, 5'-AAGGAATTCAGGAATTCTCAATTG-3' and IGS-R, 5'-GTCCACCGGCAAATCGCCG-TGCG-3' (Ehrlich et al. 2003; 2007; El Khoury et al. 2011).

**PCR amplification.** PCR was performed using 200 ng of a fungal DNA template (5 µl), 1 µl of each of the IGS-R and IGS-F (20 pM) primers (Eurofins Genomics, France), 25 µl of Econo Taq Plus Green 2× Master Mix (Euromedex, France), and 18 µl of sterile $H_2O$. The Master Mix contained: 0.1 U/µl of Econo Taq DNA polymerase – reaction buffer (pH 9.0), 400 µM each (dATP, dGTP, dCTP, and dTTP); 3 mM $MgCl_2$ and blue and yellow tracking dyes. Microtubes containing the PCR mix were transferred into a thermocycler and submitted to 34 cycles of amplification following an initial denaturation of DNA at 94°C for 5 min. Each cycle consisted of a denaturation step at 95°C for 1 min, an annealing step at 46°C for 1 min, and an extension step at 56°C for 1.5 min, with a final extension at 60°C for 10 min added to the last cycle. After amplification, the PCR products were stored at 4°C until used. PCR products were analyzed by electrophoresis separation on a 1.5 % agarose gel, and PCR-specific bands visualized by UV trans-illumination. The size of the amplicons was estimated using a 1 kb DNA ladder. The PCR products were purified using the clean-up Nucleospin kit (Machery Nagel, France), using the manufacturer's instructions.

**Restriction enzyme digestion of PCR-IGS amplicons: PCR-IGS-RFLP.** PCR-RFLP using *Bgl*II restriction endonuclease to digest the IGS product was shown to distinguish between *A. parasiticus* and *A. flavus* (El Khoury et al. 2011). Here we used this technique to examine whether the strains identified as *A.* section *Flavi* could be identified as *A. parasiticus* and/or *A. flavus.* The PCR-IGS amplicons were digested with the restriction endonuclease *Bgl*II (Promega, France). The reactions were performed using a total of 0.5 µg of purified PCR product in 10 µl, 2 µl of 10× *Bgl*II incubation buffer, 1 µl of *Bgl*II (10 U/µl), and 7 µl ultrapure $H_2O$ in a total volume of 20 µl. The mixture was incubated at 37°C for 2 h, and then separated by electrophoresis in a 2% agarose gel. Restriction bands were revealed using a UV trans-illumination and a Gel-doc Image Lab system (Bio-Rad, France).

**Sequencing, sequence alignment, and phylogenetic analysis.** A total of 1 µg of purified PCR product of each amplicon was shipped to Eurofins Genomics (Germany) for sequencing using *IGS-F* primer. Sequence data were sent as electronic files to the lab for examination and use for bioinformatic analyses.

DNA BLAST analysis of obtained sequences was done online using the NCBI/NIH website to identify the closest sequences that match our new sequences. Multiple sequence alignment was performed using Clustal Omega software (The EMBL-EBI search and sequence analysis tools APIs in 2019). Sequences were submitted to GenBank on the NCBI website (http://www.ncbi.nlm.nih.gov) under the reported accession numbers (Table I). Available sequences of *aflR-aflS(J)* intergenic region of reference strains were obtained from the GenBank database. The phylogenetic trees of isolates and their close relatives based on *aflR-aflS(J)* intergenic region were derived from sequence alignment using Clustal Omega.

Table I
*Aspergillus flavus* isolates identity based on the BLAST NCBI data.

| Strain | Identity (%) |
|---|---|
| FZM1 | *Aspergillus flavus* strain A9 chromosome 3 (97.48%) |
| FAK45 | *Aspergillus flavus* strain A9 chromosome 3 (98.12%) |
| FSZ47 | *Aspergillus flavus* strain SU-16 chromosome 3 (99.37%) |
| FDY50 | *Aspergillus flavus* strain SU-16 chromosome 3 (99.67%) |

## Results and Discussion

The *flavus* group of *Aspergillus* was reported to be a significant cause of yearly economic losses reaching over 25% (Klingelhöfer et al. 2018), because of contamination of agriculture and feed components. This type of aflatoxin-producing fungi are opportunistic pathogens that contaminate corn, wheat, peanuts, and other food crops in many places of the world and causes severe diseases when ingested. Out of 30 fungal isolates, 20 were identified as *Aspergillus*, and 15 out of the 20 were characterized as *A.* section *Flavi*. Macroscopic and microscopic examinations of these 15 strains showed yellow-green colonies after growth on PDA, with spherical and rough spores/smooth to finely rough and globose conidia.

AFPA was used to identify both *A. parasiticus* and *A. flavus* (Hossain et al. 2018). Four colonies with yellow to green color with a white border surrounding the yellow to the greenish surface and an intense yellow-orange reverse color were selected as *A. flavus* and

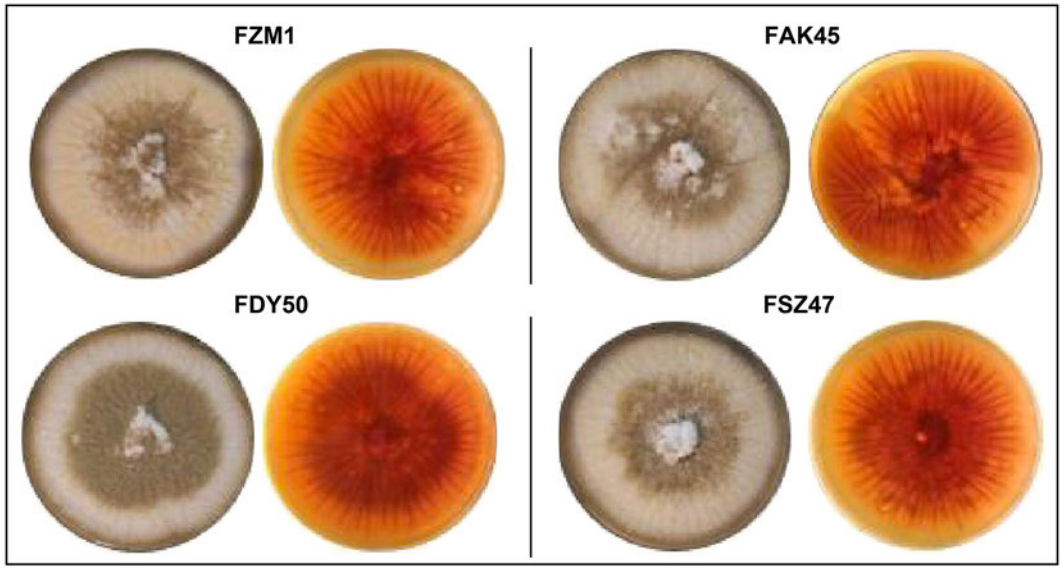


Fig. 1. Phenotypic characterization of *A. flavus* isolates grown on *A. flavus*/*parasiticus* agar (AFPA) medium. Colony color: white-green colony diameter 18 mm, colony reverse color: yellowish orange after seven days of incubation at 25°C.

*A. parasiticus* (Fig. 1). This orange color is due to the reaction of ferric citrate with aspergillic acid, forming a colored complex. The eleven remaining colonies produced creamy reverse color on AFPA, characteristic of *Aspergillus oryzae* species (Pitt et al. 1983; Rodrigues et al. 2009; Frisvad et al. 2019).

In previous studies, AFPA alone was used to identify *A. flavus* and *A. parasiticus* (Abriba et al. 2013; Fakruddin et al. 2015; Hossain et al. 2018; Krulj et al. 2020). However, based only on the phenotypic characteristics, it was impossible to distinguish between the two closely related species *A. flavus* and *A. parasiticus* because of overlapping morphological features (Rodrigues et al. 2009). Thus, molecular tools are necessary to differentiate these two species further. In the present study, we performed a molecular genetic characterization of the isolates selected to examine whether the four isolates could be *A. parasiticus* or *A. flavus.*

DNA samples from the four isolates were used as templates for PCR amplification using IGS-specific primers. These primers were highly specific for *aflR-aflS(J)* IGS fragments. DNA samples from all four fungal strains produced the expected 674 bp IGS amplicon with no additional or non-specific bands (Fig. 2). However, this 674 bp product was identical for both *A. flavus* and *A. parasiticus*. Therefore, we needed to examine the PCR product by RFLP further.

Previous studies indicated that PCR-IGS-RFLP using restriction enzymes that cleave the PCR products into sub-fragments are valuable tools for detecting and differentiating between *A. flavus* and *A. parasiticus* (El Khoury et al. 2011; Nikolic et al. 2018; Lavkor 2020). Therefore, we used the restriction endonuclease *Bgl*II to digest the four PCR products. Results shown in Fig. 3 clearly show that digestion of all the PCR products with *Bgl*II resulted in an identical profile yielding three fragments of 362, 210, and 102 bp. This typical profile demonstrated that all species were *A. flavus*. In contrast, *Bgl*II digestion should produce a profile with only two fragments of 311 bp and 362 bp with an IGS amplicon of *A. parasiticus* (El Khoury et al. 2011). Our analysis failed to detect this last profile among the four analyzed.

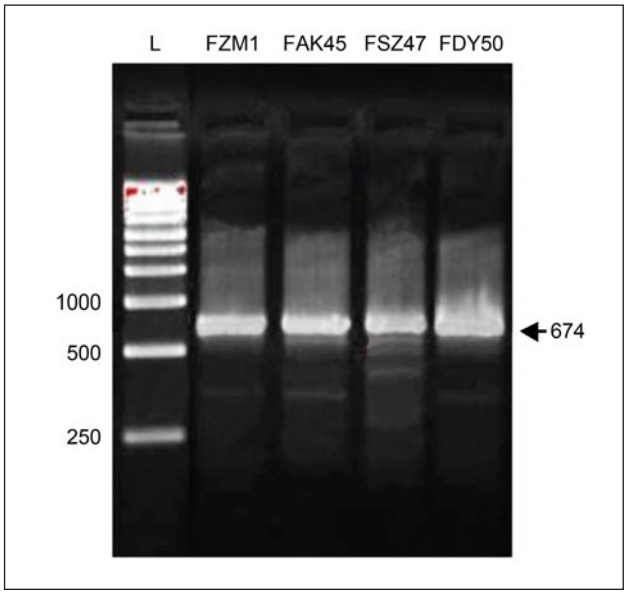


Fig. 2. PCR amplification of intergenic sequences of the four isolates. IGS-F and IGS-R primers were used for PCR amplification of the intergenic sequences in total DNA isolated from the four fungal isolates as described in Material and Methods. A total of 5 µl of each PCR product was separated in a 1.5% agarose gel by electrophoresis. Lane 1 kb ladder (L) DNA marker, *Aspergillus flavus* isolates are indicated on the top of each lane. The sizes of selected DNA fragments are indicated on the sides of the panels.

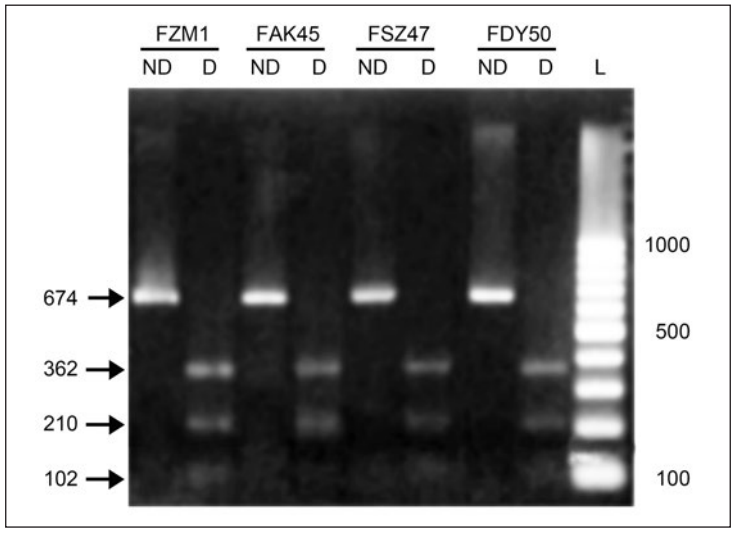


Fig. 3. PCR and RFLP analyses of fungal amplicons. A total of 5 µl of PCR products of each of the isolates (FZM1, FAK45, FSZ47 and FDY50) was digested with *Bgl*II restriction endonuclease as described in Materials and Methods. Nondigested (ND) and digested (D) products were loaded and separated by electrophoresis in a 2% agarose gel. A 100 bp DNA ladder (L) was used as molecular weight marker, the positions of 100, 500 and 1,000 bp fragments are indicated. Positions of the 362, 210 and 102 bp fragments generated by *Bgl*II digestion are indicated.

Our findings were similar to those reported by (Kana et al. 2013), which indicate that all *A. flavi* isolates recovered from all the commodities (feedstuffs and animal feed) were *A. flavus*. In contrast, other studies (Stanković et al. 2015; Nikolic et al. 2018) found the presence of *A. parasiticus* on wheat kernels and corn. This difference may result from the geographic isolation and the local atmosphere conditions (temperature, humidity), which might cause shifts in mycobiota distribution and composition of cereals observed among different regions.

Accurate identification and differentiation between this aflatoxigenic species are of great importance in determining toxicological risks due to the difference in the toxic profile of each species in the section Flavi. (Martínez-Culebras and Ramón 2007). It is well known that *A. parasiticus* produces only "B" and "G" type toxins, whereas *A. flavus* produces "B" type toxins but also cyclopiazonic acid, versicolorin, and sterigmatocystin (Wilson et al. 2002; Bailly et al. 2018). Metabolite analysis is a multistep process that requires long term culture and mycotoxin production (14 d) followed by extraction and purification for chromatographical analysis. In addition, this method requires multiple and expensive instruments to perform all these processes. In contrast, PCR-RFLP is a rapid and sensitive method requiring minimal investment and was shown to be a reliable method for taxonomic studies of *Aspergillus* species (Martínez-Culebras and Ramón 2007).

The *Aspergillus* genome is organized into eight chromosomes where the genes encoding aflatoxins are located in the 54$^{th}$ cluster, 80 kb from the telomere of chromosome 3 (Georgianna and Payne 2009). They include regulatory genes *aflR*, *aflS(J),* and several structural genes (Yu et al. 2004; Paterson 2006; Price et al. 2006). The *aflR* and *aflS(J)* genes are separated by a 737-bp intergenic region (Yu 2012). Sequence variability within this intergenic fragment has been used to establish the phylogenetic organization of *A. flavus* genotypes (Al-Wadai et al. 2013).

To confirm the PCR-RFLP data, suggesting that all our four isolates were *A. flavus*, we sequenced their amplicons using the IGS-F primer. The sequences were deposited in NCBI/Genbank under the following accession numbers (Table I). Sequence data were used for blast analysis against the Genbank DNA sequence database and to produce multiple sequence alignments (Fig. 4). The highest homology of the sequences of the isolates with those of sequences of the GenBank reference strains was used to define the isolates. All four isolates were identified as *A. flavus* with a similarity percentage ranging from 97.48% to 99.67% to *A. flavus* RefSeq from NCBI (Table II and III). In addition, sequence analysis confirmed the presence of the two restriction sites for *Bgl*II in the amplicon that yielded the three fragments (362, 210, and 102 bp). Thus, the *aflR-aflS(J)* IGS-RFLP assay with *Bgl*II is sufficient to detect *A. flavus* without sequencing. Therefore, this assay can be used for epidemiological studies to detect the prevalence of *A. flavus*.

Furthermore, this sequence analysis showed variation among the *A. flavus* isolates. This variation included single and multiple substitutions, insertions, inversions, and deletions. Sequence comparison of FSZ47 and FDY50 isolates with that of the reference strain SU 16 showed the highest sequence similarity (99,37%,

```
          1         10         20         30         40         50         60
SU-16     CGCTGAGAAT ACGGGTGATC TGAAGAGGTT TTAGATCTGA CCAGTGTAGT CCTTCCTCTG
FZM1      --C------- ---------- ---------- ---------- ---------T ----------
FDY50     --T------- ---------- ---------- ---------- ---------T ----------
FSZ47     --C------- ---------- ---------- ---------- ---------T ----------
FAK45     --C------- ---------- ---------- ---------- ---------C ----------
A9        --C------- ---------- ---------- ---------- ---------T ----------
K54A      --C------- ---------- ---------- ---------- ---------T ----------
Tox4      --C------- ---------- ---------- ---------- ---------T ----------

                   70         80         90        100        110        120
SU-16     CGTCAAGGAG TGCTGATCTG CAAGCCGGGT ACCATCTGCC GGCTCGTACT TTTTATCTTT
FZM1      ------C--- -------A-- ---------- --C------- --T------- ----------
FDY50     ------G--- -------C-- ---------- --C------- --C------- ----------
FSZ47     ------G--- -------C-- ---------- --C------- --C------- ----------
FAK45     ------C--- -------A-- ---------- --T------- --T------- ----------
A9        ------C--- -------A-- ---------- --T------- --C------- ----------
K54A      ------C--- -------A-- ---------- --T------- --C------- ----------
Tox4      ------C--- -------A-- ---------- --T------- --C------- ----------

                  130        140        150        160        170        180
SU-16     CGTCAGCATC GTTAGCCAGG CAGGCATATC TATGTCCCAT .TCTTAGAAT AGCTTCGCAG
FZM1      ---------- ---------- ---------- ---------- G--------- ----------
FDY50     ---------- ---------- ---------- ---------- .--------- ----------
FSZ47     ---------- ---------- ---------- ---------- .--------- ----------
FAK45     ---------- ---------- ---------- ---------- .--------- ----------
A9        ---------- ---------- ---------- ---------- .--------- ----------
K54A      ---------- ---------- ---------- ---------- .--------- ----------
Tox4      ---------- ---------- ---------- ---------- .--------- ----------

                  190        200        110        120        230        240
SU-16     GGTGGTATCT CAACACTGCA ACGGGACGGA TCCAGGGCTC CCTGGAGCTC ATGCAGGTGC
FZM1      ---------- ---------- ---------- ---------- ---------- ----------
FDY50     ---------- ---------- ---------- ---------- ---------- ----------
FSZ47     ---------- ---------- ---------- ---------- ---------- ----------
FAK45     ---------- ---------- ---------- ---------- ---------- ----------
A9        ---------- ---------- ---------- ---------- ---------- ----------
K54A      ---------- ---------- ---------- ---------- ---------- ----------
Tox4      ---------- ---------- ---------- ---------- ---------- ----------

                  250        260        270        280        290        300
SU-16     TAAAGATCTA GCTTGCAGGA AACAAGTCTT TTCTGGGTTC TCAGCCCGCC CATGACGGAC
FZM1      ---------- ---------- ---------- ---------- -C-------- ----------
FDY50     ---------- ---------- ---------- ---------- -C-------- ----------
FSZ47     ---------- ---------- ---------- ---------- -C-------- ----------
FAK45     ---------- ---------- ---------- ---------- -C-------- ----------

A9        ---------- ---------- ---------- ---------- -A-------- ----------
K54A      ---------- ---------- ---------- ---------- -A-------- ----------
Tox4      ---------- ---------- ---------- ---------- -A-------- ----------
```

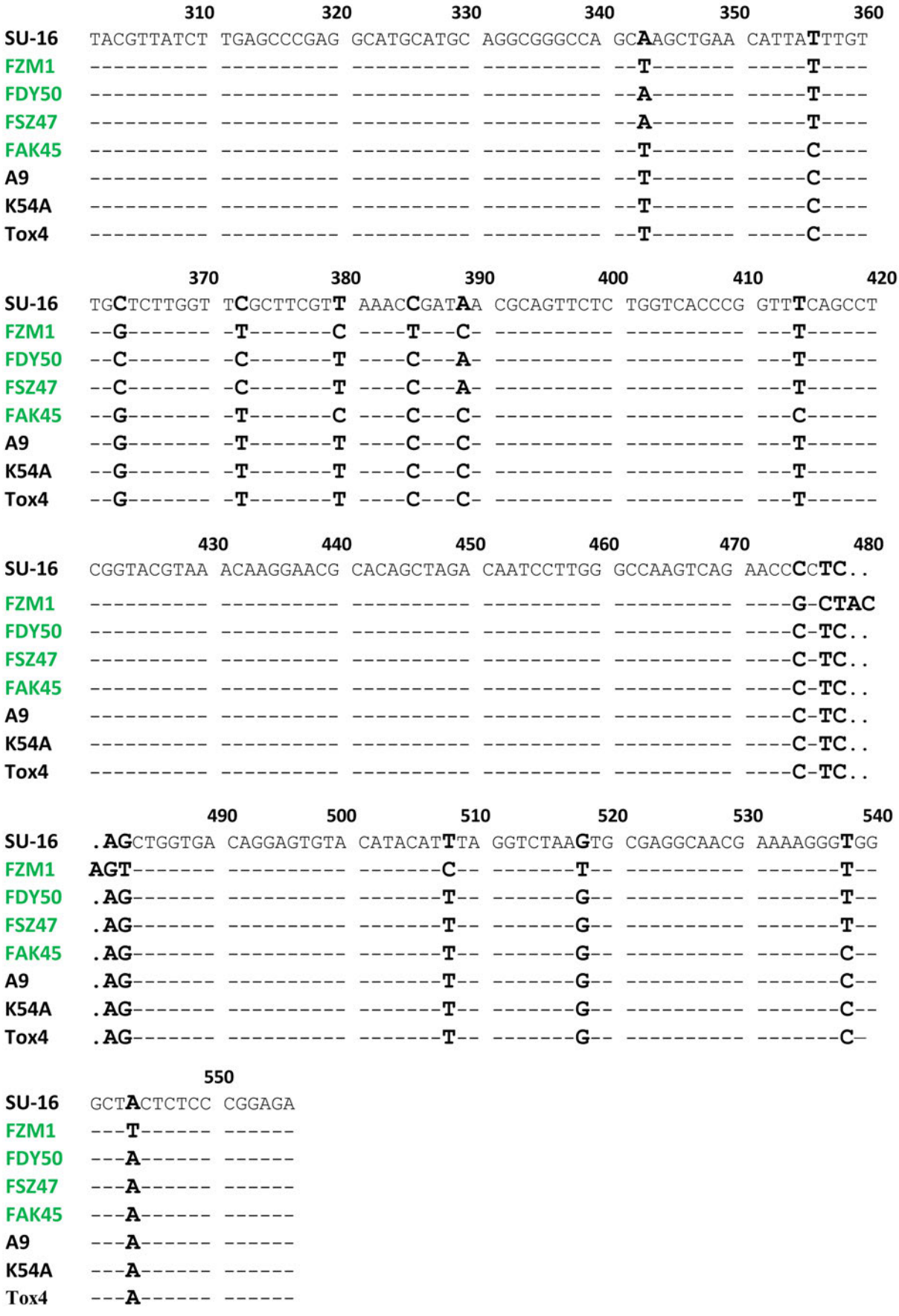


Fig. 4. Nucleotide sequence alignment of the four isolates with four reference strains. The names of the four isolates are in green. Nucleotide sequence alignment was performed using Clustal software (–) represent similarity, (.) represent deletion. Nucleotide changes are shown in bold font.

Table II
Genbank accession numbers of the *Aspergillus flavus* isolates.

| Isolate | Accession number | Strain |
|---|---|---|
| FZM1 | OL944584.1 | *A. flavus* strain FZM1 aflR-aflJ intergenic region, partial sequence |
| FAK45 | OL944586.1 | *A. flavus* strain FAK45 aflR-aflJ intergenic region, partial sequence |
| FSZ47 | OL944587.1 | *A. flavus* strain FSZ47 aflR-aflJ intergenic region, partial sequence |
| FDY50 | OL944588.1 | *A. flavus* strain FDY50 aflR-aflJ intergenic region, partial sequence |

Table III
Genbank accession numbers
of the *Aspergillus flavus* reference strains.

| Accession number | Strain |
|---|---|
| CP051037.1 | *A. flavus* strain A9 chromosome 3 |
| CP051085.1 | *A. flavus* strain K54A chromosome 3 |
| CP051045.1 | *A. flavus* strain Tox4 chromosome 3 |
| CP047251.1 | *A. flavus* strain SU-16 chromosome 3 |

and 99.67%, respectively). Since the reference strains A9, K54A, and Tox4 are 100% similar in the studied segment, their similarity with FZM1 and FAK45 isolates was found to be 97.48% and 98.12% respectively. Therefore, the highest divergence compared to the existing reference strains was seen for the sequences of the FZM1 isolate. A total of 13 positions of divergence involving single nucleotide polymorphisms (SNPs) as well as double and multiple nucleotide polymorphisms (MNPs) were observed (Fig. 4). In contrast, only minor variations were seen in FDY50 isolate corresponding to SNPs at the positions 3, 5 and 28 of the sequence. On the opposite side, the isolate FAK45 showed the highest genetic similarity with *A. flavus* reference strains A9, K54A, and Tox4 with only minor variations at the positions 50 and 103. Most of the observed polymorphisms were nucleotide substitutions, with only 10% being insertions and inversions, as shown in Table IV. Nucleotide deletions and SNPs in AF coding genes are often associated with the inability of *A. flavus* to produce aflatoxins. Deletion strains of *A. flavus* were reported in many studies (Chang et al. 2005; Donner et al. 2010; Adhikari et al. 2016; Hua et al. 2018).

However, not all AF non-producing strains have deletions in the AF biosynthesis gene cluster. The strain NRRL 30797 known as a biocontrol agent has a few substitutions in the aflatoxin biosynthesis gene cluster (Chang et al. 2012). This genetic variability may complicate the diagnosis and, therefore, the control of *A. flavus* infection and aflatoxin contamination of food and feed. Detecting particular strains of *A. flavus*, such as NRRL 30797, requires sequencing or a special PCR-RFLP capable of detecting the single substitutions. In the present study, the IGS region has been used as a target for PCR and sequencing for phylogenetic analysis. The selection of this region was motivated by the sequence variability between different species but only minor variations within isolates of the same species. The phylogenetic tree of isolates and their close relatives based on the *aflR-aflS(J)* intergenic region was constructed using Clustal Omega (Okoth et al. 2018) to illustrate

Table IV
Nucleotide variations in *aflR-aflS(J)* intergenic region sequences of *Aspergillus flavus* isolates.

| Nucleotide position | Nucleotide variation | Isolate |
|---|---|---|
| 103, 385, 478 | C with T (substitution) | FZM1: *Aspergillus flavus* strain FZM1 *aflR-aflS(J)* intergenic region, partial sequence |
| 161 | Insertion of G | |
| 380, 477, 508 | T with C (substitution) | |
| 475 | C with G (inversion) | |
| 479–481 | Insertion of ACA | |
| 482 | A with G (substitution) | |
| 483 | G with T (substitution) | |
| 544 | A with T (inversion) | |
| 50 | T with C (substitution) | FAK45: *Aspergillus flavus* strain *FAK45 aflR-aflS(J)* intergenic region, partial sequence |
| 103 | C with T (substitution) | |
| 3 | C with T (substitution) | FDY50: *Aspergillus flavus* strain *aflR-aflS(J)* intergenic region, partial sequence |
| 5, 28 | G with A (substitution) | |

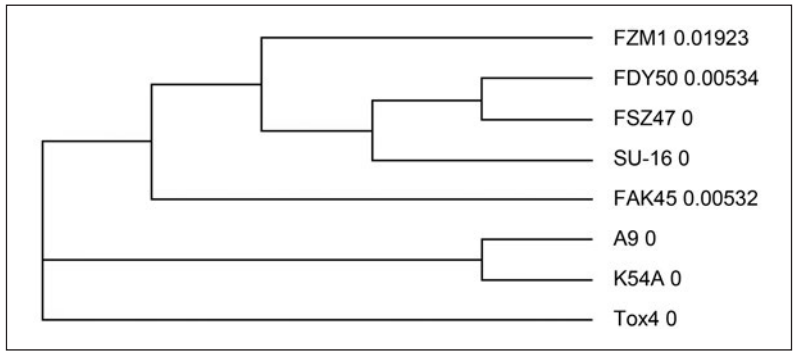


Fig. 5. Maximum Likelihood phylogenic tree showing the relationships between the examined *A. flavus* isolates and reference strains, based on *aflR/aflS(J)* intergenic sequence.

the relationships of isolates among *A. flavus* species. The phylogenetic tree obtained clearly shows that the *A. flavus* strains clustered into three major clades. In addition, several sub-clades indicate a wide variation among *A. flavus* species (Fig. 5). FSZ47 and FDY50 isolates were clustered in one clade and were found to be closely related to *A. flavus* strain SU 16 forming a mixed cluster. In contrast, FAK45 and FZM1 isolates were found to form distinct sub-clades. Variations exist among *A. flavus* isolates; those with SNPs share a closer relationship clustered with *A. flavus* strain SU16; while the isolate FAK45 clustered with a distinct sub-clade. These data agree with the previous finding reported by different groups (Krimitzas et al. 2013; Chiba et al. 2014). Recently, new direct detection methods of *A. flavus* through AF-B1 and Zearalenone by Raman spectrometry (Yang et al. 2021) or AF-B1 alone using a ortable Raman spectrometer combined with colloidal Au nanoparticles (Wang et al. 2022) were reported. This latter rapid technique provides quantitative measurement of AF-B1 in grain crops.

## Conclusions

The four diagnosis methods (phenotyping, PCR, PCR-RFLP, and amplicon sequencing) have shown different sensitivity levels of fungal characterization. Phenotypic tools were limited to *A.* section *Flavi* identification; PCR alone failed to distinguish *A. parasiticus* from *A. flavus*; PCR-RFLP in this study was able to detect *A. flavus* only. However, it failed to distinguish between different strains of *A. flavus*. Sequencing and sequence analysis was able to distinguish between the *A. flavus* strains. These data established the selection criteria of the methods to use depending on the segregation level of fungal strains. New methods based on Raman spectrometry to measure AF-B1 alone or in combination with other fungal components might provide additional help for the detection of the pathogenic *A. flavus* in grain crops.

**Acknowledgements**

This work was supported by the UTHB Algeria and both UGA and INRAE (PAVAL Lab.) in France.

**Conflict of interest**

The authors do not report any financial or personal connections with other persons or organizations, which might negatively affect the contents of this publication and/or claim authorship rights to this publication.

## Literature

**Abriba C, Lennox JA, Asikong BE, Asitok A, Ikpoh IS, Henshaw EE, Eja ME.** Isolation of aflatoxin producing species of *Aspergillus* from foodstuffs sold in Calabar markets, Cross River state, Nigeria. J Microbiol Biotechnol Res. 2013;3:8–13.

**Adhikari BN, Bandyopadhyay R, Cotty PJ.** Degeneration of aflatoxin gene clusters in *Aspergillus flavus* from Africa and North America. AMB Express. 2016 Dec;6(1):62. https://doi.org/10.1186/s13568-016-0228-6

**Ahmad MM, Ahmad M, Ali A, Hamid R, Javed S, Abdin MZ.** Molecular methods for detecting pathogenic fungi. In: Gupta VK, Tuohy M, Gaur RK, editors. Fungal biochemistry and biotechnology. Saarbrücken (Germany): Lambert; 2010. p. 154–169.

**Al-Wadai AS, Al-Othman MR, Mahmoud MA, Abd El-Aziz ARM.** Molecular characterization of *Aspergillus flavus* and aflatoxin contamination of wheat grains from Saudi Arabia. Genet Mol Res. 2013; 12(3):3335–3352. https://doi.org/10.4238/2013.September.3.10

**Bagyalakshmi R, Lily Therese K, Madhavan HN.** Nucleotide polymorphisms associated with Internal Transcribed Spacer (ITS) regions of ocular isolates of *Aspergillus flavus*. J Microbiol Methods. 2007 Jan;68(1):1–10. https://doi.org/10.1016/j.mimet.2006.05.021

**Bailly S, Mahgubi A, Carvajal-Campos A, Lorber S, Puel O, Oswald I, Bailly JD, Orlando B.** Occurrence and identification of *Aspergillus* section *Flavi* in the context of the emergence of aflatoxins in French maize. Toxins (Basel). 2018 Dec 07;10(12):525. https://doi.org/10.3390/toxins10120525

**Bothast RJ, Fennell DI.** A medium for rapid identification and enumeration of *Aspergillus flavus* and related organisms. Mycologia. 1974 Mar;66(2):365–369. https://doi.org/10.1080/00275514.1974.12019615

**Chang PK, Abbas HK, Weaver MA, Ehrlich KC, Scharfenstein LL, Cotty PJ.** Identification of genetic defects in the atoxigenic biocontrol strain *Aspergillus flavus* K49 reveals the presence of a competitive recombinant group in field populations. Int J Food Microbiol. 2012 Mar;154(3):192–196. https://doi.org/10.1016/j.ijfoodmicro.2012.01.005

**Chang PK, Horn BW, Dorner JW.** Sequence breakpoints in the aflatoxin biosynthesis gene cluster and flanking regions in nonaflatoxigenic *Aspergillus flavus* isolates. Fungal Genet Biol. 2005 Nov;42(11): 914–923. https://doi.org/10.1016/j.fgb.2005.07.004

**Chiba T, Takahashi Y, Sadamasu K, Nakama A, Kai A.** [Discrimination of *Aspergillus flavus* group fungi using phylogenetic tree analysis and multiplex PCR] (in Japanese). Food Hyg Saf Sci (Shokuhin Eiseigaku Zasshi). 2014;55(3):135–141. https://doi.org/10.3358/shokueishi.55.135

**Daghriri SH, El-Bebany AF, Alrumman SA, Hesham A.** Molecular characterisation and biological control of *Aspergillus flavus* isolates from Saudi Arabia. Arch. Phytopathol Plant Prot. 2018;51(9–10): 445–460. https://doi.org/10.1080/03235408.2018.1480262

**Donner M, Atehnkeng J, Sikora RA, Bandyopadhyay R, Cotty PJ.** Molecular characterization of atoxigenic strains for biological control of aflatoxins in Nigeria. Food Addit Contam, Part A. 2010 May; 27(5):576–590. https://doi.org/10.1080/19440040903551954

**Ehrlich K, Montalbano BG, Cotty PJ.** Sequence comparison of *afl*R from different *Aspergillus* species provides evidence for variability in regulation of aflatoxin production. Fungal Genet Biol. 2003 Feb; 38(1):63–74. https://doi.org/10.1016/S1087-1845(02)00509-1

**Ehrlich KC, Kobbeman K, Montalbano BG, Cotty PJ.** Aflatoxin-producing *Aspergillus* species from Thailand. Int J Food Microbiol. 2007 Mar;114(2):153–159. https://doi.org/10.1016/j.ijfoodmicro.2006.08.007

**El Khoury A, Atoui A, Rizk T, Lteif R, Kallassy M, Lebrihi A.** Differentiation between *Aspergillus flavus* and *Aspergillus parasiticus* from pure culture and aflatoxin-contaminated grapes using PCR-RFLP analysis of *aflR-aflJ* intergenic spacer. J Food Sci. 2011 May; 76(4):M247–M253. https://doi.org/10.1111/j.1750-3841.2011.02153.x

**Fakruddin M, Chowdhury A, Hossain MN, Ahmed MM.** Characterization of aflatoxin producing *Aspergillus flavus* from food and feed samples. SpringerPlus. 2015 Dec;4(1):159. https://doi.org/10.1186/s40064-015-0947-1

**Frisvad JC, Hubka V, Ezekiel CN, Hong SB, Nováková A, Chen AJ, Arzanlou M, Larsen TO, Sklenář F, Mahakarnchanakul W, et al.** Taxonomy of *Aspergillus* section *Flavi* and their production of aflatoxins, ochratoxins and other mycotoxins. Stud Mycol. 2019 Jun 01; 93(1):1–63. https://doi.org/10.1016/j.simyco.2018.06.001

**Gbashi S, Madala NE, De Saeger S, De Boevre M, Adekoya I, Adebo OA, Njobeh PB.** The socio-economic impact of mycotoxin contamination in Africa. In: Njobeh PB, Stepman F, editors. Mycotoxins – impact and management strategies. London (UK): IntechOpen; 2018. https://doi.org/10.5772/intechopen.79328

**Georgianna DR, Payne GA.** Genetic regulation of aflatoxin biosynthesis: from gene to genome. Fungal Genet Biol. 2009 Feb;46(2): 113–125. https://doi.org/10.1016/j.fgb.2008.10.011

**Godet M, Munaut F.** Molecular strategy for identification in *Aspergillus* section *Flavi*. FEMS Microbiol Lett. 2010 Mar;304(2):157–168. https://doi.org/10.1111/j.1574-6968.2009.01890.x

**Hamsa TAP, Ayres JC.** A differential medium for the isolation of *Aspergillus flavus* from cottonseed. J Food Sci. 1977 Mar;42(2):449–453. https://doi.org/10.1111/j.1365-2621.1977.tb01520.x

**Healy M, Reece K, Walton D, Huong J, Shah K, Kontoyiannis DP.** Identification to the species level and differentiation between strains of *Aspergillus* clinical isolates by automated repetitive-sequence-based PCR. J Clin Microbiol. 2004 Sep;42(9):4016–4024. https://doi.org/10.1128/JCM.42.9.4016-4024.2004

**Hossain MN, Talukder A, Afroze F, Rahim MM, Begum S, Haque MZ, Ahmed MM.** Identification of aflatoxigenic fungi and detection of their aflatoxin in red chilli (*Capsicum annuum*) samples using direct cultural method and HPLC. Adv Microbiol. 2018; 08(01):42–53. https://doi.org/10.4236/aim.2018.81004

**Hua SST, Palumbo JD, Parfitt DE, Sarreal SBL, O'Keeffe TL.** Development of a droplet digital PCR assay for population analysis of aflatoxigenic and atoxigenic *Aspergillus flavus* mixtures in soil. Mycotoxin Res. 2018 Aug;34(3):187–194. https://doi.org/10.1007/s12550-018-0313-6

**Ibrahim N.** Molecular identification and evaluation of genetic variability among some aflatoxigenic *Aspergillus flavus* strains isolated from fish feed in Egypt. Egypt J Microbiol. 2019;54(1):103–115. https://doi.org/10.21608/ejm.2019.16611.1114

**Kana JR, Joselin Gnonlonfin BG, Harvey J, Wainaina J, Wanjuki I, Robert A, Skilton RA, Teguia A.** Mycobiota and toxigenecity profile of *Aspergillus flavus* recovered from food and poultry feed mixtures in Cameroon. J Animal Poult Sci. 2013;2(4):98–107.

**Kim HJ, Lee MJ, Kim HJ, Cho SK, Park HJ, Jeong MH.** Analytical method development and monitoring of aflatoxin B1, B2, G1, G2 and ochratoxin A in animal feed using HPLC with fluorescence detector and photochemical reaction device. Cogent Food Agric. 2017 Jan 01;3(1):1419788. https://doi.org/10.1080/23311932.2017.1419788

**Klingelhöfer D, Zhu Y, Braun M, Bendels MHK, Brüggmann D, Groneberg DA.** Aflatoxin – publication analysis of a global health threat. Food Control. 2018 Jul;89:280–290. https://doi.org/10.1016/j.foodcont.2018.02.017

**Krimitzas A, Pyrri I, Kouvelis VN, Kapsanaki-Gotsi E, Typas MA.** A phylogenetic analysis of Greek isolates of *Aspergillus* species based on morphology and nuclear and mitochondrial gene sequences. BioMed Res Int. 2013;2013:260395. https://doi.org/10.1155/2013/260395

**Krulj J, Ćurčić N, Stančić AB, Kojić J, Pezo L, Tukuljac LP, Solarov MB.** Molecular identification and characterisation of *Aspergillus Flavus* isolates originating from Serbian wheat grains. Acta Aliment. 2020 Nov 07;49(4):382–389. https://doi.org/10.1556/066.2020.49.4.3

**Lavkor I.** Quantitative detection of aflatoxin and species identification of *Aspergillus* section *Flavi* isolates from peanuts using molecular approaches. Legume Res. 2020;43(2):195–199. https://doi.org/10.18805/LR-530

**Lee CZ, Liou GY, Yuan GF.** Comparison of the *aflR* gene sequences of strains in *Aspergillus* section *Flavi*. Microbiology. 2006 Jan 01;152(1):161–170. https://doi.org/10.1099/mic.0.27618-0

**Levy L, Castlebury LA, Carris LM, Meyer RJ, Pimentel G.** Internal transcribed spacer sequence-based phylogeny and polymerase chain reaction-restriction fragment length polymorphism differentiation of *Tilletia walkeri* and *T. indica*. Phytopathology. 2001 Oct; 91(10):935–940. https://doi.org/10.1094/PHYTO.2001.91.10.935

**Liao J, He Z, Xia Y, Lei Y, Liao B.** A review on biosynthesis and genetic regulation of aflatoxin production by major *Aspergillus* fungi. Oil Crop Sci. 2020 Oct;5(4):166–173. https://doi.org/10.1016/j.ocsci.2020.11.001

**Martínez-Culebras PV, Ramón D.** An ITS-RFLP method to identify black *Aspergillus* isolates responsible for OTA contamination in grapes and wine. Int J Food Microbiol. 2007 Jan;113(2):147–153. https://doi.org/10.1016/j.ijfoodmicro.2006.06.023

**Martinez-Miranda MM, Rosero-Moreano M, Taborda-Ocampo G.** Occurrence, dietary exposure and risk assessment of aflatoxins in arepa, bread and rice. Food Control. 2019 Apr;98:359–366. https://doi.org/10.1016/j.foodcont.2018.11.046

**Mohankumar M, Vijayasamundeeswari A, Karthikeyan M, Mathiyazhagan S, Paranidharan V, Velazhahan R.** Analysis of molecular variability among isolates of *Aspergillus flavus* by PCR-RFLP of the ITS regions of rDNA. J Plant Prot Res. 2010 Jan 1;50(4): 446–451. https://doi.org/10.2478/v10045-010-0075-4

**Nicholson P, Simpson DR, Weston G, Rezanoor HN, Lees AK, Parry DW, Joyce D.** Detection and quantification of *Fusarium cul-*

*morum* and *Fusarium graminearumin* cereals using PCR assays. Physiol Mol Plant Pathol. 1998 Jul;53(1):17–37. https://doi.org/10.1006/pmpp.1998.0170

**Nikolic M, Nikolic A, Jaukovic M, Savic I, Petrovic T, Bagi F, Stankovic S.** Differentiation between *Aspergillus flavus* and *Aspergillus parasiticus* isolates originated from wheat. Genetika. 2018;50(1): 143–152. https://doi.org/10.2298/GENSR1801143N

**Okoth S, De Boevre M, Vidal A, Diana Di Mavungu J, Landschoot S, Kyallo M, Njuguna J, Harvey J, De Saeger S.** Genetic and toxigenic variability within *Aspergillus flavus* population isolated from maize in two diverse environments in Kenya. Front Microbiol. 2018 Jan 26;9:57. https://doi.org/10.3389/fmicb.2018.00057

**Paterson RRM.** Identification and quantification of mycotoxigenic fungi by PCR. Process Biochem. 2006 Jul;41(7):1467–1474. https://doi.org/10.1016/j.procbio.2006.02.019

**Pitt JI, Hocking AD, Glenn DR.** An improved medium for the detection of *Aspergillus flavus* and *A. parasiticus*. J Appl Bacteriol. 1983 Feb; 54(1):109–114. https://doi.org/10.1111/j.1365-2672.1983.tb01307.x

**Pitt JI, Hocking AD.** Fungi and food spoilage. New York (USA): Springer New York; 2009. https://doi.org/10.1007/978-0-387-92207-2

**Price MS, Yu J, Nierman WC, Kim HS, Pritchard B, Jacobus CA, Bhatnagar D, Cleveland TE, Payne GA.** The aflatoxin pathway regulator AflR induces gene transcription inside and outside of the aflatoxin biosynthetic cluster. FEMS Microbiol Lett. 2006 Feb; 255(2):275–279. https://doi.org/10.1111/j.1574-6968.2005.00084.x

**Rao KR, Vipin AV, Venkateswaran G.** Molecular profile of non-aflatoxigenic phenotype in native strains of *Aspergillus flavus*. Arch Microbiol. 2020 Jul;202(5):1143–1155. https://doi.org/10.1007/s00203-020-01822-1

**Rodrigues P, Venâncio A, Kozakiewicz Z, Lima N.** A polyphasic approach to the identification of aflatoxigenic and non-aflatoxigenic strains of *Aspergillus* section *Flavi* isolated from Portuguese almonds. Int J Food Microbiol. 2009 Feb;129(2):187–193. https://doi.org/10.1016/j.ijfoodmicro.2008.11.023

**Singh P, Orbach M, Cotty P.** *Aspergillus texensis*: a novel aflatoxin producer with S morphology from the United States. Toxins (Basel). 2018 Dec 03;10(12):513. https://doi.org/10.3390/toxins10120513

**Stanković S, Lević J, Nikolić M, Krnjaja V, Jauković M, Nalaz P.** Prvi Nalaz *Aspergillus parasiticus* u Proizvodnji Kukuruza u Srbiji. Paper presented at: Proceedings of the XIII Savetovanje o Zaštiti Bilja; 2015 October 23–27; Zlatibor, Serbia. p. 32–33.

**Wang H, Liu M, Zhang Y, Zhao H, Lu W, Lin T, Zhang P, Zheng D.** Rapid detection of *Aspergillus flavus* and quantitative determination of aflatoxin $B_1$ in grain crops using a portable Raman spectrometer combined with colloidal Au nanoparticles. Molecules. 2022 Aug 18; 27(16):5280. https://doi.org/10.3390/molecules27165280

**Wilson DM, Mubatanhema W, Jurjević Z.** Biology and ecology of mycotoxigenic *Aspergillus* species as related to economic and health concerns. In: DeVries JW, Trucksess MW, Jackson LS, editors. Mycotoxins and food safety. Advances in experimental medicine and biology. Boston (USA): Springer; 2002(504). p. 3–17. https://doi.org/10.1007/978-1-4615-0629-4_2

**Yang XQ, Yu HC, Yin Y, Yuan YX, Wu H, Li H.** [Detection of aflatoxin $B_1$ and zearalenone in maize by Raman spectroscopy] (in Chinese). J Nucl Agric Sci. 2021;35(1):159–166. https://doi.org/10.11869/j.issn.100-8551.2021.01.0159

**Yin Y, Lou T, Yan L, Michailides TJ, Ma Z.** Molecular characterization of toxigenic and atoxigenic *Aspergillus flavus* isolates, collected from peanut fields in China. J Appl Microbiol. 2009 Dec;107(6):1857–1865. https://doi.org/10.1111/j.1365-2672.2009.04356.x

**Yu J, Chang PK, Ehrlich KC, Cary JW, Bhatnagar D, Cleveland TE, Payne GA, Linz JE, Woloshuk CP, Bennett JW.** Clustered pathway genes in aflatoxin biosynthesis. Appl Environ Microbiol. 2004 Mar;70(3):1253–1262. https://doi.org/10.1128/AEM.70.3.1253-1262.2004

**Yu J.** Current understanding on aflatoxin biosynthesis and future perspective in reducing aflatoxin contamination. Toxins (Basel). 2012 Oct 25;4(11):1024–1057. https://doi.org/10.3390/toxins4111024

**Zarrin M, Erfaninejad M.** Molecular variation analysis of *Aspergillus flavus* using polymerase chain reaction-restriction fragment length polymorphism of the internal transcribed spacer rDNA region. Exp Ther Med. 2016 Sep;12(3):1628–1632. https://doi.org/10.3892/etm.2016.3479

ORIGINAL PAPER
Polish Journal of Microbiology
2022, Vol. 71, No 4, 601–613
https://doi.org/10.33073/pjm-2022-045

# Characterization of Fecal Microbiomes of Osteoporotic Patients in Korea

ASAD UL-HAQ[2, 4#], HOONHEE SEO[1, 2#], SUJIN JO[1], HYUNA PARK[1], SUKYUNG KIM[2], YOUNGKYOUNG LEE[1], SAEBIM LEE[1, 2], JE HOON JEONG[3*] and HO-YEON SONG[1, 2*]

[1] Department of Microbiology and Immunology, School of Medicine, Soonchunhyang University, Cheonan-si, Chungnam, Republic of Korea
[2] Probiotics Microbiome Convergence Center, Soonchunhyang University, Asan, Chungnam, Republic of Korea
[3] Department of Neurosurgery, Soonchunhyang University Bucheon Hospital, Bucheon, Gyeongi-do, Republic of Korea
[4] Division of Rheumatology, Department of Internal Medicine, Soonchunhyang University Seoul Hospital, Seoul, Republic of Korea

Submitted 11 July 2022, accepted 11 September 2022, published online 19 December 2022

Abstract

An imbalanced gut microbiome has been linked to a higher risk of many bone-related diseases. The objective of this study was to discover biomarkers of osteoporosis (OP). So, we collected 76 stool samples (60 human controls and 16 OP patients), extracted DNA, and performed 16S ribosomal ribonucleic acid (rRNA) gene-based amplicon sequencing. Among the taxa with an average taxonomic composition greater than 1%, only the *Lachnospira* genus showed a significant difference between the two groups. The Linear Discriminant Effect Size analysis and qPCR experiments indicated the *Lachnospira* genus as a potential biomarker of OP. Moreover, a total of 11 metabolic pathways varied between the two groups. Our study concludes that the genus *Lachnospira* is potentially crucial for diagnosing and treating osteoporosis. The findings of this study might help researchers better understand OP from a microbiome perspective. This research might develop more effective diagnostic and treatment methods for OP in the future.

K e y w o r d s: osteoporosis, microbiomes, gut microbiota, fecal microbiomes, 16S rRNA gene-based metagenomics, *Lachnospira*

## Introduction

Osteoporosis (OP), the most common bone-related disease, is characterized by a loss of bone mass, increased bone fragility, damage to bone tissue microstructure, and increased fracture risk. It affects men and women (1–8% and 9–38%, respectively) (Wade et al. 2014; Cannarella et al. 2019). Throughout life, human bone continues the remodeling process. One remodeling cycle consists of four stages (initiation, resorption, reversal, and formation) (Ding et al. 2020). When bone resorption outpaces bone formation, bone integrity is compromised, leading to OP (Tang 2020). The pathophysiology of OP is linked to heredity, hormonal levels, diet, lifestyle, and inflammatory factors (Peng et al. 2018; Zheng et al. 2019; Li et al. 2020; Tang 2020). OP is more common in women than in men. The primary cause of OP has been linked to estrogen deprivation after menopause (Manolagas 2010). The secondary cause of OP includes smoking, type 1 diabetes (T1D), parathyroid disorder, inflammatory bowel disease (IBD), arthritis, and glucocorticoid medication (Zaheer and LeBoff 2000). Many pharmacological, hormonal, antibody and inhibitor-based therapies are currently being practiced to cure OP. However, all available treatments are associated with severe side effects like gastrointestinal diseases, rhinitis, dermatological reactions, musculoskeletal pain, dizziness, nausea, headache,

# Asad Ul-Haq and Hoonhee Seo contributed equally to this study.

* Corresponding authors: H.-Y. Song, Department of Microbiology and Immunology, School of Medicine, Soonchunhyang University, Cheonan-si, Chungnam, Republic of Korea; Probiotics Microbiome Convergence Center, Soonchunhyang University, Asan, Chungnam, Republic of Korea; **e-mail: songmic@sch.ac.kr**
J.-H. Jeong, Department of Neurosurgery, Soonchunhyang University Bucheon Hospital, Bucheon, Gyeongi-do, Republic of Korea; **e-mail: neuri71@schmc.ac.kr**

stroke, and hypercholesterolemia (Camacho et al. 2016; Tu et al. 2018). Thus, a new OP therapy with minimum or no adverse effects is urgently needed.

It has been estimated that there are 10 trillion bacteria in the human intestinal microbiota (Yan et al. 2016). Based on their involvement in human health, intestinal microorganisms are classified as beneficial, opportunistic, and commensal microbes. The beneficial bacteria (probiotics) confer health benefits to hosts (Guarner and Schaafsma 1998). Some commonly used probiotics are *Bifidobacteria*, *Lactobacillus reuter*, *Lactobacillus rhamnosus*, *Lactobacillus acidophilus*-group, *Bacillus coagulans*, *Escherichia coli* strain Nissle 1917, *Enterococcus faecium*, and certain enterococci (Pandey et al. 2015). The opportunistic microbes utilize the opportunity of weakened defense mechanisms of the host to inflict damage. Some opportunistic bacteria are *Corynebacterium equi*, *Staphylococcus aureus*, *Mycoplasma pneumoniae*, and *Salmonella* spp. The commensal bacteria defend against foreign pathogens directly by competing for living space or nutrients by toxins (bacteriocins, acids, and phenols) (Guarner and Malagelada 2003; Wang et al. 2018). Moreover, some commensal bacteria act on the host immune system (Stecher and Hardt 2008), and several commensal bacteria reside inside the human gut, like *Bacteroides fragilis*, *Bacteroides uniformis*, and *Clostridium ramosum*.

Previously, multiple studies have demonstrated the link between gut microbiome compositions and bone metabolism. Also, bone-related mineral absorption is involved in OP under different physiological conditions (Scholz-Ahrens et al. 2007; Sjögren et al. 2012; Charles et al. 2015; Li et al. 2016; D'Amelio and Sassi 2018; Uchida et al. 2018; Tavakoli and Xiao 2019; Cheng et al. 2020). Xu et al. (2017) showed that intestinal microbiota composition and structure could be influenced by both host (genetic background and gender) and environmental factors (diet, lifestyle, hygiene, antibiotics, and probiotics). A new genome-wide associated study found that the order Clostridiales and family *Lachnospiraceae* are positively related to bone mass variation, implying a linkage between microbiota and bone formation (Ni et al. 2021).

Several recent studies have investigated the effects of microbiomes on primary or secondary OP between OP patients and healthy controls (HCs) (Wang et al. 2017; Das et al. 2019; Li et al. 2019; Wei et al. 2021b). However, these previous studies were limited to Chinese, Latin American, and European populations. Thus, this study aimed to investigate the bacterial community structure and diversity alterations of gut microbiota in OP patients among Korean people. Variations in the gut microbial composition of OP patients compared to HCs were obtained based on in-depth research of microbial components connected to OP. These findings were correlated with clinical parameters. We expect that our study could serve as a platform for future research into new microbe biomarkers and processes behind the impact of gut microbiota on OP.

## Experiment

### Materials and Methods

**Sample collection, DNA extraction, amplification, and sequencing.** The present study was performed from May 2020 to November 2021 in the Healthcare Center affiliated with the Probiotics Microbiome Convergence Center at Soonchunyyang University, Asan, South Korea. It was approved by the Institutional Review Board (IRB) (IRB No. 2019-10-017-005). Seventy-six (33–82 years) adults were enrolled in this study, including 60 human controls (HC) and 16 OP patients (Table SI). OP was diagnosed by bone density test using dual-energy X-ray absorptiometry (DEXA) based on the World Health Organization (WHO) recommendations (Kanis 2008). Participants of this study were informed about the sampling method and risks involved. All of them agreed to laboratory tests and gave written consent. The first fecal samples before breakfast (5–10 g) were collected by each participant individually at the recruitment site at RT and placed at −80°C immediately. Then, samples were transported to the laboratory with dry ice (temperature ~ −78°C) and kept at −80°C until further processing. All 76 samples were used for the 16S rRNA gene V4 region sequencing.

**DNA extraction.** Using the QIAamp DNA fast Stool Mini Kit (Qiagen, Germany), microbial DNA was extracted from 180–220 mg fecal samples following the manufacturer's protocol. The DNA concentration was measured with a Qubit-4 fluorometer (Thermo Fisher Scientific, UK). The quality of DNA was checked by 0.8% agarose gel electrophoresis. All DNA samples were stored at −20°C until further use.

**PCR amplification of the 16S rRNA gene.** The 16S bacterial rRNA (V4 hypervariable region) was amplified using Illumina 16S amplicon primer set (5 μM each) (Forward primer: 5'-TCGTCGGCAGCGTCAGATGTGTATAAGAGACAG-CCTACGGGNGGCWGCAG-3', Reverse primer: 5'-GTCTCGTGGGCTCGGAGATGTGTATAAGAGACAGGACTACHVGG-GTATCTAATCC-3') with 10 ng of template DNA and KAPA HiFi HotStart ReadyMix (Kapa Biosystems, USA) following the previously described protocol by our team (Kim et al. 2021). Briefly, the PCR was performed on a Veriti 96-well Thermal cycler (Applied Biosystems, Thermo Fisher, USA) with all 76 samples, including negative control (no template DNA) and positive control (5 ng of mouse stool DNA). Amplification conditions for all

samples were: initial denaturation at 95°C for 3 min, followed by 25 cycles of denaturation at 95°C for 30 s, annealing at 55°C for 30 s, and extension at 72°C for 30 s, with a final extension step at 72°C for 5 min. PCR products were purified using AMPure beads (Beckman Coulter, UK) following the manufacturer's protocol. Indexed PCR was performed using Nextera XT DNA Library Prep Kit (Illumina, USA) according to the recommended protocol, followed by PCR clean-up using AMPure beads. Each sample was diluted to 1 nM final concentration, and samples were pooled together.

**The 16S rRNA gene-based sequencing and data analysis.** Pooled library (50 pMol) was used for sequencing with 30% PhiX spiking on an iSeqTM100 platform (Illumina, USA). Data were analyzed following the procedures described previously by our team (Kim et al. 2021; ul-Haq et al. 2022). Briefly, we analyzed data using the EzBioCloud server (http://www.ezbiocloud.net). Trimmomatic (version. 0.32) was used for quality checking and filtering of low-quality reads (< Q25). Primer trimming was done with Myers and Miller's alignment algorithm (Myers and Miller 1988). Samples without 16S rRNA encoding were identified using HMMER software and nhmmer (package ver. 3.2.1) (Wheeler and Eddy 2013). The unique reads and redundant reads were clustered using the derep_full length command in VSEARCH (Rognes et al. 2016). We employed EzBioCloud's 16S rRNA database (Yoon et al. 2017) for taxonomic assignment with VSEARCH (Myers and Miller 1988; Rognes et al. 2016). Chimeric reads were filtered using UCHIME (Edgar et al. 2011). To identify sequences at the low taxonomic level, the cluster_fast command (Rognes et al. 2016) was used to create operational taxonomic units (OTUs). Single-read OTUs were removed from further analysis. Sequences were deposited in Sequence Read Archive (SRA) (BioProject ID: PRJNA795857, accessible at https://www.ncbi.nlm.nih.gov/bioproject/795857).

**Quantitative PCR.** qPCR was used for comparative quantification of *Lachnospira* using BioRad CFX Connect Real-Time-System thermocycler equipment (BioRad, USA) and iQ SYBR® Green Supermix (BioRad, USA) with *Lachnospira*-specific primers (Forward primer 5'-CCTGACTAAGAAGCTCCGGC-3'; Reverse primer: 5'-CAAAAGCAGTTCCGGGGTTG-3') according to Liu et al. (2022). A total of 32 samples (16 OP patients and 16 HCs) with positive control (mouse stool DNA) and negative control (no template DNA) were used for this experiment. Triplicate qPCR was performed using 10 ng of genomic DNA from each sample, 10 µl of SYBR Mixture, 1 µl forward primer (1 µM), and 1 µl reverse primer (1 µM) for each PCR reaction. PCR conditions were as follows: pre-denaturation at 95°C for 5 minutes, followed by 40 cycles of denaturation at 95°C for 10 seconds, and annealing/extension at 56°C for 30 seconds. Quantitation cycle (Cq) values from HC and OP patient groups were compared using GraphPad Prism software (ver. 8.0.1, USA).

**Statistical analysis.** Alpha diversities of the samples were calculated for samples based on Chao1 (Chao 1987), ACE (Chao and Lee 1992), Shannon/Simpson (Magurran 2013), Jackknife (Burnham and Overton 1979), NPShannon (Chao and Shen 2003), and Phylogenetic diversity (Faith 1992). On the other hand, beta diversity distances were analyzed based on Generalized UniFrac (Chen et al. 2012), Fast UniFrac (Hamady et al. 2010), Jenson-Shannon (Lin 1991), and Bray-Curtis (Beals 1984). Permutational multivariate analysis of variance (PERMANOVA) was used to determine the beta set significance between OP and HC. The taxonomic biomarkers were found using statistical comparison algorithms of LEfSe (Linear discriminant analysis Effect Size) (Segata et al. 2011) and Kruskal-Wallis *H* tests (Kruskal and Wallis 1952). The Student's *t*-test was performed to evaluate the statistical significance of comparing Cq (quantification cycle) values of OP patients and HCs. Functional profiles were predicted based on the Kyoto Encyclopedia of Genes and Genomes (KEGG) (Ye and Doak 2009) using Phylogenetic Investigation of Communities by Reconstruction of Unobserved States (PICRUSt2) (Douglas et al. 2020). The differences between the groups were assessed using STAMP (statistical analysis of taxonomic and functional profiles) software and Welch's *t*-test. The $p < 0.05$ was taken as statistically significant for all the analyses.

## Results

**Characteristics of the study population.** Table SI shows a demographic data comparison between the two groups. The number of participants was 60 in the HC group and 16 in the OP group. The mean ages of the HC and OP groups were 59.1 ± 9.8 years and 66.3 ± 8.9 years, respectively. Baseline characteristics, such as age, gender, and body mass index (BMI), showed no statistically significant differences between the two groups. Mean T-scores of HCs and OP patients were – 0.75 ± 1.1 and – 2.85 ± 0.3, respectively. Lifestyle factors such as smoking and drinking did not significantly differ between OP and HC groups. Hypertension, diabetes mellitus, and blood chemistry measurements (glucose, triglyceride, protein, albumin, and blood urea nitrogen (BUN)) were not significantly different between the two groups, suggesting that these parameters did not seem to have a significant relationship with OP.

**Microbiota characteristics.** A total of 1,419,302 high-quality reads were generated among the 76 fecal samples, with 4,279 median values per sample. Compared to the HC group, OP patients had no difference

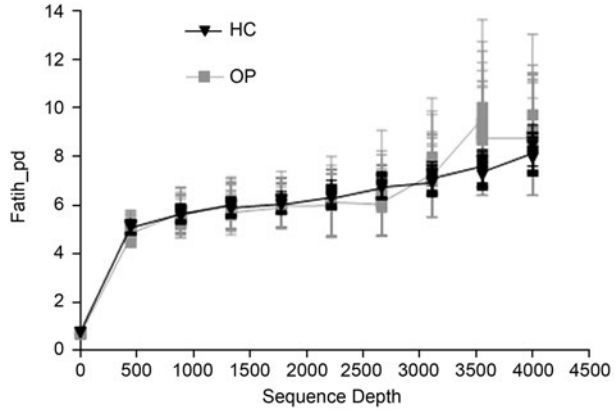


Fig. 1. Rarefaction curve for sequence depth. The Faith phylogenetic diversity (Faith_pd) rarefaction curve shows that there is no difference in species abundance and diversity between the healthy control (HC) group and the osteoporotic (OP) patient group.

in species richness and diversity, as shown in Faith phylogenetic diversity (Faith_pd) rarefraction curve (Fig. 1). Along with that, average taxonomic compositions in feces of osteoporotic patients and HCs are presented in Table SII and Fig. 2. Our data showed that average taxonomic compositions of OP patients and HC group were not significantly different at the phylum or class level. However, at the phylum level, Firmicutes showed the highest average percentage in both OP patients and HCs (HC = 50%, OP = 47%), followed by Bacteroidetes (HC = 35, OP = 39%), Proteobacteria (HC = 7.7%, OP = 8.4%), and Actinobacteria (HC = 6.2%, OP = 5.5%). Similarly, at the class level, Clostridia had the highest percentage in both OP patients and HCs (HC = 45%, OP = 44%), followed by Bacteroidia (HC = 35.6%, OP = 39%), Gam-

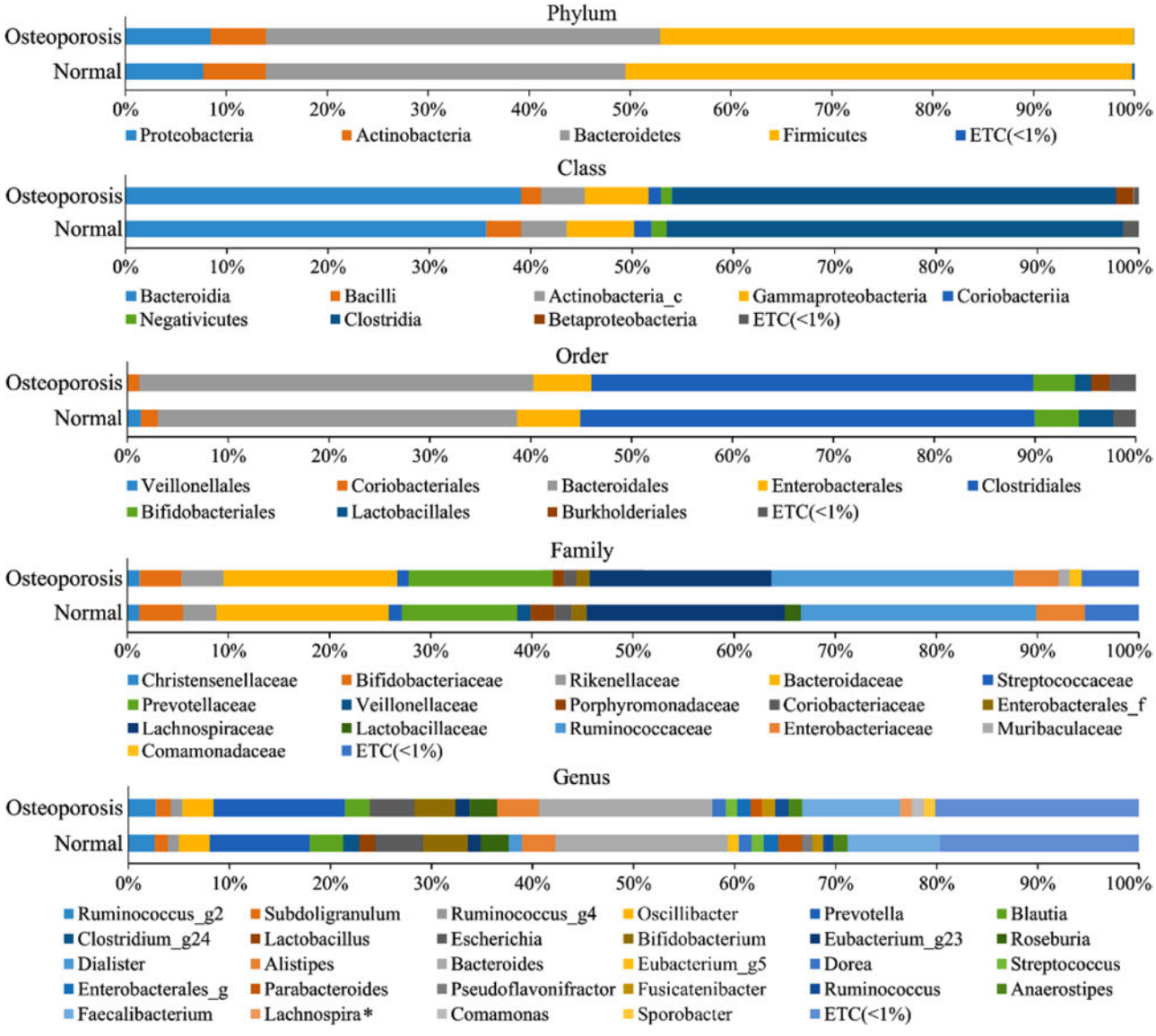


Fig. 2. Average taxonomic compositions of healthy controls (normal) and osteoporosis patient groups. The normal group and osteoporosis (OP) patients were further classified at the phylum,-class, order, family, and genus levels. Those with relative abundances less than 1% were expressed as ETC. Only the *Lachnospira* genus showed a significant difference between the two groups among taxa of all ranks. Statistical significance between groups was analyzed using the Wilcoxon rank-sum test. $^{*}p < 0.05$.

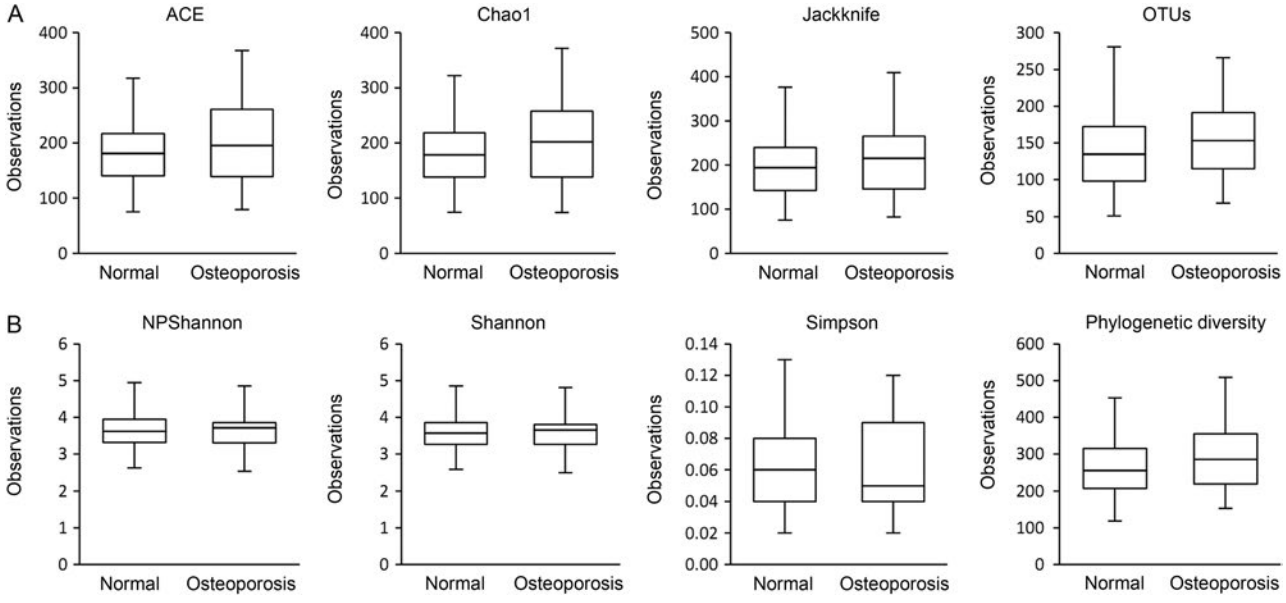


Fig. 3. Alpha diversity indices for stool samples of healthy controls (normal) and osteoporosis (OP) patients. A) Species richness was analyzed with Ace, Chao1, Jackknife, OTUs, and B) Species diversity was analyzed with NPShannon, Shannon, Simpson, and Phylogenetic diversity. The horizontal thick black band represents the median value, and boxplot margins indicate the first and third quartiles. There was no significant difference between the two groups in any analysis results.

maproteobacteria (HC = 6.6%, OP = 6.3%), Actinobacteria (Class) (HC = 4.5%, OP = 4.3%), and Bacilli (HC = 3.4%, OP = 2%). At the order level, Clostridiales (HC = 45%, OP = 43.8%), Bacteroidales (HC = 35.6%, OP = 39%), Enterobacterales (HC = 6.3%, OP = 5.8%), and Bifidobacterailes (HC = 4.4%, OP = 4.1%) were abundant in HC and OP groups. Furthermore, at the family level, *Ruminococcaceae* (HC = 23.3%, OP = 24%) had the highest percentage in abundance, followed by *Lachnospiraceae* (HC = 19.6%, OP = 17.9%), *Bacteroidaceae* (HC = 17.1%, OP = 17.2%), and *Prevotellaceae* (HC = 11.4%, OP = 14.2%). Different genera also showed varied abundance in the two groups of subjects. The five most popular genera in both study groups were *Bacteroides* (HC = 17.05%, OP = 17.7%), *Prevotella* (HC = 9.91%, OP = 13.07%), *Faecalibacterium* (HC = 9.09%, OP = 9.72%), *Escherichia* (HC = 4.75%, OP = 4.41%), and *Bifidobacterium* (HC = 4.38%, OP = 4.12%). The rest of the genera were in lower abundance (Table SI). Our data showed that the genus *Lachnosipra* had a significantly higher abundance in OP patients than in HCs according to ranks of all taxa.

**Alpha diversity analysis.** To determine the alpha diversity index for HC and OP patients' stool samples, we performed multiple statistical analyses (Fig. 3). The species richness was analyzed with Ace, Chao1, Jackknife, and OTUs (Fig. 3A). The species diversity was analyzed with NPShannon, Shannon, Simpson, and Phylogenetic diversity (Fig. 3B). We found that differences between the HC and OP groups were not statistically significant in any analysis. Hence, our data indicated that both groups do not differ in species load.

**Variations of microbiota in OP Patients and HCs.** Our beta set-significance analysis by Jensen-Shannon, Bray-Curtis, Generalized UniFrac, and UniFrac revealed no differences between OP patients and HC at the genera level (Table I). Changes in microbiota between HC and OP patients were also investigated using principal coordinate analysis (PCoA) (Fig. 4). PCoA plots were based on Jensen-Shannon divergence (Fig. 4A), Bray-Curtis (Fig. 4B), generalized UniFrac (Fig. 4C), and uniFrac (Fig. 4D) in two dimensions. Furthermore, OP patients and HCs were categorized individually according to cluster analysis based on the unweighted pair group method with arithmetic means (UPGMA) hierarchical clustering analysis (Fig. 5), including analysis by Jensen-Shannon (Fig. 5A), Bray-Curtis (Fig. 5B), generalized UniFrac (Fig. 5C), and UniFrac (Fig. 5D). UPGMA analysis resulted in no characteristic distinction between OP patients and HCs.

**Taxonomic biomarker discovery.** The results of Kruskal-Wallis *H* tests and LEfSe analysis showed that

Table I
Results of beta set-significance analysis.

| Pair-wise | Species | Genus |
|---|---|---|
| Jensen-Shannon | N.S. ($p = 0.725$) | N.S. ($p = 0.796$) |
| Bray-Curtis | N.S. ($p = 0.463$) | N.S. ($p = 0.173$) |
| Generalized UniFrac | N.S. ($p = 0.616$) | N.S. ($p = 0.631$) |
| UniFrac | N.S. ($p = 0.757$) | N.S. ($p = 0.732$) |

Permutational multivariate analysis of variance (PERMANOVA) was used to determine the beta set significance between osteoporosis (OP) and the normal group (HC).

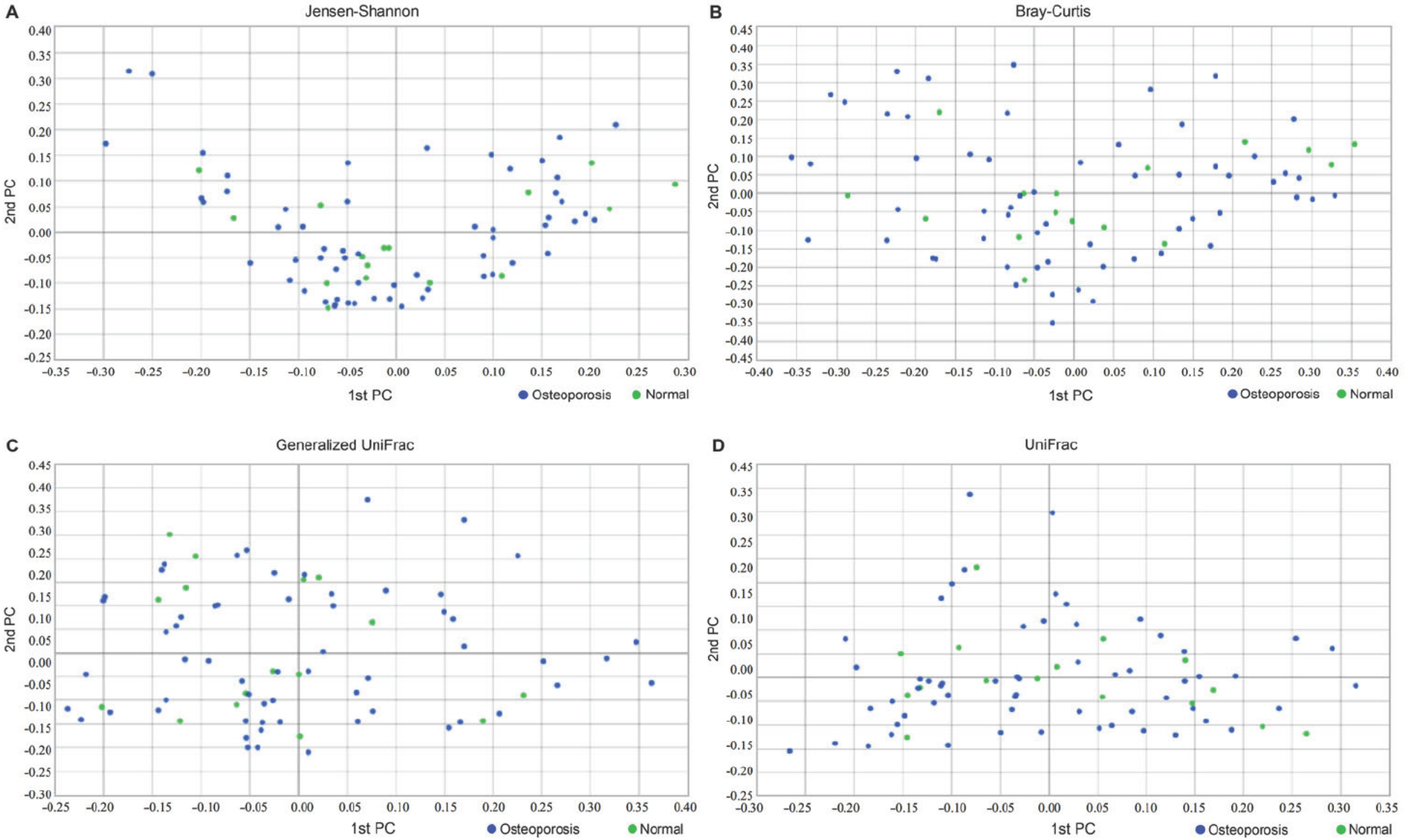


Fig. 4. Principal coordinate analysis (PCoA) of bacterial communities. Clustering using the Unweighted Pair Group Method with Arithmetic mean (UPGMA). Healthy controls (normal) and osteoporosis (OP) patients were analyzed by A) Jensen-Shannon, B) Bray-Curtis, C) Generalized UniFrac, and D) UniFrac.

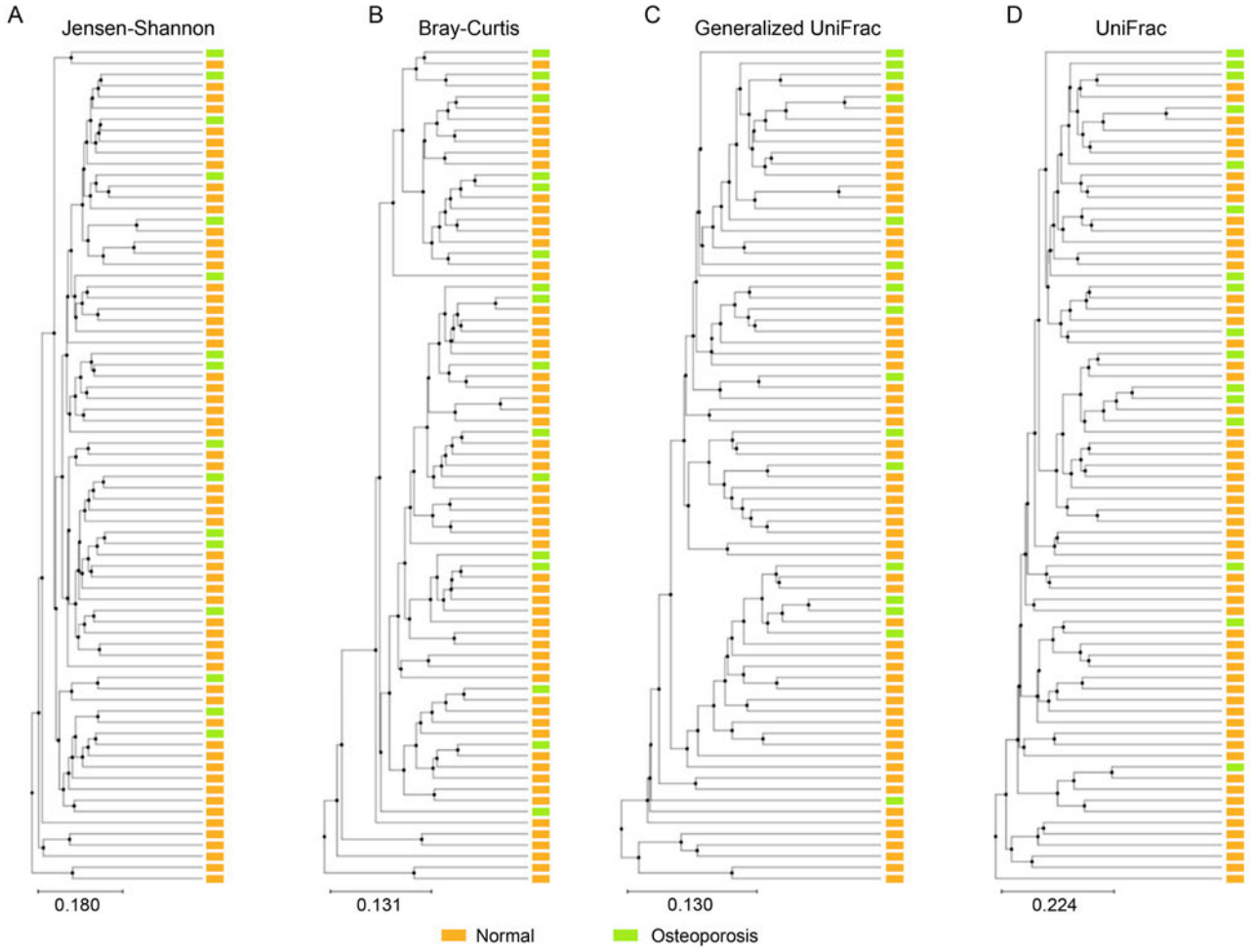


Fig. 5. Clustering using the Unweighted Pair Group Method with Arithmetic mean (UPGMA). Healthy controls (normal) and osteoporosis (OP) patients were analyzed by A) Jensen-Shannon, B) Bray-Curtis, C) Generalized UniFrac, and D) UniFrac.

one order, two families, and six genera were significantly different between the two groups (Fig. 6). The taxonomic groups with $p < 0.05$ and linear discriminant analysis (LDA) effect size > 2 are presented here. Distributions of order Micrococcales (HC = 0.02%, OP = 0.1%), family *Micrococcaceae* (HC = 0.02%, OP = 0.07%), family *Bacillaceae* (HC = 0.02%, OP = 0.06%), genus *Lachnospira* (HC = 0.74%, OP = 1.13%), genus *Solibacillus* (HC = 0.00%, OP = 0.20%), genus *PAC000195_g* (HC = 0.19%, OP = 0.30%), genus *PAC000741_g* (HC = 0.01%, OP = 0.06%), genus *PAC001435_g* (HC = 0.01%, OP = 0.04%), and genus *PAC001231_g* (HC = 0.02%, OP = 0.02%) were increased in OP patients compared to HCs. Our data showed that the *Lachnospira* and *Solibacillus* genera had LDA effect sizes exceeding three (3.26565 and 3.037, respectively). Among them, the *Lachnospira* genus had the highest LDA effect size. It was the only one that showed a significant change among taxa of all ranks.

To find out the relative abundance of *Lachnospira* in OP patients and HCs, we performed a percentage taxonomical abundance test and real-time PCR analysis (Fig. 7). After analyzing the relative taxonomic

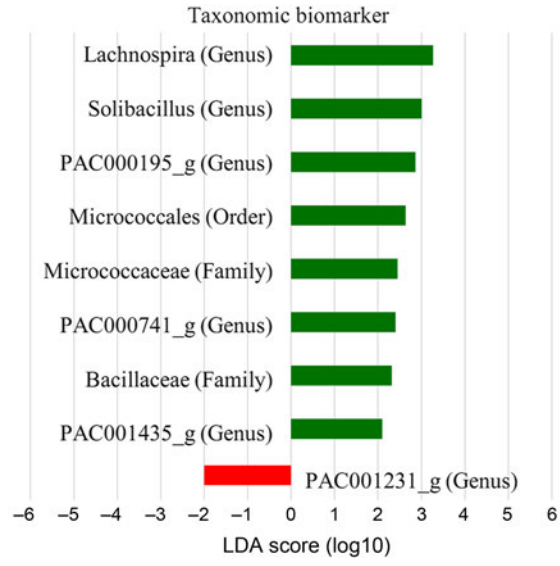


Fig. 6. Distinct taxa identified in healthy controls (normal) and osteoporosis (OP) patients using LEfSe (Linear discriminant analysis Effect Size) analysis. Taxonomic variations with linear discriminant analysis (LDA) scores greater than 2 and significance at $\alpha < 0.05$ as determined by the Kruskal-Wallis test are presented here. The raw data of the above analysis results are presented in Table SIII.

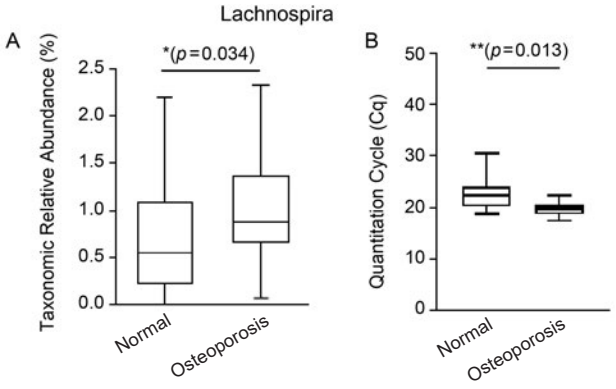


Fig. 7. The taxonomic abundance of the *Lachnospira* genus. Among taxa of all ranks, only the *Lachnospira* genus showed a significant difference in abundance between the two groups.

A) Among 16S gene-based metagenomics analysis results, the relative taxonomic abundance of the *Lachnospira* genus was analyzed, and the Wilcoxon rank-sum test was used for statistical significance, B) this result was verified by real-time PCR. Unpaired Student's *t*-test was applied for statistical significance. The quantification cycle (Cq) value of the osteoporosis (OP) group was lower than that of the normal (HC) group, confirming that the osteoporosis (OP) group contained more *Lachnospira* than the normal group (HC). * $p < 0.05$; ** $p < 0.01$

abundance of the *Lachnospira* genus based on 16S rRNA amplicon sequencing results, it was found that OP patients were significantly rich in *Lachnospira* ($p = 0.034$) (Fig. 7A). Furthermore, qPCR results confirmed the higher abundance of the genus *Lachnospira* in OP patients than in HCs (Fig. 7B). So, these data indicate that the genus *Lachnospira* can be a candidate for taxonomic biomarker discovery of OP.

**Functional pathway prediction.** To investigate the possible functions of gut microbiota found in this investigation, PICRUST was used to identify KEGG functional pathways. Eleven KEGG pathways were projected to change between the osteoporosis and control groups, as illustrated in Fig. 8. HC had functionally ten improved pathways related to peptidoglycan maturation, purine metabolism, geranyl diphosphate biosynthesis, mevalonate pathway, PCO (photorespiratory carbon oxidation) cycle, glycerol degradation pathway, nicotinate pathway, L-valine degradation, creatinine degradation, and biphenyl degradation when compared OP. In contrast, the OP group had elevated pyrimidine biosynthesis than HCs ($p < 0.05$).

## Discussion

The gut microbiota has been identified as a critical factor in several bone-related diseases like gout (Guo et al. 2016; Chu et al. 2021; Lin et al. 2021) and osteoporosis (Wang et al. 2017; Xu et al. 2017; Palacios-González et al. 2020; Rettedal et al. 2021; Wei et al. 2021a). Changes in gut microbiota have been linked to bone homeostasis and bone tissue quality (Sjögren et al. 2012; D'Amelio and Sassi 2018; Cheng et al. 2020; Ni et al. 2021). However, the precise link between gut microbiome composition and osteoporosis is unknown. In this work, the 16S rRNA gene sequencing method was employed to characterize gut microbiota compositions of OP and HC in the Korean population.

Representative indices for microbial richness were studied to explore the relationships between microbial compositions and OP risk in South Korean people. Our

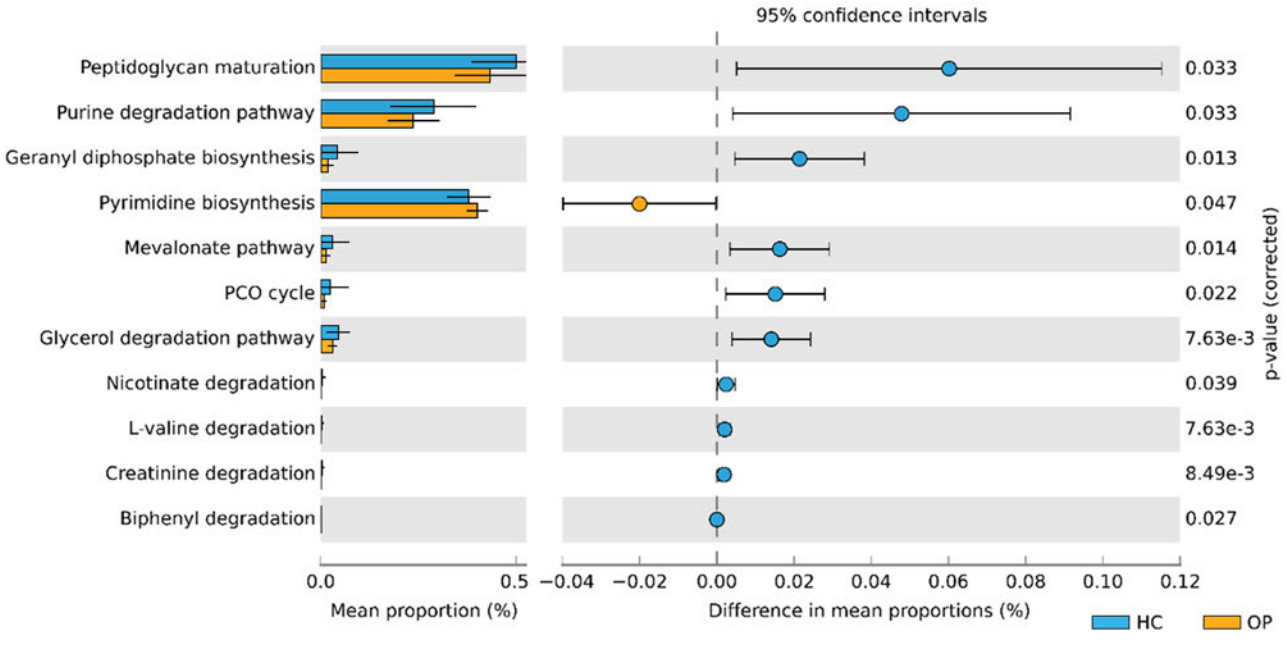


Fig. 8. Functional differences between OP and HC groups. A total of 11 metabolic pathways varied between the two groups. Tests were conducted at Kyoto Encyclopedia of Genes and Genomes (KEGG) using Phylogenetic Investigation of Communities by Reconstruction of Unobserved States (PICRUST) and MetaCyc webserver. PCO, photorespiratory carbon oxidation.

data showed no differences in the average taxonomic composition of OP and HC groups at higher taxa (phylum, class, order, and family) levels. However, only the *Lachnospira* genus was significantly higher among taxa of all ranks in the OP group. Several studies have investigated the relationship between gut microbiota based on taxa and OP proportionate abundances, yielding inconclusive results. Previous studies (Xu et al. 2020; Wei et al. 2021b) have reported increased phylum Bacteroidetes and genera *Bacteroides* in OP patients, while others (Wang et al. 2017) have shown a reduced population of phylum Bacteroidetes in OP patients. However, our data showed a slightly increased population of phylum Bacteroidetes in OP patients, although the increase was not statistically significant (HC = 35.63% vs. OP = 39.04%). Many Gram-negative bacteria of phylum Bacteroidetes have lipopolysaccharide (LPS) in their outer membrane (Eckburg et al. 2005). LPS-induced inflammation is reported to promote osteoclast and bone destruction (Abu-Amer et al. 1997; Zou and Bar-Shavit 2002). One cohort research has found that the relative abundance of the *Lachnospira* genus is increased in those with low bone marrow density (low-BMD) (Palacios-González et al. 2020), consistent with our findings.

Our data showed no significant differences in species richness or diversity between OP and HC groups. This data is consistent with earlier research showing no change in Simpson or Shannon diversity based on the same 16S rRNA sequencing to identify community variations between OP patients and HCs (Das et al. 2019; Xu et al. 2020). One research has found variations in alpha diversity between HCs and OP patients (Wang et al. 2017). However, they studied only six subjects in each group. Thus, their conclusions should be cautiously considered (Wang et al. 2017). So, HC and OP groups can probably not be differentiated based on alpha and beta diversity analysis. Using the LEfse analysis, we identified some taxonomic differences between OP patients and HCs at order, family, and genus levels. After removing possible confounders, our data showed increased abundances for order Micrococcales, families *Micrococcaceae* and *Bacillaceae*, and genera *Lachnospira*, *Solibacillus*, *PAC000195_g*, *PAC000741_g*, and *PAC001435_g* might be linked to an increased risk of OP.

The *Lachnospira* genus is a prominent member of the *Lachnospiraceae* family. *Lachnospira* bacteria are anaerobic, fermentative, and chemoorganotrophic like other family members. Some species of *Lachnospira* have significant hydrolyzing enzymatic activities (Vacca et al. 2020). Furthermore, based on diet intake data and gastrointestinal OTUs, *Lachnospira* was favorably linked to vegetables, fiber consumption, and potassium intake. In contrast, it showed a negative relationship between an omnivorous diet and cholesterol (Di Iorio et al. 2019; De Angelis et al. 2020; Vacca et al. 2020). Naderpoor et al. (2019), in their clinical trials studies, have shown that the vitamin D dose group has a higher population of *Lachnospira* than the control groups. Whisner et al. (2018) have found that the *Lachnospiraceae* family and *Lachnospira* genus are important taxa in college students reporting moderate-to-vigorous physical activity. On the contrary, *Lachnospira* spp. is significantly more abundant in female subjects with obesity and obesity plus metabolic syndrome than in male subjects (Chávez-Carbajal et al. 2019). Based on previous studies, the exact role of the *Lachnospira* genus in different study groups remains unclear. However, our findings revealed that the population of genus *Lachnospira* increased significantly in OP patients. The role of other distinctively prevalent taxa (order Micrococcales, families *Micrococcaceae* and *Bacillaceae*, and genera *Solibacillus*, *PAC000195_g*, *PAC000741_g*, and *PAC001435_g*) in LEfse analysis were not linked to osteoporosis before.

The functional prediction data indicated that several KEGG pathways might play a role in osteoporosis pathogenesis. In our data, the peptidoglycan maturation showed the highest effect size of the other pathways. Many studies have established that peptidoglycan enhances osteoclastogenesis and bone resorption and synergizes osteoclast differentiation with LPS (Kishimoto et al. 2012; Kwon et al. 2021; Ozaki et al. 2021). Some studies indicate that peptidoglycan helps in the upregulation of bone density, facilitating osteoblast differentiation, and diminishing osteoclastogenesis by reducing the RANKL (receptor activator of NF-kB ligand)/OPG (osteoprotegerin) ratio (Sato et al. 2012; Ishida et al. 2015; Chaves de Souza et al. 2016). Our data shows the increased purine degradation pathway in the HC group, but purine metabolism is usually coupled with gout disease. However, some studies indicate that purines (ATP) regulate bone and cartilage metabolism as ATP increases intracellular $Ca^{2+}$ (Yu and Ferrier 1993; 1994; Hoebertz et al. 2003) to facilitate the formation of osteoclast. Geranyl diphosphate and farnesyl pyrophosphate are necessary for protein prenylation and are produced by the mevalonate system. The increased protein prenylation promotes bone resorption rather than creation (Choi et al. 2010; Agabiti et al. 2017; Hasan et al. 2018). Our prediction showed the increased geranyl diphosphate and mevalonate system in HC, which contradicts previous studies for unknown reasons. Valine is a critical metabolic regulator of hematopoietic stem cell (HSCs) or bone marrow cell maintenance (Wilkinson et al. 2018), and Nakauchi (2017) demonstrated that dietary valine restriction emptied the mouse bone marrow niche within two weeks. A study by Huh et al. (2015) showed that creatinine is independently associated with low bone mineral density, affirming our prediction. We could not find the reasons for the elevation of other metabolisms (pyrimidine biosynthesis, PCO cycle,

glycerol degradation pathway, nicotine degradation, and biphenyl degradation) and their role in bone health.

We attempted to develop a flawless study. However, some limitations remained. Firstly, the sample size of OP patients was not large enough. Specially, we obtained only 16 OP patients and 60 HCs. Secondly, OP is more common in postmenopausal females than in males. It is the primary cause of OP (Manolagas 2010). However, we did not analyze the differences between OP males and OP females separately in the present study due to fewer OP patient samples. Furthermore, all participants were from Bucheon city and nearby areas. Because these patients came from a confined area, geographical and climatic parameter variations were minimal. Thus, our findings require confirmations from other locations. Moreover, this study did not perform metabolomics assays to determine the organic compounds involved in the metabolism. Finally, the 16S rRNA sequencing study showed insufficient depth for species identification. The weaknesses above must be addressed further by a future whole-genome sequencing (WGS) study. In addition, some studies indicate the relation between the oral microbiome and osteoporosis (Contaldo et al. 2020; 2021). So, a future study may correlate oral dysbiosis, gut dysbiosis, and osteoporosis. Despite these limitations, our findings provide essential information for the gut microbiota of Korean OP patients. They will have clinical significance for clinicians. However, these findings can be coupled with more precise and accurate techniques like whole genome sequencing and animal model studies.

## Conclusions

Our data shows that a 16S rRNA amplicon sequencing study based on stool samples of OP patients can be used as a new diagnostic parameter for OP. Furthermore, OP patients and HC groups showed differences at the genera level, with OP patients showing a higher population of *Lachnospira*. Thus, *Lachnospira* might play an essential role in OP.

**ORCID**
Asad Ul-Haq https://orcid.org/0000-0002-3602-7980
Hoonhee Seo https://orcid.org/0000-0002-5932-6633
Sujin Jo https://orcid.org/0000-0002-1260-7702
Hyuna Park https://orcid.org/0000-0002-9148-4535
Sukyung Kim https://orcid.org/0000-0002-7963-9776
Youngkyoung Lee https://orcid.org/0000-0001-5426-4050
Saebim Lee https://orcid.org/0000-0002-1017-5408
Ho-Yeon Song https://orcid.org/0000-0003-4429-1383

**Acknowledgments**
This work was supported by a technology innovation program (20018499) funded by the Ministry of Trade, Industry, and Energy (MOTIE), Korea. This research was also supported by the Soonchunhyang University Research Fund and a grant (grant no. NRF-2017R1A2B1005327) of the National Research Foundation of Korea (NRF) funded by the Korean government (MSIT). The bi0 specimens and data used for this study were provided by the Biobank of Soonchunhyang University Bucheon Hospital, a member of the Korea Biobank Network (KBN4_A06). We would also like to thank all the researchers at Soonchunhyang University PMC for their assistance in this study, and Uhjin Song, M.D., for providing medical advice and English proofreading of this manuscript.

**Conflict of interest**
The authors do not report any financial or personal connections with other persons or organizations, which might negatively affect the contents of this publication and/or claim authorship rights to this publication.

## Literature

**Abu-Amer Y, Ross FP, Edwards J, Teitelbaum SL.** Lipopolysaccharide-stimulated osteoclastogenesis is mediated by tumor necrosis factor via its P55 receptor. J Clin Invest. 1997 Sep 15;100(6):1557–1565. https://doi.org/10.1172/JCI119679

**Agabiti SS, Li J, Wiemer AJ.** Geranylgeranyl diphosphate synthase inhibition induces apoptosis that is dependent upon GGPP depletion, ERK phosphorylation and caspase activation. Cell Death Dis. 2017 Mar;8(3):e2678–e2678. https://doi.org/10.1038/cddis.2017.101

**Beals EW.** Bray-Curtis Ordination: An effective strategy for analysis of multivariate ecological data. In: MacFadyen A, Ford ED, editors. Advances in ecological research. London (UK): Academic Press; 1984. p. 1–55. https://doi.org/10.1016/S0065-2504(08)60168-3

**Burnham KP, Overton WS.** Robust estimation of population size when capture probabilities vary among animals. Ecology. 1979; 60(5):927–936. https://doi.org/10.2307/1936861

**Camacho PM, Petak SM, Binkley N, Clarke BL, Harris ST, Hurley DL, Kleerekoper M, Lewiecki EM, Miller PD, Narula HS, et al.** American Association of Clinical Endocrinologists and American College of Endocrinology Clinical Practice Guidelines for the diagnosis and treatment of postmenopausal osteoporosis – 2016 – Executive Summary. Endocr Pract. 2016;22(9):1111–1118. https://doi.org/10.4158/EP161435.ESGL

**Cannarella R, Barbagallo F, Condorelli RA, Aversa A, La Vignera S, Calogero AE.** Osteoporosis from an endocrine perspective: the role of hormonal changes in the elderly. J Clin Med. 2019 Oct 01; 8(10):1564. https://doi.org/10.3390/jcm8101564

**Chao A, Lee SM.** Estimating the number of classes via sample coverage. J Am Stat Assoc. 1992;87(417):210–217. https://doi.org/10.1080/01621459.1992.10475194

**Chao A, Shen TJ.** Nonparametric estimation of Shannon's index of diversity when there are unseen species in sample. Environ Ecol Stat. 2003;10(4):429–443. https://doi.org/10.1023/A:1026096204727

**Chao A.** Estimating the population size for capture-recapture data with unequal catchability. Biometrics. 1987 Dec;43(4):783–791. https://doi.org/10.2307/2531532

**Charles JF, Ermann J, Aliprantis AO.** The intestinal microbiome and skeletal fitness: connecting bugs and bones. Clin Immunol. 2015 Aug;159(2):163–169. https://doi.org/10.1016/j.clim.2015.03.019

**Chaves de Souza JA, Frasnelli SCT, Curylofo-Zotti FA, Ávila-Campos MJ, Spolidório LC, Zamboni DS, Graves DT, Rossa C Jr.** *NOD1* in the modulation of host-microbe interactions and inflammatory bone resorption in the periodontal disease model. Immunology. 2016 Dec;149(4):374–385. https://doi.org/10.1111/imm.12654

**Chávez-Carbajal A, Nirmalkar K, Pérez-Lizaur A, Hernández-Quiroz F, Ramírez-del-Alto S, García-Mena J, Hernández-Guerrero C.** Gut microbiota and predicted metabolic pathways in a sample of Mexican women affected by obesity and obesity plus metabolic syndrome. Int J Mol Sci. 2019 Jan 21;20(2):438. https://doi.org/10.3390/ijms20020438

**Chen J, Bittinger K, Charlson ES, Hoffmann C, Lewis J, Wu GD, Collman RG, Bushman FD, Li H.** Associating microbiome composition with environmental covariates using generalized UniFrac distances. Bioinformatics. 2012 Aug 15;28(16):2106–2113. https://doi.org/10.1093/bioinformatics/bts342

**Cheng S, Qi X, Ma M, Zhang L, Cheng B, Liang C, Liu L, Li P, Kafle OP, Wen Y, et al.** Assessing the relationship between gut microbiota and bone mineral density. Front Genet. 2020 Jan 31;11:6. https://doi.org/10.3389/fgene.2020.00006

**Choi HJ, Choi JY, Cho SW, Kang D, Han KO, Kim SW, Kim SY, Chung YS, Shin CS.** Genetic polymorphism of geranylgeranyl diphosphate synthase (GGSP1) predicts bone density response to bisphosphonate therapy in Korean women. Yonsei Med J. 2010; 51(2): 231–238. https://doi.org/10.3349/ymj.2010.51.2.231

**Chu Y, Sun S, Huang Y, Gao Q, Xie X, Wang P, Li J, Liang L, He X, Jiang Y, et al.** Metagenomic analysis revealed the potential role of gut microbiome in gout. NPJ Biofilms Microbiomes. 2021 Aug 9;7(1):66. https://doi.org/10.1038/s41522-021-00235-2

**Contaldo M, Fusco A, Stiuso P, Lama S, Gravina AG, Itro A, Federico A, Itro A, Dipalma G, Inchingolo F, et al.** Oral microbiota and salivary levels of oral pathogens in gastro-intestinal diseases: current knowledge and exploratory study. Microorganisms. 2021 May 14;9(5):1064. https://doi.org/10.3390/microorganisms9051064

**Contaldo M, Itro A, Lajolo C, Gioco G, Inchingolo F, Serpico R.** Overview on osteoporosis, periodontitis and oral dysbiosis: the emerging role of oral microbiota. Appl Sci (Basel). 2020 Aug 29; 10(17): 6000. https://doi.org/10.3390/app10176000

**D'Amelio P, Sassi F.** Gut microbiota, immune system, and bone. Calcif Tissue Int. 2018 Apr;102(4):415–425. https://doi.org/10.1007/s00223-017-0331-y

**Das M, Cronin O, Keohane DM, Cormac EM, Nugent H, Nugent M, Molloy C, O'Toole PW, Shanahan F, Molloy MG, et al.** Gut microbiota alterations associated with reduced bone mineral density in older adults. Rheumatology. 2019 Dec 01;58(12):2295–2304. https://doi.org/10.1093/rheumatology/kez302

**De Angelis M, Ferrocino I, Calabrese FM, De Filippis F, Cavallo N, Siragusa S, Rampelli S, Di Cagno R, Rantsiou K, Vannini L, et al.** Diet influences the functions of the human intestinal microbiome. Sci Rep. 2020 Dec;10(1):4247. https://doi.org/10.1038/s41598-020-61192-y

**Di Iorio BR, Rocchetti MT, De Angelis M, Cosola C, Marzocco S, Di Micco L, di Bari I, Accetturo M, Vacca M, Gobbetti M, et al.** Nutritional therapy modulates intestinal microbiota and reduces serum levels of total and free indoxyl sulfate and p-cresyl sulfate in chronic kidney disease (Medika study). J Clin Med. 2019 Sep 10; 8(9):1424. https://doi.org/10.3390/jcm8091424

**Ding K, Hua F, Ding W.** Gut microbiome and osteoporosis. Aging Dis. 2020;11(2):438–447. https://doi.org/10.14336/AD.2019.0523

**Douglas GM, Maffei VJ, Zaneveld JR, Yurgel SN, Brown JR, Taylor CM, Huttenhower C, Langille MGI.** PICRUSt2 for prediction of metagenome functions. Nat Biotechnol. 2020 Jun;38(6):685–688. https://doi.org/10.1038/s41587-020-0548-6

**Eckburg PB, Bik EM, Bernstein CN, Purdom E, Dethlefsen L, Sargent M, Gill SR, Nelson KE, Relman DA.** Diversity of the human intestinal microbial flora. Science. 2005 Jun 10;308(5728):1635–1638. https://doi.org/10.1126/science.1110591

**Edgar RC, Haas BJ, Clemente JC, Quince C, Knight R.** UCHIME improves sensitivity and speed of chimera detection. Bioinformatics. 2011 Aug 15;27(16):2194–2200. https://doi.org/10.1093/bioinformatics/btr381

**Faith DP.** Conservation evaluation and phylogenetic diversity. Biol Conserv. 1992;61(1):1–10. https://doi.org/10.1016/0006-3207(92)91201-3

**Guarner F, Malagelada JR.** Gut flora in health and disease. Lancet. 2003 Feb;361(9356):512–519. https://doi.org/10.1016/S0140-6736(03)12489-0

**Guarner F, Schaafsma GJ.** Probiotics. Int J Food Microbiol. 1998 Feb 17;39(3):237–238. https://doi.org/10.1016/S0168-1605(97)00136-0

**Guo Z, Zhang J, Wang Z, Ang KY, Huang S, Hou Q, Su X, Qiao J, Zheng Y, Wang L, et al.** Intestinal microbiota distinguish gout patients from healthy humans. Sci Rep. 2016 Feb;6(1):20602. https://doi.org/10.1038/srep20602

**Hamady M, Lozupone C, Knight R.** Fast UniFrac: facilitating high-throughput phylogenetic analyses of microbial communities including analysis of pyrosequencing and PhyloChip data. ISME J. 2010 Jan;4(1):17–27. https://doi.org/10.1038/ismej.2009.97

**Hasan WNW, Chin KY, Jolly JJ, Ghafar NA, Soelaiman IN.** Identifying potential therapeutics for osteoporosis by exploiting the relationship between mevalonate pathway and bone metabolism. Endocr Metab Immune Disord Drug Targets. 2018 Aug 28;18(5): 450–457. https://doi.org/10.2174/1871530318666180423122409

**Hoebertz A, Arnett TR, Burnstock G.** Regulation of bone resorption and formation by purines and pyrimidines. Trends Pharmacol Sci. 2003 Jun;24(6):290–297. https://doi.org/10.1016/S0165-6147(03)00123-8

**Huh JH, Choi SI, Lim JS, Chung CH, Shin JY, Lee MY.** Lower serum creatinine is associated with low bone mineral density in subjects without overt nephropathy. PLoS One. 2015 Jul 24; 10(7): e0133062–e0133062. https://doi.org/10.1371/journal.pone.0133062

**Ishida M, Kitaura H, Kimura K, Sugisawa H, Aonuma T, Takada H, Takano-Yamamoto T.** Muramyl dipeptide enhances lipopolysaccharide-induced osteoclast formation and bone resorption through increased RANKL expression in stromal cells. J Immunol Res. 2015; 2015:1–12. https://doi.org/10.1155/2015/132765

**Kanis JA.** Assessment of osteoporosis at the primary health-care level. Technical Report. Sheffield (UK): World Health Organization Collaborating Centre for Metabolic Bone Diseases, University of Sheffield; 2008. https://www.sheffield.ac.uk/FRAX/

**Kim S, Seo H, Rahim MA, Tajdozian H, Kim YS, Song HY.** Characteristics of vaginal microbiome in women with pelvic inflammatory disease in Korea. Pol J Microbiol. 2021 Sep 01;70(3):345–357. https://doi.org/10.33073/pjm-2021-033

**Kishimoto T, Kaneko T, Ukai T, Yokoyama M, Ayon Haro R, Yoshinaga Y, Yoshimura A, Hara Y.** Peptidoglycan and lipopolysaccharide synergistically enhance bone resorption and osteoclastogenesis. J Periodontal Res. 2012 Aug;47(4):446–454. https://doi.org/10.1111/j.1600-0765.2011.01452.x

**Kruskal WH, Wallis WA.** Use of ranks in one-criterion variance analysis. J Am Stat Assoc. 1952;47(260):583–621. https://doi.org/10.1080/01621459.1952.10483441

**Kwon Y, Park C, Lee J, Park DH, Jeong S, Yun CH, Park OJ, Han SH.** Regulation of bone cell differentiation and activation by microbe-associated molecular patterns. Int J Mol Sci. 2021 May 28; 22(11):5805. https://doi.org/10.3390/ijms22115805

**Li C, Huang Q, Yang R, Dai Y, Zeng Y, Tao L, Li X, Zeng J, Wang Q.** Gut microbiota composition and bone mineral loss – epidemiologic evidence from individuals in Wuhan, China. Osteoporos Int. 2019 May;30(5):1003–1013. https://doi.org/10.1007/s00198-019-04855-5

**Li JY, Chassaing B, Tyagi AM, Vaccaro C, Luo T, Adams J, Darby TM, Weitzmann MN, Mulle JG, Gewirtz AT, et al.** Sex steroid deficiency-associated bone loss is microbiota dependent and prevented by probiotics. J Clin Invest. 2016 Apr 25;126(6):2049–2063. https://doi.org/10.1172/JCI86062

**Li S, Mao Y, Zhou F, Yang H, Shi Q, Meng B.** Gut microbiome and osteoporosis: a review. Bone Joint Res. 2020 Aug 01;9(8):524–530. https://doi.org/10.1302/2046-3758.98.BJR-2020-0089.R1

**Lin J.** Divergence measures based on the Shannon entropy. IEEE Trans Inf Theory. 1991 Jan;37(1):145–151. https://doi.org/10.1109/18.61115

**Lin S, Zhang T, Zhu L, Pang K, Lu S, Liao X, Ying S, Zhu L, Xu X, Wu J, et al.** Characteristic dysbiosis in gout and the impact of a uric acid-lowering treatment, febuxostat on the gut microbiota. J Genet Genomics. 2021 Sep;48(9):781–791. https://doi.org/10.1016/j.jgg.2021.06.009

**Liu R, Peng C, Jing D, Xiao Y, Zhu W, Zhao S, Zhang J, Chen X, Li J.** Lachnospira is a signature of antihistamine efficacy in chronic spontaneous urticaria. Exp Dermatol. 2022 Feb;31(2):242–247. https://doi.org/10.1111/exd.14460

**Magurran AE.** Measuring biological diversity. Malden (USA), Oxford (UK), Carleton (Australia): Wiley-Blackwell; 2013.

**Manolagas SC.** From estrogen-centric to aging and oxidative stress: a revised perspective of the pathogenesis of osteoporosis. Endocr Rev. 2010 Jun 01;31(3):266–300. https://doi.org/10.1210/er.2009-0024

**Myers EW, Miller W.** Optimal alignments in linear space. Comput Appl Biosci. 1988 Mar;4(1):11–17. https://doi.org/10.1093/bioinformatics/4.1.11

**Naderpoor N, Mousa A, Fernanda Gomez Arango L, Barrett HL, Dekker Nitert M, de Courten B.** Effect of vitamin D supplementation on faecal microbiota: A randomised clinical trial. Nutrients. 2019 Nov 27;11(12):2888. https://doi.org/10.3390/nu11122888

**Nakauchi H.** Valine as a key metabolic regulator of hematopoietic stem cell maintenance. Blood. 2017 Dec 07;130(Suppl_1):SCI-20. https://doi.org/10.1182/blood.V130.Suppl_1.SCI-20.SCI-20

**Ni JJ, Yang XL, Zhang H, Xu Q, Wei XT, Feng GJ, Zhao M, Pei YF, Zhang L.** Assessing causal relationship from gut microbiota to heel bone mineral density. Bone. 2021 Feb;143:115652. https://doi.org/10.1016/j.bone.2020.115652

**Ozaki Y, Kishimoto T, Yamashita Y, Kaneko T, Higuchi K, Mae M, Oohira M, Mohammad AI, Yanagiguchi K, Yoshimura A.** Expression of osteoclastogenic and anti-osteoclastogenic cytokines differs in mouse gingiva injected with lipopolysaccharide, peptidoglycan, or both. Arch Oral Biol. 2021 Feb;122:104990. https://doi.org/10.1016/j.archoralbio.2020.104990

**Palacios-González B, Ramírez-Salazar EG, Rivera-Paredez B, Quiterio M, Flores YN, Macias-Kauffer L, Moran-Ramos S, Denova-Gutiérrez E, Ibarra-González I, Vela-Amieva M, et al.** A multi-omic analysis for low bone mineral density in postmenopausal women suggests a relationship between diet, metabolites, and microbiota. Microorganisms. 2020 Oct 22;8(11):1630. https://doi.org/10.3390/microorganisms8111630

**Pandey KR, Naik SR, Vakil BV.** Probiotics, prebiotics and synbiotics – A review. J Food Sci Technol. 2015 Dec;52(12):7577–7587. https://doi.org/10.1007/s13197-015-1921-1

**Peng X, Wu X, Zhang J, Zhang G, Li G, Pan X.** The role of CKIP-1 in osteoporosis development and treatment. Bone Joint Res. 2018 Feb;7(2):173–178. https://doi.org/10.1302/2046-3758.72.BJR-2017-0172.R1

**Rettedal EA, Ilesanmi-Oyelere BL, Roy NC, Coad J, Kruger MC.** The gut microbiome is altered in postmenopausal women with osteoporosis and osteopenia. JBMR Plus. 2021 Mar;5(3):e10452. https://doi.org/10.1002/jbm4.10452

**Rognes T, Flouri T, Nichols B, Quince C, Mahé F.** VSEARCH: a versatile open source tool for metagenomics. PeerJ. 2016 Oct 18; 4:e2584. https://doi.org/10.7717/peerj.2584

**Sato T, Watanabe K, Kumada H, Toyama T, Tani-Ishii N, Hamada N.** Peptidoglycan of *Actinomyces naeslundii* induces inflammatory cytokine production and stimulates osteoclastogenesis in alveolar bone resorption. Arch Oral Biol. 2012 Nov;57(11):1522–1528. https://doi.org/10.1016/j.archoralbio.2012.07.012

**Segata N, Izard J, Waldron L, Gevers D, Miropolsky L, Garrett WS, Huttenhower C.** Metagenomic biomarker discovery and explanation. Genome Biol. 2011 Jun 24;12(6):R60. https://doi.org/10.1186/gb-2011-12-6-r60

**Scholz-Ahrens KE, Ade P, Marten B, Weber P, Timm W, Açil Y, Glüer CC, Schrezenmeir J.** Prebiotics, probiotics, and synbiotics affect mineral absorption, bone mineral content, and bone structure. J Nutr. 2007 Mar 01;137(3) Suppl 2:838S–846S. https://doi.org/10.1093/jn/137.3.838S

**Sjögren K, Engdahl C, Henning P, Lerner UH, Tremaroli V, Lagerquist MK, Bäckhed F, Ohlsson C.** The gut microbiota regulates bone mass in mice. J Bone Miner Res. 2012 Jun;27(6):1357–1367. https://doi.org/10.1002/jbmr.1588

**Stecher B, Hardt WD.** The role of microbiota in infectious disease. Trends Microbiol. 2008 Mar;16(3):107–114. https://doi.org/10.1016/j.tim.2007.12.008

**Tang CH.** Osteoporosis: from molecular mechanisms to therapies. Int J Mol Sci. 2020 Jan 22;21(3):714. https://doi.org/10.3390/ijms21030714

**Tavakoli S, Xiao L.** Depletion of intestinal microbiome partially rescues bone loss in sickle cell disease male mice. Sci Rep. 2019 Dec; 9(1):8659. https://doi.org/10.1038/s41598-019-45270-4

**Tu KN, Lie JD, Wan CKV, Cameron M, Austel AG, Nguyen JK, Van K, Hyun D.** Osteoporosis: a review of treatment options. PT. 2018 Feb;43(2):92–104.

**Uchida Y, Irie K, Fukuhara D, Kataoka K, Hattori T, Ono M, Ekuni D, Kubota S, Morita M.** Commensal microbiota enhance both osteoclast and osteoblast activities. Molecules. 2018 Jun 23; 23(7):1517. https://doi.org/10.3390/molecules23071517

**ul-Haq A, Lee KA, Seo H, Kim S, Jo S, Ko KM, Moon SJ, Kim YS, Choi JR, Song HY, Kim HS.** Characteristic alterations of gut microbiota in uncontrolled gout. J Microbiol. 2022 Dec;60(12):1178–1190. https://doi.org/10.1007/s12275-022-2416-1

**Vacca M, Celano G, Calabrese FM, Portincasa P, Gobbetti M, De Angelis M.** The controversial role of human gut *Lachnospiraceae*. Microorganisms. 2020 Apr 15;8(4):573. https://doi.org/10.3390/microorganisms8040573

**Wade SW, Strader C, Fitzpatrick LA, Anthony MS, O'Malley CD.** Estimating prevalence of osteoporosis: examples from industrialized countries. Arch Osteoporos. 2014 Dec;9(1):182. https://doi.org/10.1007/s11657-014-0182-3

**Wang H, Wei CX, Min L, Zhu LY.** Good or bad: gut bacteria in human health and diseases. Biotechnol Biotechnol Equip. 2018 Sep 03; 32(5):1075–1080. https://doi.org/10.1080/13102818.2018.1481350

**Wang J, Wang Y, Gao W, Wang B, Zhao H, Zeng Y, Ji Y, Hao D.** Diversity analysis of gut microbiota in osteoporosis and osteopenia patients. PeerJ. 2017 Jun 15;5:e3450. https://doi.org/10.7717/peerj.3450

**Wei M, Li C, Dai Y, Zhou H, Cui Y, Zeng Y, Huang Q, Wang Q.** High-throughput absolute quantification sequencing revealed osteoporosis-related gut microbiota alterations in Han Chinese elderly. Front Cell Infect Microbiol. 2021a Apr 30;11:630372. https://doi.org/10.3389/fcimb.2021.630372

**Wei M, Li C, Dai Y, Zhou H, Cui Y, Zeng Y, Huang Q, Wang Q.** High-throughput absolute quantification sequencing revealed osteoporosis-related gut microbiota alterations in Han Chinese elderly. Front Cell Infect Microbiol. 2021b Apr 30;11(381):630372. https://doi.org/10.3389/fcimb.2021.630372

**Wheeler TJ, Eddy SR.** nhmmer: DNA homology search with profile HMMs. Bioinformatics. 2013 Oct 1;29(19):2487–2489. https://doi.org/10.1093/bioinformatics/btt403

**Whisner CM, Maldonado J, Dente B, Krajmalnik-Brown R, Bruening M.** Diet, physical activity and screen time but not body

mass index are associated with the gut microbiome of a diverse cohort of college students living in university housing: a cross-sectional study. BMC Microbiol. 2018 Dec;18(1):210–210. https://doi.org/10.1186/s12866-018-1362-x

**Wilkinson AC, Morita M, Nakauchi H, Yamazaki S.** Branched-chain amino acid depletion conditions bone marrow for hematopoietic stem cell transplantation avoiding amino acid imbalance-associated toxicity. Exp Hematol. 2018 Jul;63:12–16.e1. https://doi.org/10.1016/j.exphem.2018.04.004

**Xu X, Jia X, Mo L, Liu C, Zheng L, Yuan Q, Zhou X.** Intestinal microbiota: a potential target for the treatment of postmenopausal osteoporosis. Bone Res. 2017 Dec;5(1):17046. https://doi.org/10.1038/boneres.2017.46

**Xu Z, Xie Z, Sun J, Huang S, Chen Y, Li C, Sun X, Xia B, Tian L, Guo C, et al.** Gut microbiome reveals specific dysbiosis in primary osteoporosis. Front Cell Infect Microbiol. 2020 Apr 21;10(160):160. https://doi.org/10.3389/fcimb.2020.00160

**Yan J, Herzog JW, Tsang K, Brennan CA, Bower MA, Garrett WS, Sartor BR, Aliprantis AO, Charles JF.** Gut microbiota induce IGF-1 and promote bone formation and growth. Proc Natl Acad Sci USA. 2016 Nov 22;113(47):E7554–E7563. https://doi.org/10.1073/pnas.1607235113

**Ye Y, Doak TG.** A parsimony approach to biological pathway reconstruction/inference for genomes and metagenomes. PLoS Comput Biol. 2009 Aug;5(8):e1000465. https://doi.org/10.1371/journal.pcbi.1000465

**Yoon SH, Ha SM, Kwon S, Lim J, Kim Y, Seo H, Chun J.** Introducing EzBioCloud: a taxonomically united database of 16S rRNA gene sequences and whole-genome assemblies. Int J Syst Evol Microbiol. 2017 May;67(5):1613–1617. https://doi.org/10.1099/ijsem.0.001755

**Yu HS, Ferrier J.** ATP induces an intracellular calcium pulse in osteoclasts. Biochem Biophys Res Commun. 1993 Mar;191(2):357–363. https://doi.org/10.1006/bbrc.1993.1225

**Yu H, Ferrier J.** Mechanisms of ATP-induced $Ca^{2+}$ signaling in osteoclasts. Cell Signal. 1994 Nov;6(8):905–914. https://doi.org/10.1016/0898-6568(94)90023-X

**Zaheer S, LeBoff MS.** Osteoporosis: prevention and treatment. [Updated 2018 Nov 26]. In: Feingold KR, Anawalt B, Boyce A, Chrousos G, de Herder WW, Dhatariya K, Dungan K, Hershman JM, Hofland J, Kalra S, et al, editors. Endotext [Internet]. South Dartmouth (USA): MDText.com, Inc.; 2000– [cited 2022 May 30]. Available from https://www.ncbi.nlm.nih.gov/books/NBK279073/

**Zheng W, Liu C, Lei M, Han Y, Zhou X, Li C, Sun S, Ma X.** Evaluation of common variants in the *CNR2* gene and its interaction with abdominal obesity for osteoporosis susceptibility in Chinese postmenopausal females. Bone Joint Res. 2019 Nov;8(11):544–549. https://doi.org/10.1302/2046-3758.811.BJR-2018-0284.R1

**Zou W, Bar-Shavit Z.** Dual modulation of osteoclast differentiation by lipopolysaccharide. J Bone Miner Res. 2002 Jul;17(7):1211–1218. https://doi.org/10.1359/jbmr.2002.17.7.1211

Supplementary materials are available on the journal's website.

Polish Journal of Microbiology
2022, Vol. 71, No 4

# CONTENTS

## Vol. 71, 1–4, 2022

## No 1

## No 2

MINIREVIEWS



ORIGINAL PAPERS

## No 3

ORIGINAL PAPERS

## No 4

**Polish Journal of Microbiology**
**Vol. 71, 1–4, 2022**

## ACKNOWLEDGEMENTS

**The editors of the Polish Journal of Microbiology wish to express their gratitude to colleagues who have reviewed the manuscripts submitted to our Journal in the past year**

**A**

Abbas Aqleem (China), Adams Philip (USA), Ahire Jayesh J. (India), Akimbekov Nuraly (Kazakhstan), Albarracin Virginia H. (Argentina), Aljohny Bassam (United Kingdom), Andreani Nadia Andrea (Germany), Azman Kasan Nor (Malaysia)

**B**

Bai Peter (Hungary), Balmaseda Rubina Aitor (Spain), Balzan Claudia (Brazil), Banerjee Aparna (Chile), Baxter Katherine (United Kingdom), Beev Georgi (Bulgaria), Beresfort Tony (Ireland), Berger Fabian (Germany), Bhagat Neeta (India), Bogut Agnieszka (Poland), Bottalico Lucrezia (Italy), Bowers Samuel J. (USA), Bucha Michał (Poland), Buttimer Colin (Ireland)

**C**

Cabrera Vignoli Rafael (Uruguay), Capozzi Vittorio (Italy), Chen Kaisen (China), Clayton Salano (Kenya), Codella Roberto (Italy), Consolato M. Sergi (Canada), Cowan Ashton Keith (South Africa), Cyplik Paweł (Poland)

**D**

D'Erme Maria (Italy), Dalisay Doralyn (Philippines), Dandekar Ajai A. (USA), Das Shankar Prasad (India), de Cock Hans (Netherlands), Drywień Małgorzata (Poland) Du Xin (USA)

**E**

Effmert Uta (Germany), Evanovich Eliane (Brazil)

**F**

Fasciana Teresa (Italy), Foster Tim (Ireland), Frôhlich Eleonore (Germany), Furusawa Go (Malaysia)

**G**

Gautam Ablesh (India), Gebel Jürgen (Germany), Ghosh Abjrajyoti (India), Gong Bin (China), Gonzales-Garcia Natalia (Ireland), Grudlewska-Buda Katarzyna (Poland), Guran Mumtaz (Turkey), Guzek Aneta (Poland)

**H**

Haddad Gabriel G. (USA), Haddix Pryce L. (USA), Hampl Richard (Czech Republic), Hannan Anthony (Australia), He Qi (China), Hemamalini Nallaiah (India), Hong Xiang (China), Horth Roberta Z. (USA)

**I**

Iseppi Ramona (Italy)

**J**

Jarvis Karen (USA), Jenneman Gary E. (USA), Jha Hem Chandra (India), Job Katarzyna (Poland), Johny Lidiya C. (India)

**K**

Kalka Joanna (Poland), Kampf Günter (Germany), Kiriakidis Joannis (Greece), Kobayashi Nobumuchi (Japan), Komatsu Yasuhiko (Japan), Kopke Salinas Roberto (Brazil), Kot Barbara (Poland), Kruyova Marcela (Czech Republic), Krzowski Łukasz (Polska), Kunicka-Styczyńska Alina (Poland), Kunishima Hiroyuki (Japan), Kuyukina Maria S. (Russian Federation)

**L**

Leon Felix Josefina (Mexico), Liu Bing-Bing (China), Liu Huan (China), Liu Mao Ke (China), Lohans Christopher (Canada)

**M**

Maki Katherine (USA), Maki Katherine (USA), Malm Anna (Poland), Mandal Santi M. (India), Markovska Rumyana (Bulgaria), Marschall Jonas (USA), Martirosian Gayane (Poland), Masi Chandran (Ethiopia), Mastroleo Felice (Belgium), Meaden Sean (United Kingdom), Menes Rodolfo Javier (Uruguay), Merakou Christina (Italy), Międzobrodzki Jacek (Poland), Miller Aaron (USA), Mirzazadeh Majid (USA), Mistry Nerges (India), Morales Megan (USA), Moya-Elizando Ernesto A. (Chile), Mwirichia Romano (Kenya)

**N**

Narsing Rao Manik Prabhu (China), Nimaichand Salam (Indonesia), Nweze Justus Amuche (Nigeria)

**P**

Pancer Katarzyna (Poland), Pessione Enrica (Italy), Petrova Penka (Bulgaria), Pirs Mateja (Slovenia), Plociński Przemysław (Poland), Prajapati Ajay Kumar (India), Prisic Sladjana (USA)

**R**

Rajasabapathy Raju (India), Rega Martina (Italy), Rivera-Morales Lydia Guadalupe (Mexico), Root-Bernstein Robert (USA), Rotondo John Charles (Italy), Różalska Barbara (Poland), Różanska Anna (Poland), Rubina Aitor Balmaseda (Spain)

**S**

Saginala Kaylan (USA), Sahoo Suban K. (India), Schröder Maria (Germany), Sharma Dipali (USA), Sharma Savitri (India), Sharna Rohit (India), Sieniawska Elwira (Poland), Sikora Anna (Poland), Sitarz Robert (Polska), Smułek Wojciech (Poland), Sturov Nikolay (Russian Federation), Swift Joel (USA), Szymańska-Czerwińska Monika (Poland)

**T**

Taylor-Brown Alyce (Unied Kingdom), Tessier Elisabeth M. (USA), Tileklioglu Evren (Turkey), Tong Ai-Zi (China), Touchette David (Canada), Trafny Elżbieta Anna (Poland)

**U**

Ugbenyen Anthony M. (South Africa), Ullah Hanif (China)

**V**

Vahdati Kourosh (Iran), Valencia Rivera Dora E. (Mexico), Velazquez-Guadarrama Norma (Mexico), Velkov Tony (Australia), Vielot Nadja A. (USA), Vu Loi (Germany)

**W**

Wang Tao (USA), Wang Yingjie (China), Westerveld Sean (Canada), Wolff Jose Luiz (Brazil)

**X**

Xu Henglong (China), Xu Ming (China)

**Z**

Zadjelovic Vinko (United Kingdom), Zhang Lujia (China), Zheng Mengyuan (USA), Zilbeyaz Kani (Turkey)

**Polish Journal of Microbiology**
**Vol. 71, 1–4, 2022**

# Author Index

Polish Journal of Microbiology
2022, Vol. 71, No 4, 625–628

# INFORMACJE Z POLSKIEGO TOWARZYSTWA MIKROBIOLOGÓW

Od ostatniej informacji o działalności Zarządu Głównego Polskiego Towarzystwa Mikrobiologów, zamieszczonej w zeszytach nr 3 z 2022 r. kwartalników *Advancements of Mikrobiologia – Postępy Mikrobiologii* i *Polish Journal of Microbiology*, ZG PTM zajmował się następującymi sprawami:

1. Z głębokim żalem zawiadamiamy, że w dniu 27 września 2022 r. zmarł Pan dr n. farm. Bohdan Jerzy Starościak specjalista w dziedzinie mikrobiologii farmaceutycznej. Pan Doktor całe życie zawodowe związany był z Zakładem Mikrobiologii Farmaceutycznej Akademii Medycznej w Warszawie – Warszawskiego Uniwersytetu Medycznego, prowadząc zajęcia dydaktyczne i badania naukowe oraz przez wiele lat kierując Zakładem. Przez pół wieku należał do Polskiego Towarzystwa Mikrobiologów, pełniąc szereg funkcji w Oddziale Terenowym PTM w Warszawie. Przez 30 lat był sekretarzem redakcji kwartalnika PTM – *Postępy Mikrobiologii.* Jako sekretarz bardzo rzetelnie recenzował i wykonywał korekty nadsyłanych manuskryptów, korzystając z ogromnej wiedzy mikrobiologicznej jaką posiadał.

2. Na stronie PTM utworzono zakładkę FEMS, do której są zamieszczane informacje otrzymywane z FEMS, powinno to zachęcić do szerszego korzystania z możliwości – korzyści jakie daje przynależność PTM do FEMS.

3. Wice-Prezes FEMS Pani prof. dr hab. Elżbieta A. Trafny i Pani Sekretarz dr. hab. Agnieszka Laudy wręczyły jubileuszowy dyplom PTM Pani Profesor dr hab. Zofii Zwolskiej, Członkowi Honorowemu PTM, na Konferencji „Światowy Dzień Gruźlicy 2022" z uroczystą sesją naukową z okazji Jubileuszu Pani Profesor, w dniu 14 października 2022 r., w Pałacu Staszica w Warszawie.

4. Z powodu rosnącej inflacji tj. wzrostu kosztów cen papieru, energii, opłat pocztowych, itp. podniesiono o 10% koszty prenumeraty papierowych zeszytów czasopism PTM nabywanych przez osoby prywatne. Obecnie będą one wynosiły – koszt 1 zeszytu *AM-PM* i *PJM* 40 zł + 4 zł (10%) = 44 zł × 4 zeszyty = 176 zł + VAT 8% = 190,08 zł
   Natomiast koszt prenumeraty roczników dla firm i bibliotek, zostanie zwiększony o 20% i wyniesie:
   koszt 1 zeszytu 40 zł + 8 zł (20%) = 48,– zł × 4 zeszyty = 192,– zł + 15,36 (VAT 8%) = 207,36 zł
   Dla prenumeratorów zagranicznych – ARS POLONA
   *PJM* – 500 zł + 100 zł (20%) = 600 zł + VAT 8% = 648 zł
   *AM-PM* – 266 zł + 53,20 (20%) = 319,20 zł + VAT 8% = 344,74 zł

5. Podjęto **Uchwałę Nr 29-2022** w sprawie zatrudnienia Pani Moniki Kucharskiej na stanowisku sekretarki w biurze ZG PTM od 01.11.2022 r. do 31.12.2023 r.

6. Podjęto **Uchwałę Nr 30-2022** w sprawie przyjęcia 12 nowych Członków Zwyczajnych PTM.

7. Podjęto **Uchwałę Nr 31-2022** w sprawie objęcia patronatem honorowym wydarzenia „Antybiotykoterapia pod Lupą Farmaceuty" które odbywa się cyklicznie, w tym roku w dniach 14–18.11.2022. Organizatorem wydarzenia jest Polskie Towarzystwo Studentów Farmacji. Celem wydarzenia jest edukacja młodego pokolenia, szczególnie młodzieży w wieku szkolnym, w zakresie antybiotyków i roli farmaceuty w przebiegu prawidłowej antybiotykoterapii.

8. Podjęto **Uchwałę Nr 32-2022** w sprawie współorganizowania konferencji on-line „VIII Ogólnopolskie Spotkanie Mikrobiologów i Epidemiologów", która odbyła się on-line w dniu 14 listopada 2022 roku. Kierownikiem Naukowym Konferencji była Pani prof. dr hab. Ewa Augustynowicz-Kopeć, Konsultant Wojewódzki w dziedzinie mikrobiologii lekarskiej. Współorganizatorem wydarzenia jest również Instytut Gruźlicy i Chorób Płuc oraz firma Medicare S.C.

9. Podjęto **Uchwałę Nr 33-2022** w sprawie przyjęcia 3 nowych Członków Zwyczajnych PTM.

10. W dniu 03.11.2022 r. odbyło się spotkanie redakcji czasopism *PJM*, *AM-PM* oraz kierownictwa PTM z przedstawicielami firmy Sciendo na temat współpracy wydawniczej czasopism PTM. Zgłoszono szereg uwag do dotychczasowej współpracy oraz rozpoczęto rozmowy na temat nowych umów wydawniczych na okres 4-letni. Firma Sciendo odniosła się do zgłaszanych zastrzeżeń. Obiecano wyjaśnić szereg z nich a także przygotować projekty umów dotyczących wydawania on-line kwartalników *PJM* i *AM-PM*. Trwają negocjacje w sprawie nowych umów wydawniczych.

11. Po raz pierwszy opłacono nowo wprowadzoną roczną składkę członkowską PTM w ESCMID – 250 Euro.

12. W dniu 22.11.2022 r. w ramach spotkania naukowego Sekcji Mikrobiologii Środowiskowej PTM został wygłoszony wykład pt. „Nowe rozwiązania bio(techno)logiczne dla rozwoju zrównoważonych strategii uprawy roślin, z uwzględnieniem diagnostyki, zwalczania i monitoringu kluczowych fitopatogenów" przez Panią prof. dr hab. Magdalenę Frąc z Instytutu Agrofizyki im. Bohdana Dobrzańskiego Polskiej Akademii Nauk.

13. W dniu 16.11.2022 r. odbyły się w Krakowie Warsztaty z okazji Europejskiego Dnia Wiedzy o Antybiotykach i Światowego Tygodnia Wiedzy o Antybiotykach organizowane we współpracy z Krakowskim Oddziałem PTM. W ramach Warsztatów, wykłady wygłosili: prof. dr hab. Waleria Hryniewicz, prof. dr hab. Marek Gniadkowski, dr hab. Anna Czajka prof. UR, dr Anna Bialecka i dr Alicja Kuch.

14. W dniach 29–30.11.2022 r., z okazji 200 rocznicy urodzin Ludwika Pasteura, odbyła się międzynarodowa konferencja, współorganizowana przez Warszawski Oddział PTM "The last word belongs to microbes, celebrating the 200$^{th}$ anniversary of birth of Louis Pasteur". Na konferencję przyjechało grono naukowców z Instytutu Pasteura w Paryżu oraz innych instytutów zagranicznych, którzy oprócz badaczy polskich wygłosili szereg wykładów. Zorganizowano również sesje plakatów i e-plakatów. Na konferencji obecna była m.in. Pani Prezydent FEMS, prof. Hilary Lappin-Scott. Materiały konferencyjne zawarto w opracowanej książce konferencyjnej.

15. Zakończono proces retrakcji 5 artykułów – plagiatów z zeszytów *AM-PM*, co jest już widoczne na stronach internetowych, m.in. kwartalnika *AM-PM* i *WoS*.

16. Oddział Terenowy PTM we Wrocławiu wraz z Katedrą Mikrobiologii i Biologii Molekularnej WLNZ UZ, Zakładem Mikrobiologii WNB UWr oraz Zakładem Fizykochemii Drobnoustrojów WNB UWr zorganizował w Zielonej Górze w dniu 09.12.2022 r. Sympozjum „Dolnośląsko-Lubuskie spotkania z mikrobiologią". Omówiono zagadnienia poświęcone drobnoustrojom tworzącym biofilm i sposobom zwalczania biofilmu.

17. Sekcja Mikrobiologii Środowiskowej PTM w dniu 14.12.2022 r. zorganizowała seminarium on-line z wykładem „Ameby skorupkowe w badaniach torfowisk: paleoekologia, monitoring, eksperyment", który wygłosił Pan prof. dr hab. Mariusz Lamentowicz z Pracowni Ekologii Zmian Klimatu Wydziału Nauk Geograficznych i Geologicznych Uniwersytetu im. Adama Mickiewicza w Poznaniu.

18. Do dnia 12.12.2022 r. przeprowadzono wybory nowych władz Oddziałów Terenowych i ich komisji rewizyjnych w większości oddziałów PTM. Mamy nadzieję, że do końca roku pozostałe OT PTM przeprowadzą wybory wśród swoich członków. Nowo wybranym władzom Oddziałów Terenowych PTM życzymy dużo sił, pomysłów i zaangażowania, aby nasze Towarzystwo rozwijało się dynamicznie.

19. Prezydium PTM postanowiło, z końcem 2022 r. zrezygnować z umieszczania informacji o działalności Zarządu Głównego Polskiego Towarzystwa Mikrobiologów w zeszytach kwartalników *Advancements of Microbiologia – Postępy Mikrobiologii* i *Polish Journal of Microbiology.* Dotychczasowe i nowe informacje o PTM zamieszczane będą co kwartał w utworzonej zakładce „Bieżące informacje z ZG PTM" na głównej stronie internetowej PTM.

20. Pan prof. dr hab. Jacek Bielecki zrezygnował z funkcji Redaktora Naczelnego kwartalnika *Postępy Mikrobiologii – Advancements of Microbiology* z końcem roku. Polskie Towarzystwo Mikrobiologów wyraża swoje wielkie uznanie dla 25. letniej oddanej pracy Pana Profesora w Redakcji *Postępów Mikrobiologii* i dziękuje za poświęcenie sprawom czasopisma. Pan Profesor zapisał się na trwałe w historii działalności i rozwoju czasopisma.

21. W związku z rezygnacją Pana prof. dr hab. Jacka Bieleckiego z funkcji Redaktora Naczelnego czasopisma *Postępy Mikrobiologii – Advancements of Microbiology* Prezydium ZG PTM **Uchwałą Nr 34-2022** postanowiło z dniem 01.01.2023 r. powierzyć funkcję Redaktora Naczelnego *Advancements of Microbiology* (nowa nazwa) Panu prof. dr hab. n. med. Tomaszowi Gosiewskiemu, specjaliście mikrobiologii z Katedry Mikrobiologii Zakładu Molekularnej Mikrobiologii Medycznej Wydziału Lekarskiego Uniwersytetu Jagiellońskiego Collegium Medicum w Krakowie.

22. Sprawy czasopism PTM
PTM od 2023 roku będzie wydawało on-line kwartalnik *Postępy Mikrobiologii – Advancements of Microbiology* pod nazwą *Advancements of Microbiology.* Ponadto PTM negocjuje umowę czteroletnią na wydawanie on-line czasopism *Advancements of Microbiology* (dawniej *Postępy Mikrobiologii*) oraz *Polish Journal of Microbiology* przez firmę Sciendo, polską filię firmy De Gruyer. Opłaty wydawnicze będą wyższe niż w poprzednich latach, co zmusza PTM do podniesienia opłat redakcyjnych.
a) Ponadto wzrosła ranga czasopisma *Polish Journal of Microbiology* – nastąpił wzrost wskaźników oceny (m.in. do $IF_{2021}$ = 2,019, 5-letni IF = 1,806, CiteScore = 2,7).
W związku z powyższym podjęto **Uchwałę Nr 35-2022** w sprawie zwiększenia opłat redakcyjnych *PJM*:
* dla autora korespondencyjnego – członka PTM (z opłaconą składką na rok bieżący), z 500 USD do 800 USD + VAT 23%
* dla autorów korespondencyjnych nie będących członkami PTM z 800 USD do 1000 USD + VAT 23% (jeżeli się stosuje).
Zwiększona opłata dotyczyć będzie manuskryptów przysłanych do Redakcji *PJM* od 01.03.2023 r.
b) W przypadku *Advancements of Microbiology* zrezygnowano z funkcjonującej przez 4 lata nazwy *Postępy Mikrobiologii – Advancements of Microbiology*, co ma ułatwić dostęp autorów zagranicznych do czasopisma i ponownej oceny kondycji czasopisma przez firmę Scopus. Ponadto w związku z podniesieniem rangi czasopisma i wzrostu wskaźników oceny (m.in. $IF_{2020}$ z 0,947 do $IF_{2021}$ = 1,106), podjęto **Uchwałę Nr 36-2022** w sprawie zwiększenia opłat redakcyjnych:
* dla autora korespondencyjnego – członka PTM (z opłaconą składką na rok bieżący), gdy manuskrypt jest w wersji anglojęzycznej lub przysyłane są obie wersje językowe (angielska i polska) opłata wzrasta z 200 zł + VAT 23% (tj. 246 zł brutto) do 400 zł + VAT 23% (tj. 492 zł brutto), gdy manuskrypt jest przysłany tylko w języku polskim – opłata wzrasta z 400 zł + VAT 23% (tj. 492 zł brutto) do 800 zł + VAT 23% (tj. 984 zł brutto);
* dla pozostałych autorów korespondencyjnych, którzy nie są aktywnymi członkami PTM (nie mają opłaconych składek w roku bieżącym), gdy manuskrypt jest w wersji anglojęzycznej lub przysyłane są obie wersje językowe (angielska i polska) opłata wzrasta z 300 zł + VAT 23 % (tj. 369 zł brutto), do 1000 zł + VAT 23% (tj. 1230 zł brutto), gdy manuskrypt jest przysłany tylko w języku polskim – opłata wzrasta z 600 zł + VAT 23% (tj. 738 zł brutto) do 1400 zł + VAT 23% (tj. 1722 zł brutto).
Zwiększona opłata dotyczyć będzie manuskryptów przysłanych do Redakcji AM od 01.03.2023 r.

23. W związku z podjęciem się obowiązku uzupełniania na bieżąco informacji na stronie PTM, podjęto **Uchwalę Nr 37-2022** o zwiększeniu uposażenia miesięcznego sekretarki ZG PTM o 200 zł.

24. Podjęto **Uchwałę Nr 38-2022** w sprawie przyjęcia nowych Członków Zwyczajnych PTM.

25. Z okazji nadchodzących Świąt Bożego Narodzenia i Nowego Roku 2023 dziękujemy wszystkim członkom PTM za współpracę w minionym okresie oraz życzymy dużo zdrowia, pomyślności oraz sukcesów na polu zawodowym, rodzinnym, a także społecznym.

Warszawa, 09.12.2022 r.

SEKRETARZ
Polskiego Towarzystwa Mikrobiologów
*dr hab. n. farm. Agnieszka E. Laudy*

PREZES
Polskiego Towarzystwa Mikrobiologów
*prof. dr hab. Stefan Tyski*

## CZŁONKOWIE WSPIERAJĄCY PTM

**Członek Wspierający PTM – Srebrny**
**od 12.09.2017 r.**

Firma Ecolab Sp. z o.o. zapewnia: najlepszą ochronę środowiska pracy przed patogenami powodującymi zakażenia podczas leczenia pacjentów, bezpieczeństwo i wygodę personelu, funkcjonalność posiadanego sprzętu i urządzeń. Firma jest partnerem dla przemysłów farmaceutycznego, biotechnologicznego i kosmetycznego.

**Członek Wspierający PTM – Zwyczajny**
**od 12.09.2017 r.**

Merck Sp. z o.o. jest częścią międzynarodowej grupy Merck KGaA z siedzibą w Darmstadt, Niemcy i dostarcza na rynek polski od roku 1992 wysokiej jakości produkty farmaceutyczne i chemiczne, w tym podłoża mikrobiologiczne